Stratospheric ozone in the Earth system

Fernando Iglesias-Suarez BSc, MSc
Lancaster Environment Centre, Lancaster University, UK
September 2017

This dissertation is submitted for the degree of Doctor of Philosophy

Abstract

Stratospheric ozone in the Earth system

Fernando Iglesias-Suarez B.A., MSc
Lancaster Environment Centre, Lancaster University, UK

September 2017

Ozone in the stratosphere protects life on Earth by absorbing much of the ultraviolet solar radiation, as well as being a major source of ozone to the troposphere. A number of factors can influence stratospheric ozone levels and explain past, present and future changes. While there is a large literature exploring changes in stratospheric ozone due to, for example, ozone depleting substances (ODSs) and climate change, the study of its interactions with the rest of the Earth system is relatively recent. The work presented in this thesis investigates changes in stratospheric ozone and its links with other elements of the Earth system (tropospheric chemical composition and climate), using observations, a global chemistry-climate model (CESM1-WACCM), and existing multi-model output.

This work evaluates past changes and explores future evolution of stratospheric ozone and associated climate impacts using multi-model output (ACCMIP simulations) from the pre-industrial period to the end of the 21st century. ACCMIP multi-model mean total column ozone trends compare favourably against observations. These models show a strong link between the Antarctic ozone hole and surface climate, which demonstrates that stratospheric ozone changes are coupled with the troposphere.

A series of sensitivity simulations is conducted to investigate multi-decadal variability. A striking finding is that low frequency variability of ozone in the tropical middle stratosphere resembles multi-decadal climate variability in Pacific Ocean sea surface temperatures. This analysis also shows that internally generated climate variability is the leading factor explaining recent negative trends of mid-stratospheric tropical ozone.

Finally, an additional set of sensitivity simulations is performed to quantify future radiative forcing between 2000s and 2100s that results from changes in ozone due to climate change, ODSs and methane concentrations. These results highlight the importance of stratosphere-troposphere exchange, as well as the key role of the stratosphere controlling the tropospheric ozone forcing.

Acknowledgements

I am sincerely grateful to my supervisors Dr Paul Young and Prof Oliver Wild for being my beacon during this thesis. Paul has been my weekly (and even daily) support and guidance, and Oliver has promptly provided sensible perspective during toughest periods. I am also grateful to Dr Fernando Govantes for supporting me to change my career path from environmental-related advise to science-based research. I would like to thank the UK Natural Environment Research Council for providing me with the funding that allowed to conduct this work, share my findings at conferences, and meet so many remarkable scientists.

An important part of my research was a short stay in Boulder (Colorado, US). Dr Jean-François Lamarque hosted me at NCAR, where Dr Doug Kinnison, Dr Mike Mills, Dr Simone Tilmes and Dr Louisa Emmons helped me to get started with their chemistry-climate model. Also Dr Dan Marsh, Dr Rolando Garcia, Dr Anne Smith and Dr Bill Randel from NCAR, and Dr Karen Rosenlof, Dr Bob Portman, Dr Sean Davis, Dr Birgit Hassler and Dr Amy Butler from NOAA, gave me the opportunity to share my research and provided valuable insight to this thesis.

At Lancaster University, I thank Prof Gail Whiteman for letting me join an outstanding multidisciplinary research group at the Pentland Centre for Sustainability in Business. Particularly, Dr Dmitry Yumashev guided me to bridge climate science with global socio-economic risks. I am also grateful to my PhD and postdocs fellows with who I shared so many experiences, especially Dr Alfonso Lag-Brotons for distracting me from science on daily basis.

To my friends and family, you all know that I felt your unconditional understanding and encouragement throughout this bumpy journey. Thank you mum and sibs for the many (often unearned) privileges I enjoyed. I wish dad could see me becoming a doctor(-ate), not the kind he may have probably expected though. Especial thanks to Juan for the amazing flamenco guitar that accompanied me destroying classic songs. I feel really fortunate to have spent these years with ‘La Milla de Oro’ in Lancaster, os quiero cabesitas. And thank you Maria, you are my rock. I am ready for the next adventure!

Nando
September 2017

to my dad

Contents

List of figures

List of tables

Chapter 1

Introduction and thesis aims

The work in this thesis concerns past changes, present, and future evolution of ozone in the stratosphere, the role of different drivers in those changes, such as ozone depleting substances (ODSs), climate change and natural variability, and how such changes interact with other parts of the Earth system (tropospheric composition and climate).

The stratosphere is a distinct region of the atmosphere (~ 12–50 km) with a particular chemical composition and dynamics, and is strongly influenced by the presence of ozone (WMO, 2014). It can affect – and be influenced by – the troposphere, both directly (e.g. transport of trace gases) and indirectly (e.g. radiative processes). Ozone is mainly found in the stratosphere, where it protects life on Earth by absorbing most of the incoming solar ultraviolet radiation. Also stratospheric ozone is an important source of ozone to the troposphere, affecting its abundance and distribution (e.g. Zeng and Pyle, 2003). In the troposphere, however, ozone is a pollutant (affecting ecosystems, crops and human health), greenhouse gas (GHG), and influences the oxidising capacity of the atmosphere (hydroxyl radicals) (Prather et al., 2001; UNEP, 2015). Therefore, understanding how different drivers affect stratospheric ozone and the implications of past and future changes is important for a range of issues.

Stratospheric ozone abundance and distribution is in balance between photochemical production and loss reactions, and transport processes. Anthropogenic emissions of ODSs since the 2nd half of the 20th century have perturbed this balance,

leading to net ozone losses (WMO, 2014). The Antarctic in austral spring experiences largest ozone losses in stratospheric ozone, the so-called 'ozone hole'. In turn, the ozone hole due to dynamical and radiative coupling can affect tropospheric and surface climate, such as temperatures, winds and precipitation (e.g. Thompson and Solomon, 2002). Owing to international efforts, the ozone layer is expected to recover from anthropogenic ODSs during the 21st century. Yet natural variability acting at different timescales complicates a clear detection of ozone recovery (e.g. Solomon et al., 2016).

Furthermore, stratospheric ozone may be influenced by other factors and never return to pre-industrial levels. Due to increasing concentrations of GHGs, climate change results in tropospheric warming, but cooling in the stratosphere with associated feedbacks, such as ozone chemistry and transport processes (e.g. Haigh and Pyle, 1982). Global models project an acceleration of the Brewer-Dobson circulation (BDC) – i.e. mean meridional transport of air mass in the stratosphere – which would affect the distribution of stratospheric ozone and stratosphere-troposphere exchange (e.g. Garcia and Randel, 2008). In addition, increased abundances of GHGs such as nitrogen oxide and methane would not only contribute to climate change, but also affect stratospheric ozone chemistry (e.g. Randeniya et al., 2002). The above drivers and related feedbacks complicate our understanding of stratospheric ozone responses and their implications.

The aim of this thesis is to investigate stratospheric ozone changes, including their interactions with other elements of the Earth system, and to assess their implications. Using previously completed multi-model experiments, I have explored past changes and future evolution of stratospheric ozone and related climate impacts. Furthermore, I have used a global chemistry-climate model to complete my own simulations and examined links between modelled ozone changes, natural variability and tropospheric composition and climate.

The remainder of this thesis is organised as follows. Chapter 2 presents our current understanding and the overall background relevant for this work. I describe the main processes determining stratospheric ozone abundances and distribution, before discussing recent observed changes and stratosphere-troposphere links. Here, I also provide a brief description of chemistry-climate models and discuss projected changes of stratospheric ozone during the 21st century.

Chapter 3 quantifies stratospheric ozone changes and related climate impacts in the Atmospheric Chemistry and Climate Model Intercomparison Project (ACCMIP) (Lamarque et al., 2013b) from pre-industrial times (1850) to the 21st century (2100). In addition, this analysis also includes the simulations from the phase 5 of the Coupled Model Intercomparison Project (CMIP5) (Taylor et al., 2012) and the phase 2 of the Chemistry-Climate Model Validation activity (CCMVal2) (Morgenstern et al., 2010b) as a benchmark for the former models.

Chapter 4 demonstrates internal low frequency variability in ozone in the tropical middle stratosphere related to dynamical (BDC) and chemical (NO_x-catalysed loss) processes. Also, this chapter discusses that acknowledging multi-decadal internal climate variability can help interpret recent observationally derived changes in the BDC.

Chapter 5 explores future changes in stratospheric ozone and related radiative forcing due to climate change, stratospheric ozone recovery, and methane emissions. In this chapter, particular attention is given to non-linearities and the robustness of the forcing attributed to individual drivers. For the first time, this work unambiguously identifies ozone forcing based on its origin (i.e. stratospheric- and tropospheric-produced ozone forcing).

Chapter 6 summarises the findings of the previous chapters as well as discussing the limitations and caveats of this thesis. Finally I discuss how future work may help better understand stratospheric ozone changes and climate interactions.

Chapter 2

Literature review

Investigating stratospheric ozone and its interactions with the rest of the Earth system requires understanding of the chemical and dynamical processes controlling the stratosphere, as well as global features determining atmospheric composition and climate in the troposphere. Anthropogenic emissions of radiatively active greenhouse gases (GHGs), ozone depleting substances (ODSs) and ozone precursors have altered chemistry and energy balances in the atmosphere and will continue doing so in the coming century, with distinct changes occurring in the stratosphere and the troposphere (IPCC, 2013). Observations (direct and indirect) have provided fundamental knowledge of the mechanisms involved in such changes, although they may be limited in time (e.g. satellite records extend only few decades) and/or coverage (e.g. fewer ground-based measurements are available in the Southern Hemisphere, SH) (WMO, 2014). Numerical models are generally able to capture observed changes, can provide insight on the important processes and make projections following possible socio-economic developments (i.e. future emission scenarios) (e.g. Morgenstern et al., 2017).

In this chapter, I introduce our current understanding to provide the overall background to the experiments and analyses in subsequent chapters. In Section 2.1, I describe chemical and dynamical processes determining stratospheric ozone, recent observed changes and their causes. Then I present the salient factors of tropospheric climate and composition in Section 2.2, before discussing key interactions between the stratosphere and the troposphere in Section 2.3. This is

followed by a discussion on stratospheric ozone evolution during the 21st century and its drivers in Section 2.4, along with a brief description of chemistry-climate models (CCMs) used for future simulations in Section 2.5. Finally, I provide a summary of the chapter in Section 2.6.

2.1. The stratosphere and the ozone layer

First, this section presents a general overview of the stratospheric ozone layer, focusing on the early observations and photochemical theory (Sect. 2.1.1). Then, I describe the important features of the stratosphere, including chemistry (Sect. 2.1.2) and dynamics (Sect. 2.1.3). Finally, this section also presents past changes of ozone, distinguishing between polar and extra-polar regions, and discusses their causes (Sect. 2.1.4).

2.1.1. The stratospheric ozone layer

The stratosphere, broadly defined as the region of the atmosphere from ~ 10–15 km (lower at high latitudes and higher in the tropics) to ~ 50 km, holds the vast majority of ozone in the atmosphere. In this region, heating by ozone due to the absorption of incoming solar radiation leads to a positive temperature lapse rate – higher temperature with altitude – (e.g. Andrews, et al., 1987). The absorption of high-energy ultraviolet radiation by ozone (Cornu, 1879; Hartley, 1880) not only determines stratospheric temperature and dynamics but also protects living things on Earth (WMO, 2014). Reductions in stratospheric ozone, therefore, results in increases of harmful ultraviolet radiation with negative consequences for human health, plants and animals (UNEP, 2015).

Observations

First measurements of ozone in the stratosphere date from 1924 (Dobson and Harrison, 1926). Dobson and Harrison (1926) recorded the measurements using the total thickness of ozone in a column of air at standard conditions (1013.25 hPa and 273.15 K) using a spectrograph (Dobson, 1968), the so-called Dobson Units (DU). 1 DU is defined as 2.687×10^6 molec cm^{-2} of ozone. For example, 100 DU brought to the surface occupies 1 mm thick layer of ozone.

Comprehensive up-to-date description of available data sets of ozone and other trace gases (e.g. ODSs, H_2O) can be found in the latest World Meteorological Organization (WMO) Scientific Assessment of Ozone Depletion report (WMO, 2014), and is summarised in Figure 2.1. Briefly, total column ozone ground-based measurements, using Dobson and Brewer spectrometers, provide the longest data records available since 1960s (Fioletov et al., 2002, 2008; Hendrick et al., 2011). However, observations are sparse and biased toward the Northern Hemisphere (NH) – i.e. fewer data records exist in the SH, with best coverage over North America, Europe and Japan (WMO, 2014).

Satellite records are available since the late 1970s (i.e. sparse and more uncertain observations in the early 1970s), providing near-global and continuous coverage (e.g. Stolarski and Frith, 2006; Weber et al., 2011). Because the lifetime of satellite instruments – such as the Solar Backscatter Ultraviolet (SBUV) – is limited (e.g. drifts), long-term records require merging and homogenisation to overcome differences between instruments, local time measurements, vertical and temporal resolution, and coordinate systems (e.g. pressure- or altitude-based system) (e.g. Bodeker et al., 2005, 2013).

Ozone profiles – vertically resolved measurements – are also available from ground-based stations (i.e. balloon-borne ozonesondes) and satellites (limb- and nadir-viewing instruments). While the ground-based network station provides high vertical resolution profiles (~ 100 m) since the 1970s, they reach as high as the middle stratosphere (~ 33 km) (e.g. Thompson et al., 2012). Recent activities have merged and homogenised various satellite instruments – e.g. the Stratospheric Aerosol and Gas Experiment instruments (SAGE I and II), HALogen Occultation Experiment (HALOE), and Microwave Limb Sounder (MLS) – to provide a gap free record since the early 1980s, which cover the upper troposphere to the upper stratosphere (~ 1–300 hPa) with a coarser resolution (e.g. Davis et al., 2016).

Photochemistry

An oxygen only theory of the formation and destruction of ozone was first proposed by Chapman (1930). The production of stratospheric ozone is initiated by the ultraviolet photolysis of O_2,

$$O_2 + h\nu\ (\lambda < 242\ \text{nm}) \quad \rightarrow \quad 2O \qquad (2.1)$$

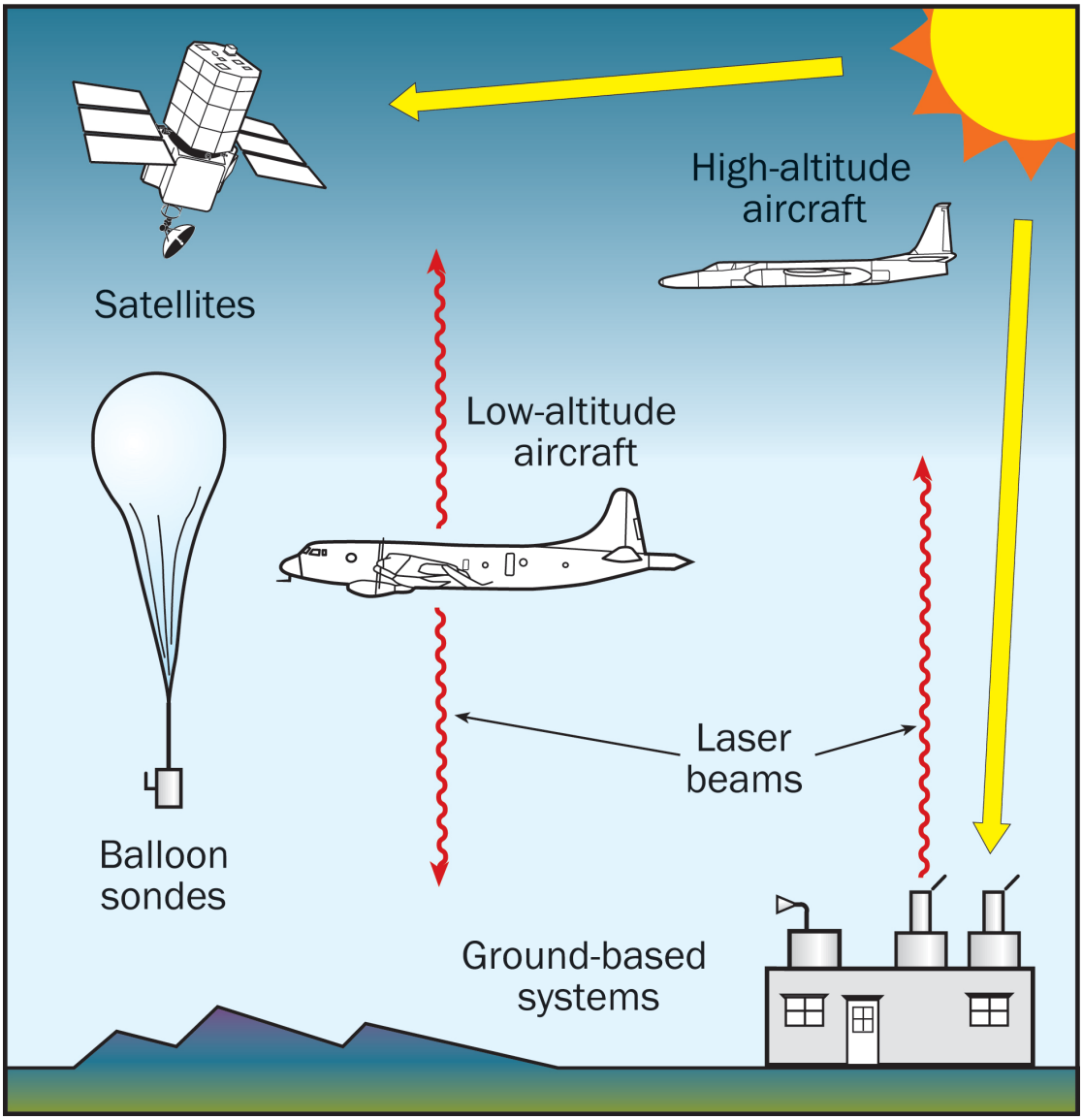

Figure 2.1. Summary of ozone measurements (from WMO, 2014).

where hν is a photon, and λ represents wavelength. The resultant oxygen atom (O) reacts very rapidly with O_2 to form ozone (O_3),

$$O + O_2 + M \rightarrow O_3 + M^* \qquad (2.2)$$

where M is a third body (N_2 or O_2), which dissipates energy from the collision. Photolysis of O_3 is also rapid,

$$O_3 + h\nu\ (\lambda < 320\ \text{nm}) \rightarrow O + O_2. \qquad (2.3)$$

As commented above, the absorption of ultraviolet radiation by O_3 (reaction 2.3) determines the thermal structure of the stratosphere (positive gradient with altitude). Chapman pointed out that O_3 and O are in photochemical equilibrium (rapid

interchange between one another, reactions 2.2–2.3). Therefore, it is useful to consider the sum of O_3 and O together as an "odd oxygen family" (O_x), because the latter is produced or destroyed much more slowly. Note that in the stratosphere O_3 largely dominates the partitioning of the O_x family. This concept allows to distinguish between net production or loss of O_3 over time.

A very small fraction of the O_x family (via O_3 and O interaction) produces O_2, resulting in this case in a net loss of O_3,

$$O + O_3 \rightarrow 2O_2. \quad (2.4)$$

2.1.2. Stratospheric ozone chemistry

Gas-phase ozone loss

However, stratospheric ozone loss via the O_x family interaction (reaction 2.4) is not able to explain alone observed ozone abundances. Further research demonstrated that stratospheric ozone is also destroyed by hydrogen (Bates and Nicolet, 1950), and nitrogen oxide chemistry (Crutzen, 1970). Active (great reactivity) species of hydrogen (H + OH + HO_2; HO_x) and nitrogen (NO + NO_2; NO_x) are involved in catalytic cycles that destroy ozone. In other words, HO_x and NO_x species are regenerated after destroying ozone. The general form of the catalytic cycles is:

$$XO + O \rightarrow X + O_2 \quad (2.5)$$

$$X + O_3 \rightarrow XO + O_2 \quad (2.6)$$

$$\text{Cycle 1; net: } O + O_3 \rightarrow 2O_2$$

where the "X" refers to reactive hydrogen, nitrogen, and halogen elements (X = H, OH, NO, Cl, Br) – chlorine is particularly important for this cycle, and is further discussed below. In addition, reactions between HO_x and O compete with ozone production, making it less effective. While anthropogenic perturbations to levels of stratospheric hydrogen (e.g. via emissions of methane, CH_4, and increased water vapour, H_2O, concentrations) and nitrogen oxides (e.g. via emissions of nitrous oxide, N_2O) may result in enhanced ozone loss, observed depletion in recent decades is primarily due to halogen-related chemistry (e.g. WMO, 2014).

The important halogen elements are chlorine, bromine and iodine. While, fluorine shows very low catalytic efficiency destroying ozone, as it rapidly reacts with methane to form a stable hydrogen fluoride (HF) reservoir (Stolarski et al., 1975), iodine is found in very small amounts in the stratosphere though it may affect

significantly ozone in the troposphere (e.g. Butz et al., 2009). Of particular importance for ozone chemistry are chlorine and bromine (e.g. due to their abundance and catalytic chemistry), therefore halogen chemistry will be referred to them herein.

Although chlorine chemistry has a long history, it was not shown until the early 1970s, that chlorine could destroy ozone in a catalytic cycle (Stolarski and Cicerone, 1974). It was also realized that anthropogenic emissions of chlorofluorocarbons (CFCs) were perturbing natural abundances of chlorine in the atmosphere, and that they could reside very long periods (i.e. removal is only via breakup by ultraviolet radiation in the stratosphere) (Molina and Rowland, 1974). Today it is well established that chlorine (Molina and Molina, 1987) and bromine (McElroy et al., 1986; Tung et al., 1986) can destroy ozone in catalytic cycles (e.g. such as cycle 1).

The above catalytic ozone loss cycle 1 is effective when oxygen atoms are available. Because the abundance of oxygen atoms increases with height by the photo-dissociation of oxygen and ozone molecules (i.e. higher intensity of ultraviolet radiation), the cycle 1 is the dominant catalytic ozone loss cycle in the upper stratosphere – peaking ~ 40 km. However, chlorine and bromine can also destroy ozone interacting with other chemical families (e.g. HO_x and NO_x). Ozone destruction can occur via chlorine (Johnson et al., 1995; Kovalenko et al., 2007) and bromine (Poulet et al., 1992) monoxides interacting with HO_x,

$$O_3 + OH \rightarrow HO_2 + O_2 \quad (2.7)$$
$$XO + HO_2 \rightarrow HOX + O_2 \quad (2.8)$$
$$HOX + h\nu \rightarrow X + OH \quad (2.9)$$
$$O_3 + X \rightarrow XO + O_2 \quad (2.10)$$
$$\text{Cycle 2; net:} \quad 2O_3 \rightarrow 3O_2$$

and NO_x (Toumi et al., 1993; Burkholder et al., 1995; Lary et al., 1996),

$$NO + O_3 \rightarrow NO_2 + O_2 \quad (2.11)$$
$$XO + NO_2 + M \rightarrow XONO_2 + M \quad (2.12)$$
$$XONO_2 + h\nu \rightarrow X + NO_3 \quad (2.13)$$
$$NO_3 + h\nu \rightarrow NO + O_2 \quad (2.14)$$
$$O_3 + X \rightarrow XO + O_2 \quad (2.10)$$
$$\text{Cycle 3; net:} \quad 2O_3 \rightarrow 3O_2$$

where $XONO_2$ (i.e. $ClONO_2$ or $BrONO_2$) represent halogen "reservoirs" (non-ozone destroying species), where X in cycles 2 and 3 refers to halogen atoms. In addition, chlorine can also reacts with nitrogen as follows,

$$O_3 + h\nu\ (\lambda < 320\ nm) \rightarrow O + O_2 \quad (2.3)$$
$$O + NO_2 \rightarrow NO + O_2 \quad (2.15)$$
$$NO + ClO \rightarrow NO_2 + Cl \quad (2.16)$$
$$O_3 + Cl \rightarrow ClO + O_2 \quad (2.10a)$$

Cycle 4; net: $2O_3 \rightarrow 3O_2$.

The Antarctic ozone hole and heterogeneous halogen chemistry

Although the above gas-phase catalytic cycles can significantly destroy ozone, the large reduction in total ozone reported over Antarctica during austral spring (ozone hole) in 1985 (Farman et al., 1985; Komhyr et al., 1986; Stolarski et al., 1986) was not expected. It was proposed that very high concentrations of reactive chlorine could occur in the presence of polar stratospheric clouds (PSCs) – via heterogeneous reactions (Solomon et al., 1986). Under high concentrations of reactive chlorine (ClO_x), ozone can be depleted without the presence of oxygen atoms (Molina and Molina, 1987),

$$ClO + ClO \rightarrow ClOOCl \quad (2.17)$$
$$ClOOCl + h\nu \rightarrow Cl + ClOO \quad (2.18)$$
$$ClOO + M \rightarrow Cl + O_2 + M \quad (2.19)$$
$$2[Cl + O_3 \rightarrow ClO + O_2] \quad (2.10a)$$

Cycle 5; net: $2O_3 \rightarrow 3O_2$.

The ClO dimer cycle (cycle 5; photolysis of Cl_2O_2 produces atomic chlorine) contributes to ~ 75 % in the formation of the Antarctic ozone hole. Interactions between ClO and BrO in catalytic chemistry also contribute to ~20 % to the formation of the ozone hole (McElroy et al., 1986; Tung et al., 1986; Anderson et al., 1989),

$$ClO + BrO \rightarrow Cl + Br + O_2 \quad (2.20a)$$
$$\rightarrow BrCl + O_2 \quad (2.20b)$$
$$\rightarrow ClOO + Br \quad (2.20c)$$
$$ClBr + h\nu \rightarrow Cl + Br \quad (2.21)$$
$$O_3 + Cl \rightarrow ClO + O_2 \quad (2.10a)$$
$$O_3 + Br \rightarrow BrO + O_2 \quad (2.10b)$$

Cycle 6; net: $2O_3 \rightarrow 3O_2$.

High concentrations of reactive chlorine and bromine, and therefore ozone loss via cycles 5 and 6, can only occur in the presence of PSCs. Here, a brief description of their composition and important heterogeneous halogen activation is provided – see Solomon (1999) for an in-depth review. PSCs are generally classified in two major groups: Type I (nitric acid, HNO_3, containing PSCs); and Type II (ice PSCs) (Biele et al., 2001). Type I can also be separated into Type Ia and Type Ib subclasses. PSCs Type Ia are composed by solid and liquid particles of nitric acid trihydrate (NAT), and can form at temperatures well above the frost point, the so-called NAT-temperature ($T_{NAT} \approx 195$ K). Type Ib clouds (liquid PSCs) form at temperatures below the dew point of HNO_3 ($T_{dew} \approx 192$ K). At those temperatures, binary aerosols droplets of sulfuric acid (H_2SO_4) and H_2O take up HNO_3 to form supercooled ternary solution droplets (STS). Ice PSCs (Type II) are less frequent, as they form only below the frost point ($T_{ice} \approx 188$ K). PSCs Type I, however, are of especial interest for polar ozone depletion since they can form at higher temperatures than ice PSCs (~ 7 K) and limit the abundance of nitrogen oxide available to form halogen reservoir species – i.e. formation of HNO_3 and irreversible denitrification of the stratosphere by sedimentation of large solid particles (Crutzen and Arnold, 1986; Toon et al., 1986). A number of heterogeneous reactions have been demonstrated to be important for polar halogen activation, such as:

$$HCl + ClONO_2 \rightarrow HNO_3 + Cl_2 \quad (2.22)$$

$$N_2O_5 + H_2O \rightarrow HNO_3 \quad (2.23)$$

$$ClONO_2 + H_2O \rightarrow HNO_3 + HOCl \quad (2.24)$$

$$HCl + OHCl \rightarrow H_2O + Cl_2 \quad (2.25)$$

$$BrONO_2 + H_2O \rightarrow HNO_3 + HOBr \quad (2.26)$$

$$HCl + BrONO_2 \rightarrow HNO_3 + BrCl \quad (2.27)$$

$$HCl + OHBr \rightarrow H_2O + BrCl \quad (2.28)$$

Chlorine and bromine partitioning

Halogen source gases (organic halogens such as CFCs, halons and hydrochlorofluorocarbons, HCFCs; further discussed below) enter the stratosphere through the tropopause – boundary layer that 'separates' the troposphere and the stratosphere – mainly in the tropics. High–energy ultraviolet radiation breaks up the halogen source gases releasing reactive atomic halogens (Cl and Br), which increases efficiency with altitude and peaks in the upper stratosphere – see Bedjanian and Poulet

(2003) and Wayne et al. (1995) for a detailed discussion. However, chlorine and bromine show a rather different reactivity with reactive species, particularly with methane. This reactivity ultimately determines the partitioning between active (reactive) and inactive (reservoir) species of the total inorganic chlorine and bromine, Cl_y and Br_y respectively (Sander et al., 2006, 2009). While chlorine atoms react with methane to form hydrogen chlorine (HCl) reservoir species (Stolarski and Cicerone, 1974), bromine is less tightly bounded (Wofsy et al., 1975; Yung et al., 1980). Chlorine and bromine atoms show similar reactivity with ozone, forming halogen monoxide (XO). Halogen monoxides, in turn, react at similar rates with NO_2 to form reservoirs of halogen nitrates ($XONO_2$). Although halogen nitrates photolyse to reform halogen monoxides, $BrONO_2$ is more photolabile than $ClONO_2$ (Lary, 1996). Therefore, Cl_y is found mainly in reservoir species (HCl and $ClONO_2$), and Br_y is skewed towards the reactive oxide (BrO) under sunlight conditions – i.e. at night it will be primarily found in reservoir species. Although bromine shows ~ 60 times higher efficiency than chlorine destroying ozone, the latter is ~ 160 times more abundant in the stratosphere and the dominant driver of ozone loss in present-day atmospheric conditions (e.g. Chipperfield and Pyle, 1998; WMO, 2014).

Stratospheric ozone chemistry regimes

Different chemical regimes exist in the upper and lower stratosphere controlling stratospheric ozone. In the upper stratosphere ozone is in photochemical equilibrium – very short-lived in the order of seconds to minutes (Chapman, 1930). Therefore, its abundance is controlled by the balance between photochemical production (Chapman's photochemistry) and gas-phase catalytic ozone loss (cycle 1) (Bates and Nicolet, 1950; Crutzen, 1970; Molina and Rowland, 1974; Stolarski et al., 1975). However, ozone lifetime significantly increases in the lower stratosphere (in the order of few months or longer) (Sankey and Shepherd, 2003). Because transport processes are of a similar time scale compared to photochemistry, dynamics largely influences ozone abundances in this region (e.g. Shepherd, 2008).

From a photochemistry point of view and to understand the relative importance of different catalytic ozone loss cycles, it is important to bear in mind that photochemistry ozone rates increase with altitude – production and loss along with atomic oxygen (e.g. Crutzen et al., 1995; Grenfell et al., 2006). In the lowermost stratosphere, HO_x-catalysed chemistry dominates gas-phase ozone loss (i.e. where

oxygen atoms are limited). In the lower and middle stratosphere (~ 25–40 km), NO_x-catalysed chemistry largely determines gas-phase ozone loss via cycles 1 and 3 – photo-dissociation of N_2O releases reactive NO_x. Ozone loss is primarily controlled by HO_x-catalysed chemistry via cycle 1 above ~ 45 km, where atomic oxygen is relatively abundant. Although gas-phase halogen-induced ozone loss is not a dominant process (i.e. a maximum is found around 40 km via cycle 1), heterogeneous halogen chemistry (cycles 5 and 6) drives localised largest total ozone losses in the polar lower stratosphere during springtime (e.g. Solomon, 1999).

Source gases affecting stratospheric ozone

Substances that affect stratospheric ozone can have natural and anthropogenic sources. International efforts routinely monitor these substances and provide very detailed reports, including past changes, recent trends, detection and attribution to ozone changes and 'expected' future abundances according to current regulations (see WMO, 2014; and references therein for the most recent update). Thus, this section only presents a brief overview of the most important source gases for stratospheric ozone chemistry.

The atmospheric composition of trace gases has been perturbed by human activities. Intense emissions of ODSs such as CFCs (e.g. CFC-11, CFC-12, CFC-113) and halons (e.g. halon-1202, halon-1211, halon-1301, halon-2402) in the late 20th century have largely driven the observed decreased of stratospheric ozone (Solomon et al., 1986; deZafra et al., 1987; Anderson et al., 1989). The Montreal Protocol (1987) and its Amendments and Adjustments was agreed to limit the emissions of ODSs (note that it continues to be reviewed and adjusted if recommended). As a result, the total combined anthropogenic ODSs abundance in the troposphere peaked in 1994 and declined since by about 10 % in 2012 compared to its peak levels (i.e. total organic chlorine and bromine abundances from controlled ODSs in 2012 are 3300 pptv and 15.2 ± 0.2 pptv respectively) (WMO, 2014). Although the overall production of many ODSs has decreased – e.g. HCFCs continue to grow due to their temporary use as substitutes of the more 'damaging' CFCs, their abundance in the atmosphere respond with a delay and at different time scales (Ko et al., 2013). This is the result of both large emissions from banks or reservoirs (equipment in use) and their relative long lifetime (i.e. only small fraction is photochemically destroyed in the stratosphere).

To put natural sources in context, they contribute to ~ 16 % of the total stratospheric inorganic chlorine (e.g. methyl chloride, CH_3-Cl), and about half to the total inorganic bromine in the stratosphere, which is likely to come from methyl bromide (CH_3-Br) and very short-lived brominated substances – i.e. these are difficult to estimate due to their lifetimes are less than 6 months (e.g. Hossaini et al., 2012; 2013).

Other non-halogenated substances, such as methane and nitrous oxide, can impact stratospheric ozone significantly and have both natural and anthropogenic sources. Methane plays various roles in stratospheric ozone chemistry and its concentration has more than doubled since pre-industrial times due to human activities (i.e. 1808 ppbv in 2012) (Hartmann et al., 2013). Increased concentrations of methane results in a total stratospheric ozone increased due to smog-like chemistry and reduced abundance of ClO_x – i.e. controlling the partitioning of active and inactive chlorine species –, which is partially offset by ozone reductions in the upper stratosphere due to enhanced HO_x-catalysed loss (e.g. Randeniya et al., 2002; Revell et al., 2012).

In the early 1970s, it was noticed that NO_x – emitted by supersonic aircrafts – can destroy stratospheric ozone (Crutzen, 1970; Johnston, 1971). The photochemical degradation of N_2O results in N_2, O_2 and a small fraction of nitrogen oxides (i.e. ~ 10 % of NO_x). The latter directly destroys stratospheric ozone (Ravishankara et al., 2009; Portmann et al., 2012). N_2O atmospheric levels have increased ~ 20 % since the pre-industrial period and is currently the most important single substance emitted to the atmosphere affecting stratospheric ozone. Nevertheless, methane and N_2O contributions to stratospheric ozone changes in the recent past (last three decades) are estimated to be small (WMO, 2011).

2.1.3. Stratospheric dynamics

Photochemical production and destruction (Chapman and catalytic chemistry), and dynamics (transport) determine the distribution of ozone in the stratosphere. This section describes the important features governing stratospheric circulation. Detailed description and discussion can be found in Baldwin et al. (2001), Dameris and Baldwin (2011), and Butchart (2014) and references therein.

The global mean mass transport of air in the stratosphere is characterised by upwelling in the tropics (tropospheric air enters the stratosphere) and poleward flow

motion before descending at mid- and high latitudes (stratospheric air returns to the troposphere) (e.g. Butchart, 2014). The global meridional circulation was described by Alan Brewer (1949) and Gordon Dobson (1929; 1956) to explain distributions of water vapour and ozone respectively, and it is referred to as the "Brewer-Dobson circulation" (BDC). The term BDC is used to describe the overall overturning circulation in the stratosphere (Holton et al., 1995), but has no formal definition as different physical models can describe it – e.g. the Transform Eulerian Mean, TEM, describes the residual mean circulation (Andrews et al., 1987). The stratosphere-troposphere exchange (STE) is largely determined by the BDC (e.g. Shepherd, 2008; Li et al., 2009**)**.

The poleward mean motion of air in the middle and upper stratosphere – during the winter hemisphere – is driven by planetary-scale Rossby waves (wave lengths in the order of thousand km), mechanism generally known as the "extra-tropical pump" or "Rossby-wave pump" (Holton et al., 1995; Plumb, 2002; Young et al., 2011). These stationary or quasi-stationary waves are the result of the combined effects of large-scale orography (e.g. Himalaya, Rocky Mountains, Andes), equator-to-pole temperature gradient and the Coriolis force – i.e. inertial force in response to the rotation of the Earth. They propagate from the troposphere upwards, and can dissipate throughout the stratosphere up to the lower mesosphere (<100 km), depositing momentum or wave drag. Drag from dissipating waves always deposits easterly momentum – decelerating stratospheric westerly winds –, and as a consequence a small poleward flow balances the angular momentum, which ultimately drives the residual mean circulation (Andrews et al., 1987).

The BDC is usually split in a shallow branch, controlling the lower stratosphere region all year around, and a deep branch controlling the middle and upper stratosphere during the winter hemisphere (Birner and Bonish, 2011). In addition, the stirring of air – two-way mixing – by planetary-scale Rossby waves during the winter hemisphere at mid-latitudes (between the polar and subtropical barriers, "surf zone") results in a rapid isentropic (adiabatic) transport compared to the residual mean circulation. Two-way isentropic mixing of air also occurs all year around in the subtropical lower stratosphere (i.e. also important for STE). Therefore, the transport of air in the stratosphere can be described by the relatively slow residual mean circulation (i.e. controlling the vertical motion) and rapid isentropic two-way horizontal mixing (Plumb, 2007).

Another important driver of interannual variability is the quasi-biennial oscillation (QBO), which controls the variability of the tropical stratospheric zonal winds between ~ 16 to 50 km (~ 1–100 hPa). The QBO can be thought to consist in downward propagating easterly and westerly winds, with a mean period of ~ 28 months (22–34 month range) (Baldwin et al., 2001). Interestingly, large-scale equatorial waves driving this phenomenon show periodicities that are unrelated to the mean oscillation of the QBO (Baldwin et al., 2001). Easterlies are usually stronger (~ 35 m s^{-1}) than the westerlies counterpart (~ 20 m s^{-1}), with a maximum peaking around 20 hPa (Baldwin and Gray, 2005). Although constrained to the tropics, the QBO affects the extra-tropical circulation and temperature gradient in the stratosphere by modulating waves propagation (Baldwin et al., 2001).

Figure 2.2 presents dynamics in the stratosphere modulating the distribution of chemical constituents such as ozone. In the middle and upper stratosphere (>30 km), the impact of transport processes is limited, where ozone is in photochemical equilibrium (WMO, 2014). However, the transition region between the upper stratosphere (chemically controlled) and the lowermost stratosphere (dynamically controlled) is important for transport of ozone (e.g. Solomon et al., 1985). Due to the mean stratospheric mass transport (see above), ozone is transported from lower to higher latitudes and accumulated at seasonal time scale in the lower stratosphere (e.g. Fortuin and Kelder, 1998). Thus, total column ozone is greater at mid- and high latitudes compared to the tropics.

Although long-term changes in the BDC, for example, due to climate change are surrounded by large uncertainties (e.g. Engel et al., 2009; Hardiman et al., 2014), these can have important consequences for ozone distribution and abundances in the stratosphere and the troposphere.

2.1.4. Past changes and variability in stratospheric ozone

To explore past changes and trends in stratospheric ozone there are available a number of observational data and re-analysis data sets (WMO, 2014; Fujiwara et al., 2017), which are described above in more detail.

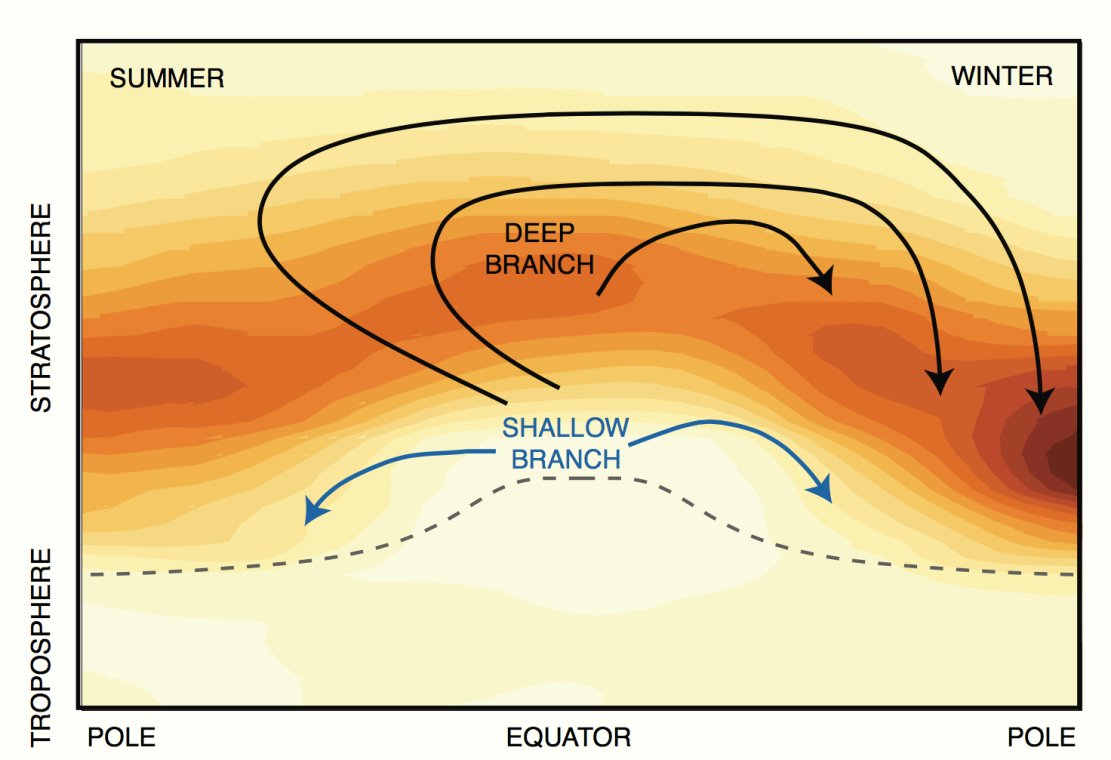

Figure 2.2. Illustration of the Brewer-Dobson circulation along with the climatological stratospheric ozone distribution at solstices (from WMO, 2014).

Global ozone changes

Near-global stratospheric ozone is usually referred to the extra-polar regions (60ºN–60ºS) (e.g. WMO, 2014), and this section uses the term to global stratospheric ozone for simplicity. Because largest changes observed in global ozone since 1979 (satellite era) occur in mid-latitudes (35º–60º N/S) compared to the almost unchanged tropical region (20ºN–20ºS) (e.g. WMO, 2014), the following discussion gives special consideration to the first. Changes in mid-latitude ozone are the result of a complex interaction between various factors, particularly due to changes in dynamics from the tropical source region (e.g. transport of relatively ozone-rich air), changes in the isentropic horizontal mixing of air with polar regions (e.g. potentially ozone-depleted mass air along with higher levels of activated halogens), and in-situ changes in catalysed ozone loss.

According with the last WMO 2014 report (2014) and based on various observational data sets, present-day (2008–2013) annual mean global total column ozone is ~ 2 % lower than 1960–1980 levels, but ~ 0.5 % higher since the previous

WMO 2010 report (2011). Observed global total column ozone shows a positive trend of 1 ± 1.7 % between 2000 and 2013, though not significant at the 95 % confidence interval (i.e. substantial disagreement on the significance of the trend is found between the data sets) (WMO, 2014). On the vertical profile of ozone, largest changes are typically observed in the upper stratosphere (chemically controlled) and a secondary peak in the lower stratosphere (both chemical and dynamical processes can affect ozone changes). Since 2000, ozone concentrations show significant increases in the upper stratosphere (~ 3 % dec^{-1} and 2 % dec^{-1} in the mid-latitudes and the tropics respectively), and positive but not significant trend in the lower stratosphere (i.e. region that dominates total column ozone due to larger ozone densities).

A number of natural factors affect global stratospheric ozone variability and have to be taken into account to understand long-term changes, which are largely dominated by anthropogenic emissions of ODSs (WMO, 2014). Natural variability operates at different time scales. Internally generated variability, for example, can affect global ozone at intra-annual (i.e. the annual cycle is largely associated with seasonal variability of the BDC) and inter-annual (e.g. the QBO and El Niño/Southern Oscillation, ENSO) time scales (WMO, 2007; Hood and Zaff, 1995). Externally forced natural variability can also significantly affect global ozone. The 11-year solar cycle has been shown to modulate total column ozone globally by about 3 % between solar maximum and solar minimum (e.g. WMO, 2007, 2011), with a maximum peak of ~ 4 % in the upper stratosphere and a secondary peak in the lower stratosphere of ~ 2 % (Soukharev and Hood, 2006; Randel and Wu, 2006). Global ozone variability associated with the 11-year solar cycle is likely due to changes in the BDC (Hood and Soukharev, 2012), though the mechanism is not fully understood (Gray et al., 2010). Volcanic eruptions can significantly enhance stratospheric sulfate aerosols, which impact global ozone levels directly via heterogeneous loss chemistry and indirectly due to changes in temperature and transport (e.g. Solomon et al., 1996; WMO, 1999). Recent major volcanic eruptions, El Chichón in 1982 and Mt. Pinatubo in 1991, resulted in approximately two orders of magnitude in stratospheric aerosol optical depth and a global reduction in total column ozone of ~ 2 % (maximum of 5 %) in the next few years (WMO, 1999).

In addition, chemical and radiative feedbacks (e.g. effect of temperature in ozone chemistry) and associated non-linearities (e.g. Eyring et al., 2010b, 2013a; Banerjee et al., 2016), further complicates the attribution and detection of ozone

recovery from ODS-induced chemistry (WMO, 2014). Although the first signs of global ozone recovery have already emerged, a clear separation of chemically-induced ozone recovery (i.e. due to ODSs) from the large natural variability is still difficult (WMO, 2014; Chipperfield et al., 2017).

Polar ozone changes

Dynamical features during winter in polar regions have played a key role in recent observed stratospheric ozone changes, particularly in the NH (WMO, 2014). The stratospheric polar vortex is a relatively isolated area of low pressure and cold air over the Earth's poles during the winter hemisphere (caused by the lack of solar heating) (e.g. Farman, 1977). This cold air results in a sharp temperature gradient between high and middle latitudes, edged by polar night jet (e.g. strong east-west zonal air) (e.g. Solomon, 1999). In the SH, the polar vortex is relatively strong and well-isolated – centered over the pole surrounding Antarctica – with minimum temperatures as cold as ~ 185 K. On the other hand, the Arctic vortex is more disturbed due to large-scale land-ocean masses lead to more active tropospheric meteorology and planetary-Rossby waves. This results in a relatively warmer, more variable (weaker), and less persistent Arctic vortex (e.g. IPCC, 2007; Solomon et al., 2014). The structural difference between the NH and the SH polar vortex determines the conditions at which heterogeneous ozone loss chemistry can occur, leading to significantly different ozone changes in recent decades as halogen loadings increased (e.g. Rienecker et al., 2011).

Over the Antarctic, total column ozone decreased by over 50 % in October between the 1960s and the mid-1990s (WMO, 2011). Historical minimum levels were observed around 1993–1995, and since then remained fairly constant. While minimum total column ozone in October are ~ 100 DU, ozone is virtually destroyed between 15–20 km (WMO, 2011). Observationally-based multivariate regression analyses and studies combining observations and model experiments have argued that the first fingerprints of the Antarctic ozone hole "healing" (i.e. chemically-driven due to reductions in ODS levels) are already seen (Salby et al., 2011, 2012; Kuttippurath et al., 2013; Shepherd et al., 2014; Solomon et al., 2016).

Over the Arctic, significantly less ozone loss is observed compared to its Antarctic counterpart. The presence of PSCs is more limited in abundance and time because of higher temperatures, meaning that denitrification rarely occurs, and

sunlight exposure of halogenated active air is reduced (vortex displacements and asymmetry) (WMO, 2014). The large variability in the Arctic vortex results in boreal springs with negligible ozone losses, and springs with relatively large ozone losses of ~ 30 % in total column ozone and up to ~ 70 % in ozone volume mixing ratios in specific regions (WMO, 2011, 2014).

2.2. The troposphere and the climate system

To understand the dynamical, chemical and radiative coupling between the stratosphere and the troposphere, a description of the important features governing the observed changes in tropospheric climate and composition is needed. Ozone in the troposphere is a short-lived trace gas that plays an important role in the Earth's radiative balance and atmospheric composition. This section presents a general overview of changes in the climate system during the 'Industrial Era' and their likely causes; then, the radiative forcing concept as a measure of energy perturbation of the Earth system is addressed; finally, this section also presents a short review on the tropospheric ozone budget.

2.2.1. Past changes in the climate system

Instrumental observations of the climate system, as discussed above, are based on ground-based stations (e.g. using direct physical and biogeochemical techniques) and satellites (e.g. using remote sensing techniques), and extend back to ~ 1850s (Hartmann et al., 2013). Paleoclimate reconstructions, such as tree rings and ice cores, provide useful information of past climates back hundreds to million of years (e.g. Hansen et al., 2008; Mann, 2011), allowing to assess more recent changes in the context of natural climate variability. Numerical models that represent the climate system (e.g. climate models typically include physical laws and different degree of chemistry and biology representation) are important means to, for example, understand causality of past changes – detection and attribution experiments – and explore future changes under given conditions (e.g. future climate emission scenarios). This section relies on observed and modelled temperature changes and radiative budgets – based on atmospheric composition changes – to provide an overall picture and understanding of the climate system and its recent changes over the Industrial Era (i.e. instrumental record observations). A comprehensive review of past

changes in the climate system – including multiple lines of evidence such as changes in precipitation, winds, sea level, cryosphere – and current understanding is provided in the latest Assessment Report of the Intergovernmental Panel on Climate Change (IPCC, 2013).

The global mean surface temperature (GMST) during the instrumental record period (1880–2012), which combines land and ocean data using three independent data sets (Hansen et al., 2010; Morice et al., 2012; Vose et al., 2012), has increased 0.85 (0.65–1.06) ºC (IPCC, 2013). The assessment of temperature changes in the free troposphere and stratosphere can be made using radiosonde and satellite products, however, is more difficult (i.e. revisions and versions of the data sets along with their intrinsic data uncertainties). Despite larger uncertainty on the trends between radiosonde and satellite data sets (Christy et al., 2003; Free et al., 2005; Mears and Wentz, 2009; Zou and Wang, 2011; Haimberger et al., 2012), the global troposphere has warmed and the stratosphere has cooled during the 2nd half of the 20th century (IPCC, 2013).

The Earth's energy budget is briefly introduced here to understand the possible causes of the relatively rapid and sustain warming of the troposphere in the last decades (e.g. Trenberth et al., 2009). The climate system of the Earth is fueled by an average incoming solar radiation (i.e. shortwave radiation, SWR) of 1361 Wm^{-2} (Kopp and Lean, 2011). The Earth's surface, clouds, gases and aerosols absorb about 70 % of the SWR, and the remaining 30 % is reflected back to space (albedo). As the surface of the Earth warms, it emits outgoing energy mostly in the infrared spectrum (i.e. longwave radiation, LWR). A large fraction of the LWR is absorbed by a number of gases in the atmosphere – H_2O, CO_2, CH_4, N_2O, O_3 and other greenhouse gases (GHGs) – and clouds, which ultimately results in an 'extra' warming of the lower layers of the atmosphere, the so-called greenhouse effect. Therefore, observationally derived small and positive imbalance in the Earth's radiative budget (Murphy et al., 2009; Trenberth et al., 2009; Hansen et al., 2011), may result from changes in the incoming solar radiation or changes in the outgoing radiation (SWR and LWR).

Solar radiation is the only external natural forcing that shows small increase over the pre-industrial period, but also a small decrease during the satellite era (1986–2008) when largest GMST increases are observed (Klopp and Lean, 2011). Hence, solar forcing is not consistent with the magnitude of the warming in the troposphere and the cooling in the stratosphere. Overall, the contribution of internal climate

variability to the GMST over the 1951–2010 period has been assessed to be small (−0.1 ºC to 0.1 ºC) (Bindoff et al., 2013). Moreover, climate model simulations driven only by natural forcing and internal climate variability show that simulated GMST anomalies since ~ 1950s are largely inconsistent with those observed (e.g. Jones et al., 2013; Knutson et al., 2013).

Changes in the atmospheric composition – e.g. CO_2, CH_4, N_2O – since the pre-industrial period (1750), associated with the rapid development of human activities, is consistent with the observed small positive imbalance in the Earth's radiative budget (Murphy et al., 2009; Trenberth et al., 2009; Hansen et al., 2011). Simulated GMST anomalies by climate model simulations, which included both anthropogenic (e.g. increasing concentration of GHGs) and natural forcing, are consistent with observationally derived GMST (e.g. Gillett et al., 2012, 2013; Knutson et al., 2013). The observed GMST increase over the 1951–2010 period has been largely attributed – over 50 % of the change – to increases in GHGs concentrations (Bindoff et al., 2013), and is consistent with the former IPCC Forth Assessment Report (IPCC, 2007; Hegerl et al., 2007).

2.2.2. Radiative forcing

Radiative forcing is a valuable metric to understand and measure the contribution of individual agents or drivers to climate change (i.e. typically assessing the influence on the GMST). This section introduces the main concepts that form the backdrop to ozone radiative forcing addressed in subsequent chapters. Broadly speaking, radiative forcing (RF) is the net imbalance or change in the Earth's radiative budget due to an imposed perturbation (e.g. change in atmospheric concentration of a radiatively active gas). However, there are different 'flavours' on the precise definition, with their advantages and limitations. RF is defined here as the net change in downward radiation flux (between incoming SWR and outgoing LWR) at the tropopause, after stratospheric temperatures adjust to radiative equilibrium, while other variables are held fixed to the unperturbed state (e.g. tropospheric temperature, clouds and water vapour) (Myhre et al., 2013). The RF discussed in this section refers to the 1750–2011 period, unless otherwise specified. While the RF concept is a very useful metric for climate forcers such as well-mixed GHGs (WMGHGs) and ozone to characterise the climate response, other climate forcers such as anthropogenic aerosols can

significantly influence other tropospheric state variables (e.g. clouds and snow-ice cover). Effective radiative forcing (ERF) is used to measure the net change in radiative flux at the top of the atmosphere, after allowing rapid adjustments on atmospheric variables (troposphere and stratosphere), while holding GMST fixed at unperturbed values (Myhre et al., 2013). RF and ERF for CO_2, tropospheric ozone and solar irradiance perturbations show negligible differences, and fairly similar values for CH_4, N_2O and stratospheric ozone perturbations (Hansen et al., 2005; Shindell et al., 2013b), although a better characterisation of the climate response due to, for example, black carbon is provided by the ERF (Bond et al., 2013).

Solar radiation and volcanic eruptions are the main natural external forcing to the climate system, although the latter can only contribute to a net decrease in the Earth's radiative balance. The overall contribution of the solar forcing over the Industrial Era has been estimated to be small but positive (0.08–0.18 W m^{-2}), and yet a better constrained estimate (via satellite measurements) between two minimums in 1986 and 2008 has shown a small negative forcing (−0.04–0.00 Wm^{-2}) (Klopp and Lean, 2011). RF that results from volcanic eruptions is well characterised (Myhre et al., 2013), being largely the result of sulfate aerosol precursors injected into the atmosphere (i.e. emissions of mineral dust and CO_2 are considered to have a negligible effect on climate). After Mt. Pinatubo eruption (1991), causing a large negative forcing of ~ 3.0 W m^{-2} the year following the eruption (Forster et al., 2007), several minor volcanic eruptions over the 2008–2011 period (Nagai et al., 2010; Vernier et al., 2011; Neely et al., 2013) have resulted in approximately −0.11 (−0.15 to −0.08) W m^{-2} (Myhre et al., 2013).

Figure 2.3 shows RF of important GHGs contributing to climate change. Human activities have led to profound atmospheric composition changes. Direct emissions of WMGHGs (CO_2, CH_4, N_2O and halocarbons) have increased their concentration over the Industrial Era. WMGHGs concentrations, using direct measurements and ice-core, and their radiative properties are well constrained (Hartmann et al., 2013). The estimated total RF due to WMGHGs is 2.83 (2.54–3.12) Wm^{-2} (Myhre et al., 2013). CO_2, CH_4 and N_2O are responsible for approximately 65 %, 17 % and 6 % respectively of the total WMGHGs forcing, whereas halocarbons account for the remaining ~ 22 % (Myhre et al., 2013). Ozone concentrations have also changed substantially – in the troposphere and the

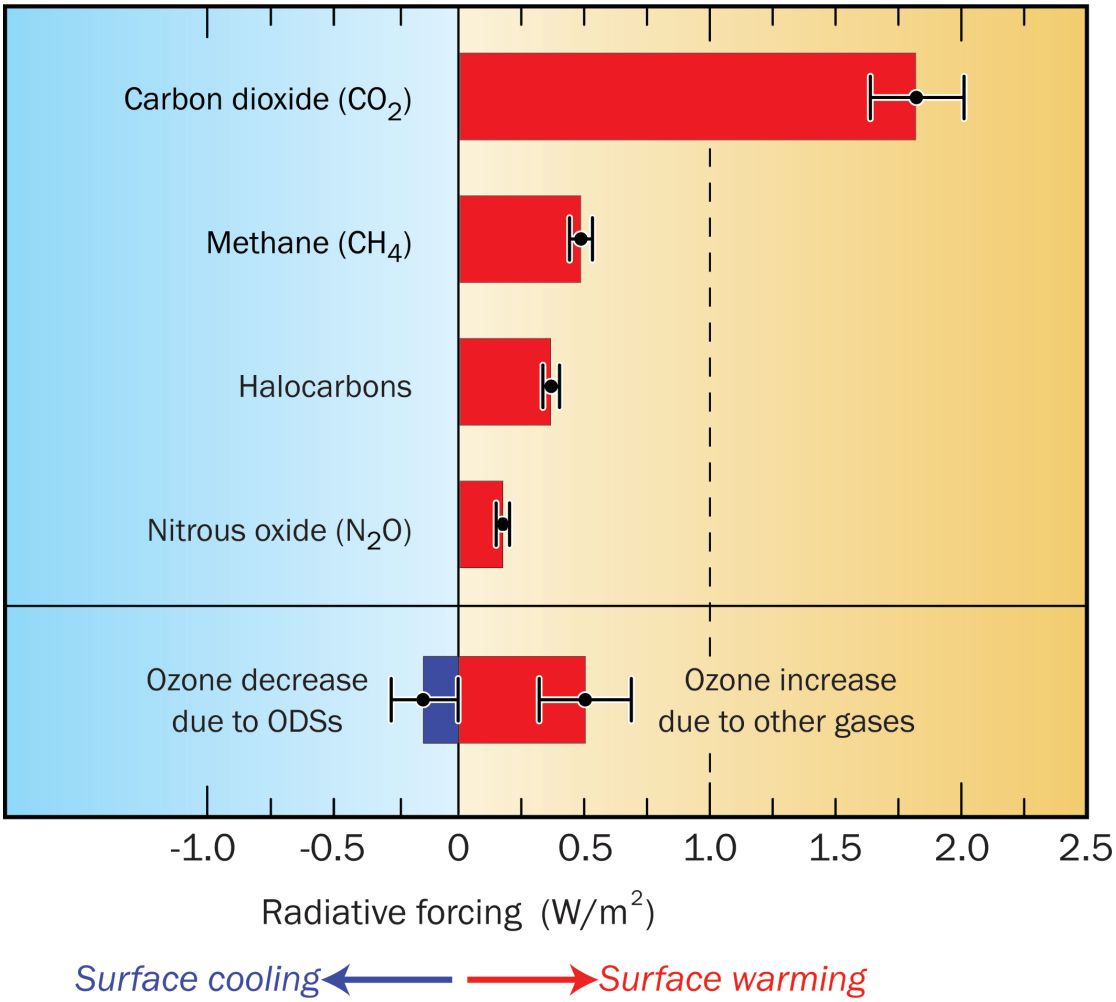

Figure 2.3. Radiative forcing of major greenhouse gases contributing to climate change over 1750–2011 (from WMO, 2014).

stratosphere – as a consequence of human activity (i.e. indirectly via atmospheric chemistry), which is largely associated to ozone precursor and ODS emissions (e.g. Young et al., 2013a; Iglesias-Suarez et al., 2016; Chapter 3 of this thesis). The total RF associated with ozone is 0.35 (0.15–0.55) W m^{-2}, which results from the interplay between tropospheric – 0.40 (0.20–0.60) W m^{-2} – and the stratospheric – −0.05 (−0.15–0.05) W m^{-2} – forcing (Myhre et al., 2013). The stratospheric water vapour RF, resulting from CH_4 oxidation, is 0.07 (0.02–0.12) W m^{-2} (Myhre et al., 2013). Other human activities have somewhat offset the above RF. For example, changes in aerosols concentrations have led to an uncertain but negative ERF of −0.9 (−0.25 to −0.05) W m^{-2}, and a RF of −0.15 (−0.25 to −0.05) W m^{-2} due to changes in land use (e.g. deforestation) (Myhre et al., 2013).

2.2.3.Tropospheric ozone

In the troposphere, ozone is a trace gas with important consequences for the Earth's energy balance, the oxidising capacity of the atmosphere and air pollution. This section discusses main processes – sources and sinks – determining tropospheric ozone abundances and historical changes.

Tropospheric ozone chemistry has received much attention since the 2nd half of the 20th century and its production, loss and distribution are relatively well understood (e.g. Crutzen, 1974, 1979; Sillman, 1999; Atkinson, 2000; Fishman, 2003; Monks et al., 2015). The tropospheric ozone budget is typically characterised by in-situ ozone chemistry (photochemical production and destruction) (e.g. Haagen-Smit, 1952; Crutzen, 1974, 1979; Jenkin and Clemitshaws, 2000), influx from the stratosphere (stratosphere-troposphere exchange) (Danielsen and Mohnen, 1977; Logan, 1985; Holton et al., 1995) and removal via dry deposition (Wesley and Hicks, 2000; Hardacre et al., 2015). Despite climate models show a reasonable good representation of global tropospheric ozone features, significant uncertainties remain in the characterisation of the tropospheric ozone budget (Stevenson et al., 2006; Wild, 2007; Young et al., 2013a).

Our understanding of the tropospheric ozone budget largely relies on chemistry models. At the global and annual scale, present-day (year 2000) net chemical ozone production is about 618 ± 275 Tg yr^{-1}, as reported in the last IPCC Assessment Report (Myhre et al., 2013; Young et al., 2013a), which is constrained by a relatively large uncertainty in the magnitude of the ozone production and loss terms (Wild, 2007). Photochemical ozone production maximises in the tropical lower troposphere (i.e. oxidation of hydrocarbons by greatest abundances of OH from the $O(^1D) + H_2O$ reaction), over continental regions, and in the upper troposphere (i.e. relatively high concentrations of NO_x from lightning) (e.g. Bloss et al., 2005; Wild and Palmer, 2008; Banerjee et al., 2014). On the other hand, chemical ozone loss is greatest in the lower troposphere and in highly polluted continental regions (i.e. elevated concentrations of NO results in ozone titration via an enhanced $NO + O_3$ flux) (von Kuhlmann et al., 2003; Wild and Palmer, 2008). Together net chemical production of ozone largely dominates the continental boundary layer (i.e. high concentration of ozone precursors) and the upper troposphere (i.e. low temperatures slow ozone loss), whereas net chemical loss dominates the marine boundary layer and the middle troposphere (i.e. high concentration of OH and low levels of ozone

precursors) (von Kuhlmann et al., 2003; Wild and Palmer, 2008). Present-day global and annual STE as derived from observations is approximately 550 ± 140 Tg yr^{-1} (McLinden et al., 2000; Olsen et al., 2001). Tropospheric ozone with stratospheric origin largely dominates the upper troposphere, particularly at mid- and high latitudes (Banerjee et al., 2016), where ozone shows greatest radiative efficiency (Riese et al., 2012; Rap et al., 2015). Finally, dry deposition of ozone to vegetation, oceans and other surfaces balances the tropospheric ozone budget, though is surrounded by large uncertainties (e.g. Hardacre et al., 2015). Simulated present-day global and annual dry deposition of ozone is about 1094 ± 264 Tg yr^{-1} (Myhre et al., 2013; Young et al., 2013a).

Tropospheric ozone levels have increased since the pre-industrial times due to enhanced ozone precursor emissions by human activities. Surface ozone measurements before 1950s are subject of large uncertainty (i.e. semi-quantitative techniques were used based on the Schonbein ozonoscope) (Bojkov, 1986; Marenco et al., 1994). Observations indicate that surface ozone concentrations may have increased by approximately 3–5 times over the late 1800s–1900s period in Western Europe, and have approximately doubled over the 1950s–1990s period (Cooper et al., 2014; and references therein). Modelling studies show that tropospheric ozone burden has increased ~ 30 % over the Industrial Era (1850s–2000s) (Lamarque et al., 2005; Young et al., 2013a), with largest changes occurring in the extra-tropical NH (i.e. largest ozone precursor emissions). However, current global chemistry models fail to represent observed surface ozone low concentrations at Montsouris (France) during the pre-industrial period (Hauglustaine and Brasseur, 2001; Parrella et al., 2012; Young et al., 2013a). Despite the large increase in ozone precursor emissions and the concomitant tropospheric ozone increase since the 19th century, the distribution of chemical ozone regimes (i.e. net chemical production-loss; see above) remained fairly unchanged (Wild and Palmer, 2008).

2.3. Interactions between the stratosphere and the troposphere

The stratosphere and the troposphere are two relatively distinct regions of the atmosphere (e.g. chemistry and dynamics determine their composition and climate), though they are closely linked by radiative, dynamical and chemical processes. First, this section presents the impacts of polar stratospheric ozone depletion on the

troposphere, discussing current understanding and gaps in our knowledge; and then, the effects of climate change – changes in temperature and transport – on stratospheric ozone are addressed with a focus on chemistry-climate feedbacks and non-linear processes.

2.3.1. Impact of polar stratospheric ozone loss on the troposphere

The effects of polar stratospheric ozone depletion on the troposphere and surface climate have received much attention in the last 15 years or so (e.g. WMO, 2007; Forster et al., 2011). The fingerprint of the Antarctic ozone hole on SH troposphere surface and climate is relatively well characterised, and will be revisited in this section (i.e. changes in tropospheric circulation). However, Arctic ozone loss during boreal spring is substantially less pronounced compared to the SH, and its signature on the NH tropospheric climate is much weaker (Morgenstern et al., 2010a) and difficult to assess (Gillett et al., 2013). Thus this section will not further address the linkages between polar stratospheric ozone loss and tropospheric response in the NH. Recent reviews provide a detailed description of tropospheric responses to polar stratospheric ozone loss in both hemispheres (Forster et al., 2011; Thompson et al., 2011; Canziani et al., 2014; Previdi and Polvani, 2014; and references therein).

The Antarctic ozone hole and tropospheric circulation response

As discussed above, the absorption of incoming solar shortwave radiation (i.e. ultraviolet spectrum) largely determines stratospheric climate and its thermal structure. A large and significant cooling in the SH polar lower stratosphere of ~ 8 K over the 1960–2000 period is observed during austral spring, and associated with the ozone hole (e.g. Randel et al., 2009b). The seasonality of this cooling – weaker during austral summer and not significant in autumn and winter – also suggest that increased concentrations of greenhouse gases (GHGs) have had a relatively small impact on polar lower stratospheric temperatures in the recent past. Current chemistry-climate models represent fairly well stratospheric cooling in response to the ozone hole (e.g. Young et al., 2013b; Iglesias-Suarez et al., 2016).

As a consequence of the cooling in the lower stratosphere over Antarctica in austral spring, the meridional temperature gradient between middle and high latitudes increases – thermal wind balance – and results in a strengthening of the polar nigh jet or polar vortex (e.g. Solomon, 1999). Observations show that the SH polar vortex has strengthened and become more persistent – breakdown occurs ~ 2 weeks later – between 1980s and 2000s (e.g. Waugh et al., 1999; Thompson and Solomon, 2002). The downward propagation of stratospheric circulation changes reaches the troposphere in ~ 1–2 month time (Baldwin and Dunkerton 1999, 2001; Thompson et al., 2005). Therefore, tropospheric circulation changes associated with the Antarctic ozone hole maximises during austral summer (Thompson and Solomon, 2002; Gillett and Thompson, 2003). The SH "midlatitude jet", defined here as the band of strongest westerly winds situated at midlatitudes (~ 50ºS), shifts poleward (i.e. zonal mean zonal winds strengthens at higher latitudes and weakens at lower latitudes relative to the climatological mean) (e.g. Previdi and Polvani, 2014). In turn, this results in a poleward shift of the storm track (Simmonds and Keay, 2000; Wang et al., 2013) and other changes in surface climate, such as temperature (e.g. Thompson and Solomon, 2002).

The Southern Annular Mode (SAM) is the leading mode of variability of the SH extra-tropical circulation (Thompson and Wallace, 2000). Both observational (Thompson and Solomon 2002; Marshal 2003, 2007) and modelling studies (Gillett and Thompson, 2003; Son et al., 2008, 2009, 2010; Polvani et al., 2010; Gillett and Fyfe, 2013; Keeble et al., 2014; Iglesias-Suarez et al., 2016) show a positive (poleward) and significant shift in the SAM during austral summer in the 2nd half of the 20th century. Evidence suggests that SH extra-tropical circulation changes in the last decades are linked to stratospheric ozone depletion, such as the seasonal feature of the observed and simulated changes. In addition, detection and attribution studies using models of different complexity and/or observations show that the positive trend of the SAM in summertime is primarily the response to the ozone hole (McLandress et al., 2011; Polvani et al., 2011; Gillett and Fyfe, 2013). Only one modelling study attributes comparable contributions to increases in GHGs concentrations and stratospheric ozone depletion (Fyfe et al., 2012). The prescribed ozone depletion used in their simulations may be weaker than observed (Fyfe et al., 2012), and therefore would skew the climate response in the troposphere (Young et al., 2014).

The expected stratospheric ozone recovery during the 21st century, as ODS abundances decrease in the atmosphere, will result in the opposite climate response to the impacts of ozone depletion. Thus ozone recovery will tend to drive the extra-tropical circulation equatorward (i.e. negative shift of the SAM), opposing the effects of increasing concentrations of GHGs. During austral summer, climate models project that the effects of the ozone hole recovery and increasing GHGs on the SAM will largely cancel each other in the first half of the 21st century, resulting in small extra–tropical tropospheric circulation changes (e.g. McLandress et al., 2011; Polvani et al., 2011; Gillett and Fyfe, 2013; Iglesias-Suarez et al., 2016). By mid-century, projected total column ozone over the SH polar cap in austral spring will be similar to 1980 levels (Eyring et al., 2010a), thus changes in the extra-tropical tropospheric circulation will be largely governed by GHGs. Under a low-intense future emission scenario (GHGs decrease) the SAM will tend to return to "normal" levels (pre-ozone hole), whereas further poleward shift of the SAM is projected under a high-intense future emission scenario (GHGs increase) (McLandress et al., 2011; Gillett and Fyfe, 2013; Iglesias-Suarez et al., 2016).

2.3.2. Climate change and stratosphere-troposphere interactions

Changes in climate can affect the stratosphere and the ozone layer due to changes in temperature, atmospheric composition and transport. This section reviews climate impacts on stratospheric radiation, chemistry and dynamics, as well as, the coupling between the stratosphere and the troposphere. Although many processes and mechanisms governing stratospheric responses to changes in climate are not fully understood, a comprehensive discussion of current understanding can be found in recent assessments and reviews (e.g. WMO, 2007, 2014; Dameris and Baldwin, 2011; Forster et al., 2011).

Effects on stratospheric radiation and chemistry

While increasing concentrations of GHGs (e.g. CO_2, CH_4 and N_2O) since pre-industrial times associated with human activities have warmed the troposphere, they have cooled the stratosphere along with ozone depletion in recent decades (e.g. Pyle et al., 2005; Dameris and Baldwin, 2011; Myhre et al., 2013). Enhanced concentrations of GHGs in the stratosphere results in a net stratospheric cooling, as they emit more

outgoing infrared radiation compared to that absorbed. As emission of infrared radiation by GHGs increases with temperature, stratospheric cooling peaks in the upper stratosphere around 50 km (i.e. highest temperatures).

Stratospheric cooling, in turn, slows gas-phase ozone loss rates, primarily via the Chapman reactions in the upper stratosphere, NO_x-catalysed cycle in the middle stratosphere and HO_x-catalysed ozone loss in the lower stratosphere (Barnet et al., 1975; Zeng and Pyle, 2003). Although heterogeneous-driven ozone loss is relatively insensitive to changes in temperature in the extra-polar lower stratosphere (i.e. hydrolysis of N_2O_5 and bromine nitrate) (e.g. McElroy et al., 1992; Pyle et al., 2005), its efficiency increases substantially in the polar lower stratosphere, due to higher and more persistent abundances of PSCs and greater denitrification.

Satellites provide global coverage measurements of the stratosphere with a coarse vertical resolution since ~ 1979. Microwave sounding Unit (MSU) instrument provides measurements of the lower stratosphere (channel 4: near–20 km), whereas Stratospheric Sounding Unit (SSU) provides measurements of the middle (channel 1: 25–35 km) and upper (channel 2: 40–50 km) stratosphere (Hartmann et al., 2013). The Advance Microwave Sounding Unit (AMSU; in production since 1998) has replaced MSU and SSU instruments. Overall, observations show a cooling trend in the stratosphere, which increases (more negative) with height (in agreement with physical understanding). The global lower stratospheric temperature has cooled approximately 1 K over the 1979–2012 period (MSU channel 4) (Hartmann et al., 2013). While current climate models typically underestimate global lower stratospheric cooling (e.g. Thompson et al., 2012; Charlton-Perez et al., 2013; Santer et al., 2013), recent modelling studies suggest that ozone depletion (due to ODSs) is the dominant driver (Eyring et al., 2006; Ramaswamy et al., 2006; Dall'Amico et al., 2010; Gillett et al., 2011; Lott et al., 2013). Although two independent data sets show a significant disagreement of the cooling trend in the middle stratosphere, as large as 0.5 K dec^{-1} (SSU channels 1–2), they show good agreement in the upper stratosphere (SSU channel 3) between 1979 and 2005 (Thompson et al., 2012). Climate models show cooling trends in the middle stratosphere that lie within observational uncertainties (i.e. large disagreement), but underestimate the cooling observed in the upper stratosphere (Forster et al., 2011; Thompson et al., 2012; Santer et al., 2013).

Using observations (SSU) and model simulations, the separate influence of GHGs and ozone depletion on mid- and upper stratospheric temperatures was not detectable (Gillett et al., 2011). Interestingly, since ~ year 2000 lower stratospheric temperatures stopped cooling, which may be associated with the interplay between increasing GHGs abundances (direct radiative cooling) and decreasing ODS concentrations (indirect warming due to ozone recovery) (Ferraro et al., 2015). Changes in stratospheric temperatures will play an important role driving stratospheric ozone during the 21st century. In the future, the effects of ozone recovery and increasing GHGs on stratospheric temperatures will tend to counteract each other (warming and cooling respectively), and their relative importance will be emission scenario and model dependent.

Effects on stratospheric dynamics

The stratospheric circulation is characterised by the Brewer-Dobson circulation (BDC), which largely determines stratospheric ozone distribution and stratosphere-troposphere exchange (STE). A robust feature of model simulations is the acceleration of the BDC (shallow and deep branches) in response to climate change through changes in wave activity (dissipation of different types of atmospheric waves), in spite of the exact mechanism is not fully understood (e.g. Butchart, 2014; and references therein). An enhanced BDC would have notable consequences during the 21st century. For example, it would affect stratospheric ozone distribution (e.g. greater abundances in the extra-tropics and lesser abundances in the tropics along with the concomitant changes in temperatures), increase STE (e.g. affecting tropospheric ozone abundances and distribution), and reduce the mean age of air in the stratosphere (e.g. with important consequences for ODSs) (Austin et al., 2006; Garcia and Randel, 2008; Oman et al., 2009; Butchart et al., 2010).

However, observations provide a conflicting picture with regard to the expected acceleration of the BDC due to climate change in the recent past (since ~ 1979). Observational estimates of the BDC are derived indirectly – e.g. using changes in other chemical species, age of air, and temperatures – and are surrounded by large uncertainties (Engel et al., 2009; Thompson and Solomon, 2009; Fu et al., 2010; Free, 2010; Young et al., 2011; Stiller et al., 2012; Kawatani and Hamilton, 2013). Moreover, changes in the BDC are small and it is proven difficult to assess a long-term trend from the relatively large natural variability (e.g. Forster et al., 2011;

Arblaster et al., 2014). Briefly, observational estimates and model simulations show a strengthening in the shallow branch of the BDC (lower stratosphere) in the recent past. However, recent changes in the deep branch of the BDC (mid- and upper stratosphere) are more difficult to interpret, as an acceleration is derived from temperature analyses while no significant changes or even a weakening is found in age of air analyses. The extent of future changes in the BDC – associated with climate change – adds to the overall uncertainty of model projections.

Stratosphere-troposphere interactions

A large literature – based on both observational and modelling studies – has shown strong relationships between the stratosphere and the troposphere and their modes of variability, such as annular modes (e.g. Baldwin et al., 1994; Perlwitz and Graf, 1995; Kodera et al., 1996; Baldwin and Thompson, 2009; Kiesewetter et al., 2010), the El Niño/Southern Oscillation (ENSO) (e.g. Marsh and Garcia, 2007; Garfinkel and Hartmann, 2008; Randel et al., 2009a; Calvo et al., 2010; Calvo and Marsh, 2011) and the quasi-biennial oscillation (QBO) (e.g. Holton and Tan, 1980; Baldwin et al., 2001; Naoe and Shibata, 2010; Watson and Gray, 2013; Anstey and Shepherd, 2014). These connections are important since they influence stratospheric ozone variability on intra-seasonal, seasonal, inter-annual and decadal time scales through transport and dynamics (e.g. SPARC, 2010; Forster et al., 2011; Arblaster et al., 2014). This section only describes some important features.

Leading modes of tropospheric circulation, such as the Northern Annular Mode (NAM) and the Southern Annular Mode (SAM), can directly and indirectly (via atmospheric wave activity – propagation and dissipation) influence ozone abundances in the troposphere and the stratosphere. This is particularly important for stratospheric ozone in the NH. For example, the NAM is strongly anti-correlated with total ozone at high latitudes (approximately >50ºN) (e.g. Lamarque and Hess, 2004; Kiesewetter et al., 2010). Extreme positive phase of the NAM (strong and cold polar vortex) is associated with negative total column ozone anomalies due to reduced transport in the stratosphere (i.e. the opposite is true for extreme negative phase of the NAM).

ENSO is a Pacific Ocean's tropical atmosphere-ocean phenomenon and a leading source of inter-annual variability in the troposphere (e.g. Trenberth et al., 2002). A number of studies have explored its influence on the stratosphere. For example, enhanced planetary wave activity and a strengthened BDC (shallow branch)

is associated with strong warm phases of ENSO (El Niño), which results in higher total ozone in the extra-tropics and lower total ozone in the tropics (e.g. Garfinkel and Hartmann, 2008; Randel et al., 2009a).

Also the QBO can affect the activity of atmospheric waves, therefore modulating the strength of the polar vortex (e.g. Baldwin et al., 2001). In the case of an easterly-phase of the QBO, the polar vortex tends to be more disturbed due to higher planetary wave activity (relatively weaker and warmer), which results in higher total column ozone anomalies at high latitudes (e.g. Anstey and Shepherd, 2014). On the other hand, relative strong ozone depletion can occur during westerly-phases of the QBO, especially when it is coincident with an ENSO cold phase (La Niña), such as the prevailing conditions during the boreal winter in 2011 that resulted in Arctic ozone losses comparable to that in the Antarctic ozone hole (Hurwitz et al., 2011; Manney et al., 2011).

2.4. Future changes in stratospheric ozone

Increasing concentrations of ozone depleting substances (ODSs) has been the major driver of stratospheric ozone depletion in the second half of the 20th century. As a consequence of international efforts to limit and cease the production of ODSs, their abundance in the atmosphere is expected to decrease and stratospheric ozone to recover during the 21st century. However, climate change (due to increased greenhouse gas, GHG, concentrations) will also affect the ozone layer. Focused in the 21st century, this section discusses the dominant factors driving stratospheric ozone, and describes stratospheric ozone evolution as projected in model simulations.

2.4.1. Drivers of stratospheric ozone

The future evolution of the ozone layer is explored using chemistry-climate models that include stratospheric chemistry and dynamics forced by different drivers. Here, the changes in the dominant factors (i.e. ODSs, temperature, stratospheric circulation, N_2O and water vapour) that will shape the projected evolution of ozone are discussed.

Due to the successful implementation of the Montreal Protocol and its Amendments and Adjustments, the total combined anthropogenic ODSs abundance in the troposphere peaked in 1994 and has slowly decreased since then. The slow decrease in total abundance of ODSs is expected to continue, returning to 1980 levels

around 2030s and below 1970s levels by the end of the 21st century (WMO, 2014). The Effective Equivalent Stratospheric Chlorine (EESC) is a useful metric to quantify the impact of ODSs on stratospheric ozone. EESC quantifies the reactive chlorine (Cl_y) and bromine (Br_y) in the stratosphere, based on a combination of observed and simulated troposphere-stratosphere transit times and the ratio of inorganic halogen released from different ODSs by location and time (Daniel et al., 1999; Newman et al., 2007). Model simulations project an EESC returning date to 1980 levels around 2040 in middle latitudes (~ 3 year mean age of air), and around 2065 in polar regions (~ 5.5 year mean age of air) (Eyring et al., 2010a**)**. While there is only 2.5 years difference in the mean age of air between polar and mid-latitude regions, the difference in EESC returning dates is around 25 years. This is explained by the rapid increase in ODS abundances between 1980s and 1990s and the much slower decline afterwards (SPARC, 2010). Typically model simulations use a common future scenario for ODS boundary conditions (surface concentrations). Although projected future evolution of stratospheric Cl_y and Br_y are qualitatively similar, there are significant differences in their peak levels and returning dates to historical values. For example, chemistry-climate models project a Cl_y peak value in the range of 2.2–3.3 ppbv over the polar lower stratosphere, whereas a returning date to its 1980 level varies between 2040–2080 (SPARC, 2010).

As discussed above, climate change can affect gas-phase and heterogeneous ozone loss chemistry (i.e. stratospheric temperatures) and distribution of ozone (i.e. transport). Stratospheric temperature changes will be largely the result of the interplay between ozone recovery (warming) and increasing GHGs (cooling), and the latter being the dominant driver during the second half of the century (Eyring et al., 2010b; SPARC, 2010). In addition, changes in the Brewer-Dobson circulation (BDC), which describes the general circulation in the stratosphere, can affect the distribution of ozone directly (i.e. via transport from lower to higher latitudes) and indirectly (i.e. via distribution of chemical species affecting ozone chemistry). A robust result in model simulations is the strengthening of the BDC associated with climate change (SPARC, 2010; Hardiman et al., 2014).

The future evolution of stratospheric ozone can also be influenced by other chemical constituents such as nitrogen oxide (N_2O) and methane (CH_4), which are sources of nitrogen oxides (NO_x) and hydrogen oxides (HO_x) species respectively. During the second half of the 21st century, when low anthropogenic ODS abundances

are expected, stratospheric ozone loss chemistry will be primarily controlled by NO_x- and HO_x-catalytic cycles. Furthermore, non-linear interactions between GHGs prevent a clear separation of their impact on ozone (Portmann et al., 2012; Banerjee et al., 2016). Simulated global mean total column ozone is reduced approximately 5 DU by mid-21st century compared to pre-industrial levels (Fleming et al., 2011; Portmann et al., 2012; Revell et al., 2012). This N_2O-induced ozone depletion is around a quarter of the ODSs-induced depletion in 2000 (Fleming et al., 2011). However, climate change-related feedbacks (i.e. stratospheric cooling and strengthening of the BDC) have been shown to reduce N_2O-induced ozone loss between 20–50 % (Plummer et al., 2010; Portmann et al., 2012). CH_4-related stratospheric ozone chemistry is complex, which includes direct (smog-like chemistry) and indirect (partitioning of active/inactive chlorine) processes. Nevertheless, future model simulations consistently show an increase in global ozone column, which is largely dependent on the emission scenario (Fleming et al., 2011; Portmann et al., 2012).

In addition, changes in stratospheric water vapour can affect ozone. Enhanced abundances of stratospheric water vapour would result in HO_x increases, which dominates ozone loss in the lower and upper stratosphere, and enhanced heterogeneous chemistry in the polar lower stratosphere. Increases in stratospheric water vapour may result from CH_4 oxidation and a warming of the tropical tropopause layer due to climate change (i.e. the tropical cold point controls dehydration of air masses entering the stratosphere) (Forster et al., 2011; Arblaster et al., 2014). Although most future model projections show a warming of the tropical cold point associated with climate change and a concomitant increase in stratospheric water vapour (Eyring et al., 2007), this increase is relatively small compared to the contribution from CH_4 oxidation (Oman et al., 2008). The overall impact of future increases in stratospheric water vapour on ozone has been assessed to be small (Forster et al., 2011; Arblaster et al., 2014).

2.4.2. Evolution of stratospheric ozone

Major factors controlling stratospheric ozone during the 21st century, previously discussed, will have distinct impacts between regions. This section describes the evolution of the ozone layer focusing on different regions (tropics, mid- and high latitudes) as projected by current climate models, and is illustrated in Fig. 2.4.

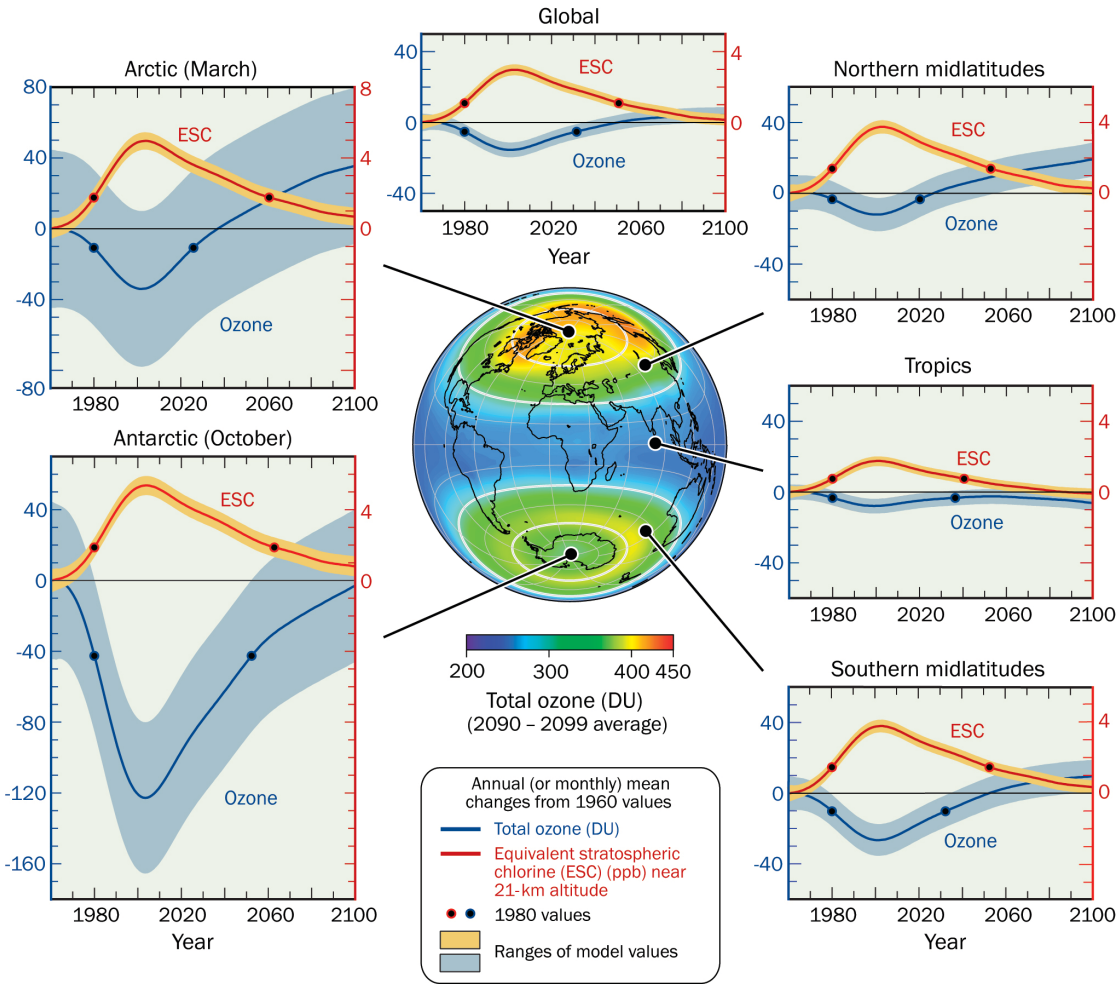

Figure 2.4. Total column ozone and Equivalent Stratospheric Chlorine (ESC) changes from 1960 to 2100, normalized to 1960 levels. Year 1980 levels are represented by dots. In addition, total column ozone climatology by the end of the 21st (2090–2099) century is shown (from WMO, 2014).

In the tropics (25ºN–25ºS), the evolution of ozone in the lower stratosphere (~ 15–30 km) and the upper stratosphere (~ 30–50 km; <15 hPa) is starkly different. Ozone is in photochemical equilibrium in the upper stratosphere. Decreasing anthropogenic ODS abundances (chlorine and bromine) reduces catalytic cycles that destroy ozone, and GHGs-induced cooling slows down ozone loss chemistry. Therefore, ozone in the upper stratosphere is projected to increase (Eyring et al., 2013a; Iglesias-Suarez et al., 2016), with comparable contributions from the above mechanisms (Waugh et al., 2009a; Oman et al., 2010; Eyring et al., 2010b). On the other hand, transport processes largely control ozone in the lower stratosphere. Climate models robustly project an acceleration of the BDC (tropical upwelling) due

to climate change (Hardiman et al., 2014), thus ozone is projected to decrease in the lower stratosphere (i.e. increase in tropospheric ozone-poor air) (Eyring et al., 2013a; Iglesias-Suarez et al., 2016). Because ozone density is largest in the lower stratosphere, tropical stratospheric column ozone is not expected to return to pre-industrial levels over the 21st century (Eyring et al., 2010a, 2013a; Iglesias-Suarez et al., 2016).

Unlike in the tropics, mid-latitude ozone is projected to increase throughout the stratosphere during the 21st century (Eyring et al., 2010a, 2013a; Iglesias-Suarez et al., 2016). While ozone increases in the upper stratosphere are due to the slow decline in anthropogenic ODSs and GHGs-induced cooling, in the lower stratosphere the strengthening of the BDC and transport of more rich-ozone air from lower to higher latitudes drive ozone increases (e.g. Shepherd, 2008; Li et al., 2009). Thus stratospheric column ozone by 2100 is projected to recover to 1980 values or above (up to ~ 20 DU or 6 %), which is dependent on the future emission scenario and associated climate-chemistry feedbacks (Eyring et al., 2013a; Pawson et al., 2014). Although mid-latitude stratospheric ozone evolution in the NH and SH are qualitatively similar, stratospheric column changes are larger in the NH by 2100 compared to pre-1960 due to differences in transport (i.e. greater in the NH) (Shepherd, 2008; Eyring et al., 2013a).

Due to largest ozone loss is observed in the polar lower stratosphere during springtime, largest stratospheric ozone changes are expected to occur in these regions by 2100. Over the Antarctic (65ºS–90ºS) in austral spring (ozone hole), stratospheric column ozone is projected to return to 1980 levels by mid-century, although there is a relatively large spread among models (Eyring et al., 2010a, 2013a). Because stratospheric ozone over Antarctica in springtime is largely insensitive to climate change (temperature and transport), its evolution closely follows the slow decline in ODS abundances (Cl_y and Br_y) (Austin et al., 2010; Eyring et al., 2007, 2010a). For example, models simulating a smaller Cl_y peak and ozone loss typically project an earlier returning date to 1980 levels. Moreover, chemistry-climate models based on EESC parameterisation and polar temperatures project somewhat a later recovery of the ozone hole (~ 2070) (Newman et al., 2006), though consistent with dynamic and transport biases in climate models (Eyring et al., 2007).

In contrast, over the Arctic (65ºN–90ºN) in boreal spring, climate change affects significantly the evolution of stratospheric ozone speeding up ozone recovery

due to anthropogenic ODSs. Thus models project an earlier returning date to 1980 levels (before mid-century and around 2030) compared to its Antarctic counterpart (Eyring et al., 2010a, 2013a). This is largely explained by a hemispheric asymmetry in meridional transport associated with the strengthening of the BDC (Austin et al., 2006, 2010; Hardiman et al., 2014). Ozone "super-recovery" – higher ozone levels compared to pre-industrial times – is consistently projected under high-intense emission scenarios by 2100, with a stratospheric column ozone difference of up to ~ 40 DU between scenarios (Eyring et al., 2013a).

2.5. Global numerical models

Numerical models that include interactive chemistry and dynamics in the troposphere and the stratosphere are important tools for our understanding of past, present and future changes of the ozone layer. They allow addressing research questions in a consistent framework. How has the ozone layer changed in the past (e.g. filling gaps in observations)? What processes can explain such changes (e.g. detection and attribution analysis)? How is stratospheric ozone expected to evolve in the coming century (e.g. projections)? This research relies on global numerical models to gain understanding on the roles of stratospheric ozone within the Earth system. Therefore, this section provides an overall introduction to chemistry-climate models (above-mentioned), and various types of simulations commonly performed. Also, I describe the general performance for present day (stratospheric) ozone, and discuss important limitations and biases in global models.

2.5.1. Chemistry-climate models

Chemistry-climate models (CCMs) are 3-D (altitude, latitude and longitude) global atmospheric models with coupled chemistry and radiation schemes, and usually constrained by prescribed sea surface temperatures (SSTs) and sea ice concentrations (SICs) following either a previous ocean model simulation or observations (see Morgenstern et al., 2010b for a recent review). Each time step, CCMs calculate chemistry reactions, radiation rates (heating and cooling) and dynamics (e.g. temperature and winds). In other words, chemistry reactions drive changes in radiatively active substances (gases and aerosols), which in turn affect dynamics (atmospheric energy balance) and feeds back on atmospheric chemistry.

Stratospheric chemistry scheme in CCMs has been developed and implemented in the last few decades (e.g. Pyle, 1980; Garcia and Solomon, 1994; De Grandpré et al., 1997; Morgenstern et al., 2010b, 2017). This typically includes gas-phase and heterogeneous reactions. Chemistry and physics are primarily coupled through changes in temperatures and transport. For example, changes in temperatures modulate ozone in the upper stratosphere through reaction rates, whereas changes in transport control ozone abundances in the lower stratosphere due to longer lifetimes. Tropospheric chemistry and aerosols have been implemented and used in CCMs more recently (e.g. Morgenstern et al., 2017 and references therein for the most recent update), which allows addressing stratospheric ozone and climate interactions in a more consistent framework.

The radiation scheme solves photolysis and heating rates. Photolysis rates control the fate of many chemical species (e.g. ozone and hydroxyl oxide) and can be derived using schemes of different complexity (e.g. from a simple look-up table to interactive calculations) (e.g. Sudo et al., 2002; Watanabe et al., 2011; Lamarque et al., 2012; Naik et al., 2013a; Shindell et al., 2013c; O'Connor et al., 2014). In turn, heating rates are derived using radiatively active species – e.g. GHGs and ODSs – and determine radiative energy balances. Dynamics are calculated by solving the "primitive equations" describing atmospheric flows. An appropriate representation of the atmosphere climatological mean state is essential (e.g. variability on different timescales and inter–hemispheric differences) (e.g. Flato et al., 2013). The Brewer-Dobson circulation and horizontal mixing largely control transport and dynamics in the stratosphere (e.g. Holton et al., 1995). This involves explicit representation of planetary-scale Rossby waves, and parameterisation of gravity and orographic waves both propagation and dissipation (e.g. Butchart, 2014).

2.5.2. Simulations

Different types of simulations can be performed with regard to the research question and purpose of the analysis. Transient simulations are usually performed to explore time-varying (time series) responses to changing boundary conditions, such as abundances of ODSs or GHGs (e.g. Eyring et al., 2010a, 2013a). On the other hand, time slice simulations are usually preferred to investigate mean changes and significance due to specific forcings, for example, by repeating the simulation a

number of years with fixed boundary conditions (i.e. each integration captures both atmospheric mean state and internal climate variability for significance) (e.g. Young et al., 2013a; Iglesias-Suarez et al., 2016).

Model simulations can also be classified into historical (past) and future simulations (Eyring et al., 2010a, 2013a; Young et al., 2013a; Iglesias-Suarez et al., 2016). Historical simulations are forced by observed boundary conditions (e.g. ODSs, GHGs and SSTs-SICs) to evaluate the performance of CCMs (e.g. how well simulated ozone depletion agrees with observed changes). Future simulations (projections) are driven by emission scenarios (e.g. emission or concentration of trace gases) under certain socio-economic assumptions to explore future climate and atmospheric composition changes.

Sensitivity simulations – or idealised realizations – are particularly useful to clearly separate the effects of specific forcing agents (e.g. detection and attribution analysis) (e.g. Gillett et al., 2012, 2013; Knutson et al., 2013). For example, they could be performed by changing one or more forcing agents at a time while holding fixed other boundary parameters (e.g. Banerjee et al., 2016). Furthermore, coordinated multi-model activities, making use of "reference simulations" (i.e. same conditions and equivalent setup), are valuable to explore not fully understood processes, chemistry-climate feedbacks and different model parameterizations (e.g. Taylor et al., 2012; Lamarque et al., 2013b; Morgenstern et al., 2017).

2.5.3. General performance

Evaluation of CCMs simulating stratospheric ozone and the processes affecting its distribution and abundances provides insight on their skills reproducing observational estimates. Confidence in future projections heavily relies on models performance against observations and the ability to represent important processes controlling ozone. Due to a large number of CCMs and the spread in stratospheric ozone projections, multi-model intercomparison projects (MIPs) complement single model evaluations (Eyring et al., 2005).

In the last 15 years several MIPs have assessed the ability of CCMs on simulating past changes in stratospheric ozone. An early MIP identified deficiencies in models simulating stratospheric dynamics in polar regions, leading to significant cold biases in winter and spring (i.e. important for heterogeneous chemistry and ozone

loss) (Pawson et al., 2000; Austin et al., 2003). The Chemistry-Climate Model Validation (CCMVal-1) activity was instructed to include similar boundary conditions (e.g. ODSs, GHGs and SSTs-SICs), eliminating many uncertainties concerning experimental setups (Eyring et al., 2005). Evaluations of the CCMVal-1 activity revealed significant differences in the simulated stratospheric inorganic chlorine (Cl_y) (Eyring et al., 2006; Waugh and Eyring, 2008), particularly over Antarctica in austral spring (2–3.5 ppbv range). In turn, this uncertainty leads to a large inter-model spread in the simulated future ozone recovery (Eyring et al., 2007). Although CCMs capture the structure of the tropical tropopause layer, they fail to represent observed trends of the tropical cold point (e.g. important for water vapour entering the stratosphere) (Gettelman et al., 2009).

The second phase of the CCMVal activity (CCMVal-2) included updated model versions of the former activity and several new participating models (SPARC, 2010). A more comprehensive evaluation assessed stratosphere-troposphere interactions in addition to chemical, radiative and dynamical processes. The overall performance of the CCMVal-2 models is similar compared to the former activity (SPARC, 2010). While the representation of several diagnostics shows some improvement, such as Cl_y, other important diagnostics show similar performance or even larger inter-model spread (e.g. tropical cold point and stratospheric water vapour). The CCMVal activities (phases 1 and 2) have informed the latest WMO Scientific Assessment reports on stratospheric ozone (WMO, 2007, 2011, 2014).

Recently, tropospheric chemistry and aerosols have also been included in CCMs (e.g. Lamarque et al., 2013b; Morgenstern et al., 2017), which enables a consistent framework for chemistry-climate analyses. The Tropospheric Ozone Assessment Report (TOAR) has evaluated current models simulating tropospheric ozone against observations (Young et al., 2018). For present day (year 2000), simulated tropospheric ozone burden and stratosphere-troposphere exchange compare favorably against observational estimates (e.g. Stevenson et al., 2006; Myhre et al., 2013; Young et al., 2013a). However, observations are not available for global net chemical production (production minus loss) and dry deposition, and models show a wide spread in these terms (Young et al., 2018). While the wide spread in net chemistry production may be related to the complexity of chemistry schemes (e.g. Wild, 2007; Jenkin et al., 2008), the inter-model range for dry deposition may be the consequence of planetary boundary layer dynamics and parameterisation of uptake

fluxes (e.g. Hardacre et al., 2015). Models are consistently high biased in the NH and low biased in the SH for ozone throughout the troposphere compared to observational estimates (Tilmes et al., 2012; Eyring et al., 2013a; Stevenson et al., 2013; Young et al., 2013a). The common NH/SH biases among models suggest that emission inventories may play a significant role, though further evaluation is required (Young et al., 2018).

2.6. Summary

In this chapter, I have presented an overview of the main concepts that support the analyses in subsequent chapters. I have introduced the main features controlling stratospheric ozone abundance and distribution along with past changes observed in recent decades (Sect. 2.1). Due to the stratosphere is far from being an isolated region of the atmosphere, I have presented the important features of the troposphere for climate and ozone (Sect. 2.2), before describing stratosphere-troposphere interactions (Sect. 2.3). Finally, I have discussed projected changes of stratospheric ozone in the 21st century (Sect. 2.4), and briefly described chemistry-climate models that are routinely used in such projections (Sect. 2.5).

Chapter 3

Stratospheric ozone change and related climate impacts over 1850–2100 as modelled by the ACCMIP ensemble

F. Iglesias-Suarez[1], P. J. Young[1] and O. Wild[1]

[1]Lancaster Environment Centre, Lancaster University, Lancaster, UK

Correspondence to: F. Iglesias-Suarez (n.iglesiassuarez@lancaster.ac.uk)

The following work has been published in Atmospheric Chemistry and Physics on 18 January 2016 (citation: Stratospheric ozone change and related climate impacts over 1850–2100 as modelled by the ACCMIP ensemble, Atmos. Chem. Phys., 16, 343-363, doi:10.5194/acp-16-343-2016, 2016). The authors and their contributions are listed below.

Fernando Iglesias-Suarez: Processed the data, analysed the data, and wrote the manuscript. **Paul J. Young and Oliver Wild:** Helped to synthesise, interpret the results and compile the manuscript.

Abstract

Stratospheric ozone and associated climate impacts in the Atmospheric Chemistry and Climate Model Intercomparison Project (ACCMIP) simulations are evaluated in the recent past (1980–2000), and examined in the long-term (1850–2100) using the Representative Concentration Pathways (RCPs) low and high emission scenarios (RCP2.6 and RCP8.5, respectively) for the period 2000–2100. ACCMIP multi-model mean total column ozone (TCO) trends compare favourably, within uncertainty estimates, against observations. Particularly good agreement is seen in the Antarctic austral spring (−11.9 % dec^{-1} compared to observed ~ −13.9 ± 10.4 % dec^{-1}), although larger deviations are found in the Arctic's boreal spring (−2.1 % dec^{-1} compared to observed ~ −5.3 ± 3.3 % dec^{-1}). The simulated ozone hole has cooled the lower stratosphere during austral spring in the last few decades (−2.2 K dec^{-1}). This cooling results in Southern Hemisphere summertime tropospheric circulation changes captured by an increase in the Southern Annular Mode (SAM) index (1.3 hPa dec^{-1}). In the future, the interplay between the ozone hole recovery and greenhouse gases (GHGs) concentrations may result in the SAM index returning to pre-ozone hole levels or even with a more positive phase from around the second half of the century (−0.4 hPa dec^{-1} and 0.3 hPa dec^{-1} for the RCP2.6 and RCP8.5, respectively). By 2100, stratospheric ozone sensitivity to GHG concentrations is greatest in the Arctic and Northern Hemisphere midlatitudes (37.7 DU and 16.1 DU difference between the RCP2.6 and RCP8.5, respectively), and smallest over the tropics and Antarctica continent (2.5 DU and 8.1 DU respectively). Future TCO changes in the tropics are mainly determined by the upper stratospheric ozone sensitivity to GHG concentrations, due to a large compensation between tropospheric and lower stratospheric column ozone changes in the two RCP scenarios. These results demonstrate how changes in stratospheric ozone are tightly linked to climate and show the benefit of including the processes interactively in climate models.

3.1. Introduction

The Atmospheric Chemistry and Climate Model Intercomparison Project (ACCMIP) (Lamarque et al., 2013b) was designed to evaluate the long-term (1850–2100) atmospheric composition changes (e.g. ozone) to inform the Fifth Assessment Report of the Intergovernmental Panel on Climate Change (IPCC, 2013), supplementing phase 5 of the Coupled Model Intercomparison Project (CMIP5) (Taylor et al., 2012),

where the focus was more on physical climate change. In addition, ACCMIP is the first model intercomparison project in which the majority of the models included chemical schemes appropriate for stratospheric and tropospheric chemistry. Due to the absorption of shortwave radiation, stratospheric ozone is important for determining the stratospheric climate (e.g. Randel and Wu, 1999) and has a strong influence on tropospheric ozone through stratosphere-to-troposphere transport (e.g. Collins et al., 2003; Sudo et al., 2003; Zeng and Pyle, 2003). In addition, changes in stratospheric ozone can affect atmospheric circulation and climate, reaching to the lower troposphere in the case of the Antarctic ozone hole (e.g. Thompson and Solomon, 2002; Gillett and Thompson, 2003). This study evaluates stratospheric ozone changes and associated climate impacts in the ACCMIP simulations, quantifying the evolution since the pre-industrial period through to the end of the 21st century.

Stratospheric ozone represents approximately 90 % of ozone in the atmosphere and absorbs much of the ultraviolet solar radiation harmful for the biosphere (e.g. WMO, 2014; UNEP, 2015). Anthropogenic emissions of ozone depleting substances (ODSs) such as chlorofluorocarbons and other halogenated compounds containing chlorine and bromine have played a key role in depleting stratospheric ozone during the latter half of the 20th century (e.g. WMO, 2014). Although present globally averaged TCO levels are only ~ 3.5 % lower than pre-1980 values, about half the TCO is depleted over Antarctica between September and November (austral spring) each year (Forster et al., 2011). Globally, halogen loading peaked around 1998 (although this depends on altitude and latitude) and started to decrease afterwards due to the implementation of the Montreal Protocol and its Amendments and Adjustments (e.g. WMO, 2007, 2014). As a result, stratospheric ozone is expected to recover and return to pre-industrial values during the 21st century (e.g. Austin and Wilson, 2006; Eyring et al., 2010a). Although anthropogenic ODSs are the main cause of ozone depletion over the last decades, other species such as methane, nitrous oxide (N_2O) and carbon dioxide (CO_2) affect stratospheric ozone chemistry as well (e.g. Haigh and Pyle, 1982; Portmann et al., 2012; Revell et al., 2012; Reader et al., 2013). Randeniya et al. (2002) argued that increasing concentrations of methane can amplify ozone production in the lower stratosphere via photochemical production, though increases of water vapour from methane oxidation may have the opposite effect (Dvortsov and Solomon, 2001). Nitrogen oxides (NO_x) chemistry is important in the middle-upper stratosphere for ozone; thus, variations and trends in the source gas (N_2O) may have a

substantial influence on ozone levels (e.g. Ravishankara et al., 2009; Portmann et al., 2012; Revell et al., 2012).

As ODS levels slowly decrease, projected climate change will likely play a key role in stratospheric ozone evolution through its impacts on temperature and atmospheric circulation (e.g. IPCC, 2013). The impact of climate change on ozone in the stratosphere further complicates the attribution of the recovery (e.g. Waugh et al., 2009a; Eyring et al., 2010b) since increases in CO_2 levels cool the stratosphere, slowing gas-phase ozone loss processes (e.g. reduced NO_x abundances; reduced HO_x-catalysed ozone loss; and enhanced net oxygen chemistry) resulting in ozone increases, particularly in the middle-upper stratosphere and high latitudes (e.g. Haigh and Pyle, 1982; Randeniya et al., 2002; Rosenfield et al., 2002). Further, an acceleration of the equator-to-pole Brewer-Dobson circulation (BDC) has been predicted in many model studies under high GHG concentrations (e.g. Butchart et al., 2006; Garcia and Randel, 2008; Butchart et al., 2010), although its strength can only be inferred indirectly from observations, meaning that there are large uncertainties in recent trends (e.g. Engel et al., 2009; Bönisch et al., 2011; Young et al., 2011; Stiller et al., 2012). This BDC acceleration enhances transport in the atmosphere and stratospheric-tropospheric exchange (STE), and is likely to have a substantial role throughout the 21st century (e.g. Butchart, 2014). STE is a key transport process that links ozone in the stratosphere and the troposphere (e.g. Holton et al., 1995), characterised by downward flux of ozone-rich stratospheric air, mainly at mid-latitudes, and upward transport of ozone-poor tropospheric air in tropical regions. In contrast, ozone loss cycles could increase with higher N_2O and lower methane concentrations (e.g. Randeniya et al., 2002; Ravishankara et al., 2009).

Traditionally, chemistry-climate models (CCMs) have been used to produce stratospheric ozone projections into the past and the future (e.g. WMO, 2007, 2014), usually prescribing sea surface temperatures and sea-ice concentrations from observations or climate simulations. Some coordinated climate model experiments, such as the CMIP5 and the Chemistry-Climate Model Validation activities (CCMVal and CCMVal2) (Eyring et al., 2006; Eyring et al., 2007; Austin et al., 2010; Eyring et al., 2010a; Eyring et al., 2013a) have examined stratospheric ozone evolution. Recent past stratospheric column ozone projections (~ 1960–2000), from the above coordinated climate model experiments, show substantial decreases driven mainly by anthropogenic emissions of ODSs and agree well with observations. However, future

stratospheric ozone projections are influenced by both the slow decrease in ODS levels and the climate scenario chosen. To illustrate this, Eyring et al. (2013a) used a subgroup of CMIP5 models with interactive chemistry in the stratosphere and the troposphere to show gradual recovery of ozone levels during the next decades (as ODS abundances decrease in the stratosphere), and global multi-model mean stratospheric column ozone "super-recovery" (higher levels than those projected in the pre-ozone depletion period) for the most pessimistic emission scenario (RCP8.5) at the end of the 21st century. A main recommendation from the SPARC-CCMVal (2010) report is that CCMs should keep developing towards self-consistent stratosphere-troposphere chemistry, interactively coupled to the dynamics and radiation (e.g. enabling chemistry-climate feedbacks).

Tropospheric ozone accounts for the remaining ~ 10 % atmospheric ozone, where it is a GHG, a pollutant with significant negative effects to vegetation and human health, and a main source of hydroxyl radicals controlling the oxidising capacity of the atmosphere (e.g. Prather et al., 2001; Gregg et al., 2003; Jerrett et al., 2009). Its abundance in the troposphere is determined from the balance of STE and photochemistry production involving the oxidation of hydrocarbons and carbon monoxide (CO) in the presence of NO_x, versus chemical destruction and deposition to the surface (e.g. Lelieveld and Dentener, 2000; Wild, 2007). These terms depend in turn on climate system dynamics (e.g. STE) and on the magnitude and spatial distribution of ozone precursors emissions such as, volatile organic compounds, NO_x and CO (e.g. chemical production and destruction) (e.g. Wild, 2007). Several studies found tropospheric ozone increases due to climate change via enhanced STE (e.g. Collins et al., 2003; Sudo et al., 2003; Zeng and Pyle, 2003). Other studies have shown positive relationship between anthropogenic emissions and tropospheric ozone abundance (e.g. Stevenson et al., 2006; Young et al., 2013a). However, the ultimately net impact of climate and emissions changes remains unclear (Stevenson et al., 2006; Isaksen et al., 2009; Jacob and Winner, 2009), and it may differ substantially by region, altitude or season (e.g. Myhre et al., 2013).

Further, the ozone hole influences surface climate via temperature and circulation changes (e.g. Thompson and Solomon, 2002; Gillett and Thompson, 2003) owing to direct radiative effects (e.g. Randel and Wu, 1999; Forster et al., 2011). The ozone layer heats the stratosphere by absorbing incoming ultraviolet solar radiation, hence, trends and variations on ozone would impact stratospheric dynamics (e.g.

Ramaswamy et al., 2006; Randel et al., 2009b; Gillett et al., 2011). In the Southern Hemisphere (SH), stratospheric circulation changes associated to ozone depletion have been linked to tropospheric circulation changes primarily during austral summer (lagging the former 1–2 months), based on observations (Thompson and Solomon, 2002) and model simulations (Gillett and Thompson, 2003). These SH extratropical circulation changes could be described by the leading mode of variability or the SAM (e.g. Thompson and Wallace, 2000). Previous studies based on CCMs simulations reported positive trends in the SAM over the ozone depletion period (e.g. Sexton, 2001; Shindell and Schmidt, 2004; Arblaster and Meehl, 2006; Polvani et al., 2010; McLandress et al., 2011). Furthermore, some modelling studies have projected a poleward shift (i.e. positive change) in the SAM due to future increases in GHGs (e.g. Fyfe et al., 1999; Marshall et al., 2004). Projected ozone recovery should have the opposite effect than ozone depletion (i.e. a negative trend in the SAM), and this is important as it opposes the effect of increasing GHG concentrations. Some studies suggest that these effects will largely cancel out each other during the next several decades in austral summer owing to these competing forces (e.g. Perlwitz et al., 2008; Son et al., 2009; Arblaster et al., 2011; Polvani et al., 2011; Barnes et al., 2013; Gillett and Fyfe, 2013).

Multi-model experiments are useful for evaluating model differences in not fully understood processes and associated feedbacks, and for identifying agreements and disagreements between various parameterisations (e.g. Shindell et al., 2006; Stevenson et al., 2006). While CMIP5 provides a framework towards a more Earth System approach to intercompare model simulations and enables their improvement, it lacks comprehensive information on atmospheric composition and models with full interactive chemistry (Lamarque et al., 2013b). ACCMIP aims to fill this gap by evaluating how atmospheric composition drives climate change, and provides a gauge of the uncertainty by different physical and chemical parameterisations in models (Myhre et al., 2013). While previous work has explored tropospheric changes in the ACCMIP models, the stratosphere has received less attention. Moving towards a more comprehensive modelling capability – including both tropospheric and stratospheric processes – requires comprehensive analyses of these two domains.

This study explores modelled stratospheric ozone changes with a focus on chemistry and climate feedbacks relevant to ozone and the uncertainty associated with different physical and chemical parameterisations. We quantify the evolution of

stratospheric ozone and related climate impacts in the ACCMIP simulations from pre-industrial times (1850), recent past (1980) and present day (2000) to the near-future (2030) and the end of the 21st century (2100). First, we evaluate recent past and present-day ACCMIP stratospheric ozone simulations with observations and other model based products. Then, we assess ozone projections and ozone sensitivity to GHG concentrations using the low and high emission scenarios, due to future stratospheric ozone will be influenced by both decreased ODS levels and climate (i.e. stratospheric cooling and atmospheric circulation). Finally, a description of the associated impacts of stratospheric ozone depletion and projected recovery in the climate system is presented, with a focus in the SH. In addition, this study compares ACCMIP simulations with those from CMIP5 and CCMVal2 and identifies agreements and disagreements among different parameterisations. This paper complements previous analysis of the ACCMIP simulations on tropospheric ozone evolution (Young et al., 2013a; Parrish et al., 2014), radiative forcing (Bowman et al., 2013; Shindell et al., 2013b; Stevenson et al., 2013), hydroxyl radical and methane lifetime (Naik et al., 2013b; Voulgarakis et al., 2013), historical black carbon evaluation (Lee et al., 2013), nitrogen and sulfur deposition (Lamarque et al., 2013a), and climate evaluation (Lamarque et al., 2013b).

The remainder of this paper is organised as follows. Section 3.2 describes the models and simulations used here, with a focus on the various ozone chemistry schemes. In Section 3.3, ozone is examined in the recent past against observations, and analysed from 1850 to 2100 under the low and high RCPs emission scenarios for those models with interactive chemistry-climate feedback. Section 3.4 explores past and future stratospheric ozone evolution and climate interactions. A discussion of the results is presented in Section 3.5, followed by a brief summary and main conclusions in Section 3.6.

3.2. Models, simulations and analysis

In this section we describe main details of the ACCMIP models, simulations, and analyses conducted in this paper. A comprehensive description of the models and simulations along with further references are provided by Lamarque et al. (2013b).

3.2.1. ACCMIP models

Table 3.1 summarises the ACCMIP models analysed in this study and their important features. We considered 8 models that had time-varying stratospheric ozone, either prescribed (offline) or interactively calculated (online). From the full ACCMIP ensemble (Lamarque et al., 2013b), we have excluded: EMAC, GEOSCCM and GISS-E2-TOMAS, as these did not produce output for all the scenarios and time periods analysed here (see Sect. 3.2.2); CICERO-OsloCTM and LMDzORINCA, as these used a constant climatological value of stratospheric ozone; MOCAGE and STOC-HadAM3, which showed poor stratospheric ozone chemistry performance compared to observations; and NCAR-CAM5.1, as this model was focused on aerosol output and did not save ozone fields.

The ACCMIP models included in this study are CCMs (7) or chemistry general circulation models (1) with atmospheric chemistry modules. The CCMs implemented a coupled composition-radiation scheme, whereas the chemistry and radiation was not coupled in UM-CAM (see Table 3.1). Both sea surface temperatures and sea-ice concentrations were prescribed, except in GISS-E2-R which interactively calculated them. Similarly to Eyring et al. (2013a), we group the models into two categories: 6 models with full atmospheric chemistry (CHEM), and 2 models with online tropospheric chemistry but with prescribed ozone in the stratosphere (NOCHEM) (Figure 4 of Lamarque et al., 2013b). All CHEM models included ODSs (with Cl and Br) and the impact of polar stratospheric clouds (PSCs) on heterogeneous chemistry, although a linearised ozone chemistry parameterisation was implemented in CESM-CAM-Superfast (McLinden et al., 2000; Hsu and Prather, 2009). The other two models, HadGEM2 and UM-CAM, prescribed stratospheric ozone concentrations from the IGAC/SPARC database (Cionni et al., 2011).

A final important distinction among the models is how stratospheric changes are able to influence photolysis rates. The simplest scheme is for HadGEM2 and UM-CAM, where the photolysis rates are derived from a look-up table as a function of time, latitude and altitude only, and using a climatological cloud and ozone fields (i.e. the rates are the same for all simulations) (e.g. Zeng et al., 2008; Zeng et al., 2010; Collins et al., 2011; Martin et al., 2011). The look-up table is more complex with CESM-CAM-Superfast (Gent et al., 2010), CMAM (Scinocca et al., 2008), GFDL-AM3 (Donner et al., 2011; Griffies et al., 2011) and NCAR-CAM3.5 (Gent et al., 2010; Lamarque et al., 2012), where an adjustment is applied to take surface albedo

Table 3.1. Summary of the ACCMIP models used here

Model	Stratospheric ozone	Composition-radiation coupling	Photolysis scheme	Reference
CESM-CAM-superfast	CHEM	Yes	Adjusted look-up table	Lamarque et al. (2012)
CMAM	CHEM	Yes	Adjusted look-up table	Scinocca et al. (2008)
GFDL-AM3	CHEM	Yes	Adjusted look-up table	Donner et al. (2011); Naik et al. (2013a)
GISS-E2-R	CHEM	Yes	Online	Koch et al. (2006); Shindell et al. (2013c)
HadGEM2	NOCHEM	Yes	Look-up table + TCO overhead	Collins et al. (2011)
MIROC-CHEM	CHEM	Yes	Online	Watanabe et al. (2011)
NCAR-CAM3.5	CHEM	Yes	Adjusted look-up table	Lamarque et al. (2011; 2012)
UM-CAM	NOCHEM	No	Look-up table	Zeng et al. (2008; 2010)

and cloudiness into account, which couples with the simulated aerosols. Fully online photolysis calculations were only made for MIROC-CHEM (Watanabe et al., 2011) and GISS-E2-R (Schmidt et al., 2006; Shindell et al., 2013c).

As per Young et al. (2013a), all models were interpolated to a common grid (5º by 5º latitude/longitude and 24 pressure levels).

3.2.2. ACCMIP scenarios and simulations

The ACCMIP simulations were designed to span the pre-industrial period to the end of the 21st century. In this study, time slices from the years 1850, 1980 and 2000 comprise historical projections (hereafter Hist), whereas time slices from the years 2030 and 2100 future simulations. The latter follow the climate and composition/emission projections prescribed by the RCPs (van Vuuren et al., 2011; Lamarque et al., 2012), named after their nominal radiative forcing at the end of the 21st century relative to 1750. Here we consider RCP2.6 (referring to 2.6 Wm^{-2}) and RCP8.5 (8.5 Wm^{-2}), since they bracket the range of warming in the ACCMIP simulations, and are the scenarios that have been completed by the greatest number of models.

Future ODSs (the total organic chlorine and bromine compounds) in CHEM models follow the RCPs values from Meinshausen et al. (2011), which does not include the early phase-out of hydrochlorofluorocarbons agreed in 2007 by the Parties to the Montreal Protocol. Note that ODSs may be specified as concentrations (CMAM, GFDL-AM3 and NCAR-CAM3.5) or emissions (CESM-CAM-superfast, GISS-E2-R, MIROC-CHEM) in different models, though these were the same within each time slice simulation (except for GISS-E2-R; see below). No significant trends are found for stratospheric ozone in those years that form part of the Hist 1980 time slice for the latter models, even though ODSs were specified as emissions (i.e. any trends in ODSs concentration in the stratosphere due to transport timescales do not significantly affect ozone concentrations). This is slightly different from the modified halogen scenario of WMO (2007) used in the IGAC/SPARC ozone database employed by the NOCHEM models (described below). Nevertheless, halogen concentrations in both future scenarios peak around the year 2000 and decline afterwards, although slightly different timing of ozone returning to historical levels may be found. Tropospheric ozone precursors emissions follow Lamarque et al. (2010) for the historical period, and Lamarque et al. (2013b) for the RCPs.

Briefly, the IGAC/SPARC database includes zonal and monthly mean stratospheric ozone time series between 1850–2099 (Cionni et al., 2011). A multiple linear regression analysis based on satellite (Stratospheric Aerosol and Gas Experiment I+II) and ozonesonde (Syowa and Resolute) observations is applied for the recent past (1979–2009), and extrapolated back to 1850 using pre-1979 ODS levels. Future stratospheric ozone (2010–2099) is taken from the CCMVal2 multi-model mean REF-B2 simulations, which follow the Special Report on Emission Scenarios A1B for GHG concentrations and the A1 adjusted halogen scenario (Morgenstern et al., 2010b).

Most models completed time slice simulations for each period and scenario, usually 10 years average about each time slice (e.g. 1975–1984 for the Hist 1980 time slice, although other models simulated time slices ranging from 5 to 11 years). Notice that interannual variability for a given time slice is generally small (Young et al., 2013a). The exception is GISS-E2-R, which ran transient simulations with a coupled ocean. Equivalent time slice means were calculated by averaging 10 years centred on the desired time slice, (1975–1984 for 1980 and so forth), except for the 1850 and 2100 time slices (e.g. 1850–1859 mean).

3.2.3. CMIP5 and CCMVal2 simulations

We also include CMIP5 and CCMVal2 simulations as a benchmark for the former models. We use a subset of five "high" top CMIP5 models, defined here as those models that represented and saved ozone output above 10 hPa for the historical (1850–2005, most of the models), and future (RCP2.6 and RCP8.5, 2005–2100) emission scenarios: CESM1-WACCM, GFDL-CM3, MPI-ESM-LR, MIROC-ESM, and MIROC-ESM-CHEM. Only high top models are considered here due to the implications the upper stratosphere has on, among other factors, stratospheric dynamical variability (Charlton-Perez et al., 2013), and tropospheric circulation (Wilcox et al., 2012). Moreover, we will show how, in the tropics, upper stratospheric ozone plays a key role on TCO projections during the 21st century (see Sect. 3.3.2). Again, we group the models into two categories: 3 models with full atmospheric chemistry (CHEM: CESM1-WACCM, GFDL-CM3 and MIROC-ESM-CHEM), and 2 models with prescribed ozone (NOCHEM: MPI-ESM-LR and MIROC-ESM). While MPI-ESM-LR prescribed ozone concentrations from a modified version of the IGAC/SPARC database (Cionni et al., 2011; Jones et al., 2011), with a solar cycle included in the future; MIROC-ESM imposed ozone fields from a former simulation (Kawase et al., 2011), which neglected climate impacts on stratospheric ozone. A detailed description of the models, simulations and ozone concentrations are presented by Taylor et al. (2012) and Eyring et al. (2013a).

In addition, we include 14 CCMVal2 models that represented ozone under the REF-B1 scenario (1960–2006, most of the models): CAM3.5, CCSRNIES, CMAM, E39CA, EMAC, GEOSCCM, LMDZrepro, Niwa-SOCOL, SOCOL, ULAQ, UMETRAC, UMUKCA-METO, UMUKCA-UCAM and WACCM. All these models had interactive stratospheric chemistry and coupled composition-climate feedback, although simplified or absent chemistry in the troposphere. Morgenstern et al. (2010b) describe in detail CCMVal2 models and REF-B1 simulations.

In contrast to ACCMIP time slice simulations, these data sets were based on transient experiments, which may result in slightly different ozone levels, as simulations depart from initial conditions. Nevertheless, equivalent time slice means were calculated in the same manner as above for consistency purposes throughout all analysis involving trends or ozone changes. A caveat is that TCO was calculated from

the ozone mixing ratio field, which may slightly differ (~ 1.5 %) from that of the model's native TCO (Eyring et al., 2013a).

3.2.4. Tropopause definition

For the purpose of comparing the outputs among models, a tracer tropopause definition has been argued to be suitable (Wild, 2007). This study follows Young et al. (2013a) method, in which the tropopause is based on the 150 ppbv ozone contour (i.e. "ozone mask"), after Prather et al. (2001). For example, the "troposphere" is defined as the region that lies below the ozone mask. The definition is fitted for all time slices using ozone from the Hist 1850 time slice for each model and month; meaning that the "troposphere" is defined as a fixed volume region of the atmosphere. On the one hand, Young et al. (2013a) argued that using a monthly mean tropopause from the 1850 time slice prevents issues with different degrees of ozone depletion among the models, especially for SH high latitudes. On the other hand, this neglects the fact that the tropopause height may vary with time due to climate change (e.g. Santer et al., 2003a, b). Nevertheless, Young et al. (2013a) have shown that using ozone from the Hist 2000 time slice to define the tropopause across all time slices, generally results in tropospheric ozone columns of ±5 % compared to the Hist 1850 time slice.

3.2.5. Trend calculations

The different data sets trends are broadly comparable but differ slightly in their calculation and uncertainty determination. For ACCMIP, CMIP5 and CCMVal2 models, the trends are for the differences between the Hist 1980 and 2000 time slices with the range shown as box/whisker plots (central 50 % of trends as the box; 95 % confidence intervals as the whiskers). Note that using time slices to calculate trends will underestimate the uncertainty from interannual variability. However, least squares linear trends calculated for CMIP5 and CCMVal2 models (i.e. between 1980 and 2000) are similar to those calculated from differences between time slices.

Trends for observational estimates and ozone databases (used in Sect. 3.3.1 and 3.4) are least squares linear trends (i.e. between 1980 and 2000 for consistency reasons with time slices), with error bars indicating the 95 % confidence level based on the standard error for the fit, and corrected for lag-1 autocorrelation for the former (Santer et al., 2000). Santer et al. (2000) demonstrated the significance of least squares

linear trends based on autocorrelated data (lag-1 structure) should account for this, otherwise the significance would be too liberal.

3.3. Long-term total column ozone evolution in the ACCMIP models

This section presents an evaluation of the present-day (Hist 2000) TCO distribution and recent (1980–2000) ozone trends against observations and observationally-derived data. The evolution of TCO from the pre-industrial period (1850) to the end of the 21st century (2100) is also discussed, with a particular focus on the different contribution of trends in the tropical tropospheric, lower stratospheric, and upper stratospheric columns to the total column trend. Previously, Young et al. (2013a) have shown that TCO distribution changes in the ACCMIP multi-model mean agree well with the Total Ozone Mapping Spectrometer (TOMS) for the last few decades (their Fig. S7). However, ACCMIP models simulate weaker (not significant) ozone depletion in early boreal spring over the Arctic between Hist 1980 and 2000 compared to TOMS (see also Sects. 3.3.1 and 3.5).

3.3.1. Evaluation of ozone trends, 1980–2000

Figure 3.1 shows TCO decadal trends between 1980 and 2000 for the global mean, and a number of latitude bands. The figure compares the ACCMIP, CMIP5 and CCMVal2 models against the Bodeker Scientific TCO data set (BodSci TCO - version 2.8), combining a number of different satellite-based instruments (Bodeker et al., 2005; Struthers et al., 2009), and observations from the Solar Backscatter Ultraviolet (SBUV - version 8.6) merged ozone data set (McPeters et al., 2013). Also, Fig. 3.1 includes trends from the IGAC/SPARC ozone data set (Cionni et al., 2011), which was used by the majority of the models with prescribed ozone concentrations (both ACCMIP and CMIP5). The annual mean is used in evaluations for the global, tropical and midlatitudes regions. Additional evaluations are made for the boreal spring in the Arctic (March, April and May) and the austral spring in the Antarctic (September, October and November) when strongest ozone depletion occurs.

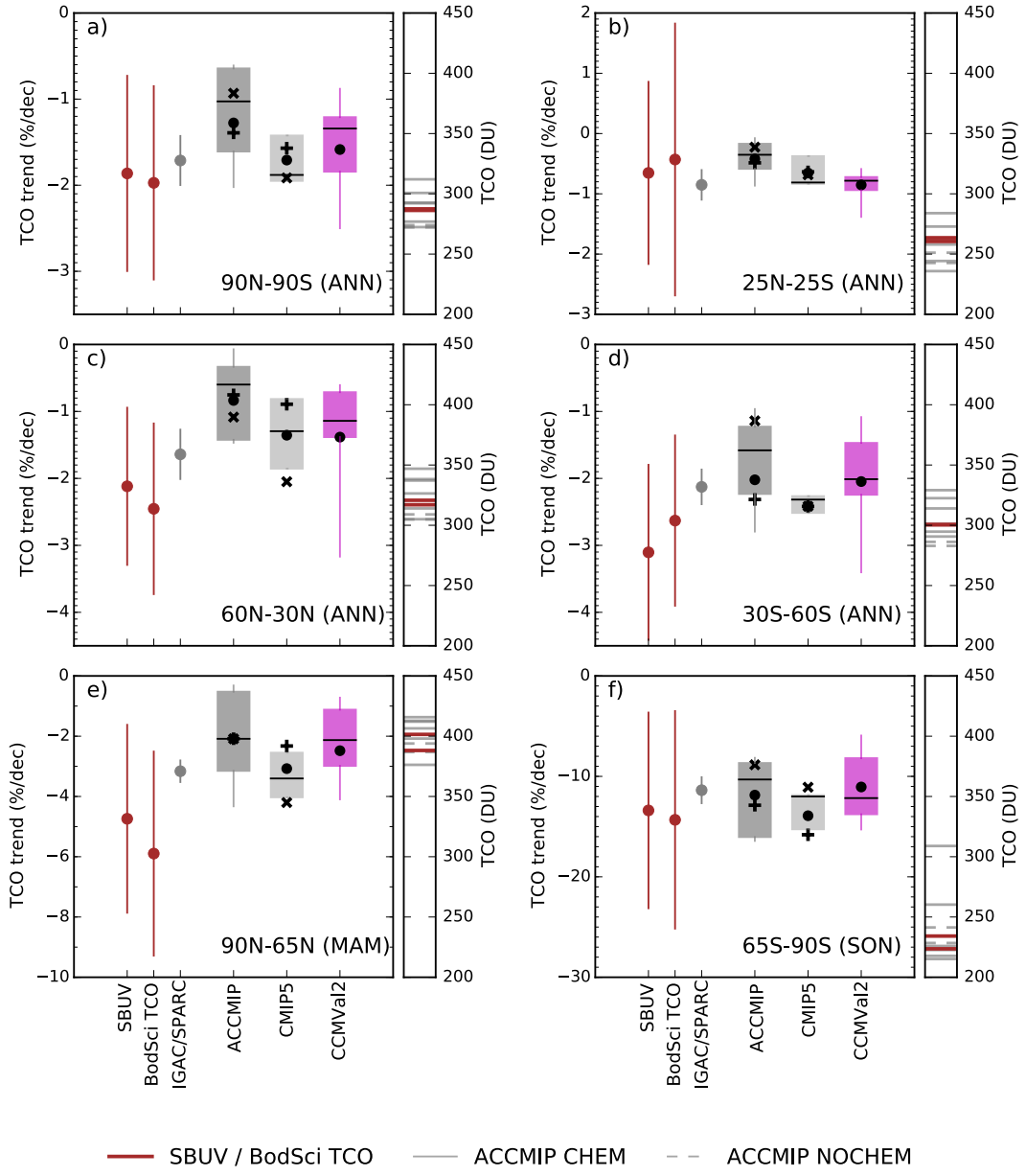

Figure 3.1. Total column ozone trends from 1980 to 2000 (% dec^{-1}) for the annual mean (ANN) (a) global, (b) in the tropics, (c) in the northern midlatitudes, (d) in the southern midlatitudes, (e) for the boreal spring in the Arctic (MAM), and (f) for austral spring in the Antarctic (SON). The box, whiskers and line indicate the interquartile range, 95 % range and median respectively, for the ACCMIP (light grey), CMIP5 (dark grey) and CCMVal2 (magenta) models. Multi-model means are indicated by dots. CHEM (models with interactive chemistry) and NOCHEM (models that prescribe ozone) means are indicated by 'plus' and 'cross' symbols, respectively. Observations and IGAC/SPARC data sets are represented by error bars indicating the 95 % confidence intervals (one tail).

Within uncertainty, the overall response for ACCMIP is in good agreement with observational data sets in terms of decadal trends and absolute values, with the Northern Hemisphere (NH) being the region where models differ most. These results also compare favourably with those reported by WMO (2014). In line with CMIP5 and CCMVal2 models, strongest changes are found over Antarctica in austral spring associated to the ozone hole, and smallest over the tropics where ODSs are least effective. ACCMIP NOCHEM models typically simulate smaller decadal trends than CHEM models, consistent with the possible underestimation of SH ozone depletion trends in the IGAC/SPARC ozone data set (Hassler et al., 2013; Young et al., 2014). However, outside extratropical SH regions, IGAC/SPARC ozone data set (i.e. used to drive the majority of ACCMIP and CMIP5 NOCHEM models) tends to show better agreement with observations than CHEM models. ACCMIP CHEM and CMIP5 CHEM models show very similar TCO decadal trends in all regions (± 0.1–0.2 % dec^{-1}), although differing somewhat more at high latitudes in the SH, where ozone depletion is greatest (± 2.9 % dec^{-1}). ACCMIP NOCHEM and CMIP5 NOCHEM models show more disparate trends (± 0.5–2.1 % dec^{-1}), which may be related to different ozone data sets and the implementation method on each model (i.e. online tropospheric chemistry in ACCMIP models).

Figure 3.2 compares vertically resolved ozone decadal trends for the same period, regions and seasons, for the ACCMIP multi-model mean and individual models against the Binary Database of Profiles (BDBP version 1.1.0.6) data set, using the so-called Tier 0 and Tier 1.4 data (Bodeker et al., 2013). Tier 0 includes ozone measurements from a wide range of satellite and ground-based platforms, whereas Tier 1.4 is a regression model fitted to the same observations. Uncertainty estimates for the BDBP Tier 1.4 trends are from the linear least square fits, as for the observations in Fig. 3.1. ACCMIP shows most disagreement with the BDBP data in the lower and middle stratosphere region and best agreement with Tier 1.4 in the upper stratosphere.

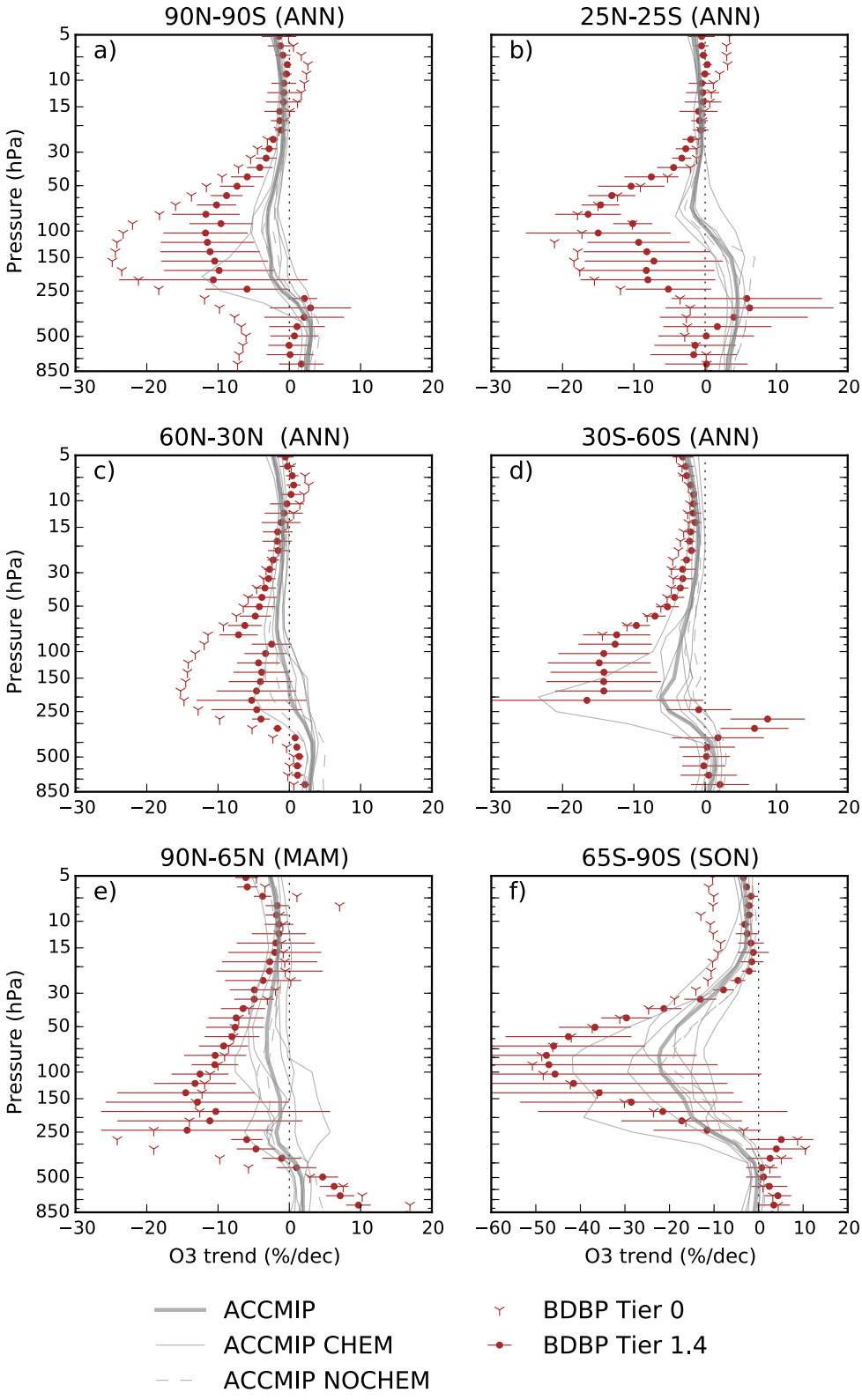

Figure 3.2. Vertically resolved ozone trends (% dec^{-1}), for ACCMIP multi-model mean, CHEM and NOCHEM models compared to BDBP Tier 1.4 (regression model fit with uncertainty estimates indicating 95 % confidence intervals, one tail) and Tier 0 (observations).

In the Tropics (Fig. 3.1b), TCO in all data sets agrees fairly well with observations. Although ACCMIP, CMIP5 and CCMVal2 simulate small decadal trends (−0.4, −0.7 and −0.9 % dec^{-1} respectively), the spread of the models at the 95 % confidence interval stays within the negative range. However, uncertainty estimates in TCO in the SBUV and BodSci TCO data sets embrace trends of different sign (−0.7 ± 1.5 % dec^{-1}, and −0.4 ± 2.3 % dec^{-1} respectively). IGAC/SPARC presents slightly larger negative decadal trends than observations in this region. CMIP5 CHEM and CCMVal2 multi-model means show slightly stronger decadal trends than ACCMIP CHEM models in this region. In terms of absolute values, the spread of the ACCMIP models overlaps the observed TCO for the Hist 2000 time slice, though most models differ by more than the observational standard deviation (7 out of 8). Biases in TCO may be attributed to different altitude regions (Fig. 3.2b). ACCMIP models fail to represent observed ozone depletion occurring in the lower and middle stratosphere region, which may be linked to a poor representation of the HO_x and upwelling in this region (e.g. Lary, 1997; Randel et al., 2007).

In the NH midlatitudes (Fig. 3.1c), TCO trends in ACCMIP and CMIP5 CHEM models (−0.8 and −0.9 % dec^{-1} respectively) underestimate larger negative trends than observation estimates (−2.3 ± 1.2 % dec^{-1}), though the CCMVal2 multi-model mean (−1.4 % dec^{-1}) is within the observational uncertainty. TCO decadal trends for IGAC/SPARC and NOCHEM models show better agreement with observations than CHEM models in this region. The ACCMIP Hist 2000 simulation agrees fairly well with observations in terms of absolute values, however, once again most models diverge by more than the observational standard deviation (7 out of 8). The ACCMIP multi-model mean falls within the BDBP Tier 1.4 uncertainty estimates for most of the lowermost and middle stratosphere, though simulates weaker ozone depletion in the lower stratosphere, which may be associated with the weaker than observed ozone depletion over the Arctic (Fig. 3.2c).

Over the Arctic in boreal spring (Fig. 3.1e), again the ACCMIP CHEM, CMIP5 CHEM and CCMVal2 data sets show weaker decadal trends than observations (−2.1, −2.3 and −2.5 % dec^{-1} respectively compared to −5.3 ± 3.3 % dec^{-1}). However, TCO for Hist 2000 in ACCMIP is in good agreement with observations, with no individual model differing by more than the observational standard deviation. In the altitude region around 150–30 hPa, the ACCMIP multi-model mean is underestimating larger negative trends compared to the BDBP data (Fig. 3.2e).

In the SH midlatitudes (Fig. 3.1d), ACCMIP simulates TCO decadal trends in better agreement with observations than in the NH midlatitudes (−2.0 % dec^{-1} compared to −2.9 ± 1.3 % dec^{-1}), except for the ACCMIP NOCHEM mean which is significantly underestimating larger negative trends (−1.1 % dec^{-1}). In terms of absolute values in present-day conditions, most ACCMIP models' TCO is either high or low biased compared to observations (7 out of 8). The ACCMIP multi-model mean is again underestimating larger negative trends compared to the BDBP data set in the altitude range between 150–30 hPa (notice that Tier 1.4 trends are more uncertain in this region), which may be associated to the influence of the tropics and in-situ HO_x catalytic loss cycle (e.g. Lary, 1997) (Fig. 3.2d).

Over Antarctica in austral spring (Fig. 3.1f), ACCMIP CHEM and CMIP5 multi-model means show best agreement compared to observations (−12.9 % dec^{-1} and −13.9 % dec^{-1} respectively compared to ~ −13.9 ± 10.4 % dec^{-1}), although all data sets fall within observational uncertainty estimates. IGAC/SPARC ozone data set and NOCHEM models simulate less ozone depletion in this region (−11.4 % dec^{-1} and −8.8 % dec^{-1} respectively) than models with interactive chemistry. Although, many ACCMIP models are in good agreement with observations in terms of absolute values for the Hist 2000 time slice, one CHEM model deviates more than the observational standard deviation. ACCMIP models show fairly good agreement with BDBP Tier 1.4 decadal trends at various altitude regions, except around 70–30 hPa, which is also the region where the modelled temperature trends are more negative than observed (see Sect. 3.5). This is consistent with previous analyses which suggested that models potentially simulate too strong negative trend for a given ozone depletion (e.g. Young et al., 2011) and this discrepancy warrants further investigation in future model intercomparison studies, where there is more model output available.

3.3.2. Past modelled and future projected total column ozone

In this section, the evolution of past modelled TCO (from 1850 to 2000) and the sensitivity of ozone to future GHG emissions (from 2030 to 2100) under the lower and higher RCPs scenarios are discussed for the regions and seasons presented in the evaluation section. In the tropical region, TCO evolution is further analysed by looking at the stratospheric (split into upper and lower regions, approximately

between 31–48 km and 17–25 km respectively) and tropospheric (<17 km) columns ozone. Historical and future global annual mean of TCO and associated uncertainty (± 1 standard deviation) for the ACCMIP and CMIP5 CHEM models and the IGAC/SPARC data set is given in Table 3.2.

To probe how different emissions of GHG affect stratospheric ozone, we only include in this section ACCMIP and CMIP5 models with full ozone chemistry (CHEM). In addition, we compare these results with the IGAC/SPARC database, generally used by those models with prescribed stratospheric ozone. Note that tropospheric column ozone under the RCPs at the end of the 21st century could lead to differences in TCO around 20 DU, due to differences in ozone precursors emissions (e.g. methane) (Young et al., 2013a). Again, vertical resolved ozone changes are presented to give insight on the vertical distribution of ozone changes (for the 1850–2100 and 2000–2100 periods).

Figure 3.3 shows, except for the extratropical regions in the SH, an increase in TCO from the pre-industrial period (Hist 1850) to the near-past (Hist 1980) owing to ozone precursors emissions. In the SH extratropical, due to special conditions (e.g. greater isolation from the main sources of ozone precursors and stratospheric cold temperatures during austral winter and early spring), there is a decrease in TCO that is particularly pronounced over Antarctica (−12.4 %). Between near-past and present-day (Hist 2000), a period characterised by ODS emissions, the TCO decreases everywhere, with the magnitude being dependent on the region. Thus, the relative change of TCO between the present-day and pre-industrial periods varies across different regions, mainly due to the competing effects of ozone precursors and ODS emissions (approximately, from 2.9 % in the NH midlatitudes and −34.9 % over Antarctica). Notice, however, that minimal stratospheric ozone depletion occurs before the 1960s.

Future TCO projected for the RCPs 2100 time slices relative to present-day are affected by the impact of the Montreal Protocol on limiting ODS emissions, climate change and ozone precursors emissions. TCO changes between 2000 and 2100 relative to the pre-industrial period for the low and high emission scenarios are in the range of approximately from −1.2 % to 2.0 % in the tropics and 28.3–31.7 % over Antarctica, respectively. Ozone “super-recovery”, defined here as higher stratospheric

Table 3.2. Global annual mean of TCO (DU)

Scenario	Year	ACCMIP*	CMIP5*	IGAC/SPARC
Hist	1850	294±16	300±19	293±1
	1980	300±19	306±20	292±2
	2000	291±16	297±20	281±1
RCP2.6	2030	295±16	301±20	288±1
	2100	297±18	302±20	294±0
RCP8.5	2030	300±17	306±20	290±1
	2100	316±23	323±11	304±0

*For the historical period and the RCPs emission scenarios considered here as calculated from the CHEM models and the IGAC/SPARC data set (see Sect. 3.2). The multi-model mean is given along with uncertainties (± 1 standard deviation).

ozone levels than those during pre-ozone depletion (1850), is found for ACCMIP CHEM models in RCP8.5 2100 in all regions and seasons, with the exception in the tropics and over Antarctica during austral spring. As expected from the above climate impacts, the biggest super-recovery is found, in the order of 12.6 % over the Arctic during boreal spring, and between 3.9–6.5 % at midlatitudes for the RCP8.5 2100 time slice. Midlatitudes inter-hemispheric difference – i.e. larger stratospheric ozone sensitivity to GHG concentrations in the NH – is likely associated with differences in transport (see also Figure 3.5b,d). Similar levels of stratospheric ozone super-recovery are found in the CMIP5 CHEM models. In contrast, the IGAC/SPARC database only projects small super-recovery in the NH polar region and at midlatitudes in the SH. These ozone super-recovery results are consistent with recent findings on stratospheric ozone sensitivity to GHG concentrations (Waugh et al., 2009a; Eyring et al., 2010b).

We give special attention to TCO projections in the tropics, since an acceleration of the BDC, due to increases in GHG concentrations would lead to a rise of tropospheric ozone-poor air entering the tropical lower stratosphere (Butchart et al., 2006; Butchart et al., 2010; SPARC-CCMVal, 2010; Butchart et al., 2011; Eyring et al., 2013a). In other words, ozone concentrations in the lower stratosphere would decrease with high GHG emissions.

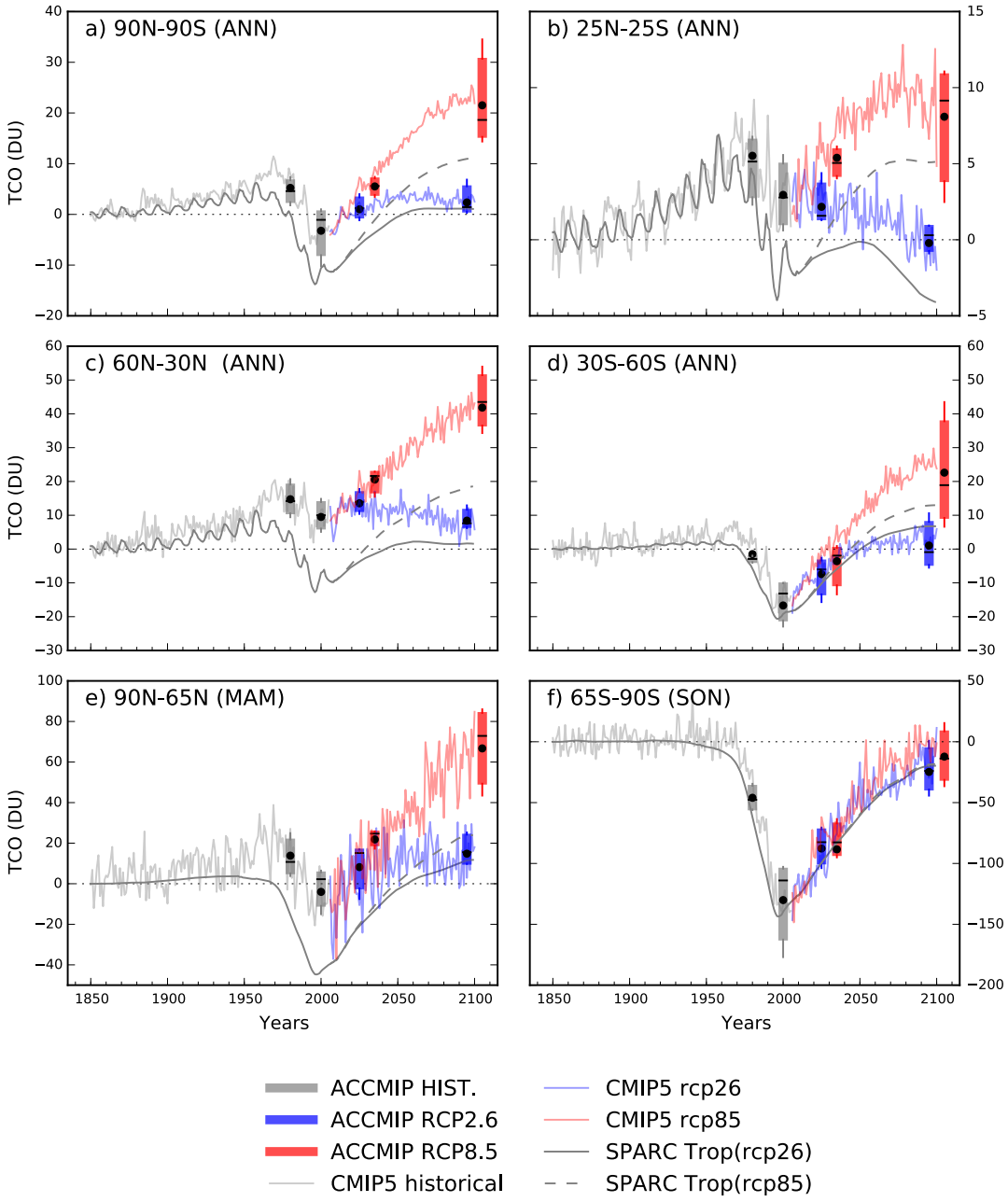

Figure 3.3. Total column ozone (DU) time series from 1850 to 2100, normalised to Hist 1850 time slice levels. The box, whiskers and line indicate the interquartile range, 95 % range and median respectively, for the ACCMIP CHEM models. In addition, the multi-model mean of the CMIP5 CHEM models and the IGAC/SPARC mean are shown.

Figure 3.4 presents upper (10–1 hPa) and lower (>15 hPa) stratospheric and tropospheric columns ozone in the tropics, from the pre-industrial period to the end of the 21st century. Tropospheric column ozone increases with higher ozone precursors

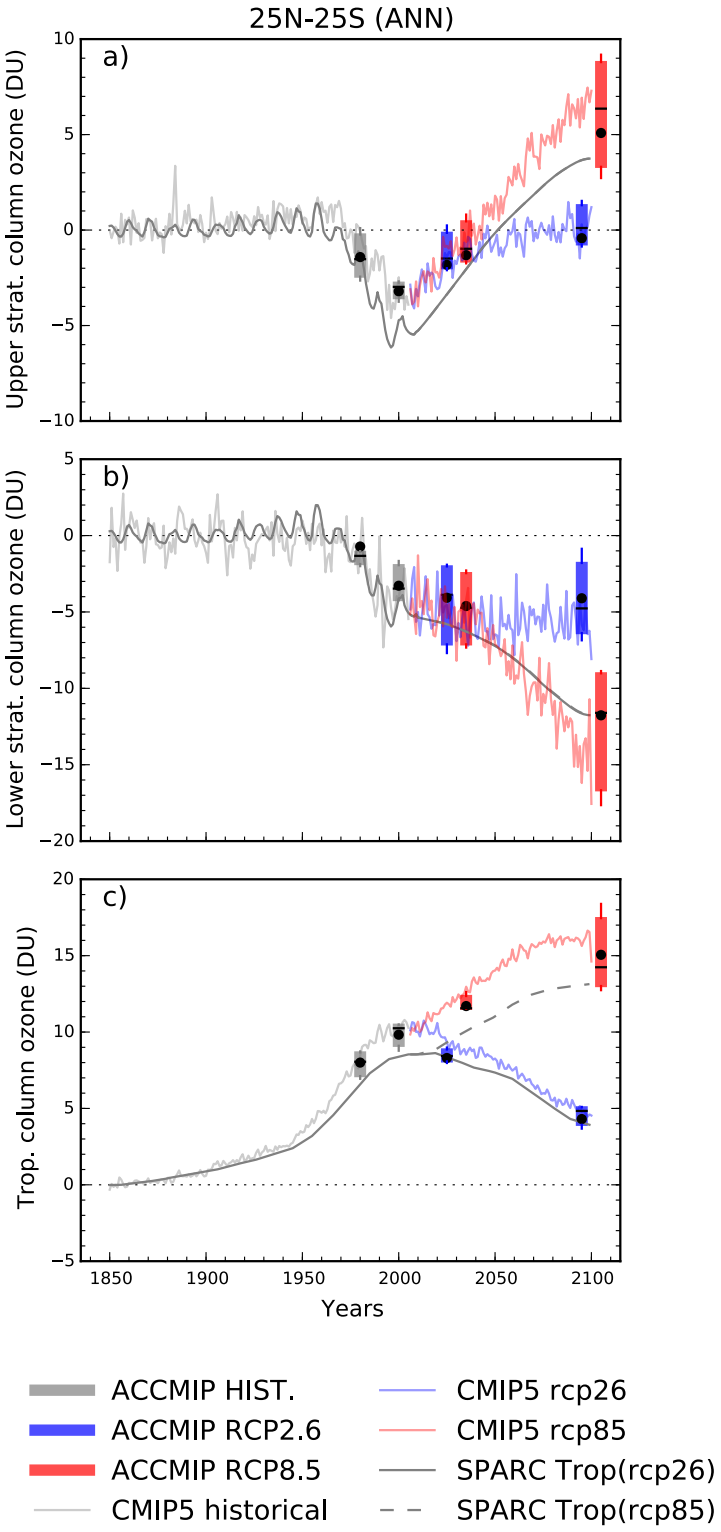

Figure 3.4. As Fig. 3.3, but for the upper stratosphere (10–1 hPa), lower stratosphere (>15 hPa) and tropospheric columns ozone (DU) in the tropics.

emissions during the historical period (1850–2000). Future emissions of ozone precursors (e.g. CO and NO_x) are fairly similar among the RCPs scenarios, decreasing to various degrees between the present-day and 2100 (van Vuuren et al., 2011). The exception is that the methane burden under the RCP8.5 scenario roughly doubles by the end of the 21st century (Meinshausen et al., 2011). Mainly due to the methane burden and the stratospheric ozone influence via STE, ACCMIP CHEM tropospheric column ozone change by 2100 relative to present-day is −5.5 DU and 5.2 DU, for the RCP2.6 and RCP8.5 scenarios respectively. For both stratospheric columns ozone, there is a small decrease from the pre-industrial period to present-day (−3.2–3.3 DU), which remained fairly constant by 2030 for both RCPs scenarios. Although ODSs concentrations decrease during the 21st century, two different stories occur in the second half of the century. In the upper stratosphere, ozone amounts return to pre-industrial levels under the low emission scenario by 2100. However, RCP8.5 2100 ozone levels relative to present-day increase 8.3 DU, due to a slow down of the ozone catalytic loss cycles, linked to the stratospheric cooling (e.g. Haigh and Pyle, 1982; Portmann and Solomon, 2007; Revell et al., 2012; Reader et al., 2013). In the lower stratosphere, ozone levels change little (−0.8 DU) by 2100 relative to the present-day for the RCP2.6, though decrease by −8.5 DU under the RCP8.5 scenario, likely due to the acceleration of the BDC. In summary, stratospheric column ozone by 2100 remains fairly similar to the present-day, although different stories are drawn in the upper and lower stratosphere. Future TCO changes in the tropics are mainly determined by the upper stratospheric ozone sensitivity to GHG concentrations, due to a large compensation between tropospheric and lower stratospheric column ozone changes in the RCP2.6 and RCP8.5 emission scenarios. Notice that tropospheric column ozone in the RCP8.5 2100 time slice is largely the result of future increase in methane.

Figure 3.5 presents vertically resolved ozone change between the Hist 1850 and RCPs 2100 time slices and between the Hist 2000 and RCPs 2100 time slices (top and bottom rows, respectively). In contrast to the tropics, the midlatitudes lower stratospheric ozone is positively correlated to GHG concentrations (Fig. 3.5, b and d) mainly due to the influx of relatively “rich” ozone air from lower latitudes (e.g. WMO, 2011) from a strengthened BDC. Additionally, the increase in methane emissions in the RCP8.5 scenario results in chemically-driven increases in ozone in this region (e.g. Randeniya et al., 2002; Revell et al., 2012; Reader et al., 2013).

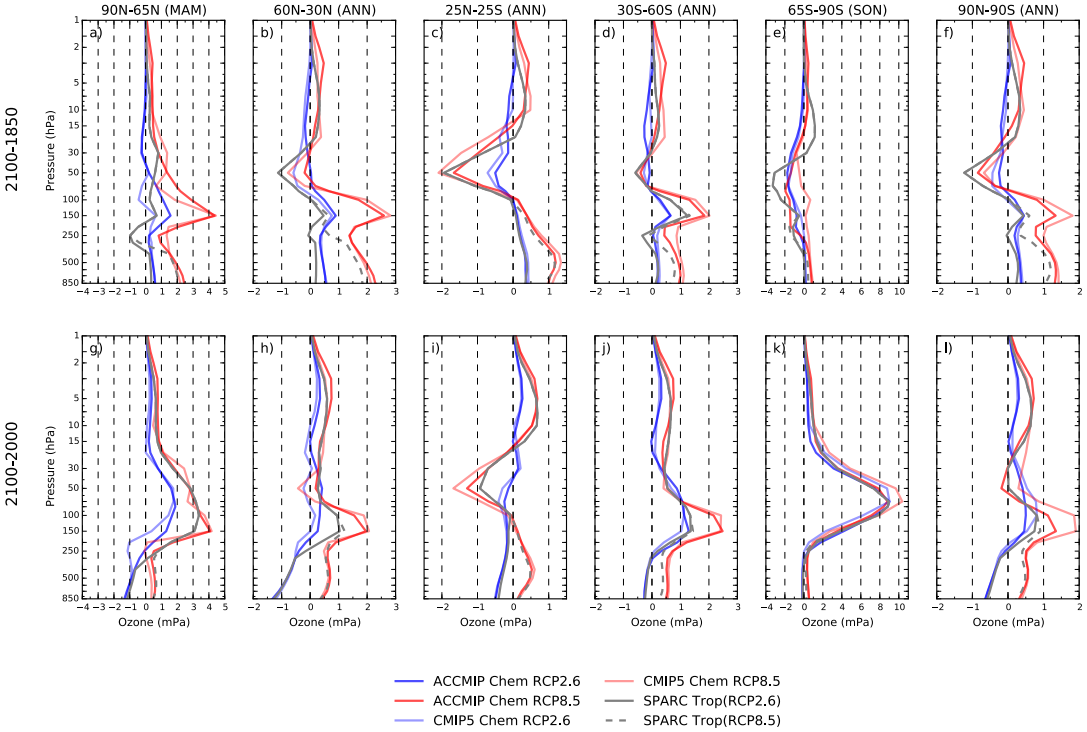

Figure 3.5. Vertically resolved ozone change between 2100 and 1850 (a to f), and 2100 and 2000 (g to l) time slices. Figures a-g are for Arctic boreal spring mean, b-h and d-j for NH and SH midlatitudes annual mean respectively, c-i for tropical annual mean, e-k for Antarctic austral spring mean, and f-l for global annual mean.

However, middle and upper stratospheric ozone sensitivity to GHG concentrations behaves the same as in the tropics. Substantial ozone increases are simulated by 2100, in the altitude region of the upper troposphere-lower stratosphere and the middle and upper stratosphere, relative to pre-industrial (1850) and present-day (2000) levels. We note that climate impact in ozone levels is weaker in the southern than in the northern midlatitudes for the ACCMIP and CMIP5 multi-model means, likely due to hemispheric differences in STE and ozone flux (Shepherd, 2008), which is in contrast to IGAC/SPARC data set. TCO for the RCP8.5 2100 time slice is 6.9–13.1 % higher than those simulated in the Hist 1850 time slice. While, the RCP2.6 2100 time slice in the northern midlatitudes is similar to present-day levels, in the southern midlatitudes is similar to pre-industrial levels. This is mainly due to regional differences in ozone precursors emissions and the tropospheric ozone contribution (Fig. 3.3, c-d).

Over the Arctic in boreal spring (Fig. 3.3e), results similar to those in the northern midlatitudes are found for all models, though higher stratospheric ozone sensitivity to GHG concentrations lead to approximately two times larger scenario differences for the 2100 time slice (37.7 DU between RCP2.6 and RCP8.5). In addition to the RCP8.5 emission scenario, ozone super recovery is also simulated under the RCP2.6 scenario by ACCMIP and CMIP5 CHEM models. The IGAC/SPARC data set projects similar results to those under the latter scenario. Note that the ACCMIP and CMIP5 multi-model means show a small increase in TCO by 1980 and no significant ozone depletion by 2000 relative to 1850. This is in sharp contrast to the polar region in the SH, which highlights both regional differences in ozone precursors sources and atmospheric conditions.

Over Antarctica during austral spring (Fig. 3.3f), TCO evolution is more isolated from GHG effects and ozone precursors than in other regions. In agreement with previous studies, ACCMIP and CMIP5 CHEM models project similar values under the lower and higher GHG scenarios (Austin et al., 2010; SPARC-CCMVal, 2010; Eyring et al., 2013a). TCO in the RCPs 2100 time slices remained below 1850s levels (−3.3–6.7 %). This suggests decreasing ODS concentrations during the 21st century as the main driver of stratospheric ozone in this region and season (i.e. ozone super-recovery is found for RCP8.5 2100 in other seasons). Furthermore, vertical distribution changes of stratospheric ozone in 2100, compared to 1850 (Fig. 3.5f1), and 2000 (Fig. 3.5f2), show small differences between the above scenarios (e.g. small sensitivity to GHG concentrations). Evolution of stratospheric ozone at high latitudes in the SH, particularly during spring season, has implications over surface climate due to modifications in temperature and circulation patterns as shown by previous studies.

3.4. Stratospheric ozone changes and associated climate impacts in the Southern Hemisphere

To probe stratospheric ozone evolution and climate interactions (1850–2100), we first examine simulated stratospheric temperatures in Sect. 3.4.1. SAM index evolution is presented in Sect. 3.4.2. Note that ozone loss over the Arctic in boreal spring is only around 25 % of the depletion observed in the Antarctic (see also Fig. 3.1e), and is not believed to have a significant role in driving NH surface climate (e.g. Grise et al., 2009; Eyring et al., 2010a; Morgenstern et al., 2010a).

3.4.1. Lower stratospheric temperature changes

Figure 3.6 shows recent stratospheric temperature decadal trends (1980–2000) at polar regions during springtime (March-April-May in the Arctic and October-November-December in the Antarctic). The figure compares temperature in the lower stratosphere (TLS) in the ACCMIP, CMIP5 and CCMVal2 models with observational estimates based on Microwave Sounding Unit (MSU) retrievals by the Remote Sensing Systems (RSS - version 3.3) (Mears et al., 2011), the Satellite Applications and Research (STAR - version 3.0) (Zou et al., 2006; Zou et al., 2009), and the University of Alabama in Huntsville (UAH - version 5.4) (Christy et al., 2003) (Fig. 3.6a-c). The TLS vertical weighting function from RSS is used to derive MSU temperature from climate models output. Temperature vertical profile decadal trends in the ACCMIP models (Fig. 3.6b-d) are compared against radiosonde products of the Radiosonde Observation Correction Using Reanalyses (RAOBCORE - version 1.5), Radiosonde Innovation Composite Homogenization (RICH-obs and RICH-tau - version 1.5) (Haimberger et al., 2008, 2012), the Hadley Centre radiosonde temperature product (HadAT2) (Thorne et al., 2005), and the Iterative Universal Kriging (IUK) Radiosonde Analysis Project (Sherwood et al., 2008) (version 2.01).

Over the NH polar cap in boreal spring, although ACCMIP, CMIP5 and CCMVal2 models are within observational estimates, all simulates weaker decadal trends (−0.5, −0.1 and −0.4 K dec^{-1}, respectively) than observed (−1.6 ± 3.4 K dec^{-1}) (Fig. 3.6a). Natural variability in models not constrained by observed meteorology is difficult to reproduce (Austin et al., 2003; Charlton-Perez et al., 2010; Butchart et al., 2011; Charlton-Perez et al., 2013; Shepherd et al., 2014) such as, the abnormally cold boreal winters in the mid-1990s (i.e. more PSCs formation), which resulted in enhanced ozone loss during boreal spring (Newman et al., 2001). Moreover, ACCMIP simulations, based on time slice experiments for most models, did not embrace that period, only those boundary conditions for 1980 and 2000 years. This weaker trend on stratospheric temperature is also seen in the vertical profile above around the tropopause (Fig. 3.6b).

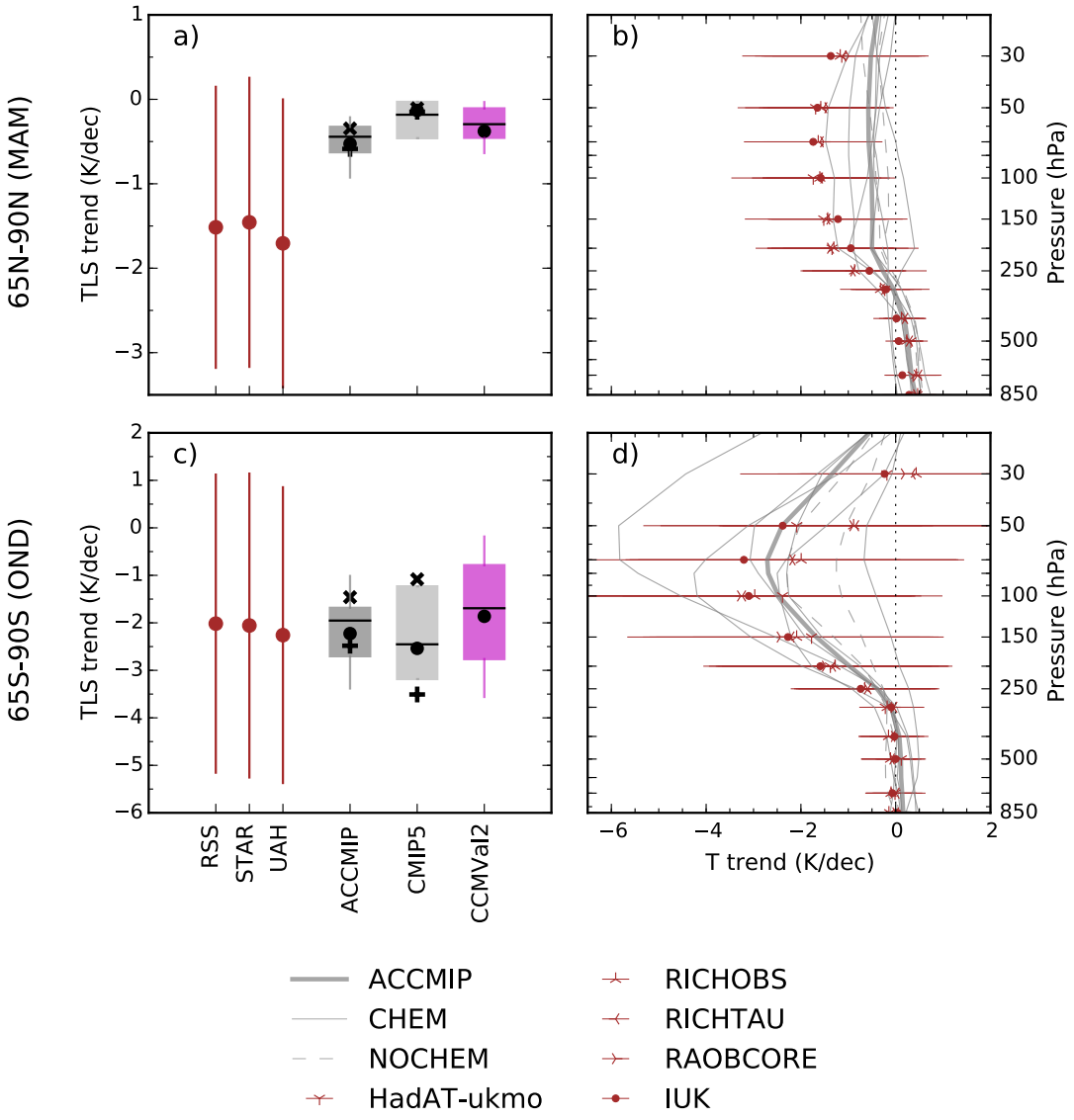

Figure 3.6. Temperature trends from 1980 to 2000 (K dec^{-1}). Figures (a) and (c) represent MSU temperature lower stratosphere (TLS) for MAM in the Arctic and for OND in the Antarctic. The box, whiskers, line, dot, 'plus' and 'cross' symbols show the interquartile range, 95 % range, median, multi-model mean, CHEM and NOCHEM means respectively, for the ACCMIP (light grey), CMIP5 (dark grey) and CCMVal2 (magenta) models. Figures (b) and (d) represent vertically resolved temperature (T) trends for the ACCMIP simulations (light grey). Observational data sets are represented by error bars indicating the 95 % confidence intervals (one tail).

Over Antarctica in austral spring, the ACCMIP and CMIP5 multi-model means are in very good agreement (−2.2 K dec^{-1}, −2.5 K dec^{-1} respectively) with satellite measurements (−2.1 ± 6.3 K dec^{-1}) (Fig. 3.6c). CHEM models (i.e. ACCMIP and CMIP5) and CCMVal2 multi-model mean tend to simulate larger negative trends than NOCHEM models, which may be due to the fact that the IGAC/SPARC ozone data set is at the lower end of the observational estimates, as has been shown in recent studies (Solomon et al., 2012; Hassler et al., 2013; Young et al., 2014). They argued the importance of the ozone data set for appropriate representation of stratospheric temperature, and in turn SH surface climate. Although, large uncertainties exist in this region and period, all ACCMIP individual models fall within the observational error estimates (Fig. 3.6d). Note that observational estimates are significant at the 95 % confidence levels, if year 2000 is removed from the linear fit (−2.95 ± 2.90, −3.02 ± 2.95 and −3.12 ± 2.87 K dec^{-1} for the RSS, STAR and UAH data sets, respectively), as this year was "anomalously" warm. The relatively large spread of the simulated stratospheric temperature trend for the observational period is consistent with the models spread of ozone in this region (Fig. 3.1f and 3.2f). The correlation between stratospheric ozone and temperature trends becomes evident by comparing TCO trends between the Hist 1980 and 2000 time slices and TLS trends for the same period between CHEM and NOCHEM models (i.e. large ozone depletion results in stronger stratospheric cooling trends).

Figure 3.7a depicts SH polar cap TLS long-term evolution (1850–2100) normalised to pre-industrial levels during austral spring. As commented above, stratospheric temperature can be perturbed by anthropogenic emissions of ODSs and GHGs, both having a net cooling effect. ACCMIP Hist 1980 and 2000 TLS time slices (−3.4 K and −7.9 K) are driven by the combination of ozone depletion and climate change since the pre-industrial period. In future projections, ozone recovery and GHG concentrations are expected to have an opposite effect on stratospheric temperatures. The slight temperature increased of the TLS by 2030 in the RCPs time slices relative to present-day, is very similar between the lower and higher RCPs emission scenarios (1.6 K and 1.2 K, respectively). By the end of the 21st century, the projected TLS under the RCP2.6 scenario returns to Hist 1980 levels, whereas it remains fairly unchanged under the RCP8.5 scenario relative to 2030. These two different stories suggest a key role of GHG concentration in the second half of the century, with significant implications for many aspects of the SH surface climate as

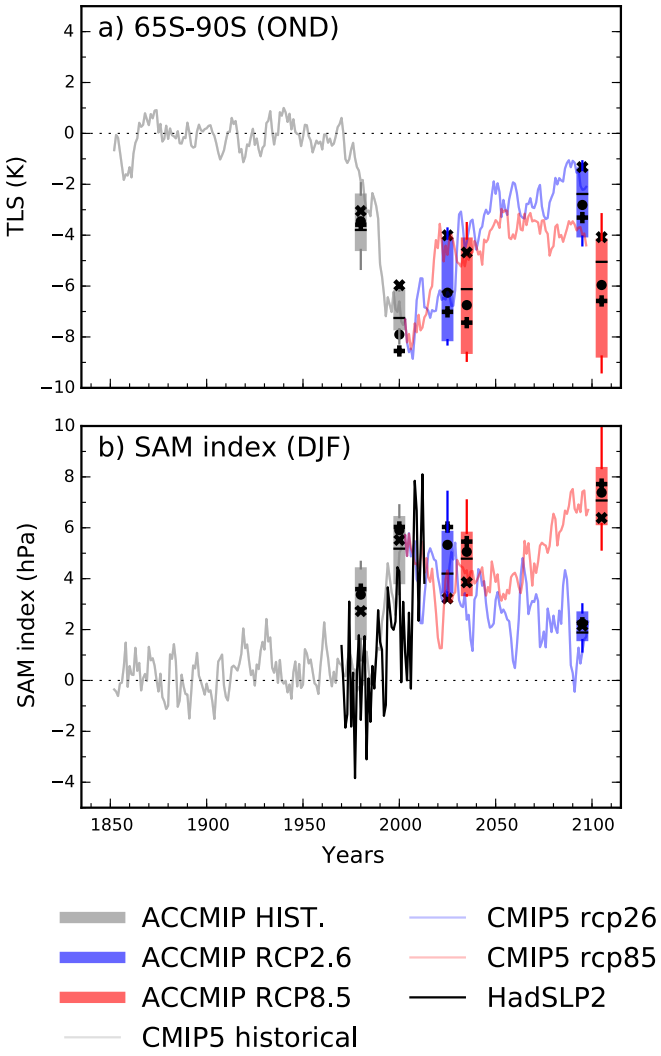

Figure 3.7. (a) MSU temperature lower stratosphere (TLS) and (b) SAM index time series from 1850 to 2100. The box, whiskers, line, dot, 'plus' and 'cross' symbols show the interquartile range, 95 % range, median, multi-model mean, CHEM and NOCHEM means respectively, for the ACCMIP models. The five years average of the CMIP5 multi-model mean is shown. In addition, HadSLP2 observational data set for (b) is represented by a solid black line. The ACCMIP models are normalised to Hist 1850 time slice levels, and the HadSLP2 data set and CMIP5 models are relative to 1860–1899 climatology.

reported previously (McLandress et al., 2011; Perlwitz, 2011; Polvani et al., 2011); see Sect. 3.4.2, Thompson et al. (2011) and Previdi and Polvani (2014) for a comprehensive review.

3.4.2. Southern Annular Mode evolution

The SAM index is defined as per Gong and Wang (1999), by subtracting the zonal mean sea level pressure (SLP) at 65ºS latitude from the zonal mean SLP at 40ºS latitude from monthly mean output. The SAM index is a proxy of variability in the jets captured by SLP anomalies at middle and high latitudes (e.g. Thompson and Wallace, 2000).

Figure 3.7b shows SAM index long-term evolution (1850–2100) normalised to 1850 levels during austral summer. Observational estimates based on the Hadley Centre Sea Level Pressure data set (HadSLP2) are shown from 1970 to 2012. The ACCMIP multi-model mean shows a positive trend between Hist 1980 and 2000 time slices (1.3 hPa dec^{-1}), coinciding with the highest ozone depletion period. Within uncertainty, this is weaker than observational estimates (2.2 ± 1.1 hPa dec^{-1}). ACCMIP CHEM and NOCHEM models show similar SAM index trends, although the latter presents weaker TLS trends (see Fig. 3.6c). As seen in Fig. 3.7a for the TLS in austral spring, by 2030 for both RCPs scenarios the ACCMIP multi-model mean shows a slight decrease in the SAM index relative to Hist 2000.

Two different stories are drawn from 2030 to 2100. The SAM index simulated under the RCP2.6 scenario tends to return to "normal" levels (−0.4 hPa dec^{-1}), as ODS concentrations and GHG emissions decrease during the second half of the century. In contrast, under the RCP8.5 scenario GHG concentrations increase, resulting in a positive trend of the SAM index (0.3 hPa dec^{-1}). By using two independent samples Student's t test, we find that SAM index changes between Hist 2000 and 2100 relative to Hist 1850, are significant for the RCP2.6 at the 5 % level, although is not significant for the RCP8.5. CMIP5 multi-model mean shows better agreement with observations during the record period (2.1 hPa dec^{-1}) than ACCMIP. During the second half of the 21st century (2030–2100), however, the CMIP5 multi-model mean shows consistent projections with the latter (−0.4 hPa dec^{-1} and 0.4 hPa dec^{-1} for RCP2.6 and RCP8.5, respectively).

3.5. Discussion

TCO trends in ACCMIP models compare favourably with observations, however, smaller ozone negative trends in the tropical lower stratosphere are simulated. It has been argued that tropical upwelling (or the BDC) is the main driver in this region

determining ozone levels (Lamarque and Solomon, 2010; Polvani and Solomon, 2012), with chemical processes playing a minor role (e.g. Meul et al., 2014). However, observed BDC and its seasonal cycle (Fu et al., 2010; Young et al., 2011) are poorly constrained in modelling studies (e.g. Butchart et al., 2006; Garcia and Randel, 2008; Butchart et al., 2010). This is important since ozone depletion determines to a large extent the temperatures in the lower stratosphere (e.g. Polvani and Solomon, 2012) (note that ACCMIP models show smaller negative temperature trends in this region compared to observations, not shown), and the latter triggers significant feedbacks in climate response (Stevenson, 2015). Models with less ozone depletion in the tropical lower stratosphere may have stronger climate sensitivity (Dietmüller et al., 2014; Nowack et al., 2015).

Long-term TCO changes relative to Hist 1850 in the ACCMIP models considered in this study, are least consistent for Hist 2000 in the Antarctic springtime (i.e. the period with large ozone losses) and for RCP8.5 2100 in general. The latter may be linked to uncertainties due to sensitivity of ozone to future GHG emissions (i.e. various direct and indirect processes affecting ozone amounts in the troposphere and the stratosphere). For example, CO_2 and methane mixing ratios increase by more than 3 and 4 times in RCP8.5 2100 relative to the pre-industrial period, respectively. Nevertheless, the ACCMIP and CMIP5 multi-model means, show consistent RCP8.5 2100 projections. Although TCO changes are relative to the Hist 1850, a period without direct measurements (e.g. estimates with large uncertainties), ACCMIP models show good agreement compared to other time slices. For example, the interquartile range (central 50 % of the data) varies approximately 3–8 % of the corresponding mean value across the regions and seasons considered here.

Stratospheric ozone has been shown to be asymmetrical over the SH polar cap (Grytsai et al., 2007). Prescribing zonal mean ozone fields in CCMs may have implications on SH climate (e.g. Crook et al., 2008; Gillett et al., 2009), particularly in early spring stratospheric temperatures (September-October) and, though less pronounced in November-December (Calvo et al., 2012; Young et al., 2013b). During strong depletion periods such as, in the recent past (1980–2000) and in the near-future (2000–2030), eliminating zonal asymmetry may result in a poor representation of stratospheric and tropospheric climate trends in the SH (Waugh et al., 2009b). Moreover, prescribing stratospheric ozone may lead to inconsistencies and skew the climate response (e.g. Nowack et al., 2015). We showed that NOCHEM models

simulated both weaker springtime TLS negative trends over the Antarctic compared to observational estimates, and stronger positive trends in the near-future compared to CHEM models. In addition, Young et al. (2014) found 20–100 % larger tropospheric climate responses in this region and season with a climate model driven by the BDBP data set compared to the SPARC/IGAC data set used in NOCHEM models here. ACCMIP CHEM and NOCHEM models show most disagreement on SAM index trends in the near-future, period with relatively strong ozone depletion (>Hist 1980). The former projects negligible trends compared to −0.57 hPa dec^{-1} and three times weaker negative trends than the latter, for the RCP2.6 and RCP8.5 respectively. This is consistent with CHEM and NOCHEM TLS springtime trends in this period and region. Nevertheless, ACCMIP models participating in this study agree with previous observational (e.g. Thompson and Solomon, 2002; Marshall, 2003, 2007) and modelling studies (e.g. Gillett and Thompson, 2003; Son et al., 2008; Son et al., 2009; Polvani et al., 2010; Son et al., 2010; Arblaster et al., 2011; McLandress et al., 2011; Polvani et al., 2011; Gillett and Fyfe, 2013; Keeble et al., 2014) on the SH surface climate response, measured here using the SAM index.

3.6. Summary and conclusions

This study has analysed stratospheric ozone evolution from 1850 to 2100 from a group of chemistry climate models with either prescribed or interactively resolved time-varying ozone in the stratosphere and participated in the ACCMIP activity (8 out of 16 models). We have evaluated TCO and vertically resolved ozone trends between 1980 and 2000, and examined past and future ozone projections under the low and high RCPs future emission scenarios (RCP2.6 and RCP8.5, respectively). Finally, we have assessed TLS and temperature profile trends at high latitudes in the recent past, and analysed TLS and SH surface climate response (diagnosed using the SAM index), from the pre-industrial period to the end of the 21st century.

Within uncertainty estimates, the ACCMIP multi-model mean TCO compares favourably with recent observational trends (1980–2000), although individual models often show significant deviations, particularly those models that include interactive chemistry. The closest agreement of TCO to observations is found over the Antarctic in austral spring (the ozone hole). The largest disagreement with observations is found for NH high latitudes during boreal spring, although this may be due to a series of

cold winters and associated additional PSCs formation during the mid- 1990s (Newman et al., 2001) – driving stronger ozone depletion – which are not captured by the use of time slice integrations (Hist 1980 and 2000). In addition, over the tropics the ACCMIP models fail to simulate ozone reductions in the lower stratosphere over the same period, which could be linked to trends in tropical upwelling (e.g. Polvani and Solomon, 2012).

The results corroborate previous findings (Waugh et al., 2009a; Eyring et al., 2010b, 2013a), suggesting that changes in stratospheric ozone due to future increases in GHG concentrations are most sensitive over the Arctic and the NH midlatitudes (37.7 DU and 16.1 DU difference between the RCP2.6 and RCP8.5 by 2100, respectively), with the smallest sensitivity in the tropics and over Antarctica (2.5 DU and 8.1 DU respectively). In the tropics, upper stratospheric ozone sensitivity to GHG concentrations will largely determine TCO future evolution, due to a trade-off between lower stratospheric and tropospheric columns ozone during the 21st century under the RCP2.6 and RCP8.5 emission scenarios.

The ACCMIP simulations of the trends in TLS and temperature profile over 1980–2000 agree well with satellite and radiosonde observations over the Antarctic in austral spring. ACCMIP CHEM models agree better with observations than the CMIP5 CHEM ensemble used here for the same period and region. However, ACCMIP models using prescribed time-varying stratospheric ozone (NOCHEM) show weaker trends than observational estimates in the recent past (1980–2000), and stronger positive trends than models with stratospheric chemistry online (CHEM) in the near-future (2000–2030). This highlights the importance of the ozone database used to drive models on the climate response. For example, Young et al. (2014) found large differences in SH surface climate responses when using different ozone data sets.

Overall, stratospheric ozone and associated climate impacts are fairly well represented by the ACCMIP ensemble mean in the recent past (1980–2000), and individual models also agree on the sign and distribution of past and future changes (1850–2100). In line with previous multi-model analyses (Son et al., 2008; Eyring et al., 2010a, 2013a; Son et al., 2010; Gillett and Fyfe, 2013), and observation studies (Thompson and Solomon, 2002; Marshall, 2003, 2007), the ACCMIP models show strong positive trends of the SAM index in austral summer during the ozone depletion period (1.3 hPa dec^{-1} 1980–2000), which is in agreement with observations

(2.2 ± 1.1 hPa dec^{-1}). While in the recent past both ozone depletion and increasing GHGs have favoured a strengthening of the SAM during summer, under projected ozone recovery they will drive the SAM into opposite directions. Under the low emission scenario, the SAM index tends to return to pre-industrial levels from around the second half of the 21st century (−0.4 hPa dec^{-1} between 2030–2100); i.e. the impact of ozone recovery is stronger than GHG. In contrast, with the higher emission scenario, the GHG-driven SAM trend exceeds the opposing ozone recovery-driven trend, and the SAM index continues on its positive trend (0.3 hPa dec^{-1} between 2030–2100).

In this study we have presented stratospheric ozone evolution (1850–2100) using a number of models that participated in the ACCMIP activity. We have shown how stratospheric ozone is represented in the ACCMIP ensemble compared to observational estimates, as well as previous multi-model activities, to put into context current model simulations. We have demonstrated both its key role in the present and future SH climate and the importance of how it is represented in climate models. Particularly, we have focused on evaluating both simulations with interactive ozone chemistry and simulations with prescribed ozone concentrations. A main outcome of this analysis is that largest disagreements between models (i.e. inter-model spread) arise from the various chemistry-climate interactions (i.e. stratospheric cooling and circulation changes). Hence these results, and work over the last decade (e.g. SPARC-CCMVal, 2010; Nowack et al., 2015), have shown that changes in stratospheric ozone are tightly coupled to the climate, supporting the idea of including these processes interactively in models. It is clear that our ability to understand future climate will depend on models that can reliably simulate these chemistry-climate feedbacks.

Acknowledgements. This work was supported by NERC, under project number NE/L501736/1. F. Iglesias-Suarez would like to acknowledge NERC for a PhD studentship. We thank the modelling groups that contributed to the ACCMIP, CMIP5 and CCMVal2 model intercomparison projects and provided the model results used in this study.

Chapter 4

Multi-decadal climate signatures in the tropical stratosphere and the contribution to recent ozone trends

F. Iglesias-Suarez[1,2], P. J. Young[1,2,3], O. Wild[1,2], E. Ryan[1,2], R. R. Garcia[4], D. E. Kinnison[4], J.-F. Lamarque[4], D. R. Marsh[4], Michael J. Mills[4] and A. K. Smith[4]

[1]Lancaster Environment Centre, Lancaster University, Lancaster, UK
[2]Data Science Institute, Lancaster University, Lancaster, UK
[3]Pentland Centre for Sustainability in Business, Lancaster University, Lancaster, UK
[4]Atmospheric Chemistry Observations and Modeling Laboratory, National Center for Atmospheric Research, Boulder, Colorado, USA
Correspondence to: F. Iglesias-Suarez (n.iglesiassuarez@lancaster.ac.uk)

The authors and their contributions are listed below.

Fernando Iglesias-Suarez: Devised research, performed simulations with WACCM, processed the data, analysed the data, and wrote the manuscript. **Paul J. Young and Oliver Wild:** Helped to synthesise, interpret the results and compile the manuscript. **Edmund Ryan:** Helped to perform Fourier transform decompositions. **Rolando R. Garcia, Doug E. Kinnison, Jean-François Lamarque, Daniel R. Marsh, Michael J. Mills and Anne K. Smith:** Supported WACCM simulations, and helped interpret the results and compile the manuscript.

Abstract

Ozone in the tropical middle stratosphere decreased around -0.16 ± 0.04 ppm dec^{-1} in the 1990s and remained persistently low since. Using chemistry-climate model simulations and observations, we show that multi-decadal climate variability in the Pacific Ocean sea surface temperatures – the Interdecadal Pacific Oscillation – can account for about 50 ± 10 % of the recent negative trends in mid-stratospheric tropical ozone, via dynamical and chemical coupling. A regression analysis indicates that acknowledging low frequency variability can help interpret previous observationally derived changes in the Brewer-Dobson circulation since year 1979. These findings also demonstrate strong links between stratosphere-troposphere variability at decadal time scales and their potential role on future ozone recovery detection.

4.1. Introduction

The global ozone layer has declined by about 3 % since the 1980s due to anthropogenic emissions of ozone-depleting substances (ODSs). In recent years the successful implementation of the Montreal Protocol and its Amendments and Adjustments has led to the first signs of recovery in the global ozone layer (WMO, 2014). Surprisingly, mid-stratospheric tropical ozone shows a negative trend since the 1990s despite a decline in the amount of ODSs in the stratosphere. The tropical middle stratosphere is a key region where most ozone is produced, and ozone loss rates here are most sensitive to reactive nitrogen (NO_y) abundance, with ozone variability being determined by both NO_y source gas emissions (nitrogen oxide, N_2O) and changes in transport (Nedoluha et al., 2015). Here we use observational estimates and model simulations to show for the first time how multi-decadal internal climate variability, namely the Interdecadal Pacific Oscillation (IPO), has an impact on mid-stratospheric tropical ozone, and can account for about half of the observed trends. We propose a mechanism that involves both dynamical and chemical processes to explain an internal low frequency variability of the ozone layer in the tropical middle stratosphere.

Ozone variations in the tropical mid-stratosphere may be driven by a number of processes on different time scales. The observed slow and steady increase in N_2O emissions may have enhanced stratospheric ozone loss chemistry, resulting in a long-term net decrease (Portmann et al., 2012). Although ozone depletion due to ODSs is

less effective in the tropics than in polar lower stratosphere, it may have played an indirect role via ozone loss at higher latitudes in the 1980s and 1990s (WMO, 2014). On decadal time scales, the 11-year solar cycle is known to affect stratospheric ozone, particularly in the tropical upper and lower stratosphere (Soukharev and Hood, 2006; Gray et al., 2010). However, recent trends in mid-stratospheric tropical ozone show little relationship with changes in solar radiation (Nedoluha et al., 2015). Other drivers of ozone change in this region include dynamical changes associated with the quasi-biennial oscillation (QBO), which is characterized by downward propagating equatorial zonal winds oscillations (~ 28 month periodicity) between easterlies and westerlies from the upper to the lower stratosphere. In addition, the El Niño/Southern Oscillation (ENSO) is known to affect the tropical stratosphere via changes in tropical upwelling (Marsh and Garcia, 2007; Randel et al., 2009a; Calvo et al., 2010). Nevertheless, the QBO and ENSO events drive changes in dynamics on a shorter time scale than the observed trends. Overall, the cause of the recent sharp decrease (1990–2000) and anomalously low values since ~ 2000 in mid-stratospheric tropical ozone are inconsistent with these recognized mechanisms.

Figure 4.1 shows the IPO fingerprints derived from the Extended Reconstructed Sea Surface Temperature (ERSST version v4) database (Huang et al., 2015). The observed IPO regression pattern over the historical period (Fig. 4.1A) shows three distinct regions, which best encapsulate multi-decadal variability of sea surface temperatures (SSTs) in the Pacific Ocean. Warming over the central-eastern equatorial Pacific and cooling over the central-west North/South Pacific are associated with the positive phase of the IPO. The observed SSTs change between 1990–1999 and 2001–2010 (Fig. 4.1B) – period of interest in this study – reveals a shift from a positive to a negative phase of the IPO. Internally generated SSTs variability, particularly in the tropics, drives changes in the stratospheric mean mass transport via the Brewer-Dobson circulation, BDC (Oman et al., 2009; Oberländer et al., 2013; Butchart, 2014). Anomalously warm tropical SSTs are associated with a relatively enhanced circulation in the stratosphere, whereas the opposite occurs for anomalously cold tropical SSTs.

Previous studies have demonstrated strong correlations between interannual and decadal shifts in Pacific Ocean SSTs and dynamics in the lower stratosphere through ENSO and the IPO (Randel et al., 2009a; Calvo et al., 2010; Jadin et al., 2010), although the QBO may mask signals in the upper atmosphere (see Sect. 4.6). In

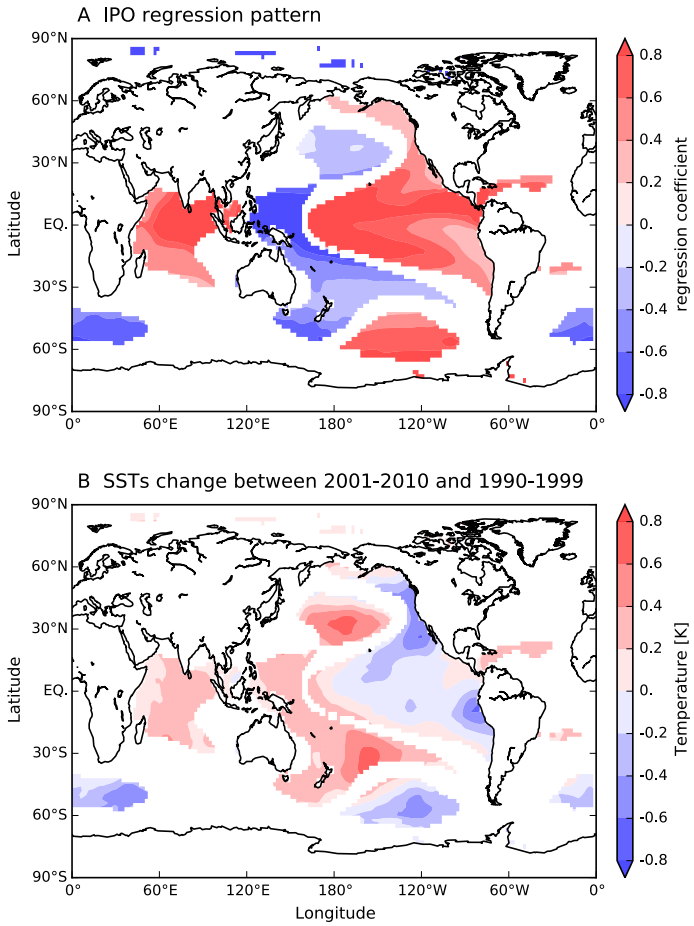

Figure 4.1. Observed IPO patterns derived from the ERSST dataset. (**A**) Regression of monthly SSTs anomalies onto the IPO time series (1901–2014). (**B**) SSTs change between 1990–1999 (positive IPO phase) and 2001–2010 (negative IPO phase). Coloring is for statistically significant correlation at the 95 % confidence interval between the IPO and SSTs.

the tropical middle stratosphere ozone loss is sensitive to catalysis by odd nitrogen (NO_y) species, and the partitioning between N_2O and the reactive NO_y is determined by the relative time scales of transport and chemistry (Nedoluha et al., 2015). For example, a relatively rapid circulation results in less N_2O photodissociated into reactive NO_y (more N_2O is transported upwards), meaning reduced ozone loss and higher ozone concentrations in the mid-stratosphere. The opposite is the case for a reduced circulation.

Here we use a combination of model simulations and recent observational estimates of ozone and Pacific SSTs to demonstrate internal low frequency variability in ozone in the tropical middle stratosphere related to this transport-N_2O/NO_y mechanism. In addition, we discuss that acknowledging multi-decadal internal climate

variability can help better constrain recent observed changes in the BDC. This result is crucial to understand ozone trends and recovery better, and distinguish between natural and forced signals.

4.2. Recent mid-stratospheric tropical ozone changes

To investigate recent decreases in mid-stratospheric tropical ozone we used observational estimates and model simulations. The Stratospheric Water and Ozone Satellite Homogenized (SWOOSH version 2.5) database provides merged and homogenized ozone measurements from a range of satellites (Davis et al., 2016). To explore the mechanism and processes driving these ozone changes, a global atmospheric model (the Whole Atmosphere Community Climate Model, WACCM) run with observed SSTs, QBO and solar variability is used here (Marsh et al., 2013; Tilmes et al., 2016). WACCM includes fully coupled ozone chemistry in the troposphere and stratosphere, which responds to changes in atmospheric composition and incoming UV radiation. Figure 4.2A presents the time series of mid-stratospheric tropical (20°N–20ºS) ozone anomalies between 1990 and 2005. Simulated 10-year running mean ozone trends – WACCM_Recent-Past, blue solid line – (-0.17 ± 0.07 ppm dec^{-1}) are in very good agreement with observational based estimates (-0.16 ± 0.04 ppm dec^{-1}) for the 1990–2000 period. Since the beginning of the 21st century, ozone levels in this region are persistently low.

Figure 4.2B shows the low-pass filtered IPO (Chebyshev low-pass filter with 13-year cutoff period and a filter order of 6 unless otherwise specified) derived from monthly means of the Extended Reconstructed Sea Surface Temperature (ERSST version v4) database (Huang et al., 2015) and the modeled WACCM_Recent-Past surface temperatures (Henley et al., 2015). A shift from a positive to negative phase of the IPO is coincident with a sharp decrease in ozone in the tropical middle stratosphere in the 1990s. After 2000, observations and simulations show a negative phase of the IPO and anomalously low ozone levels in this region. SSTs can affect dynamics in the stratosphere (Butchart, 2014) and these results are consistent with multi-decadal variability in mid-stratospheric tropical ozone being linked to internal climate variability in the troposphere – namely the IPO. However, a number of processes could also be playing a role, particularly those that involve changes in ODS and N_2O concentrations.

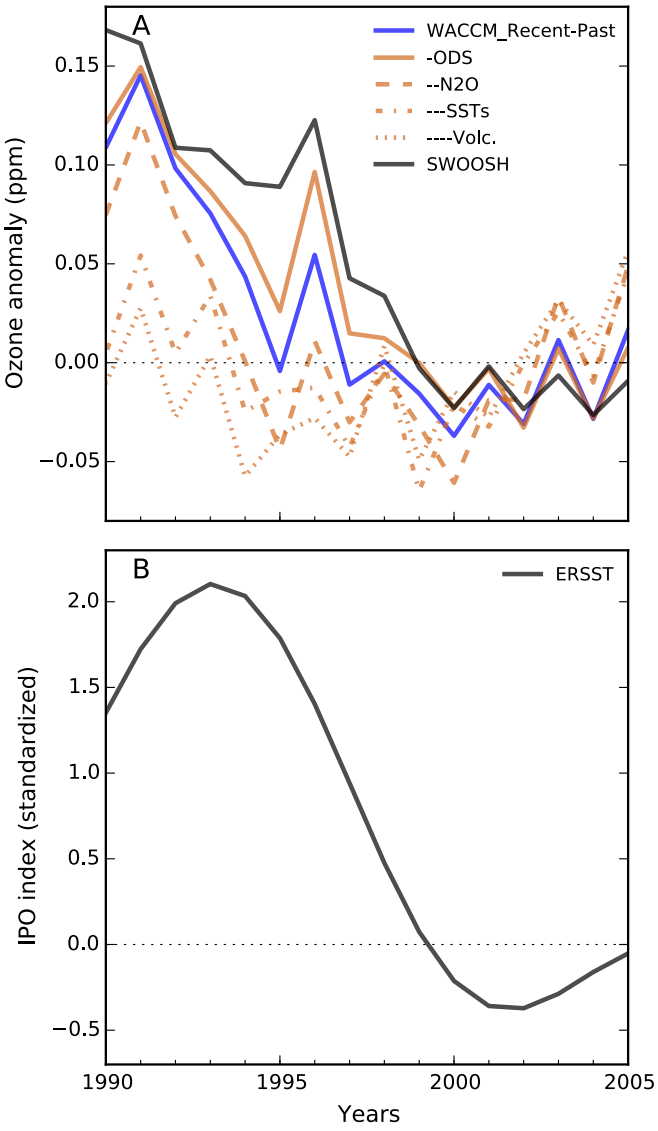

Figure 4.2. Simulated and observed recent changes in mid-stratospheric tropical ozone and the Interdecadal Pacific Oscillation (IPO) from 1990 to 2005. (A) Ozone 10-year running mean between 20ºN and 20ºS at 10 hPa relative to the period between 1995–2005, for WACCM_Recent-Past (solid blue line) and the SWOOSH data base (solid black line). In addition, the same is shown for the individual contributions of ODSs (−ODS; solid orange line), N_2O (−−N2O; dashed orange line), SSTs (−−−SSTs; dashed-dotted orange line), and mayor volcanic eruptions (−−−−Volc.; dotted orange line), by successively removing the impacts of these drivers to the WACCM-recent past simulation. (B) The IPO (standardized and low-pass filtered) as observed from the ERSST dataset (solid black line) and calculated from the WACCM_Recent-Past simulation (solid blue line).

A series of sensitivity simulations were conducted to assess the relative importance of different drivers in recent changes in mid-stratospheric tropical ozone, by imposing one single perturbation at a time: anthropogenic emissions of (1) ODSs and (2) N_2O, (3) major volcanic eruptions and (4) SSTs variability (see Sect. 4.6). Figure 4.2A shows that the impact of N_2O and ODS concentrations on ozone in the last decade of the 20th century, coinciding with the shift in the IPO phase, accounts for up to a quarter of the simulated trend (respectively 15 ± 18 % and 7 ± 23 %, with one standard error). However, in the inner tropics (5ºN–5ºS), increases in N_2O levels explain only 8 ± 35 % and the impact of ODSs is negligible. Removing major volcanic eruptions, El Chichón (1982) and Mt Pinatubo (1991), explains an additional 25 ± 15 % of the former trend. Multi-decadal variability in SSTs accounts for about 50 ± 10 % of the trend. These results indicate that recent negative trends in ozone in the tropical middle stratosphere are not primarily the result of anthropogenic emissions (N_2O and ODSs), but instead due to natural forcings, mainly associated with internally generated variability in SSTs.

4.3. Dynamical and chemical processes

Using observations to disentangle the mechanism linking internally generated decadal climate variability in SSTs with ozone in the tropical middle stratosphere is difficult, due to the interacting processes involved, changing atmospheric composition and the relatively short record period. Here we use WACCM with a fully coupled configuration (i.e. global earth system model), which includes interactions among the atmosphere, ocean, land and sea ice (Marsh et al., 2013). The model was run with full ozone chemistry with constant pre-industrial boundary conditions (WACCM_Pre-Industrial). These simulations artificially allow separation of the key processes involved in both an externally unforced system (Figure 4.3A) and the recent past (Figure 4.3B).

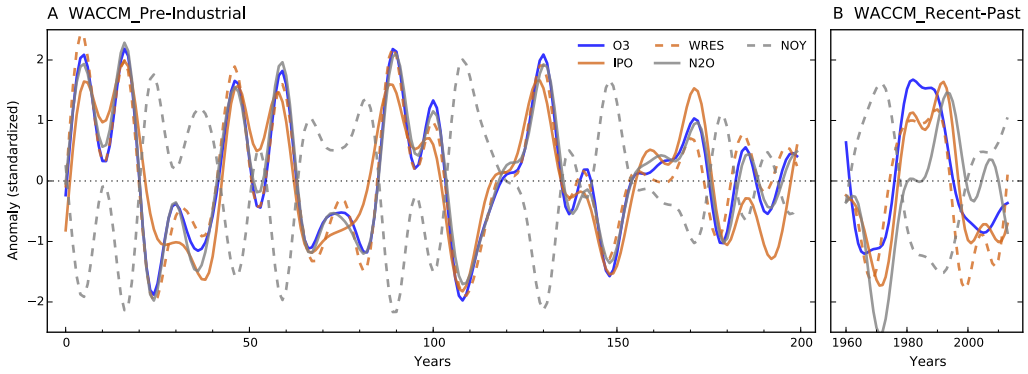

Figure 4.3. Dynamical and chemical processes linking the IPO with mid-stratospheric tropical ozone. Low pass filtered anomalies (standardized) of the IPO (solid orange line), and the residual mean vertical velocity ($\overline{w}^*$; WRES, dashed orange line), N2O (solid grey line), NOY (dashed grey line) and partial column ozone (O3, solid blue line) averaged between 20ºN–20ºS and 5–10 hPa, for (A) WACCM_Pre-Industrial (200 years with pre-industrial boundary conditions) and (B) WACCM Recent-Past (1960–2010).

Variability in SSTs can influence the BDC, which controls transport of air and trace constituents within the stratosphere and is characterized by upwelling in the tropics, poleward movement and downwelling in extratropical regions (Oberländer et al., 2013). Previously, interannual SSTs variability in the tropical Pacific Ocean associated with ENSO has been linked to changes in lower stratosphere tropical upwelling and with relatively small (0.8 %) but significant influence in the tropical middle stratosphere (Marsh and Garcia, 2007). Figure 4.3 shows the time series of standardized anomalies for the IPO and the residual mean vertical velocity – $\overline{w}^*$, a quantitative measure of the strength of the BDC (Andrews et al., 1987) – in the tropical middle stratosphere, for constant pre-industrial conditions (200 years) and recent past (50 years) simulations. Decadal variability in Pacific Ocean SSTs is strongly correlated with changes in transport in this region for both, unforced (i.e. natural variability) and perturbed (i.e. 'real world') simulations ($r=0.8$, $p < 0.01$). The low-frequency signal due to changes in SSTs in the middle stratosphere may arise from longer and sustained conditions in the background climate state associated with the position of the subtropical tropospheric jets (Palmeiro et al., 2014) and decadal variability in the QBO (see Sect. 4.6), which is consistent with the ENSO impact at shorter time scales (Marsh and Garcia, 2007).

Variability in the BDC affects thermodynamics and composition in the stratosphere. Temperature changes in the tropical middle stratosphere modulate ozone loss, but NO_y chemistry is the most important driver in this region (Lary, 1997; WMO, 1999). The abundance of NO_y species is controlled by N_2O entering the stratosphere and by dynamics. Figure 4.3 shows how decadal time scale variability in NO_y is strongly anti-correlated with the residual mean vertical velocity (−11 %/10*mms^{-1}; Fig. 4.3A) and is a robust feature in the simulated recent past (−6 %/10*mms^{-1}; Fig. 4.3B). Relatively rapid circulation results in less N_2O photodissociated or oxidized into NO_y species and vice versa, which is the result of coupled transport and chemistry processes (Olsen et al., 2001).

Figure 4.3 also demonstrates how mid-stratospheric ozone is closely associated with the leading internally generated variability in SSTs on decadal time scales. These results support a mechanism that involves dynamical (i.e. BDC) and chemical (i.e. ozone loss via NO_y chemistry) processes to explain this IPO-ozone link (Plummer et al., 2010; Nedoluha et al., 2015). Briefly, a positive phase of the IPO (anomalously warm tropical SSTs) is correlated with a relatively rapid BDC in the lower and mid stratosphere. In turn, this increases the partitioning between inactive and reactive nitrogen species (N_2O/NO_y), which reduces ozone loss here. The net result is relatively high ozone levels, whereas the opposite is true during a negative phase of the IPO. Note that the shift between the two phases in the IPO is associated with 'sharp' trends in ozone (e.g. 1990–2000), followed by a relative steady ozone levels (e.g. 2000–2010).

4.4. Brewer-Dobson circulation signals

We use the former WACCM simulation of the recent past to explore the multi-decadal variability in the BDC, i.e. the 'unforced' signal associated with the IPO. Figure 4.4 shows BDC trends over the satellite period (since 1979). Focusing on this period allows clearer comparison with previous observationally based studies. Observational estimates of the BDC are derived from indirect measurements and changes in the recent past are highly uncertain (Engel et al., 2009; Hegglin et al., 2014; Ray et al., 2014). Moreover, climate models (Butchart et al., 2006; Garcia and Randel, 2008; Li et al., 2008; Butchart et al., 2010; Lin and Fu, 2013; Aschmann et al., 2014) and reanalysis datasets (Bönisch et al., 2011; Diallo et al., 2012; Seviour et al., 2012;

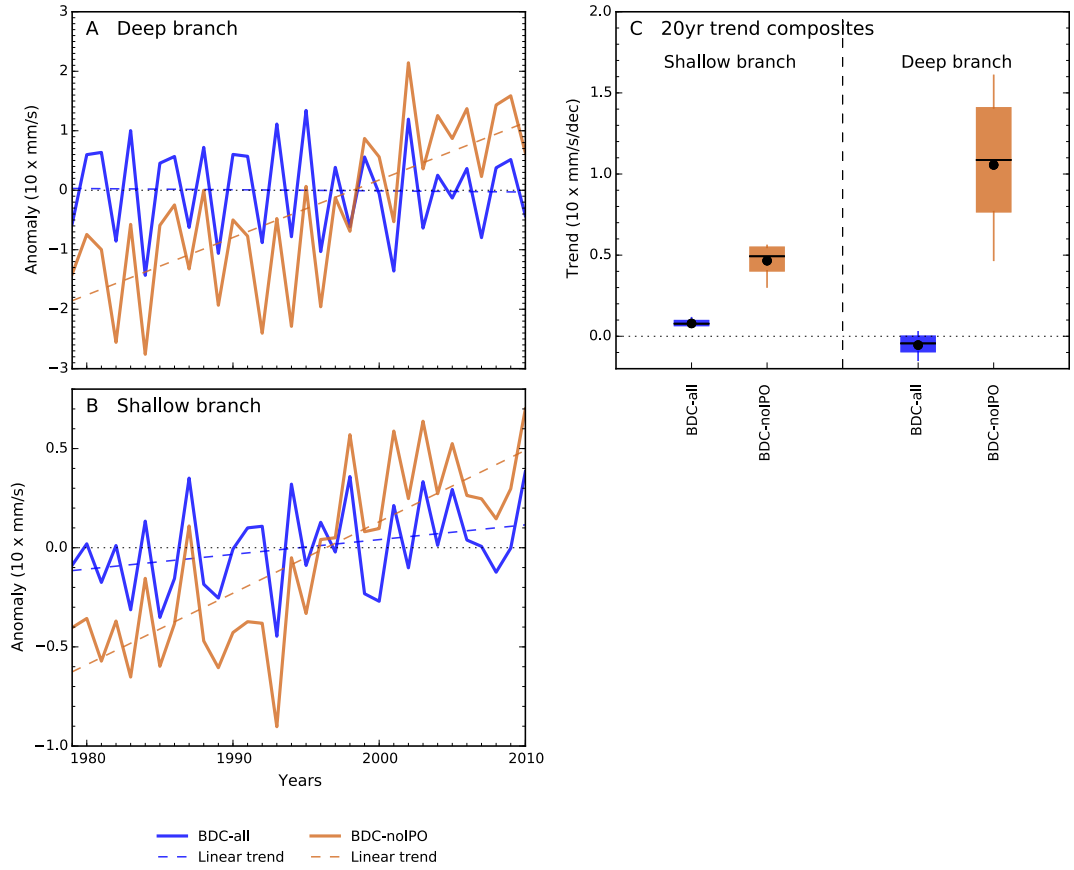

Figure 4.4. Recent past trends in the Brewer-Dobson circulation (BDC) from 1979 to 2010. (A-B) Annual mean anomalies for WACCM_Recent-Past of the residual mean vertical velocity ($\overline{w}^*$) – BDC-all, solid blue line – and $\overline{w}^*$ minus $\overline{w}^*$-IPO – BDC-noIPO, solid orange line – averaged over 20ºN–20ºS at (A) 10 hPa and (B) 70 hPa, representing the deep and shallow branches respectively. Linear trends are shown for BDC-all (dashed blue line) and BDC-noIPO (dashed orange line) from 1979 to 2009 (20 years), approximately coinciding with previous observational and assimilated data studies (Engel et al., 2009; Bönisch et al., 2011; Seviour et al., 2012; Abalos et al., 2015; Fu et al., 2015). (C) Composites of the 20-year running trend. The box, whiskers, dot, and line indicate the interquartile range, 95% range, mean and median respectively, for the BDC-all (blue) and BDC-noIPO (orange) in the shallow and deep branches.

Monge-Sanz et al., 2013; Abalos et al., 2015; Fu et al., 2015) do not necessarily agree with those changes observed in the tropical upwelling. Therefore, the focus here is not on the absolute circulation in the stratosphere but rather on its relative changes and uncertainty at multi-decadal timescale due to both internally generated and external

forcings in relatively short periods. By accounting for the IPO-like variability in the BDC time series we can analyze the long-term residual signal, which may be largely linked to the increase in the greenhouse gases (GHGs) concentration and ozone depletion in the last decades (Butchart et al., 2010). The BDC is split into shallow and deep branches (70 hPa and 10 hPa respectively) (Randel et al., 2006), corresponding to those regions where the IPO is strongly correlated with tropical upwelling in the climate model used here. The simulated annual mean circulation (BDC-all) and its residual after removing multi-decadal variability associated with the IPO (BDC-noIPO), are shown in Fig. 4.4A (deep branch) and Fig. 4.4B (shallow branch). BDC-all shows a positive trend in the shallow branch and an insignificant negative trend in the deep branch (2.9 ± 1.6 % dec^{-1} and -0.5 ± 3.6 % dec^{-1} respectively). However, the BDC-noIPO shows steeper and statistically significant positive trends in both branches (14.4 ± 2.1 % dec^{-1} and 6.8 ± 1.3 % dec^{-1} respectively).

To explore the trend sensitivity to different periods, successive 20-year trends (1979–1998, 1980–1999 etc.) are shown in Fig. 4.4C, to illustrate the robustness of secular changes in the shallow and deep branches of the BDC over 1979–2010. The 20-year running trend composites – i.e. 12 members – of the BDC-all show a positive trend in the shallow branch significant at the 5% level, and again, a not significant negative trend in the deep branch, which is consistent with above results. These ranges gauge the chances of finding either a 20-year positive or negative trend in tropical upwelling from 1979 to 2010 with regard of the chosen period. Although, the spread in the BDC-noIPO is larger as compared with the former case where internal decadal variability is neglected, both the shallow and deep branches show positive and significant trends regardless the chosen period – between 16–22 % dec^{-1} and 5–10 % dec^{-1} using the interquartile range of the corresponding branch. Note the larger spread in the 20-year trend composites of the simulated deep branch compared to that of the shallow branch is the result of a greater variance in the former, both for the BDC-all and BDC-noIPO.

Overall, Fig. 4.4 shows that trends on the BDC in relatively short periods (including current observational data sets) are very sensitive to a particular period chosen. Accounting for internal climate variability can help interpreting conflicting results, particularly from observational estimates and reanalysis datasets, and distinguish between anthropogenic and natural factors driving recent changes. Recent studies based on observations (Engel et al., 2009; Hegglin et al., 2014; Ray et al.,

2014) and assimilated data (Bönisch et al., 2011; Diallo et al., 2012; Seviour et al., 2012; Monge-Sanz et al., 2013; Abalos et al., 2015; Fu et al., 2015) have generally focused on trends in the BDC during the last three decades and found conflicting results of what it is expected due to increasing GHGs concentration. Linear trends of the BDC-all and BDC-noIPO from 1979 to 2010 (Fig. 4.4A and B) suggest that internal climate variability may have been a major factor driving the BDC. A robust signal on the BDC arises when multi-decadal natural variability is not neglected – i.e. positive trend at any given period in both branches, largely associated to increasing concentrations of GHGs and stratospheric ozone depletion (Butchart et al., 2010). The tropical upwelling in the BDC-noIPO used in Fig. 4.4 is the product of extracting the low frequency variability from the residual vertical velocity (see Sect. 4.6), which removes variability or 'noise' at multi-decadal timescale linked to the IPO (Henley et al., 2015). Although, this removes a major source of decadal variability in the Pacific Ocean's SSTs, other sources of internally generated variability may remain (Wu et al., 2011; Trenberth and Fasullo, 2013). These results can help reconcile previous findings of changes on the BDC in the last decades from observational estimates and assimilated data with previous modeling studies.

4.5. Conclusions

Observational estimates and sensitivity simulations suggest a link of the recent negative trends in the 1990s and relative low levels since year 2000 in mid-stratospheric tropical ozone with multi-decadal internal climate variability (Fig. 4.2) – i.e. predominant negative phase of the IPO – and associated reduced tropical upwelling that affects ozone loss in this region via NO_y chemistry (Fig. 4.3). Although the IPO index is used here as a proxy for multi-decadal variability in the Pacific Ocean, we acknowledge it is not a single phenomenon but rather a combination of various physical processes dominated by ENSO-like decadal variability (Newman et al., 2016). The Pacific Decadal Oscillation (PDO) is a similar proxy, but not equivalent, as it is more influenced by the Aleutian Low (Newman et al., 2016). We find strong agreement between the IPO index (Henley et al., 2015) and the PDO index (Mantua et al., 1997) ($r = 0.88$, $p < 0.01$) using the ERSST database from 1919 to 2014. This study demonstrates how internal climate variability at multi-decadal timescale can influence stratospheric ozone, and it also highlights the importance for

better understanding and representing dynamical processes in climate models aimed at distinguishing forced and unforced signals and describing future ozone recovery. In addition, stratospheric ozone variability is closely coupled to the BDC (Randel et al., 2009a), and yet the latter is surrounded by large uncertainties. Current climate models show a long-term acceleration of the BDC due to increasing GHGs concentration (Butchart et al., 2006; Garcia and Randel, 2008; Li et al., 2008; Butchart et al., 2010; Lin and Fu, 2013; Aschmann et al., 2014), though these do not necessarily agree with observations (Engel et al., 2009; Bönisch et al., 2011) and reanalysis datasets (Bönisch et al., 2011; Diallo et al., 2012; Seviour et al., 2012; Monge-Sanz et al., 2013; Abalos et al., 2015; Fu et al., 2015). This suggests that other sources of variability at decadal timescale may also play a key role driving the BDC (Fig. 4.4C).

4.6. Supporting information

This section presents details on the chemistry-climate model simulations, observational data used to evaluate modelled output, and statistical method for trends and significance. Here we also define the Interdecadal Pacific Oscillation (IPO) index, the residual vertical component of the Brewer-Dobson circulation (BDC), and present the method of statistical regression to quantify the contribution of the IPO signal on the BDC variability. Supporting figures (Figures 4.5–4.9) are included to illustrate the mechanism proposed in the main text driving much of the multi-decadal variability in mid-stratospheric tropical ozone – i.e. sea surface temperatures (SSTs) induced transport-N_2O/NO_y), and justify the method of our sensitivity simulations. To illustrate in more detail the IPO-ozone link, a series of correlation analyses are shown for the tropical middle and lower stratosphere (Figure 4.5 and Figure 4.6 respectively). Figure 4.7 shows zonal mean regressions (latitude-altitude) between the IPO and ozone, which clearly identifies the region of interest in this study. Low frequency variability in the observed QBO is illustrated in Figure 4.8. Finally, Figure 4.9 demonstrates the effect of internally generated SSTs low frequency variability on the shallow and deep branches of the BDC.

Chemistry-climate model simulations

To explore pre-industrial non-evolving conditions (WACCM_Pre-Industrial), we used a previous pre-industrial control simulation of the Community Earth System Model

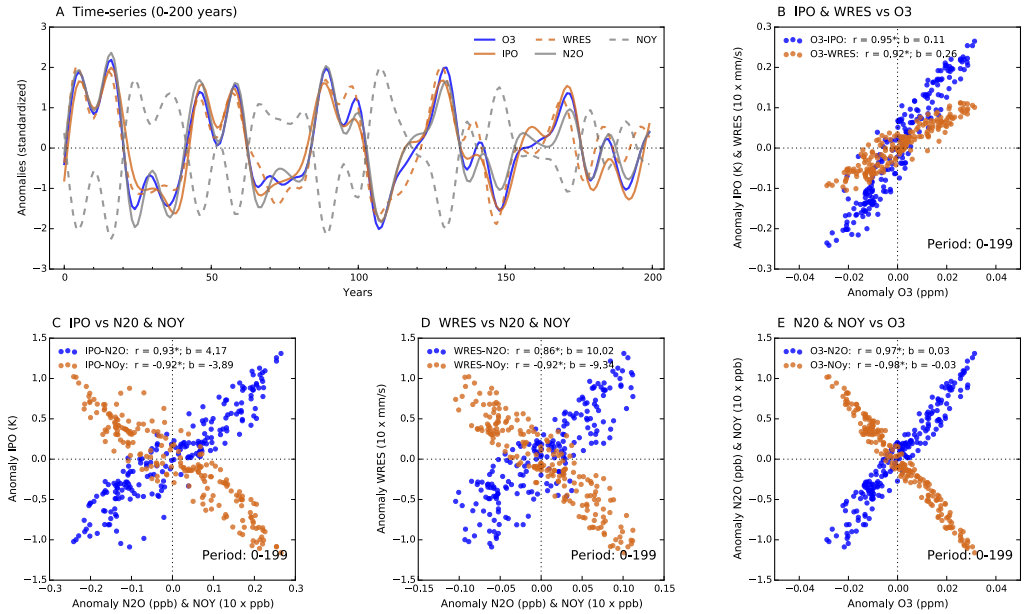

Figure 4.5. Dynamical and chemical processes linking the IPO with mid-stratospheric tropical ozone (10ºN–10ºS and 10 hPa) in constant pre-industrial conditions (WACCM_Pre-Industrial). (A) Low pass filtered anomalies (standardized) time-series of the IPO (solid orange line), WRES (residual mean vertical velocity, $\overline{w}^*$; dashed orange line), N_2O (solid grey line), NO_y (dashed grey line) and ozone (solid blue line). Correlations (r; * indicates significance at the 5 % level) and regressions (b) are shown in (B-E).

version 1 (CESM) (Marsh et al., 2013). CESM is a global coupled climate model with an approximate horizontal resolution of 1.9º latitude by 2.5º longitude, and 66 levels in the atmosphere (extending approximately to 140 km), with active coupled ocean and sea ice components. The atmosphere component is the Whole Atmosphere Community Climate Model (WACCM) version 4. The Model for Ozone and Related Chemical Tracers (MOZART) version 3 is the chemistry scheme (Kinnison et al., 2007), which includes full atmospheric chemistry from the troposphere to the lower thermosphere with gas-phase reactions, heterogeneous chemistry and photolysis. The vertical resolution varies approximately 1.1–1.4 km from the surface to the lower stratosphere (<30 km), 1.75 km near the stratopause (50 km) and 3.5 km above 65 km. A configuration of CESM that couples the atmosphere and land components was used to explore the 'real world' in the recent past (1960–2010; (WACCM_Recent-Past)

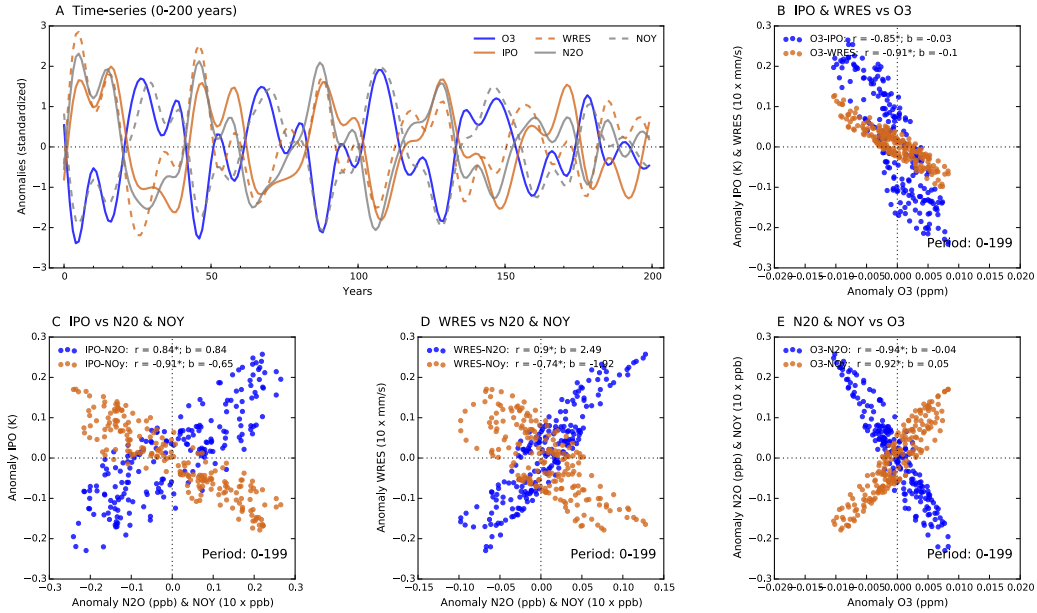

Figure 4.6. Same as in Fig. 4.5 but at 70 hPa.

(Tilmes et al., 2016; Morgenstern et al., 2017). It was forced with observed SSTs, sea-ice concentrations (SICs), solar spectral irradiance, volcanic aerosols and the quasi-biennial oscillation (QBO). Boundary conditions were specified for radiatively active species, anthropogenic, biomass burning and ozone depleting substances (ODSs for halogen compounds) emissions. Here, the version of WACCM included MOZART version 4 (Emmons et al., 2010) and recent updates (Lamarque et al., 2012; Tilmes et al., 2015). In addition, four sensitivity simulations were performed for the same period, and used in the main text to attribute recent changes in ozone: (fODS) ozone depleting substances, and (fODS+N2O) ozone depleting substances and nitrogen oxide emissions were fixed at 1955 levels; (fVolc) background stratospheric aerosol (surface area densities) is fixed at 1998–1999 averaged conditions – i.e. quiescent period without major volcanic eruptions as recommended by the CCMI activity (Eyring et al., 2013b); (fSSTs+cQBO) climatological SSTs and SICs over 1960–2010 (i.e. period with approximately equal positive-negative IPO phases) and a cyclical QBO (i.e. 28 month repeating cycle) are specified.

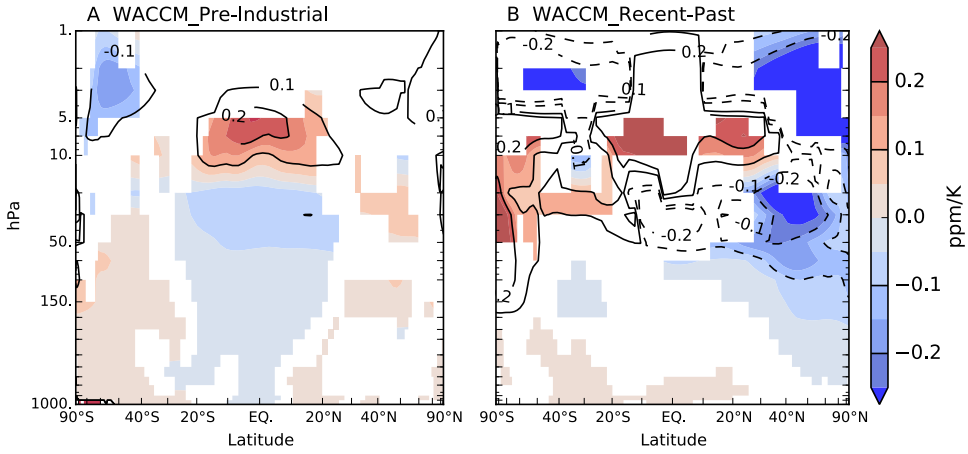

Figure 4.7. Zonal mean regression between ozone and the IPO in (A) pre-industrial conditions (WACCM_Pre-Industrial; 0–199 years), and (B) the recent past (WACCM_Recent-Past; 1960-2010). Shading is for statistically significant changes at the 95% confidence interval using two-tailed Student's t test.

The latter model does not completely represent the QBO (i.e. it is imposed by relaxing stratospheric tropical winds between 90–3 hPa). Previous studies have discussed both SSTs-QBO links and multi-decadal variability in the QBO (Gray et al., 1992ab; Brönnimann et al., 2016). Moreover, the observationally-derived QBO shows low frequency variability in phase with the observed IPO (Figure 4.8). Therefore, to investigate the effects of SSTs multi-decadal variability in ozone within a consistent framework (mediated via dynamical coupling), we imposed a QBO cycle of ~ 28 month on the above (fSSTs+cQBO) sensitivity simulation. To support this reasoning and unambiguously demonstrate the response of the BDC to the variability in SSTs, we performed an extra simulation (fSSTs), not used in the main text, imposing climatological SSTs-SICs (same as above), but with the observed QBO. Therefore, by subtracting the simulated BDC in (fSSTs+cQBO) and (fSSTs) from the 'real world' BDC (WACCM_Recent-Past), the effects of internally generated variability in SSTs coupled to the QBO are apparent. Figure 4.9 shows the residual of the simulated shallow and deep branches of the BDC over the period of interest (1980s–2000s; i.e. shift in the phase of the IPO), after subtracting internally generated variability in SSTs and the QBO (WACCM_Recent-Past minus fSSTs+cQBO; solid red line), and variability in SSTs only (WACCM_Recent-Past minus fSSTs; solid blue line). The residuals of the BDC show a positive and significant trend at the 5 % level of

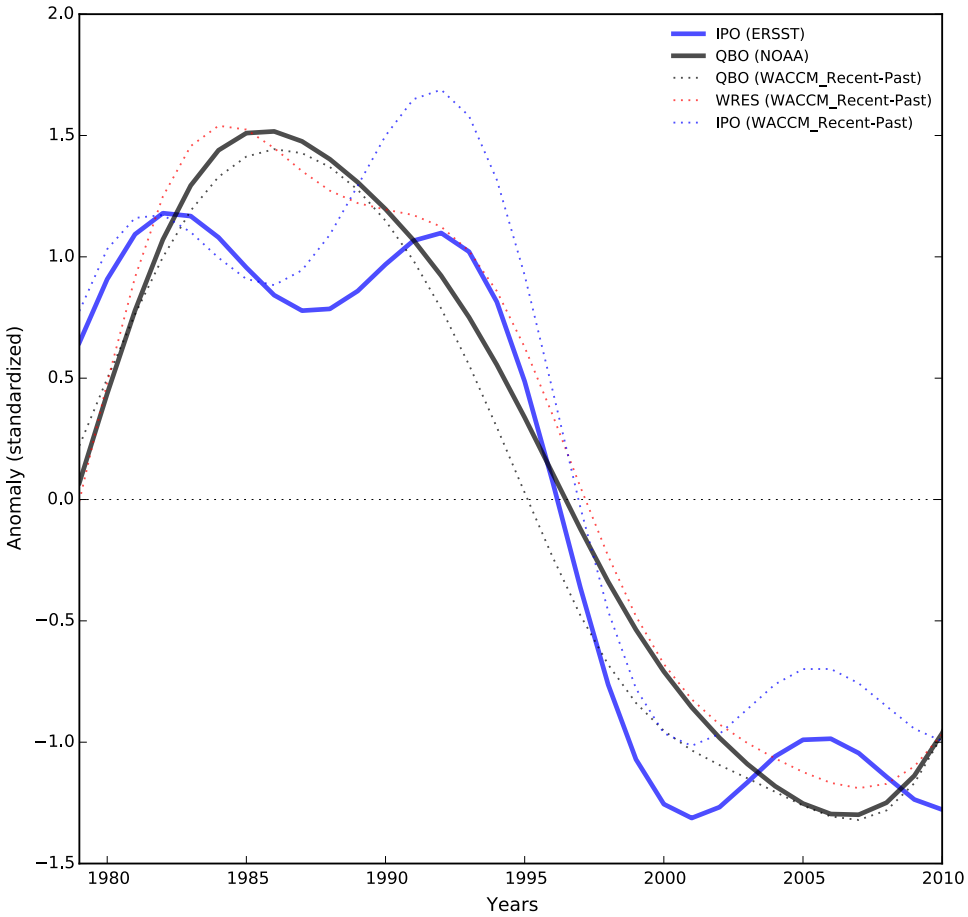

Figure 4.8. Low pass filtered anomalies time-series (1980-2010) for the IPO index (ERSST, solid blue line; and WACCM_Recent-Past, dotted blue line), the QBO (NOAA, black blue line; WACCM_Recent-Past, dotted black line), and the WRES (residual mean vertical velocity, $\overline{w}^*$, averaged over 10ºN–10ºS at 10 hPa; WACCM_Recent-Past, dotted red line). Observationally derived QBO (NOAA) is based on the zonal mean zonal wind at the equator and 30 hPa (calculated from the NCEP/NCAR Reanalysis, and retrieved from https://www.esrl.noaa.gov/psd/data/correlation/qbo.data) (accessed: 2017/09/22).

~ 0.014 ± 0.001 10 x mm/s/dec and 0.006 ± 0.002 10 x mm/s/dec for the shallow and deep ranches respectively. While the effect of imposing a cyclical QBO compared to the observed QBO (i.e. difference between the solid red and blue lines) is relatively less important in the shallow branch (e.g. strong correlation; $r = 0.95$, $p < 0.01$), it becomes apparent in the deep branch (e.g. poor correlation; $r = 0.47$, $p < 0.01$). These results support both the effects of SSTs low frequency variability on stratospheric transport and the important role of the QBO in the deep branch of the BDC.

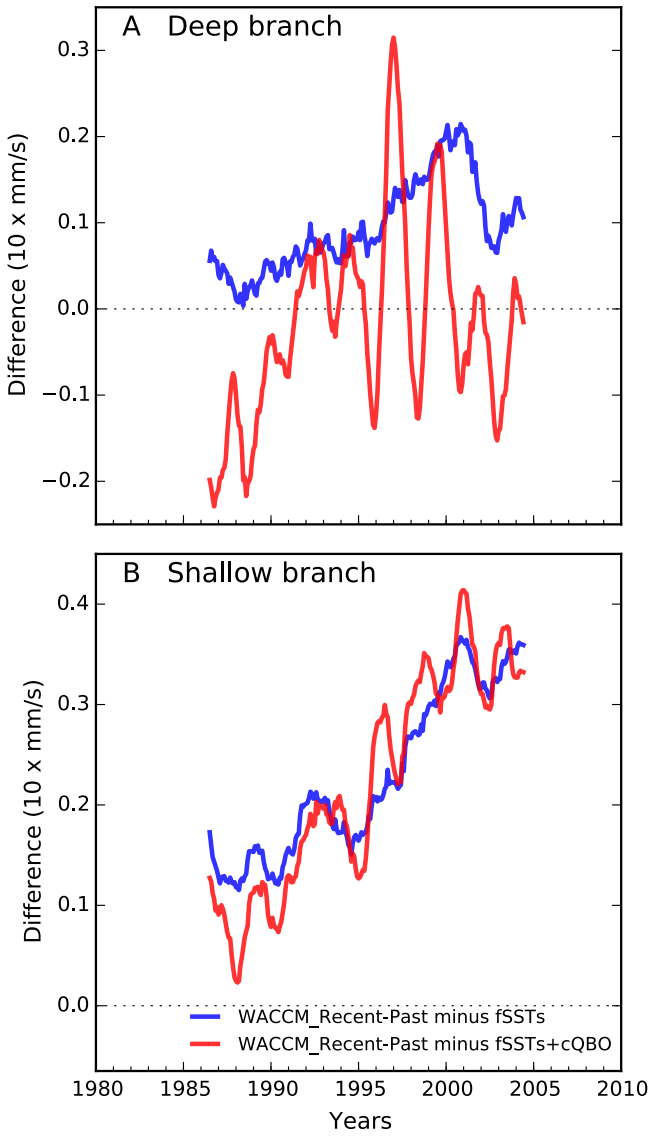

Figure 4.9. Residual changes in the simulated BDC (WACCM_Recent-Past) over 1980–2010. The 13-year running mean BDC is shown for the (A) deep branch at 10 hPa and (B) shallow branch at 70 hPa, after subtracting the BDC that results from imposing climatological SSTs and a cyclical QBO (WACCM_Recent-Past minus fSSTs+cQBO; solid red line), and from imposing climatological SSTs only (WACCM_Recent-Past minus fSSTs; solid blue line). The WRES (residual mean vertical velocity, $\overline{w}^*$, averaged over 10ºN–10ºS) is used to represent the BDC.

Internally generated climate variability

While the IPO is the leading mode of multi-decadal climate variability in SSTs, we acknowledge that there are other sources of low frequency variability in SSTs, such as the Atlantic Multidecadal Oscillation (AMO) (Meehl et al., 2016). The unambiguous

attribution of a particular pattern of variability (i.e. IPO) to mid-stratospheric tropical trends is difficult due to the interactions among the ocean basins (Kosaka and Xie, 2013). In this study, we impose SSTs-SICs climatology globally in our sensitivity simulations; therefore the attribution of internally generated variability in SSTs to ozone trends may not solely be the result of the IPO pattern. Nevertheless, we demonstrated the IPO-ozone relationship and described a plausible mechanism – involving a dynamical-chemical coupling – in the main text and supporting information.

Observed data

Observational estimates of sea surface temperatures in this work are the NOAA Extended Reconstructed Sea Surface Temperature (ERSST) version 4 (Huang et al., 2015). The ERSST reconstruction includes monthly data with horizontal resolution of 2º x 2º (latitude by longitude), retrieved from http://www.esrl.noaa.gov/psd/ (accessed: 2017/09/22).

The observed stratospheric ozone dataset used here is the Stratospheric Water and OzOne Satellite Homogenized (SWOOSH) version 2.6 (Davis et al., 2016) from 1984 to 2015, retrieved from http://www.esrl.noaa.gov/csd/groups/csd8/swoosh/ (accessed: 2017/09/22). We used merged data from a range of satellites – homogenized accounting for inter-satellite biases – of vertically resolved (316 to 1 hPa) zonal and monthly mean ozone mixing ratios with horizontal resolution of 2.5º x 2.5º.

Trends and uncertainty estimates

To derive the trends in this study, we use a least-square linear regression from deseasonalized anomaly time series. The significance of the trend indicates the 95% confidence level (1.96 sigma) calculated from the standard error of the fit and accounting the effect of lag-1 autocorrelation (Santer et al., 2000).

The Interdecadal Pacific Oscillation (IPO)

We derived the IPO using the Tripole Index (TPI) from deseasonalized sea surface temperatures (Henley et al., 2015):

$$\mathrm{TPI} = region\ 2 + \frac{region\ 1 + region\ 3}{2} \tag{4.1}$$

TPI regions are: region 1 25ºN–45ºN, 140ºE–145ºW; region 2 10ºN–10ºN, 170ºE–90ºW; and region 3 50ºS–15ºS, 150ºE–160ºW. Finally, a Chebyshev low-pass filter is applied with 13 year cutoff period and a filter order of 6. In the development of the TPI index by Henley et al. (2015), this filter showed a local maxima in the variance that explains the low-frequency portion of the IPO.

The Brewer-Dobson circulation (BDC)

In order to estimate changes in the BDC, we use the residual vertical component ($\overline{w}^*$) of the Transformed Eulerian Mean (TEM), in spherical and log pressure coordinates:

$$\overline{w}^* = \overline{w} + \frac{1}{a\cos\emptyset}\left(\cos\emptyset\ \frac{\overline{v'\theta'}}{\overline{\theta'}_z}\right)_\emptyset \tag{4.2}$$

where overbars represent zonal mean and all terms are defined as in Eq. 3.5.1b in Andrews et al. (1987).

The IPO signal on tropical upwelling

To calculate the signal on the annual mean anomaly in the shallow (70 hPa) and deep (10 hPa) branches of the tropical upwelling ($\overline{w}^*$, 20ºN–20ºS) that may be explained by the IPO, we use a simple linear regression between the two, as followed:

$$\overline{w}^{*\prime}{}_{[i]} = \overline{w}^*{}_{[i]} - \frac{\partial \overline{w}^*{}_{[i]}}{\partial IPO} * IPO \tag{4.3}$$

where $\overline{w}^{*\prime}$refers to the tropical upwelling after removing multi-decadal variability associated with the IPO, and the subscript '[i]' refers to the corresponding branch of the tropical upwelling.

Acknowledgments. This work was supported by NERC, under project number NE/L501736/1. F. Iglesias-Suarez would like to acknowledge NERC for a PhD studentship.

Chapter 5

Key drivers of ozone change and its radiative forcing over the 21st century

F. Iglesias-Suarez[1,2,*], D. E. Kinnison[3], A. Rap[4], Amanda C. Maycock[4], O. Wild[1,2] and P. J. Young[1,2,5]

[1]Lancaster Environment Centre, Lancaster University, Lancaster, UK

[2]Data Science Institute, Lancaster University, Lancaster, UK

[3]Atmospheric Chemistry Observations and Modeling Laboratory, National Center for Atmospheric Research, Boulder, Colorado, USA

[4]School of Earth and Environment, University of Leeds, Leeds, UK

[5]Pentland Centre for Sustainability in Business, Lancaster University, Lancaster, UK

[*]now at: Department of Atmospheric Chemistry and Climate Group, Institute of Physical Chemistry Rocasolano, CSIC, Madrid, Spain

Correspondence to: F. Iglesias-Suarez (figlesias@iqfr.csic.es)

The following work has been accepted in Atmospheric Chemistry and Physics on 28 March 2018 (discussion paper: Key drivers of ozone change and its radiative forcing over the 21st century, Atmos. Chem. Phys. Discuss., 1-39, doi:10.5194/acp-2017-939, 2017). The authors and their contributions are listed below.

Fernando Iglesias-Suarez: Performed simulations with WACCM, processed the data, analysed the data, and wrote the manuscript. **Doug E. Kinnison:** Supported WACCM simulations and compiled the manuscript. **Alexandru Rap and Amanda C. Maycock:** Performed radiative effect calculations, interpreted the results, and compiled the manuscript. **Paul J. Young and Oliver Wild:** Helped to plan WACCM simulations, synthesise, interpret the results, and compile the manuscript.

Abstract

Over the 21st century changes in both tropospheric and stratospheric ozone are likely to have important consequences for the Earth's radiative balance. In this study, we investigate the radiative forcing from future ozone changes, using the Community Earth System Model (CESM1), with the Whole Atmosphere Community Climate Model (WACCM), and including fully coupled radiation and chemistry schemes. Using year 2100 conditions from the Representative Concentration Pathways 8.5 (RCP8.5) scenario, we quantify the individual contributions to ozone radiative forcing of (1) climate change, (2) reduced concentrations of ozone depleting substances (ODSs), and (3) methane increases. We calculate future ozone radiative forcings and their standard error (associated with interannual variability of ozone) relative to year 2000 of (1) 33 ± 104 mWm^{-2}, (2) 163 ± 109 mWm^{-2}, and (3) 238 ± 113 mWm^{-2}, due to climate change, ODSs and methane, respectively. Our best estimate of net ozone forcing in this set of simulations is 430 ± 130 mWm^{-2} relative to year 2000, and 760 ± 230 mWm^{-2} relative to year 1750, with the 95 % confidence interval given by ±30 %. We find that the overall long-term tropospheric ozone forcing from methane chemistry-climate feedbacks related to OH and methane lifetime is relatively small (46 mWm^{-2}). Ozone radiative forcing associated with climate change and stratospheric ozone recovery are robust with regard to background climate conditions, even though the ozone response is sensitive to both changes in atmospheric composition and climate. Changes in stratospheric-produced ozone account for ~ 50 % of the overall radiative forcing for the 2000–2100 period in this set of simulations, highlighting the key role of the stratosphere in determining future ozone radiative forcing.

5.1. Introduction

Ozone is an important trace gas that plays a key role in the Earth's radiative budget, atmospheric chemistry and air quality. As a radiatively active gas, ozone interacts with both shortwave and longwave radiation. In the troposphere, ozone is an important regulator of the oxidising capacity (both itself and as the main source of hydroxyl radicals, OH), as well as being an important pollutant, with negative effects on vegetation and human health (e.g. Prather et al., 2001; UNEP, 2015). However, approximately 90% of ozone by mass is found in the stratosphere – protecting the biosphere from harmful ultraviolet solar radiation (WMO, 2014) – and is an important source of ozone in the troposphere and its budget (e.g. Collins et al., 2003; Sudo et al., 2003; Zeng and Pyle, 2003). Therefore, its future evolution – in the troposphere and the stratosphere – is an important concern for climate change and air quality during the 21st century. Future changes in emissions of ozone precursors (e.g. methane), ODSs and climate are thought to be major drivers of ozone abundances (e.g. Stevenson et al., 2006; Kawase et al., 2011; Young et al., 2013a).

Stratospheric-tropospheric exchange (STE) of ozone significantly influences the abundance and distribution of tropospheric ozone (e.g. Zeng et al., 2010; Banerjee et al., 2016). The Brewer-Dobson circulation (BDC) governs the meridional transport of air and trace constituents in the stratosphere, and is characterized by upwelling in the tropics, poleward motion in the stratosphere and sinking at middle and high latitudes (Butchart, 2014, and references therein). The BDC is commonly thought to consist of a shallow branch, controlling the lower stratosphere region, and a deep branch controlling the middle and upper stratosphere. The latter presents two cells during the spring and fall seasons, and one stronger cell into the winter hemisphere (Birner and Bönisch, 2011). Although observational estimates and climate models suggest an acceleration of the stratospheric mean mass transport via the BDC associated with climate change (e.g. Oberländer et al., 2013; Ploeger et al., 2013; Butchart, 2014; Stiller et al., 2017), significant uncertainty still remains (Engel et al., 2009; Hegglin et al., 2014; Ray et al., 2014). The tropopause is the boundary that "separates" the troposphere and the stratosphere, two chemically and dynamically distinct regions. Defining the tropopause is crucial to diagnose budget terms of trace gases such as the STE of ozone (e.g. Prather et al., 2011), although the chosen

definition may affect the resulting analysis (e.g. Wild, 2007; Stevenson et al., 2013; Young et al., 2013a).

Stratospheric ozone is expected to recover towards pre-industrial levels during the 21st century due to the implementation of the Montreal Protocol and its Amendments and Adjustments (WMO, 2014), as ODS concentrations slowly decrease in the atmosphere (e.g. Austin and Wilson, 2006; Eyring et al., 2010a). Indeed, the global ozone layer has already shown the first signs of recovery (WMO, 2014; Chipperfield et al., 2017). Future ozone recovery can affect tropospheric composition via enhanced STE of ozone and reductions in tropospheric photolysis rates, both associated with higher levels of ozone in the stratosphere. Previous modelling studies that have isolated the impacts of stratospheric ozone recovery have shown that the increased STE is the most important driver of changes in the tropospheric ozone burden (Zeng et al., 2010; Kawase et al., 2011; Banerjee et al., 2016). However, tropospheric ozone is also significantly affected by the change in ultraviolet radiation reaching the troposphere brought about by the ticker stratospheric ozone layer. In turn, reductions in ozone photolysis result in lower OH concentrations – i.e. $O_3 + h\nu\ (\lambda < 320\ \text{nm}) \rightarrow O(^1D) + O_2$ – and therefore longer methane lifetime, with consequences for long-term tropospheric ozone abundances (e.g. Morgenstern et al., 2013; Zhang et al., 2014).

The broad impacts of future climate change on the distribution of ozone are robust across a number of modelling studies and multi-model activities (Kawase et al., 2011; Young et al., 2013a; Arblaster et al., 2014; Banerjee et al., 2016; Iglesias-Suarez et al., 2016). Stratospheric cooling leads to further ozone loss in the polar lower stratosphere (through enhanced heterogeneous ozone destruction) and ozone increases in the upper stratosphere (through reduced NO_x abundances and HO_x-catalysed ozone loss, and enhanced net oxygen chemistry) (Haigh and Pyle, 1982; Rosenfield et al., 2002). In addition, a projected acceleration of the BDC leads to an enhanced STE of ozone (e.g. Garcia and Randel, 2008; Butchart et al., 2010), which results in (i) decreases in tropical lower stratospheric ozone, associated with a relatively faster ventilation and reduced ozone production (Avallone and Prather, 1996); and (ii) ozone increases in the upper troposphere, particularly in the region of the subtropical jets, linked to the descending branch of the BDC (e.g. Kawase et al., 2011; Banerjee et al., 2016). On the other hand, a warmer and wetter climate results in

reduced tropospheric ozone levels – i.e. linked to a decrease in net chemical production due to enhanced ozone chemical loss – (e.g. Wild, 2007).

Climate feedbacks associated with future ozone changes are surrounded by large uncertainties. Lightning is a major natural source of nitrogen oxides (LNO_x) in the troposphere (Galloway et al., 2004), with important consequences for atmospheric composition in the mid-upper troposphere and the lower stratosphere. The current best estimate of annual and global mean LNO_x emissions is 5 ± 3 Tg(N) yr^{-1}, with chemistry-climate models suggesting LNO_x emissions sensitivity to climate change of ~ 4–60 % K^{-1} (Schumann and Huntrieser, 2007, and references therein). Although more recent modelling studies find LNO_x emissions climate sensitivity lying at the lower end of the above estimate (Zeng et al., 2008; Banerjee et al., 2014), results from a multi-model activity suggest large uncertainty in the magnitude and even the sign of future projections response due to different parameterizations (Finney et al., 2016). Most LNO_x emissions occur in the mid-upper tropical troposphere over the continents, where photochemical production of ozone is most efficient in the troposphere – i.e. low background concentrations and longer lifetimes of NO_x, lower temperatures affecting ozone loss chemistry and abundant sunlight (e.g. Williams, 2005; Dahlmann et al., 2011). A small but significant fraction of lightning-induced NO_x emissions are converted into less photochemically active nitric acid (HNO_3, via HO_2 + NO reaction), which can be removed through wet deposition or transported into the lower stratosphere (acting as a reservoir of NO_x) (e.g. Jacob, 1999; Søvde et al., 2011). In addition, OH concentrations increase with LNO_x emissions and the resultant lightning-produced ozone – i.e. via NO + HO_2 and $O(^1D)$ + H_2O respectively – with a corresponding reduction in methane lifetime. This resulting climate feedback is important because methane is a potent greenhouse gas (GHG) and ozone precursor.

To date, ozone is the third largest contributor to the total tropospheric radiative forcing (RF) since the pre-industrial period, with overall increases in its concentration contributing a global radiative forcing over 1750–2011 of +0.35 Wm^{-2} (Myhre et al., 2013). In this study, we use the concept of radiative effect (RE) to diagnose the contribution of ozone changes on the global radiative budget. The ozone RE is the radiative flux imbalance between incoming shortwave solar radiation and outgoing longwave infrared radiation (at the tropopause, after allowing for stratospheric temperatures to re-adjust to radiative equilibrium), which results from the presence of both anthropogenic and natural ozone (Rap et al., 2015). Note that RF is therefore the

change in RE over time (e.g. Myhre et al., 2013). Ozone shows two distinct regimes with regard to its RE, with positive (longwave radiation) and negative (shortwave radiation) effects for increases in stratospheric ozone, and positive (for both longwave and shortwave radiation) effects for ozone increases in the troposphere (e.g. Lacis et al., 1990; Forster and Shine, 1997). In addition, changes in the distribution of ozone – i.e. latitudinal and vertical structure – are of a particular interest for its RE, due to horizontally varying factors such as, surface albedo, clouds and the thermal structure of the atmosphere (e.g. Lacis et al., 1990; Berntsen et al., 1997; Forster and Shine, 1997; Gauss et al., 2003). Previous studies showed highest radiative efficiency of ozone in the tropical upper troposphere (e.g. Worden et al., 2011; Riese et al., 2012; Rap et al., 2015), a region greatly influenced by changes in stratospheric influx (e.g. Hegglin and Shepherd, 2009; Zeng et al., 2010; Banerjee et al., 2016) and lightning-produced ozone (e.g. Banerjee et al., 2014; Liaskos et al., 2015) in a warmer climate.

Modelling experiments used in the latest Assessment Report of the Intergovernmental Panel on Climate Change (IPCC) followed the Representative Concentration Pathways (RCPs) emission scenarios for short-lived precursors (van Vuuren et al., 2011) and long-lived species (Meinshausen et al., 2011). The RCPs are named according to the total radiative forcing at the end of the 21st century relative to 1750. For example, while the RCP8.5 emissions scenario refers to the total 8.5 Wm^{-2} RF by 2100, future tropospheric ozone RF was projected to account for up to ~ 9 % (0.6 ± 0.2 Wm^{-2}) of the total RF (Stevenson et al., 2013). Note that the methane concentration in 2100 is more than double that in the year 2000 following the RCP8.5 emissions scenario.

Previous research has investigated impacts on ozone abundances and distributions associated to future changes in climate, ODSs and ozone precursor emissions in a processed-based approach – i.e. imposing one single forcing at a time – (Collins et al., 2003; Sudo et al., 2003; Zeng and Pyle, 2003; Zeng et al., 2008; Zeng et al., 2010; Kawase et al., 2011; Banerjee et al., 2016). Other modelling studies focused on the radiative effects of tropospheric (e.g. Gauss et al., 2003; Stevenson et al., 2013) and stratospheric (Bekki et al., 2013) ozone changes under future emission scenarios in a non processed-based fashion. One study has recently identified the indirect tropospheric and stratospheric ozone RF between 2000 and 2100 due to individual perturbations (Banerjee et al., 2018). Yet the upper limit of future ozone RF remains poorly constrained. For example, climate models do not even necessarily

agree on the sign of the indirect ozone forcing resulting from climate change and associated feedbacks (e.g. LNO_x). Furthermore, there are uncertainties arising from the interactions and non-linearities between different agents (e.g. combined forcing may differ from the sum of individual forcings due to different background conditions), as well as and long-term changes (e.g. methane feedback associated with changes in lifetimes).

Here we aim to narrow this gap by assessing how key factors drive net ozone radiative forcing, and providing an estimate of the uncertainty arising from non-linearities and long-term feedbacks. We use the Community Earth System Model (CESM1) in its "high-top" (up to 140 km) atmosphere version – the Whole Atmosphere Community Climate Model (WACCM) – and a series of sensitivity simulations to quantify the radiative effects of ozone due to (1) climate change, (2) lightning-induced NO_x emissions, (3) stratospheric ozone recovery, and (4) methane emissions between 2000 and 2100 following the RCP8.5 emissions scenario. We explore the robustness of the ozone radiative forcings associated with the above drivers under different background conditions due to non-linearities in ozone responses. Moreover, here we use a synthetic ozone tracer to unambiguously identify stratospheric- and tropospheric-produced ozone forcing. Note this study does not address reductions in anthropogenic NO_x and non-methane volatile organic compounds emissions, since they play a marginal role in future ozone RF under the RCP8.5 scenario (based on an additional simulation not presented here).

The CESM1-WACCM model, sensitivity simulations and ozone radiative effect calculations are described in Section 5.2. A present-day model evaluation, future projected ozone changes and associated radiative effects are presented in Sect. 5.3. Different sources of uncertainties are discussed and accounted for in Sect. 5.4. Finally, a summary and concluding remarks are presented in Sect. 5.5.

5.2. Methodology

5.2.1. Model description

We use the CESM (version 1.1.1) chemistry-climate model with a configuration that fully couples the atmosphere and land components. A comprehensive description of the model is given by Marsh et al. (2013, and references therein).

The atmosphere component of CESM is WACCM version 4, a high-top model that extends from the surface to approximately 140 km in the lower thermosphere, with a vertical resolution ranging from 1.2 km near the tropopause to ~ 2 km near the stratopause, and horizontal resolution of 1.9º x 2.5º (latitude by longitude). The chemical scheme is the Model for Ozone and Related Chemical Tracers (MOZART) for the troposphere (Emmons et al., 2010) and the stratosphere (Kinnison et al., 2007), including recent updates (Lamarque et al., 2012; Tilmes et al., 2015). It includes 169 chemical species with detailed photolysis, gas-phase and heterogeneous reactions (see Tables A1 and A2 in Tilmes et al., 2016). Recent updates in the orographic gravity wave forcing – reducing the cold bias in Antarctic polar temperatures – (Calvo et al., 2017; Garcia et al., 2017) and the polar stratospheric chemistry (Wegner et al., 2013; Solomon et al., 2015) are included in the model. Concentrations of radiatively active gas-phase compounds such as ozone, nitrous oxide (N_2O), methane (CH_4) and halogenated ODSs, are coupled to the model radiation scheme. Lightning-induced NO_x emissions are parameterized using the cloud top height method (Price and Vaughan, 1993), and annual global mean LNO_x emissions are scaled to simulate present-day values of between 3–5 Tg N yr^{-1}.

A stratospheric ozone tracer (O3S) is implemented to represent the abundance and distribution of stratospheric-produced ozone in the troposphere (Roelofs and Lelieveld, 1997). O3S is equivalent to ozone in the stratosphere. In the troposphere it undergoes the same chemical loss processes as ozone, but does not undergo dry deposition, following the recommendations for the Chemistry-Climate Model Initiative (CCMI) (Eyring et al., 2013b; Morgenstern et al., 2017). To account for dry deposition of O3S, we apply an annual global correction factor based on an additional model simulation (not used in the main results). This correction factor is approximately linear, ranging from 0.7 at the surface to 0.95 around 250 hPa.

The land component is the Community Land Model version 4, which has the same horizontal resolution as the atmosphere component and interactively calculates dry deposition for trace gases in the atmosphere (Val Martin et al., 2014) and biogenic emissions using the Model of Emissions of Gases and Aerosols from Nature (MEGAN) version 2.1 (Guenther et al., 2012).

5.2.2. Experimental setup

This modelling set-up uses time slice simulations driven by sea surface temperatures (SSTs) and sea ice climatologies from previous CESM1-WACCM fully coupled simulations performed as part of the CCMI (SENC2-8.5; see Morgenstern et al., 2017). An average over 1990–2009 is used to represent the year 2000; since the existing model simulation did not cover the period 2090–2109, an average over 2080–2099 is used to represent conditions at the end of the 21st century (nominally 2100). Note, however, that the perturbed concentrations of atmospheric gases are taken from year 2100 in the RCP8.5 scenario, and hence these experiments are labelled as 2100 in the manuscript. Each time slice experiment is integrated for 20 years, with the last 10 years analysed in this study (i.e. the spin-up period covered the first 10 years). Seasonally varying boundary conditions are specified for carbon dioxide (CO_2), N_2O, CH_4, and ODSs (halogen-containing compounds), as recommended for CCMI (Eyring et al., 2013b). Changes in ozone precursors – other than CH_4 – and land-use changes are not explored here (i.e. these are fixed at year 2000 levels in all experiments). Volcanic eruptions are not included in the experiments, and the incoming solar radiation is fixed at 1361 Wm^{-2}. The quasi-biennial oscillation is imposed by relaxation of equatorial winds (90–3 hPa) with an approximate 28-month period between eastward and westward phases (Marsh et al., 2013).

Table 5.1 lists the simulations used in this study. The control simulation (Cnt) had all boundary conditions set to the year 2000. Then each sensitivity simulation added one single driver (i.e. boundary condition changed to the year 2100) at a time. For example, while the climate-related ozone RF (with fixed LNO_x emission) is explored comparing the Clm−Cnt simulations, the forcing associated with changes in lightning-induced NO_x emissions is quantified comparing the Lnt−Clm simulations, and so forth. This method provides a different estimate of the overall net ozone RF compared to exploring the impact of the individual drivers alone (e.g. it accounts for non-linear effects that may be neglected by exploring each perturbation compared to the reference simulation). However, since the attribution of forcings to individual drivers may be sensitive to different background conditions, we also evaluate the robustness of the experimental design (see Sect. 5.3.5).

Table 5.1. Summary of the model simulations

Simulation	Climate[1]	ODSs[2]	CH_4[3]
Cnt	2000	2000	2000
Clm	2100 (fLNOx)[4]	2000	2000
Ltn	2100	2000	2000
O3r	2100	2100	2000
Mth	2100	2100	2100
Cnt+fLNOx	2000 (fLNOx)[4]	2000	2000

[1]Climate (SSTs, sea ice, CO_2 and N_2O, if not otherwise specified) follows the RCP8.5 emissions scenario.
[2]Relative to Cnt, ODS boundary conditions of −63.2 % (2.156 ppbv) total chlorine, −35.7 % (8.1 pptv) total bromine and −67.6 % (1.376 ppbv) total fluorine follow the halogen scenario A1.
[3]Relative to Cnt, CH_4 boundary conditions of 214.2 % (3744 ppbv) follow the RCP8.5 emissions scenario.
[4]Offline lightning-induced NO_x emissions are imposed by applying a monthly mean climatology of the Cnt simulation.

Here we provide specific details of the boundary conditions. The simulations can be classified into three main groups:

1. Sensitivity simulations that explore the impacts of climate change. Here SSTs, sea ice and main GHGs (i.e. CO_2 and N_2O) are specified to year 2100 levels (see above for explanation of SST and sea ice fields). The upper end emission scenario of the RCPs family is explored (RCP8.5). Natural biogenic emissions (e.g. isoprene) are calculated online, which are mainly governed by changes in CO_2, climate and land use (Squire et al., 2014). The indirect ozone radiative effect resulting from this climate feedback is implicitly contained in the climate signal. However, unlike LNO_x emissions it mainly impacts ozone in the lower troposphere, where ozone shows relatively small radiative efficiency (Rap et al., 2015). To isolate the impacts of lightning-produced ozone, additional experiments are performed with year 2000 levels for LNO_x emissions (fLNOx). Fixed LNO_x simulations follow the approach of Banerjee et al. (2014), imposing the monthly mean LNO_x emissions climatology from the Cnt run and switching off its interactive calculation in the model. To justify this method, we compared temperature and tropospheric ozone fields between the Cnt and Cnt+fLNOx simulations and found negligible differences (not shown).

2. Stratospheric ozone recovery due to the slow decrease of ODS concentrations (referring to the total organic chlorine and bromine species) regulated under the framework of the Montreal Protocol is investigated. Based on the CCMI recommendations, halogen species (CFC11, CFC12, CFC113, CFC114, CFC115, CCl4, HCFC22, HCFC141b, HCFC142b, CF_2ClBr, CF_3Br, CH_3Br, CH_3CCl_3, CH_3Cl, H1202, H2402, CH_2Br_2, and $CHBr_3$) are specified to year 2100 levels for the halogen scenario A1 (WMO, 2011), which includes the early phase-out of hydrochlorofluorocarbons agreed in 2007. Note that two brominated short-lived species (CH_2Br_2 and $CHBr_3$) were included in these experiments to accurately represent bromine loading and thus the associated ozone depletion, providing an additional bromine surface mixing ratio of ~ 6 pptv on top of that from the longer-lived bromine compounds.
3. Future levels of methane and its impacts on ozone are investigated. Concentrations of CH_4 are imposed to year 2100 levels from the RCP8.5 pathway – i.e. approximately double concentrations compared to year 2000. Note that methane levels were kept at year 2000 levels for the sensitivity simulations described above that explore climate change impacts.

5.2.3. Radiative transfer calculations

To calculate the resulting all-sky REs of ozone we use the ozone radiative kernel (O_3 RK) technique based on Rap et al. (2015), updated for the whole atmosphere (Figure 5.1). The O_3 RK, defined as the derivative of the radiative flux relative to small perturbations in ozone, was calculated using the offline version of the SOCRATES radiative transfer model with nine longwave (LW) and six shortwave (SW) bands, which is based on Edwards and Slingo (1996). Radiative flux calculations employed a monthly mean climatology of temperature, water vapour and ozone from the European Centre for Medium-Range Weather Forecast (ECMWF) ERA-Interim, and year 2000 surface albedo and clouds from the International Satellite Cloud Climatology Project (Rossow and Schiffer, 1999). Stratospherically adjusted REs of ozone were computed using the fixed dynamical heating approximation (Fels et al., 1980), which assumes that the atmosphere adjusts to a new equilibrium state via radiative process only – i.e. without dynamical feedbacks – on a relatively short period (~ few months). A 1 ppbv perturbation in ozone is added to each layer in turn,

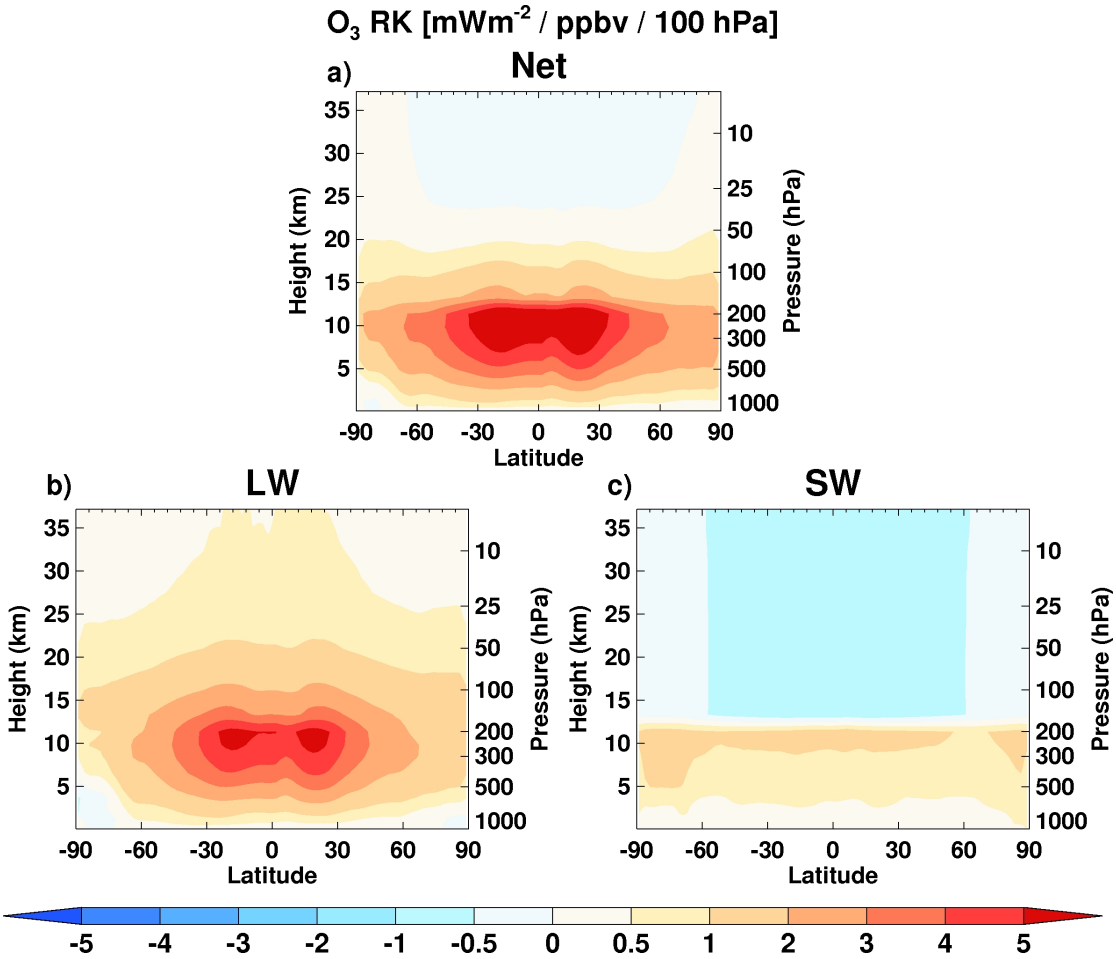

Figure 5.1. Annual zonal mean whole-atmosphere ozone radiative kernel under all-sky conditions for (a) net (LW+SW), (b) LW, and (c) SW components.

and temperatures above 200 hPa are adjusted iteratively until they converge to a new local radiative-dynamical equilibrium and the change in net flux at the 200 hPa level is diagnosed. The O_3 RK is then constructed from the changes in net flux resulting from the ozone perturbations applied to all atmospheric layers. The 200 hPa level is used for the stratospheric temperature adjustment as an approximation for the level at which the transition to local radiative-dynamical equilibrium in the stratosphere occurs. The net O_3 RK (Fig. 5.1a) illustrates the importance of the upper troposphere and lower stratosphere, particularly at low latitudes, where changes in ozone are very efficient in affecting the radiative flux of the Earth. The LW component (Fig. 5.1b) is positive throughout the atmosphere and dominates the net O_3 RK, although the SW component (Fig. 5.1c) outweighs the former in the upper stratosphere (i.e. negative sensitivity).

We compared the ozone RF calculated using the O_3 RK technique (i.e. by multiplying the simulated ozone change with the net O_3 RK interpolated to the model's grid) with the corresponding RF calculated directly with the SOCRATES radiative transfer model (see supplementary material, Fig. 5.7). The good agreement between the two methods (global mean difference of 0.01 Wm^{-2}) is consistent with the Rap et al. (2015) findings, where the O_3 RK was proposed as an efficient and accurate method to estimate ozone RFs, which is particularly well suited for multi-model intercomparison activities.

A chemical tropopause definition (Prather et al., 2001), using the 150 ppbv ozone level of the Cnt simulation, is employed to differentiate ozone changes and associated RFs occurring in the troposphere and the stratosphere. Compared to the latter, we found a negligible difference in the partitioning of tropospheric-stratospheric forcing using a consistent chemical tropopause definition to the driver investigated (i.e. higher tropopause associated with climate change).

5.3. Results

5.3.1. Present-day ozone radiative effects and model validation

A detailed present-day ozone evaluation of a similar model and experimental set-up was presented by Tilmes et al. (2016). In summary, simulated monthly mean ozone shows good agreement with observational estimates within a 25 % range in spring and summer. Zonal and annual mean tropospheric ozone shows the best agreement with observations at low and mid-latitudes (±5 DU), a key region for its radiative effect (e.g. Rap et al., 2015). Likewise, the zonal and annual mean stratospheric ozone agrees fairly well with satellite estimates in the Southern Hemisphere (SH) and low latitudes (±30 DU), but larger deviations are found at mid- and high latitudes in the Northern Hemisphere (NH), a discrepancy also apparent in the models of the Atmospheric Chemistry and Climate Model Intercomparison Project (ACCMIP) (Iglesias-Suarez et al., 2016). The tropospheric ozone budget (production, loss, dry deposition, stratospheric input), burden and lifetime for the Cnt simulation (see Table 5.2 and Fig. 5.8) are within previous multi-model activities estimates (Stevenson et al., 2013; Young et al., 2013a; Young et al., 2018).

Table 5.2. Tropospheric ozone budget, including: Ozone production (P) and loss (L) terms are based on the gas-phase reaction rates of the O_x family (O_3, O, O^1D and NO_2); Net chemical production of ozone is defined as the residual of the production and loss terms (N = P − L); Dry deposition of ozone (D) term; Stratospheric-Tropospheric exchange (S; i.e. influx from the stratosphere) term is the residual of the dry deposition and net chemistry production terms (S = D − N); Ozone burden (B) term; Ozone and methane lifetimes (τ_{O3}, τ_{CH4} respectively) is the ratio between the burden and total losses (τ = burden / total loss); τ_{CH4} includes loss with respect to OH and adjusted for soil uptake (160 years) and stratospheric sink (120 years) (Prather et al., 2012); Burden for the stratospheric ozone tracer (B_{O3S}).

Simulation	P (Tg yr^{-1})	L (Tg yr^{-1})	N (Tg yr^{-1})	D (Tg yr^{-1})	S (Tg yr^{-1})	B (Tg)	τ_{O3} (days)	τ_{CH4} (years)	B_{O3S} (Tg)
ACCENT (year 2000)	5110 ± 606	4668 ± 727	442 ± 309	1003 ± 200	552 ± 168	344 ± 39	22.3 ± 2.0	8.7 ± 1.3	----
ACCMIP (year 2000)	4877 ± 853	4260 ± 645	618 ± 275	1094 ± 264	477 ± 97	337 ± 23	23.4 ± 2.2	8.5 ± 1.1	----
Cnt	4678	4195	483	881	398	318	22.9	7.2	123
Clm[1]	5111	4809	302	811	510	309	20.1	6.9	119
Ltn	5378	5057	322	833	511	329	20.4	6.6	138
O3r	5303	5058	245	855	610	337	20.8	6.6	131
Mth	6072	5759	313	979	666	378	20.5	8.3	138
Cnt+fLNOx[1]	4648	4169	479	878	399	313	22.7	7.2	121

[1] Offline lightning-induced NO_x emissions imposed by applying a monthly mean climatology of the Cnt simulation.

Figures 5.2a-5.2b show the annual mean ozone RE calculated for the Cnt simulation (year 2000 or "present-day" hereafter) and the Tropospheric Emission Spectrometer (TES) from July 2005 until June 2008 (05–08). TES is the first product providing tropospheric ozone profiles suitable for RE studies and has been previously evaluated against other observational estimates (e.g. Osterman et al., 2008), showing small bias in the troposphere and the stratosphere of approximately 3–4 DU. The annual and global ozone RE in the Cnt simulation is 2.26 ± 0.14 Wm^{-2} (1 standard error associated with interannual variability), within the TES range of 2.21–2.26 Wm^{-2}. The spatial distribution of simulated and observed ozone REs are fairly well correlated (r = 0.6, $p < 0.01$), although note that the noisier TES signal is largely the result of averaging only three years. Both the simulated and observed present-day ozone REs reveal a positive poleward gradient, with a minimum in tropical regions (approximately 20ºN–20ºS) that is associated with the relatively low ozone levels found in the upper troposphere and lower stratosphere (see Fig. 5.8). A peak is found at high latitudes in the NH, driven by transport of relatively rich tropospheric ozone air from mid-latitudes coupled with only moderate ozone depletion in the NH stratosphere. This is in contrast with a lower RE values within the SH polar vortex, driven by the larger stratospheric ozone depletion over Antarctica (Solomon et al., 2015). Figure 5.2c compares the Cnt annual mean ozone RE against the TES data set. Compared to TES, the simulated annual mean tends to overestimate the RE in the NH and underestimate it in the SH, consistent with the bias in the ozone distribution (Tilmes et al., 2016). Significant biases are mainly confined to the tropical and subtropical regions – i.e. bias is defined here when the simulated RE ±1.96 standard error (~ 95 % confidence interval) is outside the observed range. Although tropical and subtropical regions are of particular interest for future changes in ozone and its resulting radiative forcing (i.e. highest radiative efficiency), there is a large NH/SH compensation as shown by the annual and global mean forcings. Note the RE is the radiative flux imbalance at a given time due to a radiatively active species (e.g. with and without ozone), whereas the RF refers to the change in RE over time.

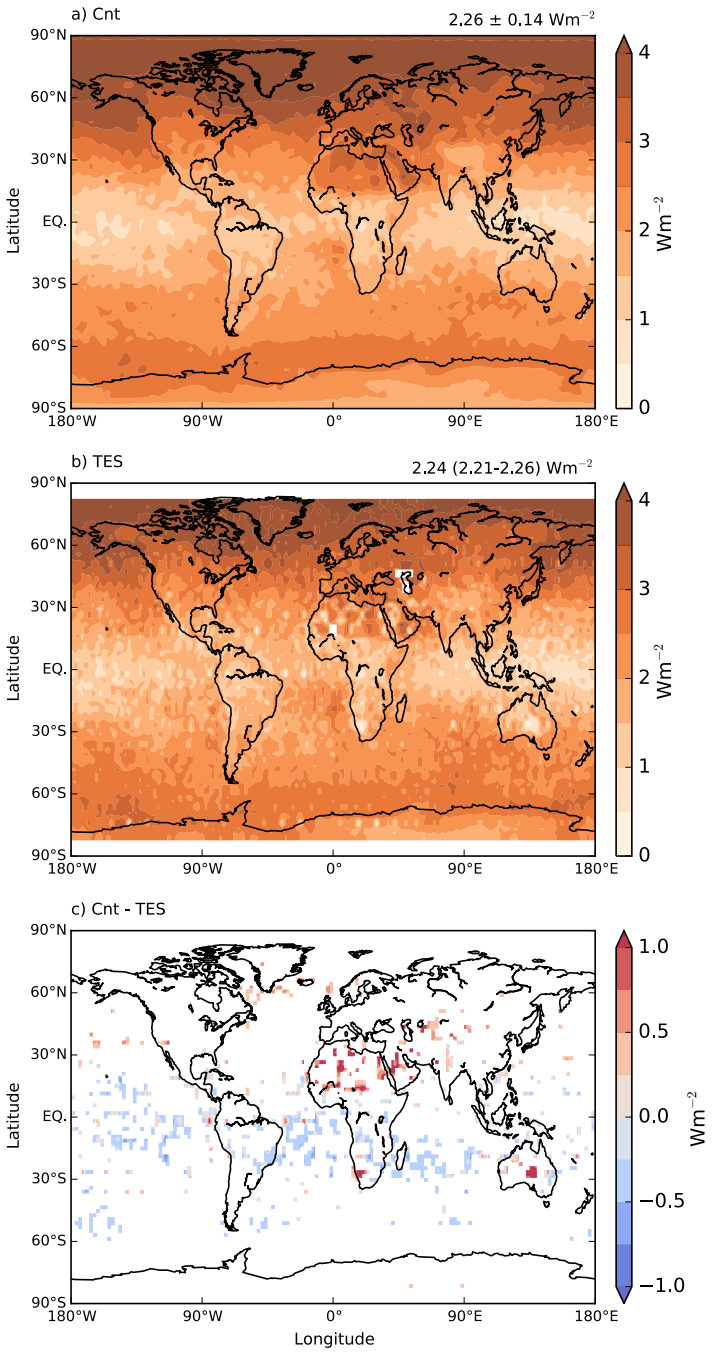

Figure 5.2. Comparison of the annual mean ozone radiative effect between (a) the Cnt simulation and (b) the Tropospheric Emission Spectrometer (TES) from July 2005 until June 2008 (05–08). (c) Cnt simulation bias compared to the TES. Differences are masked for the ±1.96 standard error within the three years observed range.

5.3.2. Ozone changes

Figure 5.3 shows modelled annual and zonal mean ozone changes by 2100 compared to present-day. We present results from adding one single perturbation at a time.

Climate (Clm−Cnt; Fig. 5.3a) shows similar pattern of ozone response to that found previously (e.g. Kawase et al., 2011; Banerjee et al., 2014). In the troposphere, ozone decreases primarily as a consequence of a warmer and more moist climate, which drives increased ozone loss via an enhanced $O(^1D) + H_2O$ flux (Johnson et al., 2001). Reduced net chemical production is partially offset by an increase in the STE (Table 5.2), driven by an enhanced BDC (Zeng and Pyle, 2003). The fingerprint of this change in the BDC can be seen in the lower stratosphere, both for decreases in the tropics and increases at mid-latitudes, respectively associated with the enhanced ascending and descending regions (Hegglin and Shepherd, 2009). In this simulation, the 70 hPa tropical (20°N-20°S) and zonal mean upwelling (Andrews et al., 1987) increases by 3.4 % dec^{-1} compared to Cnt (100 year trend). This trend is in agreement with current climate models projections of ~ 3.2 ± 0.7 % dec^{-1} between 2005–2099 following the RCP8.5 (Hardiman et al., 2014). Additional ozone depletion over the Antarctic is consistent with stratospheric cooling due to enhanced GHG levels (Fig. 5.10a), driving enhanced heterogeneous ozone loss chemistry (WMO, 2014). In contrast, cooling in the upper stratosphere results in ozone increases associated with a slowdown of catalytic O_x cycles (Haigh and Pyle, 1982; Rosenfield et al., 2002).

Future lightning (Lnt−Clm; Fig. 5.3b) shows an increase in LNO_x emissions by ~ 33 %, which results in ozone increases mainly in the tropical and subtropical upper troposphere. However, present-day LNO_x emissions have significant uncertainties and climate models do not agree even on the sign of the change due to different lightning parameterizations (Finney et al., 2016). Nevertheless, the simulated present-day LNO_x emissions of 4.8 ± 1.6 Tg(N) yr^{-1} lies within observationally-derived estimates, and the model's LNO_x sensitivity to climate of 10.8 % K^{-1} is at the upper end of the two standard deviation climate model range (8.8 ± 2 % K^{-1}) (Finney et al., 2016). The net global tropospheric ozone responses to climate will be largely determined by the interplay between (non-lightning) climate-induced ozone losses and lightning-induced ozone production.

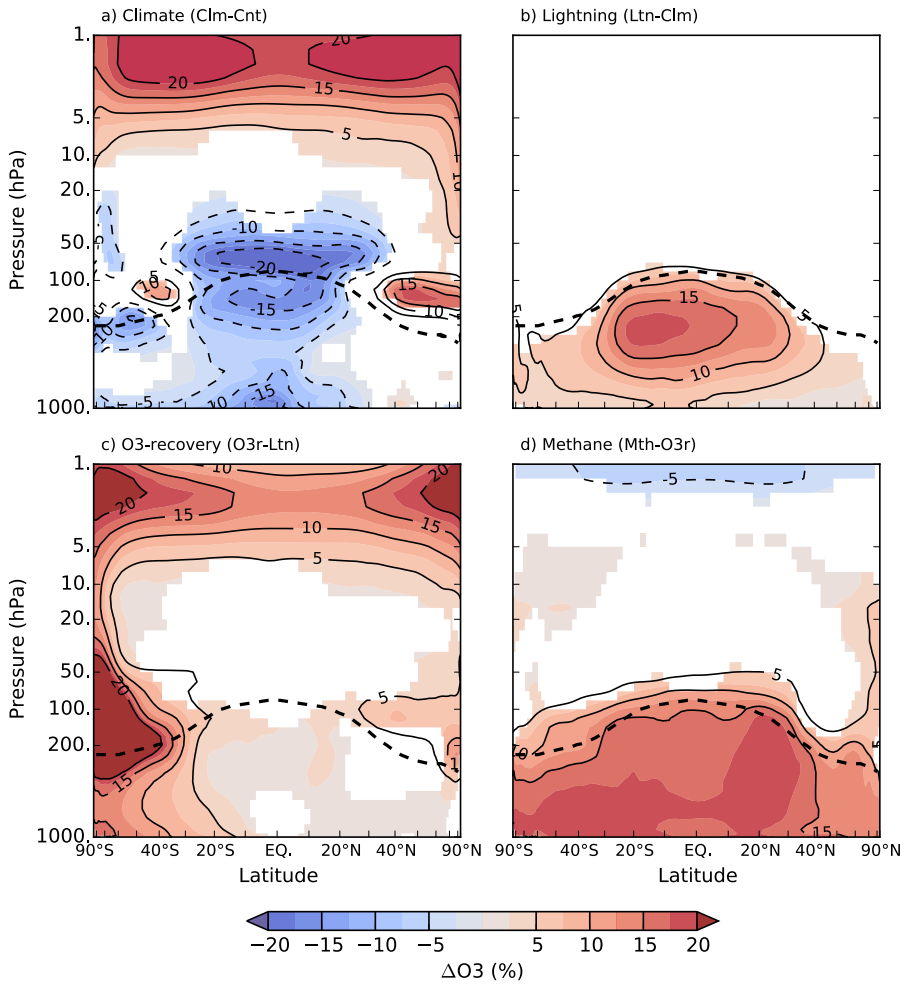

Figure 5.3. Changes in annual and zonal mean ozone due to (a) Climate, (b) Lightning, (c) O3-recovery, and (d) Methane. Contour colours are for statistically significant changes at the 95 % confidence interval using two-tailed Student's t test. The black dashed line represents the chemical tropopause based on the Cnt 150 ppbv ozone contour.

Reductions in inorganic chlorine and bromine abundances (O3r−Ltn; Fig. 5.3c) result in stratospheric ozone increases. Upper stratospheric ozone recovers largely due to decreases in ClO_x-catalysed ozone destruction. Due to reduced heterogeneous ozone loss chemistry, the largest changes are found in polar regions in the lower stratosphere, with increases of ~ 450 % over the Antarctic (November) and ~ 45 % over the Arctic (April). Greater abundances of stratospheric ozone result in an approximately 20 % increase in the STE (Table 5.2) driving higher levels of tropospheric ozone, particularly at mid- and high latitudes in the SH (related to ozone hole recovery) and tropical and subtropical upper troposphere (the descending region

of the BDC), which is consistent with previous model estimates (Banerjee et al., 2016). The BDC-driven increases are somewhat offset by the larger overhead ozone column reducing actinic fluxes and therefore ozone photochemical production (Table 5.2) (Banerjee et al., 2016).

Methane is a greenhouse gas, an ozone precursor in the troposphere and plays various roles in the stratosphere, and these processes are difficult to isolate from the rest. Future methane (Mth−O3r; Fig. 5.3d) emissions show a widespread increase of ozone in the troposphere, with annual and global tropospheric column ozone increase of 15 ± 8 % (Table 5.4). Previous modelling studies reported similar increases of 10–13 % (Brasseur et al., 2006; Kawase et al., 2011). Compensation between ozone decreases in the upper stratosphere (enhanced HO_x-catalysed chemistry) and increases in the lower stratosphere (smog-like chemistry and the partitioning of active/inactive chlorine) (Randeniya et al., 2002; Stenke and Grewe, 2005; Portmann and Solomon, 2007; Fleming et al., 2011; Revell et al., 2012), results in small changes of 2 ± 5 % for the annual and global stratospheric column ozone.

5.3.3. Ozone radiative forcing

Figure 5.4 shows maps of annual mean radiative forcing between 2000 and 2100 due to changes in ozone for the whole atmosphere, along with zonal mean forcings associated with changes in the troposphere and the stratosphere for single perturbation simulations. Note that zonal mean forcings are weighted by latitudinal area (i.e. cosine-latitude), allowing direct comparison with the total forcing. Annual and global mean forcing values and their standard error (i.e. due to ozone changes only) are listed in Table 5.3. Ozone radiative forcing shows strong dependence on the vertical distribution of the change (e.g. Lacis et al., 1990; Forster and Shine, 1997; Rap et al., 2015) and to a lesser extent on the horizontal distribution (e.g. Berntsen et al., 1997). Differences can be seen in both the geographical pattern of the forcing and in the magnitude related to the drivers.

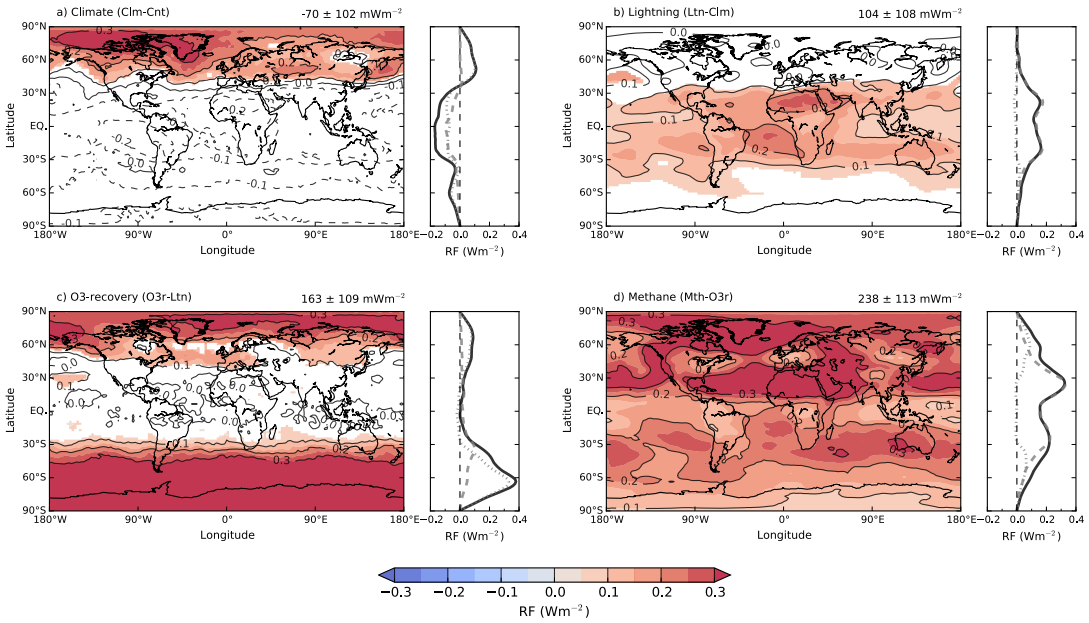

Figure 5.4. Annual mean maps of ozone radiative forcing (whole atmosphere) due to (a) Climate, (b) Lightning, (c) O3-recovery, and (d) Methane. Contour colours are for statistically significant changes at the 95 % confidence interval using two-tailed Student's t test. The annual and global mean is shown on the top right corner (mWm^{-2}). Right panels show zonal mean ozone forcings for the whole atmosphere (solid black), troposphere (dashed grey), and stratosphere (dotted grey). The zonal mean forcings are latitudinally-weighted, i.e. cosine(latitudes).

The global forcing associated with climate (Clm−Cnt; Fig. 5.4a) of -70 ± 102 mWm^{-2} is relatively small and not highly statistically significant (errors denote 1 standard error associated with the 10 year interannual variability of ozone change unless otherwise specified). The geographical pattern shows a relatively strong and significant forcing at high latitudes in the NH, related to ozone increases in the lower stratosphere (transport from enhanced BDC) and upper stratosphere (reduced chemical loss due to cooling). However, this is outweighed by a negative tropospheric forcing in the tropics and a negative stratospheric forcing in the SH extra-tropical region. The latter is largely due to additional ozone depletion in the lower stratosphere (i.e. reduction of STE; not shown).

Table 5.3. Global and annual mean ozone RF and the standard error[a] (mWm^{-2}) by driver and region for the 2000–2100 period.

		Region		Source		CH_4[b]
	Whole-atmosphere	Tropo.	Strat.	Tropo.	Strat.	Tropo.
Climate (Clm−Cnt)[c]	−70 ± 102	−40 ± 42	−30 ± 35	−20 ± 21	−50 ± 57	−8
Lightning (Ltn−Clm)[c]	104 ± 108	105 ± 45	1 ± 37	79 ± 34	24 ± 48	−11
O3-recovery (O3r−Ltn)[d]	163 ± 109	46 ± 47	117 ± 38	1 ± 1	163 ± 84	2
Methane (Mth−O3r)[c]	238 ± 113	193 ± 51	45 ± 39	160 ± 42	78 ± 48	63
Total	435 ± 108	303 ± 48	132 ± 37	220 ± 13	214 ± 72	46

[a] The annual global mean is given along with the (±) standard error (i.e. associated with 10-year interannual variability of ozone).
[b] Long-term ozone forcing due to methane chemistry-climate feedback.
[c,d] RCP8.5 and halogen A1 emission scenarios by 2100 compared to year 2000 (Cnt run) respectively.

Future lightning-induced NO_x emissions (Ltn−Clm; Fig. 5.4b) shows relatively large though not significant global ozone forcing of 104 ± 108 mWm^{-2}, mainly the result of simulated tropospheric ozone changes of 2.1 ± 2.3 DU. Two distinct peak regions are evident around the subtropical belts, where large ozone changes are coincident with relatively cloud-free areas, higher temperature, and a low solar zenith angle. The strongest positive forcing is found over the Sahara and Middle East deserts, associated with greater surface albedo.

Ozone recovery (O3r−Ltn; Fig. 5.4c) drives a significant forcing of 163 ± 109 mWm^{-2}. This forcing is largely confined to the mid- and high latitudes, particularly in the SH (due to ozone hole recovery), and is mainly linked to the stratosphere. Extra-tropical STE is especially important in the SH. This is demonstrated by tropospheric forcing of about ~ 100 mWm^{-2} in this region, which is largely the result of stratospheric-produced ozone transported to the troposphere.

Methane emissions show a large positive forcing around the subtropical belts (Mth−O3r; Fig. 5.4d), which is principally confined to the troposphere, as there is a compensation between changes in the lower and upper stratosphere (Fig. 5.3d). In the tropical and subtropical troposphere, methane is more readily oxidised partly associated with higher OH levels, which results in relatively large ozone increases (Fig. 5.3d). In addition, significant forcings at high latitudes, particularly over the

Arctic, are linked to the stratosphere (i.e. reduced ozone loss via decreased active/inactive chlorine partitioning).

Figure 5.5 shows maps of annual mean normalised tropospheric ozone radiative forcing (NRF) between 2000 and 2100 for the four sensitivity simulations. The NRF – defined here as the tropospheric ozone radiative forcing divided by the tropospheric column ozone – is a useful diagnostic to gain insight into radiative effects of ozone changes. Very similar global NRFs of ~ 39 mWm^{-2} DU^{-1} due to (non-lightning) climate and methane, indicates relatively evenly distributed ozone changes in the troposphere. In contrast, more localised lightning-produced ozone results in higher global NRF of 46 mWm^{-2} DU^{-1}, whereas ozone increases at high latitudes due to ozone recovery results in smaller NRF of 35 mWm^{-2} DU^{-1}. This highlights the dependence of the resulting forcings on the vertical and horizontal distribution of changes in ozone.

Previous studies have shown that the radiative forcing from tropospheric and stratospheric ozone do not have distinct drivers (Søvde et al., 2011; Shindell et al., 2013a). Our results support this and show that climate change, ODSs and methane have consequences for both tropospheric and stratospheric ozone radiative forcing (Table 5.3). In this set of simulations, changes in ozone occurring in the troposphere and the stratosphere respectively contribute ~ 70 % and 30 % to the total annual and global forcing of 435 ± 108 mWm^{-2}.

Further insight can be gained by attributing ozone forcing based on its origin in the stratosphere or the troposphere. In these simulations, we used a stratospheric ozone tracer (see Sect. 5.2) to unambiguously differentiate ozone with tropospheric origin (O3T) from that with stratospheric origin (O3S). Table 5.3 shows such "source classified" ozone radiative forcings, using the "O3S/ozone" and "O3T/ozone" ratios for tropospheric and stratospheric forcings respectively. Stratospheric-produced ozone contributes to ~ 50 % of the annual and global future ozone forcing in this set of simulations, which strongly reinforces the importance of stratospheric-tropospheric interactions.

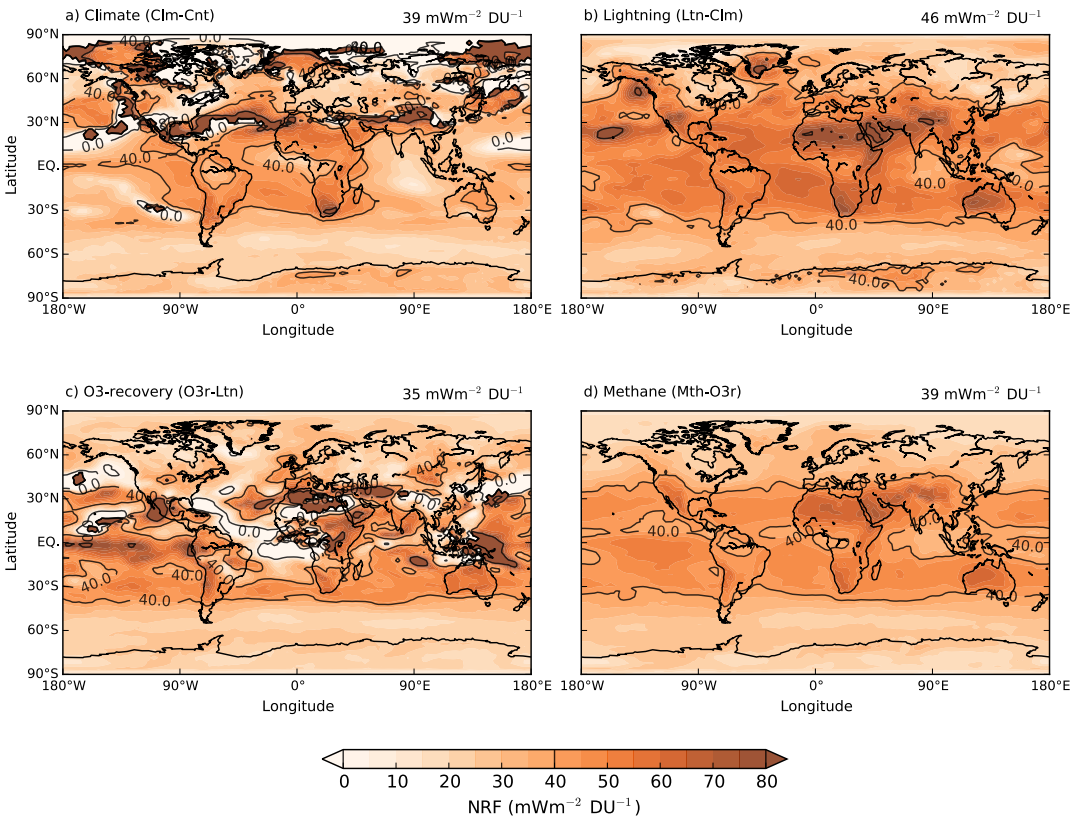

Figure 5.5. Annual mean maps of normalised tropospheric ozone radiative forcing (i.e. divided by the tropospheric column ozone change) due to (a) Climate, (b) Lightning, (c) O3-recovery, and (d) Methane. The annual and global mean is shown on the top right corner (mWm^{-2} DU^{-1}).

5.3.4. Methane feedback and resulting ozone forcing

Future climate change and emissions of ODSs and methane will affect the oxidising capacity of the atmosphere (e.g., via hydroxyl radicals, OH), which influences the methane lifetime (τCH_4) and its concentration. In turn, changes in methane concentrations result in a "long-term" response of tropospheric ozone at decadal time scales (e.g. Fuglestvedt et al., 1999; Wild and Prather, 2000; Holmes et al., 2013). The simulations considered here neglect this feedback by imposing fixed and uniform lower boundary conditions for methane. However, we can estimate how methane concentrations would have adjusted if they were free to evolve, as well as the associated ozone response and radiative forcing. Using the method described by Fiore et al. (2009, and refences therein), we calculate global mean equilibrium methane abundances, $[CH_4]_{eq}$, by

$$[\mathrm{CH_4}]_{\mathrm{eq}} = [\mathrm{CH_4}]_{\mathrm{Cnt}} \times \left(\frac{\tau\mathrm{CH_4}(p)}{\tau\mathrm{CH_4}(r)}\right)^{f} \quad (5.1)$$

where Cnt represents the fixed boundary conditions for year 2000; *(p)* and *(r)* refer to the perturbation and reference simulations respectively; and *f* is a feedback factor which accounts for the response of methane to its own lifetime. The feedback factor is explicitly calculated for WACCM using the O3r "(a)" and Mth "(b)" simulations, as follows

$$f = \frac{1}{(1-s)} \quad (5.2)$$

where *s* is calculated by

$$s = \frac{[\ \ln(\ \tau\mathrm{CH_4(b)}\ ) - \ln(\ \tau\mathrm{CH_4(a)}\ )]}{[\ \ln(\ \mathrm{BCH_4(b)}\ ) - \ln(\ \mathrm{BCH_4(a)}\ )]} \quad (5.3)$$

and where $\mathrm{BCH_4}$ is the annual and global mean methane burden. We calculate a value of *f* of 1.43 which is at the upper end of the literature range (1.19–1.53) (Prather et al., 2001; Stevenson et al., 2013; Voulgarakis et al., 2013) but within 7 % of the observationally constrained best estimate of 1.34 (Holmes et al., 2013).

The ozone response to this methane feedback is estimated by linear interpolation:

$$\Delta\mathrm{O3(eq\ -\ Cnt)} = \left[\frac{\Delta\mathrm{CH_4(eq-Cnt)}}{\Delta\mathrm{CH_4(b-a)}}\right] \times \Delta\mathrm{O3(b-a)} \quad (5.4)$$

where ΔO3 is the change in annual and global mean of tropospheric column ozone (Table 5.4). Assuming the relationships between changes in methane, ozone and radiative forcings are linear; the associated tropospheric ozone forcings to methane feedback are given by the product of ΔO3 and the NRF due to methane perturbation (39 $\mathrm{mWm^{-2}\ DU^{-1}}$; Fig. 5.5d) and are shown in Table 5.3. The overall long-term tropospheric ozone forcing related to the methane feedback in this set of simulations is a moderate increase of ~ 15 %. Climate change (Clm and Ltn simulations) enhances the oxidising capacity of the atmosphere, which results in a small negative forcing of −19 $\mathrm{mWm^{-2}}$ due to the methane feedback. In the Mth simulation, OH concentrations are strongly reduced and the associated forcing of 63 $\mathrm{mWm^{-2}}$ outweighs the climate forcing. This forcing is within the range of ~ 40–120 (mean value of 60) $\mathrm{mWm^{-2}}$ from the ACCMIP ensemble (Table 8 in Stevenson et al., 2013), when considering the same change in methane concentrations (note their values have been linearly extrapolated).

5.3.5. Background conditions and forcing

Since the ozone response to a given perturbation is dependent on the background conditions (e.g. temperature, radiative heating, trace gas levels), the resulting forcing associated to individual drivers may be sensitive to the experimental design. For example, lightning-induced ozone forcing due to climate change may differ significantly under present-day or doubled methane concentrations (i.e. year 2000 or year 2100-RCP8.5 abundances). In the present study, we imposed single perturbations successively. Therefore, the total ozone forcing calculated from this set of simulations includes chemistry-climate feedbacks arising from the interactions between the various perturbations. Yet the attribution of indirect ozone forcings to individual drivers may be sensitive to the order considered (Table 5.1).

We also completed an additional set of simulations (Table 5.5) to assess the robustness of the calculated RF to the order the perturbations were applied (Table 5.3). Lightning-induced net ozone forcing (104 ± 108 mWm^{-2} from Table 5.3) is not significantly different at the 95 % confidence interval (due to interannual variability only unless otherwise specified) compared to that calculated under approximately doubled methane concentrations (Ltn_Mth−Clm_Mth). Although the reported lightning net ozone forcing is 50 mWm^{-2} lower relative to the latter, both lie within the interannual uncertainty (~ 100 mWm^{-2}). The forcing associated with ozone recovery (163 ± 109 mWm^{-2}) is calculated under climate change (i.e. including lightning feedbacks) and present-day methane concentrations, though it also can be derived under present-day climate (O3r_Ods−Cnt) or doubled methane concentrations (Mth−Ltn_Mth). We find no significant differences between the forcings associated with these background conditions, although the reported mean forcing resulting from ozone recovery is greater by ~ 30 mWm^{-2}. Finally, methane-induced net ozone forcing due to doubling its concentrations relative to present-day under ozone recovery conditions (238 ± 113 mWm^{-2}), is not significantly different to that under present-day ODS concentrations (Ltn_Mth−Ltn) or without lightning feedbacks (Clm_Mth−Clm). The reported forcing associated with methane lies within the latter forcings (i.e. 50 mWm^{-2} range). Therefore, we conclude that future ozone forcings due to lightning, ozone recovery and methane concentrations – presented in Table 5.3 – are robust, with regard to background conditions.

The fact that global and annual ozone forcings associated with single perturbations are not significantly different with regard to background conditions is perhaps somewhat surprising, given that, for instance, ozone production is sensitive to the relative abundances of volatile organic compounds and NO_x (e.g. Sillman, 1999). However, while the globally averaged forcing is not significantly affected by the order in which the perturbations are considered, there are significant differences in budget terms (e.g. ozone burden differences due to lightning can be as large as 4.5 ± 1.4 Tg), as well as ozone levels in particular regions of the atmosphere. Therefore, the non-linear additivity of the perturbations is important when considering their impacts on quantities such as ozone profiles and surface air quality (not shown).

5.4. Uncertainties and outlook

We calculate a net ozone radiative forcing of 435 ± 108 mWm^{-2} corresponding to the year 2100 under the RCP8.5 emissions scenario compared to present-day, with the one standard error uncertainty arising from variability in ozone between the years of the time slice simulations. This variability indicates a ±25 % uncertainty, which is slightly larger than the spread across the ACCMIP ensemble of approximately ±20 % (Stevenson et al., 2013). However, additional sources of uncertainty exist in the ozone forcing. Previously, uncertainties arising from the tropopause definition (±3 %), the radiation scheme or forcing calculation (±10 %), and the extent to which clouds and stratospheric temperature adjustment influence ozone forcing (±7 % and ±3 % respectively) have been estimated (Stevenson et al., 2013). Climate feedbacks, land-use change, natural ozone precursor emissions, and future changes in the structure of the tropopause (Wilcox et al., 2012) may introduce at least an additional ±20 % uncertainty (Stevenson et al., 2013). Following Stevenson et al. (2013), we assume that the above individual uncertainties are independent and combine them to estimate an overall uncertainty of ±30 %, which represents the 95 % confidence interval. We note that Skeie et al. (2011) from an independent analysis estimated the same overall uncertainty.

Figure 5.6 summarises the global and annual net ozone forcing as well as the forcings by driver and region. Overall, our annual global mean best estimate for the net ozone radiative forcing between 2000 and 2100 is 430 ± 130 mWm^{-2}, with tropospheric and stratospheric forcings of $300 \pm 90\ mWm^{-2}$ and $130 \pm 40\ mWm^{-2}$,

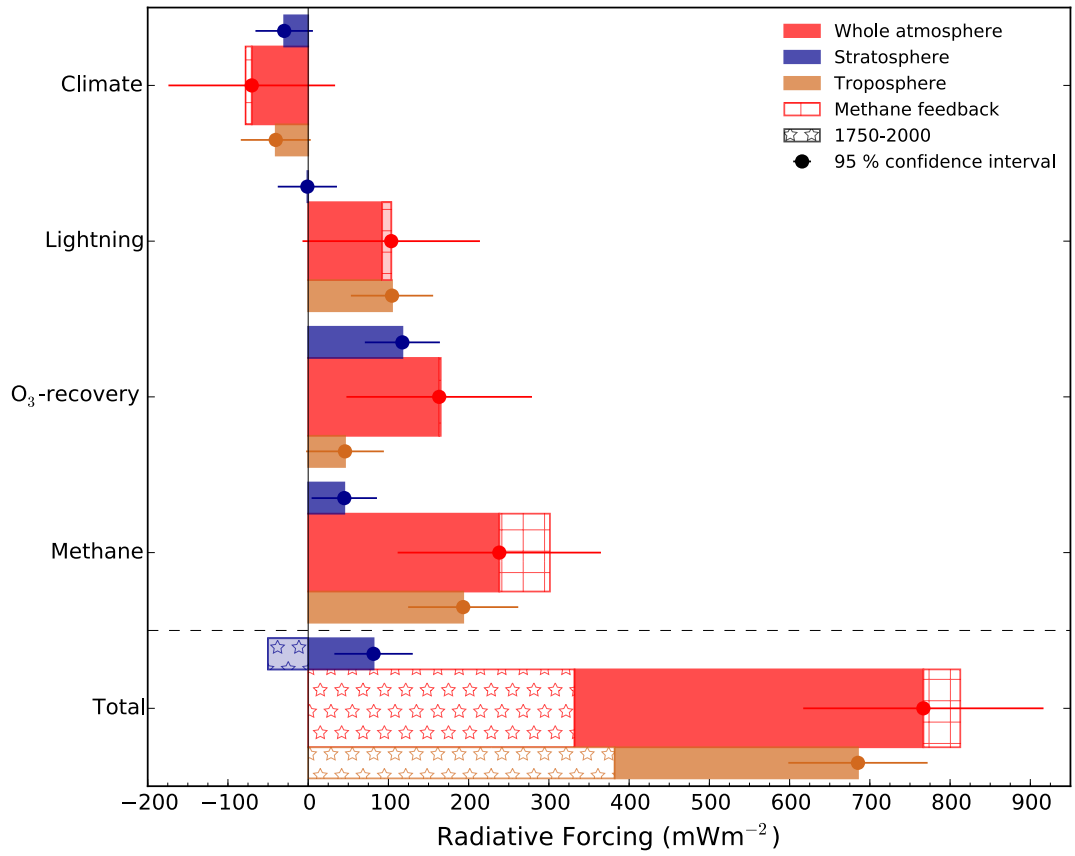

Figure 5.6. Ozone radiative forcings by drivers (2000–2100; mWm^{-2}). Tropospheric (brown), stratospheric (blue) and net (whole atmosphere, red) forcings are shown. Associated ozone forcings to methane feedback (square-hatched) are shown along with the net forcings. The overall ozone forcing (Total) is the sum of the individual forcings (Climate, Lightning, O_3-recovery and Methane from Table 5.3) scaled to 1750 (star-hatched). Dots and error bars indicate the mean and the 95 % confidence intervals of the forcings respectively. The information on pre-industrial ozone forcing (1750–2000) and sources of uncertainty are detailed in Sect. 5.4.

respectively. Current estimates for tropospheric and stratospheric ozone forcings from 1750 to 2011 are 400 ± 20 mWm^{-2} and −50 ± 100 mWm^{-2}, respectively (Myhre et al., 2013). An increase of 0.5 DU in tropospheric ozone was estimated in Skeie et al. (2011) from 2000 to 2010, and a tropospheric ozone normalized radiative forcing of 42 mWm^{-2} DU^{-1} calculated from the ACCMIP ensemble (Stevenson et al., 2013). Therefore, we estimate a net ozone forcing of 760 ± 230 mWm^{-2} from 1750 to 2100 based on our simulations, which is the result of the forcings in the troposphere and the stratosphere (690 ± 210 mWm^{-2} and 70 ± 20 mWm^{-2} respectively). Our tropospheric

forcing is within the range estimated from the ACCMIP models of 600 ± 120 mWm^{-2} (Table 12 in Stevenson et al., 2013).

Previous work has shown that NRF is an appropriate tool for estimating annual and global tropospheric forcings derived from changes in tropospheric column ozone, which in turn reduces the multi-model uncertainty (Gauss et al., 2003). The NRF in our analysis of 43 mWm^{-2} DU^{-1} is similar to that from the ACCMIP models between the 1850s and 2000s, but larger compared to that in Gauss et al. (2003). This supports the future tropospheric ozone forcings and their uncertainties during the 21st century derived from the ACCMIP ensemble (calculated using the NRF), and may be used as a benchmark for individual studies.

Although previous studies have examined key drivers of ozone during the 21st century and future changes are relatively well understood (e.g. Kawase et al., 2011; Banerjee et al., 2014; Banerjee et al., 2016), the resulting forcings have been explored in less detail (e.g. Gauss et al., 2003; Bekki et al., 2013; Stevenson et al., 2013). Following a process-based approach that includes chemistry-climate feedbacks, we calculate that climate-only, lightning, ozone recovery and methane emissions contribute respectively −16 ± 24 %, 24 ± 25 %, 38 ± 25 %, and 55 ± 26 % to the net ozone RF between 2000 and 2100 (Table 5.3 and Fig. 5.6). Further uncertainties arise from the long-term ozone response to methane changes, which could increase the overall tropospheric forcing by ~ 15 %. Climate change (including lightning feedbacks) alone produces a relatively small tropospheric ozone forcing of 64 ± 44 mWm^{-2}. A subset of eight models from the ACCMIP activity shows a small negative but not significant tropospheric forcing of −33 ± 42 mWm^{-2}, with few models reporting positive forcings (Table 12 in Stevenson et al., 2013). The impact of climate change on ozone forcing is surrounded by large uncertainties, which are associated with chemistry-climate feedbacks and the lack of confidence in the LNO_x sensitivity to global mean surface temperature, due to different parameterizations and the vertical distributions of the emissions (Banerjee et al., 2014; Finney et al., 2016), as well as changes in the BDC (Butchart, 2014). For example, the climate change-induced net ozone forcing between 2000–2100 – following the future emission scenario RCP8.5 in an independent chemistry-climate model – is of the same order of magnitude but different sign (−70 mWm^{-2}) (Banerjee et al., 2018). While they found similar tropospheric ozone forcing of 70 mWm^{-2}, their negative stratospheric ozone forcing outweighs the latter (−150 mWm^{-2}). Methane- and ODSs-induced ozone

forcings have respectively a substantial contribution from the stratosphere (~ 14 %) and the troposphere (~ 34 %), recently shown in modelling studies (Søvde et al., 2011; Shindell et al., 2013a; Banerjee et al., 2018). A striking result, however, is the contribution of the stratospheric-produced ozone to the net forcing of ~ 30 ± 20 % and ~ 99 ± 50 % due to methane and ODS concentrations respectively, which is consistent with the findings from an independent chemistry-climate model (Banerjee et al., 2016, 2018). This reflects the roles that methane plays in stratospheric ozone chemistry (i.e. particularly in the lower stratosphere), and that ozone recovery principally occurs in the stratosphere.

5.5. Summary and conclusions

This study has explored future changes in ozone by the end of the 21st century and the resulting radiative forcing following a process-based approach, imposing one forcing at a time. We have used the RCP8.5 emissions scenario to represent an upper limit on these responses. This is a different approach to previous studies, which typically have either explored future changes in ozone concentrations or ozone forcing. The methane feedbacks (due to the changing oxidising capacity of the atmosphere, and due to the long-term tropospheric ozone response) and its forcing have also been accounted for. In addition, non-linearities arising from chemistry-climate interactions have been investigated.

The simulated present-day ozone radiative effect (RE) is in good agreement with estimates based on observed ozone from TES, particularly in terms of its spatial distribution. However, there are systematic biases: RE is overestimated in the NH and underestimated in the SH, with significant biases in the subtropics. These RE biases are mostly consistent with the biases in tropospheric ozone in current global chemistry-climate models (Young et al., 2018), although the simulated annual global present-day tropospheric column ozone (28.9 ± 1.5 DU) is within observed interannual variability of 28.1–34.1 DU (Young et al., 2013a). The fact that similar spatial distribution biases are apparent in many climate models suggests a common deficiency, and emissions data have been proposed as a likely candidate (Young et al., 2013a; Young et al., 2018).

Our analysis shows that the net ozone radiative forcing arising from climate driven changes is relatively small and not significant (33 ± 104 mWm^{-2}), which is

largely the result of the interplay between lightning-produced ozone and enhanced ozone destruction (via increased temperatures and humidity). Higher methane concentrations and reduced ODS levels also have consequences for ozone forcing in the stratosphere (45 ± 39 mWm^{-2}) and the troposphere (46 ± 47 mWm^{-2}) respectively. We have demonstrated both the importance of stratospheric-tropospheric interactions and the stratosphere as a key region controlling a large fraction of the tropospheric ozone forcing (i.e. from the source point of view compared to the more common division by recipient-region).

Future annual and global tropospheric and stratospheric column ozone changes from year 2000 to 2100 in this set of simulations (7.0 DU and 21.3 DU respectively) are mainly driven by methane and ODS emissions, respectively (Table 5.4). These changes lead to a net ozone radiative forcing of 430 ± 130 mWm^{-2} compared to present-day, with an overall uncertainty of ±30 % (i.e. representing the 95 % confidence interval). Relative to the pre-industrial period (year 1750), our best estimate for the year 2100 net ozone radiative forcing is 760 ± 230 mWm^{-2}.

This study highlights the key role of the stratosphere in determining future ozone radiative forcing in spite of the fact that the impacts largely take place in the troposphere. Increasing confidence in present-day observations of the Brewer-Dobson circulation and the stratospheric-tropospheric exchange will therefore play a crucial role in improving chemistry-climate models and better constraining ozone radiative forcing. A future study will address the importance of the stratosphere on future air quality commitments, which may better inform emission regulations.

5.7. Supporting information

This section presents additional information to evaluate the updated ozone radiative kernel (O_3 RK) and illustrate in more detail present-day tropospheric ozone (Cnt; year 2000), changes in column ozone and temperature due to the different drivers investigated in this study, and additional sensitivity simulations to further assess the robustness of the results presented in the main manuscript. Tables 5.4 and 5.5 present global and annual column ozone changes for the above drivers and period, and additional model simulations used in the main text to explore non-linearities respectively. Figure 5.7 compares an ozone RF calculated using the O_3 RK technique with the corresponding RF calculated directly with the SOCRATES radiative transfer

Table 5.4. Global and annual mean ozone columns (DU)[a].

Simulation	Total column	Tropospheric column	Stratospheric column
Cnt	280.6 ± 8.7	28.9 ± 1.5	251.7 ± 8.1
Clm	281.5 ± 9.9	27.7 ± 1.6	253.8 ± 9.3
Ltn	284.2 ± 9.7	29.8 ± 1.7	254.4 ± 9.1
O3r	299.0 ± 9.5	31.2 ± 1.7	267.8 ± 8.8
Mth	308.9 ± 9.5	35.9 ± 1.9	273.0 ± 8.8
Cnt+fLNOx	280.3 ± 8.6	28.4 ± 1.5	251.9 ± 8.1

[a] The annual global mean is given along with the (±) standard error.

model, which is based on Edwards and Slingo (1996). Figures 5.8 and 5.9 show annual mean tropospheric burden distribution for ozone and stratospheric ozone tracer (O3S) respectively. Finally, Figure 5.10 shows changes in annual and zonal mean temperature due to climate, lightning, ozone depleting substances (ODSs), and methane over 2000–2100.

Table 5.5. Additional model simulations

Simulation	Climate[1]	ODSs[2]	CH_4[3]
Clm_Mth	2100 (fLNOx)[4]	2000	2100
Ltn_Mth	2100	2000	2100
O3r_Ods	2000	2100	2000

[1]Climate (sea surface temperatures, sea ice, CO_2 and N_2O, if not otherwise specified) follows the RCP8.5 emissions scenario.

[2]Relative to Cnt, ODS boundary conditions of −63.2 % (2.156 ppbv) total chlorine, −35.7% (8.1 pptv) total bromine and −67.6 % (1.376 ppbv) total fluorine follow the halogen scenario A1.

[3]Relative to Cnt, CH_4 boundary conditions of 214.2 % (3744 ppbv) follow the RCP8.5 emissions scenario.

[4]Offline lightning-induced NO_x emissions (fLNOx) are imposed by applying a monthly mean climatology of the Cnt simulation.

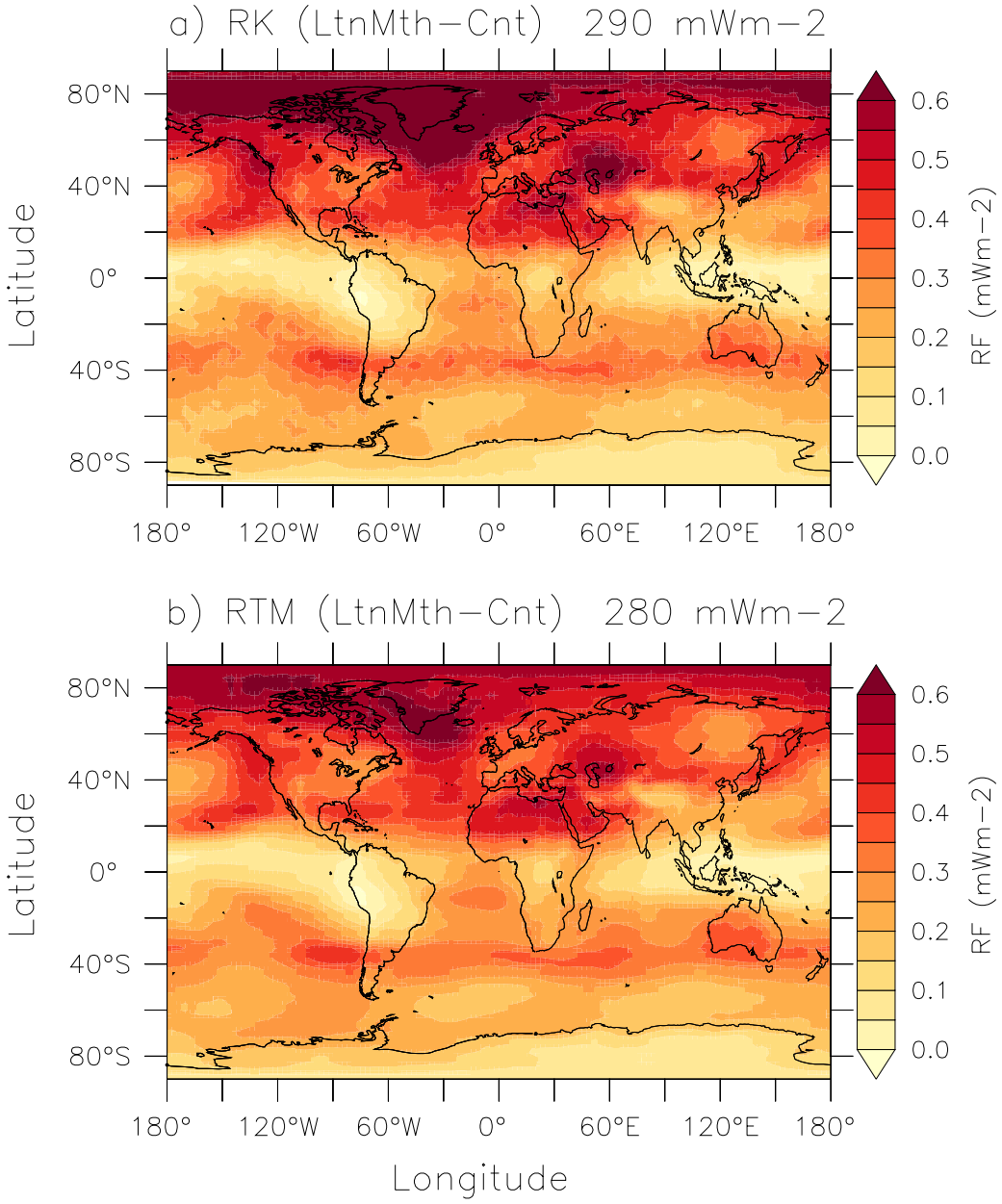

Figure 5.7. Annual mean maps of net ozone radiative forcing (Ltn_Mth−Cnt) calculated using a) the radiative kernel (RK) technique and b) the SOCRATES radiative transfer model (RTM). The annual and global mean is shown on the top (mWm^{-2}).

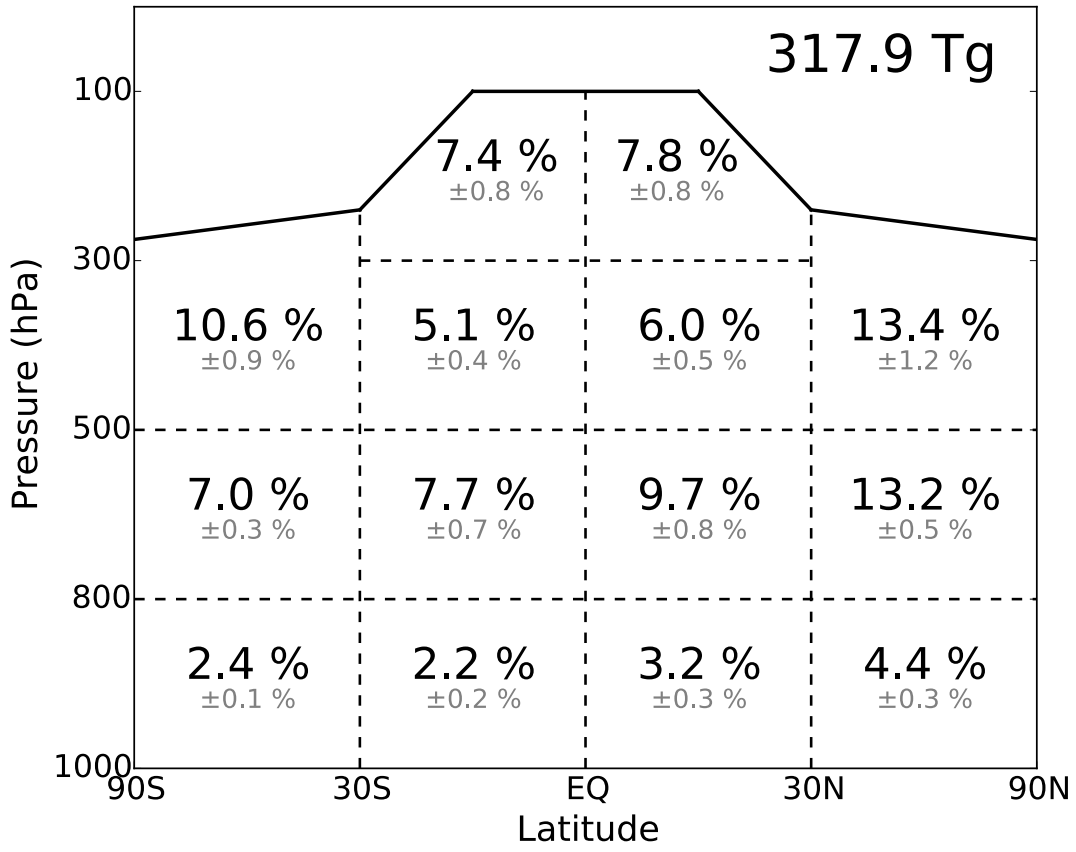

Figure 5.8. Present-day (Cnt) annual mean tropospheric ozone burden distribution (black) and the ±1 standard deviation (grey), represented by "boxes" (dashed black lines) of approximately equal air masses, as per Young et al. (2013). The tropopause is represented by the black thick line (i.e. regions below 150 ppbv ozone levels). The annual and global tropospheric ozone burden mean is shown in the top right corner.

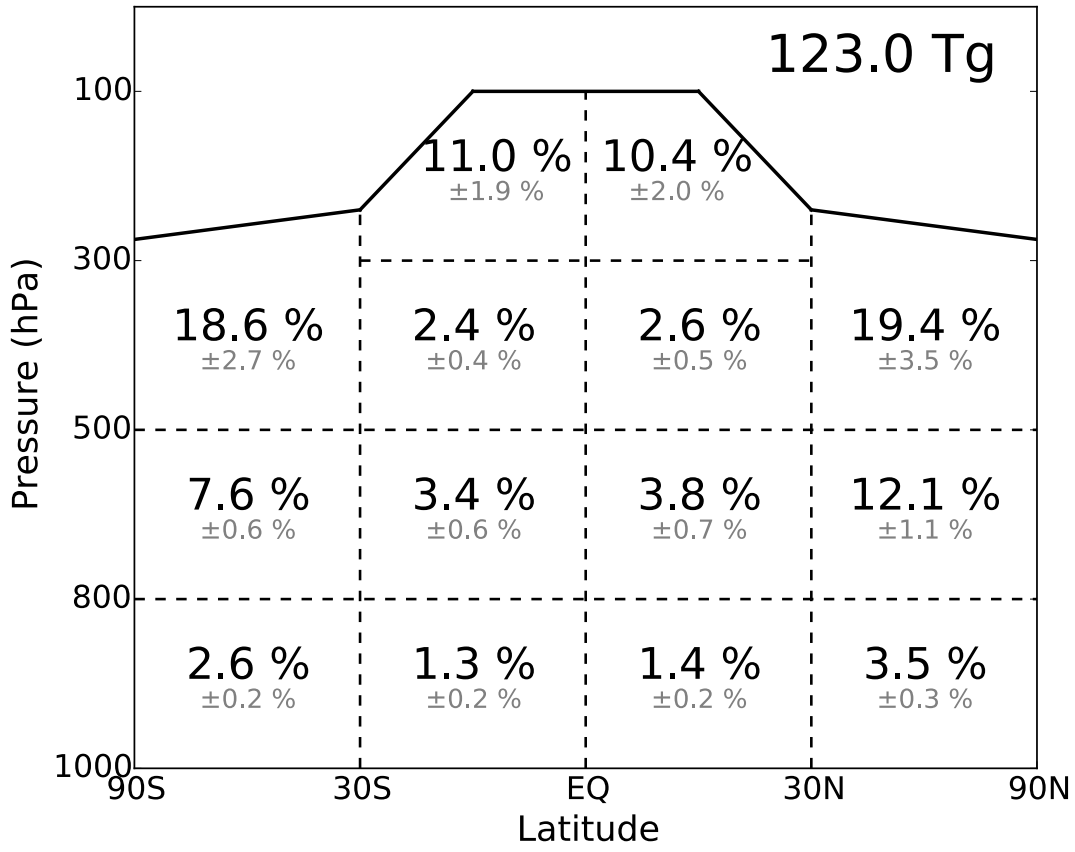

Figure 5.9. Same as Fig. 5.8 but for stratospheric ozone tracer (O3S).

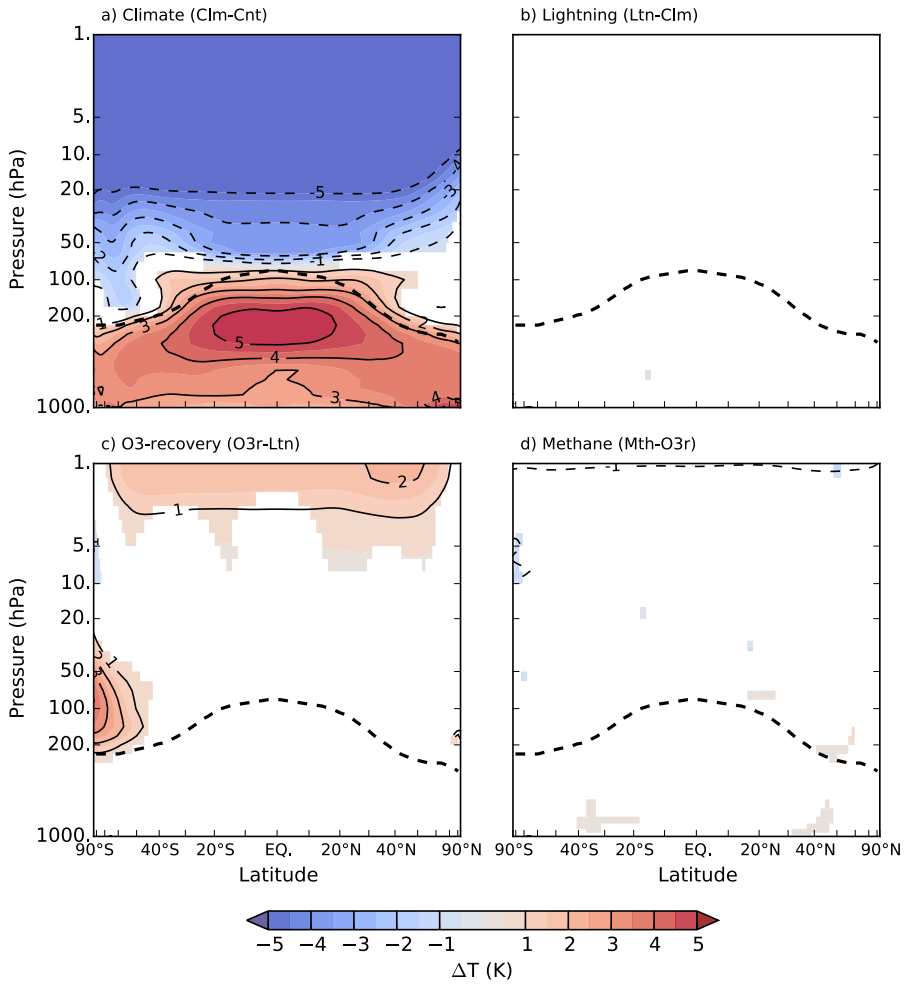

Figure 5.10. Same as Fig. 5.3 in the main text, but for temperature (K).

Competing interests. The authors declare that they have no conflict of interest.

Data availability. The model output used here can be available upon request from the corresponding author (figlesias@iqfr.csic.es). The whole atmosphere ozone radiative kernel can also be available upon request from A. Rap (a.rap@leeds.ac.uk).

Acknowledgements. This work was supported by NERC, under project number NE/L501736/1. F. Iglesias-Suarez would like to acknowledge NERC for a PhD studentship and thank Fernando Govantes for hosting him at the Centro Andaluz de Biología del Desarrollo (CABD) while he completed some of this work. WACCM is a component of the Community Earth System Model (CESM), which is supported by the NSF and the Office of Science of the U.S. Department of Energy. Computing resources were provided by NCAR's Climate Simulation Laboratory, sponsored by the NSF and other agencies. This research was enabled by the computational and storage resources of NCAR's Computational and Information Systems Laboratory (CISL). We thank the NASA JPL TES team for releasing the TES ozone.

Chapter 6

Conclusions and outlook

This thesis explored past, present and future changes in stratospheric ozone, and how these are linked to tropospheric compositions and climate. Chapter 2 presented an overview of the concepts that form the background to stratospheric ozone, as well as the major chemical and dynamical processes governing its abundance and distribution. This chapter also described tropospheric composition and climate with a focus on anthropogenic perturbations, before discussing linkages between the stratosphere and the troposphere. The evolution of stratospheric ozone in the coming century will be largely determined by human activities. I described future changes of stratospheric ozone by region and altitude, and how potential socio-economic pathways are used to drive chemistry-climate model (CCM) projections.

Chapter 3 presented an analysis of stratospheric ozone changes and associated climate impacts in the Atmospheric Chemistry and Climate Model Intercomparison Project (ACCMIP). ACCMIP was the first multi-model activity to have a number of models representing ozone chemistry in the stratosphere and the troposphere. This chapter explored the evolution of stratospheric ozone from 1850 to 2100 using a number of chemistry-climate models that participated in the ACCMIP activity (8 out of 16 models), which included time-varying stratospheric ozone (i.e. prescribed or interactively calculated). In ACCMIP, the multi-model mean total column ozone trends for the 1980–2000 period compare favourably against observational estimates, best agreement was found over the Antarctic (−11.9 % dec^{-1} compared to observed −13.9 ± 10.4 % dec^{-1}) and largest deviations were seen in the Arctic (−2.1 % dec^{-1}

compared to observed −5.3 ± 3.3 % dec^{-1}) during springtime. These models showed that the Antarctic ozone hole cooled the lower stratosphere during the same period and season (−2.2 K dec^{-1}). In turn, stratosphere-troposphere dynamical and radiative coupling drives summertime tropospheric circulation changes in the Southern Hemisphere, for example, the modelled Southern Annular Mode (SAM) index increase approximately 1.3 hPa dec^{-1}. Whether these circulation changes return to "normal" levels (pre-industrial conditions) or are further disrupted during the 21st century, will be the result of the interplay between the ozone hole recovery and greenhouse gases (GHGs) concentrations. Furthermore, ozone sensitivity to GHG abundances in the upper stratosphere will largely determine future total column ozone changes in the tropics, due to a trade off between lower stratospheric and tropospheric column ozone in the socio-economic pathways explored.

Chapter 4 proposed a mechanism that links internal low frequency variability of ozone in the middle tropical stratosphere and surface climate. Interestingly, ozone variability in this region of the stratosphere resembles multi-decadal climate variability in Pacific Ocean sea surface temperatures, the so-called Interdecadal Pacific Oscillation (IPO). Using observational data and chemistry-climate model simulations, this chapter identified a plausible mechanism that involves both dynamical (Brewer-Dobson circulation, BDC) and chemical (NO_x-catalysed loss) processes to drive multi-decadal variability in mid-stratospheric tropical ozone. Sensitivity CCM simulations showed that negative ozone trends since the 1990s in the tropical mid-stratosphere are primarily explained by internal climate variability (50 %). Major volcanic eruptions, nitrogen dioxide and ozone depleting substances (ODSs) emissions are also important factors, respectively contributing to approximately 25 %, 18 % and 6 % to the former trends. The results also indicated internally generated low frequency variability in the shallow and deep branches of the BDC, which is important for interpreting observationally derived changes in recent decades and isolating long-term trends.

Chapter 5 investigated future ozone radiative forcing between present-day (2000) and the end of the 21st century (2100), due to climate change (with and without lightning-related feedbacks), ODS and methane concentrations. This chapter presented an upper limit of projected ozone forcing by exploring a high intense emission socio-economic development. The model captured well both present-day ozone radiative effect (2.26 ± 0.14 Wm^{-2} compared to observationally derived

2.21–2.26 Wm^{-2}) and its spatial distribution ($r = 0.6$, $p < 0.01$; correlation against observed data). The results showed small and not highly significant net ozone forcing of 33 ± 104 mWm^{-2} associated with climate change, which arises from the trade off between lightning-produced ozone (104 ± 108 mWm^{-2}) and increased ozone loss in a warmer and wetter atmosphere (−70 ± 102 mWm^{-2}). This chapter highlighted the role of both (1) stratosphere-troposphere interactions and (2) the importance of the stratosphere controlling a large fraction of the tropospheric ozone forcing: (1) reduced ODS abundances and increased methane concentrations had implications for ozone forcing in the troposphere (46 ± 47 mWm^{-2}) and the stratosphere (45 ± 39 mWm^{-2}) respectively; (2) stratospheric-produced ozone (i.e. source point of view) contributes to approximately 50 % of the total ozone forcing (i.e. including the troposphere and stratosphere) in this set of simulations. Overall, the best estimate of net ozone forcing in this chapter – including above drivers and different sources of uncertainty – is 430 ± 130 mWm^{-2} relative to 2000 (i.e. 20 % of the modelled present-day ozone radiative effect), and 760 ± 230 mWm^{-2} relative to 1750 (i.e. pre-industrial reference year).

Overall, in this thesis I demonstrated that changes in stratospheric ozone are intrinsically linked to other elements of the Earth system, specifically to the climate and composition of the troposphere. I quantified the evolution of stratospheric ozone and related climate impacts using both, existing model simulations to evaluate not fully understood processes and associated feedbacks, and own sensitivity simulations to assess radiative forcings in a process-based approach. I addition, I demonstrated for the first time a link between decadal to inter-decadal internal climate variability in sea surface temperatures and ozone in the tropical middle stratosphere, and proposed a mechanism which involves dynamical and chemical processes.

As global climate models evolve to further complexity to become Earth System Models, it allows scientists to address research questions in a more consistent framework. CCMs more routinely include tropospheric and stratospheric chemistry and climate feedbacks relevant to ozone, yet they have a number of limitations (e.g. dynamical processes and chemical reactions represented, parameterisations, horizontal and vertical resolution, top lid and so forth). New multi-model activities can be used to assess model developments – do they capture observed changes in trace gases due to the correct processes, or is their uncertainty associated with chemistry-climate feedbacks better constrained? Also, multi-model activities are useful for exploring

more thoroughly linkages between the stratosphere and the troposphere due to climate change and internally generated climate variability, and for identifying key deficiencies in models. For example, stratospheric ozone chemistry is particularly sensitive to GHGs in the upper stratosphere (temperature dependence of catalytic chemistry). Thus, future studies considering changes in total column ozone should include the whole stratosphere (up to ~ 50 km height), which may be particularly important for the tropics. In addition, CCMs not constrained by observed meteorology struggle to capture natural variability. As the Arctic vortex is more disturbed, variable and relatively warmer compared to its Antarctic counterpart, simulating heterogeneous chemistry (i.e. processes on polar stratospheric clouds) and stratospheric ozone interannual variability remains a challenge in this region. Furthermore, current CCMs typically simulate smaller ozone negative trends in the tropical lower stratosphere compared to observations, which may be associated to deficiencies in the underlying general circulation model and transport processes (i.e. BDC). This is an active area of research because ozone determines to a large extent temperatures in the lower stratosphere, and the latter may be involved in significant chemistry-climate feedbacks. Also CCMs consistently project an acceleration of the BDC due to climate change with the concomitant increase in stratosphere-troposphere exchange. Due to this is particularly important for the upper troposphere and lower stratosphere (e.g. region with highest radiative efficiency of ozone), more research based on observational estimates is needed to better constrained the BDC and its seasonal cycle.

Nevertheless, the development and use of CCMs to become increasingly complex enables us to formulate more detailed questions. For example, the quasi-biennial oscillation (QBO) modulates transport and dynamical processes in the stratosphere, as well as ozone catalysed chemistry indirectly. An interactive and "realistic" representation of the QBO in CCMs can be used to explore linkages between the stratosphere and the troposphere due to climate change and internally generated climate variability. However, there is a suggestion that in some CCMs, a strong tropical upwelling may prevent an interactive representation of the QBO, whereas a weak tropical upwelling may lead to simulate shorter QBO periods. Also, due to the ever-increasing computational capacity, additional processes are being included in CCMs after laboratory and field experiments identify new relevant chemistry influencing the composition of the atmosphere. For example, very short

lived species containing halogen radicals (i.e. Cl, Br, I) have a significant influence on tropospheric and stratospheric composition. With regard to climate, halogen chemistry affects methane, ozone and other species (i.e. oxidation), which are radiatively active and affect the Earth's energy balance via direct and indirect processes. In the last decade, new observations and the implementation of halogen chemistry in CCMs have led to groundbreaking findings, yet its impacts on the global chemical composition and climate feedbacks remain poorly understood. More research is needed to improve our understanding on the chemical composition of the atmosphere and the concomitant chemistry-climate feedbacks, which will benefit from the continuous monitoring of trace gases, laboratory experiments and the ever-evolving Earth System Models.

Bibliography

Abalos, M., Legras, B., Ploeger, F., and Randel, W. J.: Evaluating the advective Brewer-Dobson circulation in three reanalyses for the period 1979–2012, J. Geophys. Res., 120, 2169-8996, doi:10.1002/2015JD023182, 2015.

Anderson, J. G., Brune, W. H., and Proffitt, M. H.: Ozone destruction by chlorine radicals within the Antarctic vortex: The spatial and temporal evolution of ClO-O3 anticorrelation based on in situ ER-2 data, J. Geophys. Res., 94, 11465-11479, doi:10.1029/JD094iD09p11465, 1989.

Andrews, D. G., Holton, J. R., and Leovy, C. B.: Middle atmosphere dynamics, International Geophysics Series, Academic press, San Diego, USA, 1987.

Anstey, J. A., and Shepherd, T. G.: High-latitude influence of the quasi-biennial oscillation, Quart. J. Roy. Meteor. Soc., 140, 1-21, doi:10.1002/qj.2132, 2014.

Arblaster, J. M., and Meehl, G. A.: Contributions of External Forcings to Southern Annular Mode Trends, J. Clim., 19, 2896-2905, doi:10.1175/JCLI3774.1, 2006.

Arblaster, J. M., Meehl, G. A., and Karoly, D. J.: Future climate change in the Southern Hemisphere: Competing effects of ozone and greenhouse gases, Geophys. Res. Lett., 38, 1944-8007, doi:10.1029/2010GL045384, 2011.

Arblaster, J. M., and Gillett, N. P. (Lead Authors), Calvo, N., Forster, P. M., Polvani, L. M., Son, S. W., Waugh, D. W., and Young, P. J., Stratospheric ozone changes and climate, Chapter 4 in Scientific Assessment of Ozone Depletion: 2014, Global Ozone Research and Monitoring Project – Report No. 55, World Meteorological Organization, Geneva, Switzerland, 2014.

Aschmann, J., Burrows, J. P., Gebhardt, C., Rozanov, A., Hommel, R., Weber, M., and Thompson, A. M.: On the hiatus in the acceleration of tropical upwelling since the beginning of the 21st century, Atmos. Chem. Phys., 14, 12803-12814, doi:10.5194/acp-14-12803-2014, 2014.

Atkinson, R.: Atmospheric chemistry of VOCs and NOx, Atmos. Environ., 34, 2063-2101, doi:10.1016/S1352-2310(99)00460-4, 2000.

Austin, J., Shindell, D., Beagley, S. R., Brühl, C., Dameris, M., Manzini, E., Nagashima, T., Newman, P., Pawson, S., Pitari, G., Rozanov, E., Schnadt, C., and Shepherd, T. G.: Uncertainties and assessments of chemistry-climate models of the stratosphere, Atmos. Chem. Phys., 3, 1-27, doi:10.5194/acp-3-1-2003, 2003.

Austin, J., and Wilson, R. J.: Ensemble simulations of the decline and recovery of stratospheric ozone, J. Geophys. Res., 111, 2156-2202, doi:10.1029/2005JD006907, 2006.

Austin, J., Scinocca, J., Plummer, D., Oman, L., Waugh, D., Akiyoshi, H., Bekki, S., Braesicke, P., Butchart, N., Chipperfield, M., Cugnet, D., Dameris, M., Dhomse, S., Eyring, V., Frith, S., Garcia, R. R., Garny, H., Gettelman, A., Hardiman, S. C., Kinnison, D., Lamarque, J. F., Mancini, E., Marchand, M., Michou, M., Morgenstern, O., Nakamura, T., Pawson, S., Pitari, G., Pyle, J., Rozanov, E., Shepherd, T. G., Shibata, K., Teyssèdre, H., Wilson, R. J., and

Yamashita, Y.: Decline and recovery of total column ozone using a multimodel time series analysis, J. Geophys. Res., 115, 2156-2202, doi:10.1029/2010JD013857, 2010.

Avallone, L. M., and Prather, M. J.: Photochemical evolution of ozone in the lower tropical stratosphere, J. Geophys. Res., 101, 1457-1461, doi:10.1029/95JD03010, 1996.

Baldwin, M. P., Cheng, X., and Dunkerton, T. J.: Observed correlations between winter-mean tropospheric and stratospheric circulation anomalies, Geophys. Res. Lett., 21, 1141-1144, doi:10.1029/94GL01010, 1994.

Baldwin, M. P., and Dunkerton, T. J.: Propagation of the Arctic Oscillation from the stratosphere to the troposphere, J. Geophys. Res., 104, 30937-30946, doi:10.1029/1999JD900445, 1999.

Baldwin, M. P., and Dunkerton, T. J.: Stratospheric Harbingers of Anomalous Weather Regimes, Science, 294, 581-584, doi:10.1126/science.1063315, 2001.

Baldwin, M. P., Gray, L. J., Dunkerton, T. J., Hamilton, K., Haynes, P. H., Randel, W. J., Holton, J. R., Alexander, M. J., Hirota, I., Horinouchi, T., Jones, D. B. A., Kinnersley, J. S., Marquardt, C., Sato, K., and Takahashi, M.: The quasi-biennial oscillation, Rev. Geophys., 39, 179-229, doi:10.1029/1999RG000073, 2001.

Baldwin, M. P., and Gray, L. J.: Tropical stratospheric zonal winds in ECMWF ERA-40 reanalysis, rocketsonde data, and rawinsonde data, Geophys. Res. Lett., 32, 1944-8007, doi:10.1029/2004GL022328, 2005.

Baldwin, M. P., and Thompson, D. W. J.: A critical comparison of stratosphere–troposphere coupling indices, Quart. J. Roy. Meteor. Soc., 135, 1661-1672, doi:10.1002/qj.479, 2009.

Banerjee, A., Archibald, A. T., Maycock, A. C., Telford, P., Abraham, N. L., Yang, X., Braesicke, P., and Pyle, J. A.: Lightning NOx, a key chemistry–climate

interaction: impacts of future climate change and consequences for tropospheric oxidising capacity, Atmos. Chem. Phys., 14, 9871-9881, doi:10.5194/acp-14-9871-2014, 2014.

Banerjee, A., Maycock, A. C., Archibald, A. T., Abraham, N. L., Telford, P., Braesicke, P., and Pyle, J. A.: Drivers of changes in stratospheric and tropospheric ozone between year 2000 and 2100, Atmos. Chem. Phys., 16, 2727-2746, doi:10.5194/acp-16-2727-2016, 2016.

Banerjee, A., Maycock, A. C., and Pyle, J. A.: Chemical and climatic drivers of radiative forcing due to changes in stratospheric and tropospheric ozone over the 21st century, Atmos. Chem. Phys., 18, 2899-2911, doi:10.5194/acp-18-2899-2018, 2018.

Barnes, E. A., Barnes, N. W., and Polvani, L. M.: Delayed Southern Hemisphere Climate Change Induced by Stratospheric Ozone Recovery, as Projected by the CMIP5 Models, J. Clim., 27, 852-867, doi:10.1175/JCLI-D-13-00246.1, 2013.

Barnett, J. J., Houghton, J. T., and Pyle, J. A.: The temperature dependence of the ozone concentration near the stratopause, Quart. J. Roy. Meteor. Soc., 101, 245-257, doi:10.1002/qj.49710142808, 1975.

Bates, D. R., and Nicolet, M.: The photochemistry of atmospheric water vapor, Journal of Geophysical Research, 55, 301-327, doi:10.1029/JZ055i003p00301, 1950.

Bedjanian, Y., and Poulet, G.: Kinetics of Halogen Oxide Radicals in the Stratosphere, Chemical Reviews, 103, 4639-4656, doi:10.1021/cr0205210, 2003.

Bekki, S., A. Rap, V. Poulain, S. Dhomse, M. Marchand, F. Lefevre, P. M. Forster, S. Szopa, and M. P. Chipperfield: Climate impact of stratospheric ozone recovery, Geophys. Res. Lett., 40, 2796–2800, doi:10.1002/grl.50358, 2013.

Berntsen, T. K., Isaksen, I. S. A., Myhre, G., Fuglestvedt, J. S., Stordal, F., Larsen, T. A., Freckleton, R. S., and Shine, K. P.: Effects of anthropogenic emissions on tropospheric ozone and its radiative forcing, J. Geophys. Res., 102, 2156-2202, doi:10.1029/97JD02226, 1997.

Biele, J., Tsias, A., Luo, B. P., Carslaw, K. S., Neuber, R., Beyerle, G., and Peter, T.: Nonequilibrium coexistence of solid and liquid particles in Arctic stratospheric clouds, J. Geophys. Res., 106, 2156-2202, doi:10.1029/2001JD900188, 2001.

Bindoff, N. L., Stott, P. A., AchutaRao, K. M., Allen, M. R., Gillett, N., Gutzler, D., Hansingo, K., Hegerl, G., Hu, Y., Jain, S., Mokhov, I. I., Overland, J., Perlwitz, J., Sebbari, R. and Zhang, X.: Detection and Attribution of Climate Change: from Global to Regional. In: Climate Change 2013: The Physical Science Basis. Contribution of Working Group I to the Fifth Assessment Report of the Intergovernmental Panel on Climate Change [Stocker, T.F., D. Qin, G. K. Plattner, M. Tignor, S.K. Allen, J. Boschung, A. Nauels, Y. Xia, V. Bex and P.M. Midgley (eds.)]. Cambridge University Press, Cambridge, United Kingdom and New York, NY, USA, 2013.

Birner, T., and Bönisch, H.: Residual circulation trajectories and transit times into the extratropical lowermost stratosphere, Atmos. Chem. Phys., 11, 817-827, doi:10.5194/acp-11-817-2011, 2011.

Bloss, C., Wagner, V., Jenkin, M. E., Volkamer, R., Bloss, W. J., Lee, J. D., Heard, D. E., Wirtz, K., Martin-Reviejo, M., Rea, G., Wenger, J. C., and Pilling, M. J.: Development of a detailed chemical mechanism (MCMv3.1) for the atmospheric oxidation of aromatic hydrocarbons, Atmos. Chem. Phys., 5, 641-664, doi:10.5194/acp-5-641-2005, 2005.

Bodeker, G. E., Shiona, H., and Eskes, H.: Indicators of Antarctic ozone depletion, Atmos. Chem. Phys., 5, 2603-2615, doi:10.5194/acp-5-2603-2005, 2005.

Bodeker, G. E., Hassler, B., Young, P. J., and Portmann, R. W.: A vertically resolved, global, gap-free ozone database for assessing or constraining global climate

model simulations, Earth Syst. Sci. Data, 5, 31-43, doi:10.5194/essd-5-31-2013, 2013.

Bojkov, R. D.: Surface Ozone During the Second Half of the Nineteenth Century, Journal of Climate and Applied Meteorology, 25, 343-352, doi:10.1175/1520-0450(1986)025<0343:SODTSH>2.0.CO;2, 1986.

Bond, T. C., Doherty, S. J., Fahey, D. W., Forster, P. M., Berntsen, T., DeAngelo, B. J., Flanner, M. G., Ghan, S., Kärcher, B., Koch, D., Kinne, S., Kondo, Y., Quinn, P. K., Sarofim, M. C., Schultz, M. G., Schulz, M., Venkataraman, C., Zhang, H., Zhang, S., Bellouin, N., Guttikunda, S. K., Hopke, P. K., Jacobson, M. Z., Kaiser, J. W., Klimont, Z., Lohmann, U., Schwarz, J. P., Shindell, D., Storelvmo, T., Warren, S. G., and Zender, C. S.: Bounding the role of black carbon in the climate system: A scientific assessment, J. Geophys. Res., 118, 5380-5552, doi:10.1002/jgrd.50171, 2013.

Bönisch, H., Engel, A., Birner, T., Hoor, P., Tarasick, D. W., and Ray, E. A.: On the structural changes in the Brewer-Dobson circulation after 2000, Atmos. Chem. Phys., 11, 3937-3948, doi:10.5194/acp-11-3937-2011, 2011.

Bowman, K. W., Shindell, D. T., Worden, H. M., Lamarque, J. F., Young, P. J., Stevenson, D. S., Qu, Z., de la Torre, M., Bergmann, D., Cameron-Smith, P. J., Collins, W. J., Doherty, R., Dalsøren, S. B., Faluvegi, G., Folberth, G., Horowitz, L. W., Josse, B. M., Lee, Y. H., MacKenzie, I. A., Myhre, G., Nagashima, T., Naik, V., Plummer, D. A., Rumbold, S. T., Skeie, R. B., Strode, S. A., Sudo, K., Szopa, S., Voulgarakis, A., Zeng, G., Kulawik, S. S., Aghedo, A. M., and Worden, J. R.: Evaluation of ACCMIP outgoing longwave radiation from tropospheric ozone using TES satellite observations, Atmos. Chem. Phys., 13, 4057-4072, doi:10.5194/acp-13-4057-2013, 2013.

Brasseur, G. P., Schultz, M., Granier, C., Saunois, M., Diehl, T., Botzet, M., Roeckner, E., and Walters, S.: Impact of Climate Change on the Future Chemical Composition of the Global Troposphere, J. Clim., 19, 3932-3951, doi:10.1175/JCLI3832.1, 2006

Brewer, A. W.: Evidence for a world circulation provided by the measurements of helium and water vapour distribution in the stratosphere, Quart. J. Roy. Meteor. Soc., 75, 351-363, doi:10.1002/qj.49707532603, 1949.

Brönnimann, S., Malik, A., Stickler, A., Wegmann, M., Raible, C. C., Muthers, S., Anet, J., Rozanov, E., and Schmutz, W.: Multidecadal variations of the effects of the Quasi-Biennial Oscillation on the climate system, Atmos. Chem. Phys., 16, 15529-15543, doi:10.5194/acp-16-15529-2016, 2016.

Burkholder, J. B., Ravishankara, A. R., and Solomon, S.: UV/visible and IR absorption cross sections of BrONO2, J. Geophys. Res., 100, 16793-16800, doi:10.1029/95JD01223, 1995.

Butchart, N., Scaife, A. A., Bourqui, M., de Grandpré, J., Hare, S. H. E., Kettleborough, J., Langematz, U., Manzini, E., Sassi, F., Shibata, K., Shindell, D., and Sigmond, M.: Simulations of anthropogenic change in the strength of the Brewer–Dobson circulation, Clim. Dynam., 27, 727-741, doi:10.1007/s00382-006-0162-4, 2006.

Butchart, N., Cionni, I., Eyring, V., Shepherd, T. G., Waugh, D. W., Akiyoshi, H., Austin, J., Brühl, C., Chipperfield, M. P., Cordero, E., Dameris, M., Deckert, R., Dhomse, S., Frith, S. M., Garcia, R. R., Gettelman, A., Giorgetta, M. A., Kinnison, D. E., Li, F., Mancini, E., McLandress, C., Pawson, S., Pitari, G., Plummer, D. A., Rozanov, E., Sassi, F., Scinocca, J. F., Shibata, K., Steil, B., and Tian, W.: Chemistry–Climate Model Simulations of Twenty-First Century Stratospheric Climate and Circulation Changes, J. Clim., 23, 5349-5374, doi:10.1175/2010JCLI3404.1, 2010.

Butchart, N., Charlton-Perez, A. J., Cionni, I., Hardiman, S. C., Haynes, P. H., Krüger, K., Kushner, P. J., Newman, P. A., Osprey, S. M., Perlwitz, J., Sigmond, M., Wang, L., Akiyoshi, H., Austin, J., Bekki, S., Baumgaertner, A., Braesicke, P., Brühl, C., Chipperfield, M., Dameris, M., Dhomse, S., Eyring, V., Garcia, R., Garny, H., Jöckel, P., Lamarque, J. F., Marchand, M., Michou, M.,

Morgenstern, O., Nakamura, T., Pawson, S., Plummer, D., Pyle, J., Rozanov, E., Scinocca, J., Shepherd, T. G., Shibata, K., Smale, D., Teyssèdre, H., Tian, W., Waugh, D., and Yamashita, Y.: Multimodel climate and variability of the stratosphere, J. Geophys. Res., 116, D05102, doi:10.1029/2010JD014995, 2011.

Butchart, N.: The Brewer-Dobson circulation, Rev. Geophys., 52, 157-184, doi:10.1002/2013RG000448, 2014.

Butz, A., Bösch, H., Camy-Peyret, C., Chipperfield, M. P., Dorf, M., Kreycy, S., Kritten, L., Prados-Román, C., Schwärzle, J., and Pfeilsticker, K.: Constraints on inorganic gaseous iodine in the tropical upper troposphere and stratosphere inferred from balloon-borne solar occultation observations, Atmos. Chem. Phys., 9, 7229-7242, doi:10.5194/acp-9-7229-2009, 2009.

Calvo, N., Garcia, R. R., Randel, W. J., and Marsh, D. R.: Dynamical Mechanism for the Increase in Tropical Upwelling in the Lowermost Tropical Stratosphere during Warm ENSO Events, J. Atmos. Sci., 67, 2331-2340, doi:10.1175/2010JAS3433.1, 2010.

Calvo, N., and Marsh, D. R.: The combined effects of ENSO and the 11 year solar cycle on the Northern Hemisphere polar stratosphere, J. Geophys. Res., 116, D23112, doi:10.1029/2010JD015226, 2011.

Calvo, N., Garcia, R. R., Marsh, D. R., Mills, M. J., Kinnison, D. E., and Young, P. J.: Reconciling modeled and observed temperature trends over Antarctica, Geophys. Res. Lett., 39, L16803, doi:10.1029/2012gl052526, 2012.

Calvo, N., Garcia, R. R., and Kinnison, D. E.: Revisiting Southern Hemisphere polar stratospheric temperature trends in WACCM: The role of dynamical forcing, Geophys. Res. Lett., 44, 2017GL072792, doi:10.1002/2017GL072792, 2017.

Canziani, P. O., O'Neill, A., Schofield, R., Raphael, M., Marshall, G. J., and Redaelli, G.: World Climate Research Programme Special Workshop on Climatic

Effects of Ozone Depletion in the Southern Hemisphere, Bull. Am. Meteorol. Soc., 95, ES101-ES105, doi:10.1175/BAMS-D-13-00143.1, 2014.

Chapman, S.: On ozone and atomic oxygen in the upper atmosphere, Philosophical Magazine and Journal of Science, 10, 369-383, doi:10.1080/14786443009461588, 1930.

Charlton-Perez, A. J., Hawkins, E., Eyring, V., Cionni, I., Bodeker, G. E., Kinnison, D. E., Akiyoshi, H., Frith, S. M., Garcia, R., Gettelman, A., Lamarque, J. F., Nakamura, T., Pawson, S., Yamashita, Y., Bekki, S., Braesicke, P., Chipperfield, M. P., Dhomse, S., Marchand, M., Mancini, E., Morgenstern, O., Pitari, G., Plummer, D., Pyle, J. A., Rozanov, E., Scinocca, J., Shibata, K., Shepherd, T. G., Tian, W., and Waugh, D. W.: The potential to narrow uncertainty in projections of stratospheric ozone over the 21st century, Atmos. Chem. Phys., 10, 9473-9486, doi:10.5194/acp-10-9473-2010, 2010.

Charlton-Perez, A. J., Baldwin, M. P., Birner, T., Black, R. X., Butler, A. H., Calvo, N., Davis, N. A., Gerber, E. P., Gillett, N., Hardiman, S., Kim, J., Krüger, K., Lee, Y. Y., Manzini, E., McDaniel, B. A., Polvani, L., Reichler, T., Shaw, T. A., Sigmond, M., Son, S. W., Toohey, M., Wilcox, L., Yoden, S., Christiansen, B., Lott, F., Shindell, D., Yukimoto, S., and Watanabe, S.: On the lack of stratospheric dynamical variability in low-top versions of the CMIP5 models, J. Geophys. Res., 118, 2494-2505, doi:10.1002/jgrd.50125, 2013.

Chipperfield, M. P., and Pyle, J. A.: Model sensitivity studies of Arctic ozone depletion, J. Geophys. Res., 103, 28389-28403, doi:10.1029/98JD01960, 1998.

Christy, J. R., Spencer, R. W., Norris, W. B., Braswell, W. D., and Parker, D. E.: Error Estimates of Version 5.0 of MSU–AMSU Bulk Atmospheric Temperatures, J. Atmos. Ocean. Tech., 20, 613-629, doi:10.1175/1520-0426(2003)20<613:EEOVOM>2.0.CO;2, 2003.

Cionni, I., Eyring, V., Lamarque, J. F., Randel, W. J., Stevenson, D. S., Wu, F., Bodeker, G. E., Shepherd, T. G., Shindell, D. T., and Waugh, D. W.: Ozone database in support of CMIP5 simulations: results and corresponding radiative forcing, Atmos. Chem. Phys., 11, 11267-11292, doi:10.5194/acp-11-11267-2011, 2011.

Collins, W. J., Derwent, R. G., Garnier, B., Johnson, C. E., Sanderson, M. G., and Stevenson, D. S.: Effect of stratosphere-troposphere exchange on the future tropospheric ozone trend, J. Geophys. Res., 108, 8528, doi:10.1029/2002JD002617, 2003.

Collins, W. J., Bellouin, N., Doutriaux-Boucher, M., Gedney, N., Halloran, P., Hinton, T., Hughes, J., Jones, C. D., Joshi, M., Liddicoat, S., Martin, G., O'Connor, F., Rae, J., Senior, C., Sitch, S., Totterdell, I., Wiltshire, A., and Woodward, S.: Development and evaluation of an Earth-System model – HadGEM2, Geosci. Model Dev., 4, 1051-1075, doi:10.5194/gmd-4-1051-2011, 2011.

Cooper, O. R., Parrish, D. D., Ziemke, J., Balashov, N. V., Cupeiro, M., Galbally, I. E., Gilge, S., Horowitz, L., Jensen, N. R., Lamarque, J. F., Naik, V., Oltmans, S. J., Schwab, J., Shindell, D. T., Thompson, A. M., Thouret, V., Wang, Y., and Zbinden, R. M.: Global distribution and trends of tropospheric ozone: An observation-based review, Elem. Sci. Anth., 2, doi:10.12952/journal.elementa.000029, 2014.

Cornu, A.: Observation de la limite ultraviolette du spectre solaire a` diverses altitudes, C. R. Hebd. Seances Acad. Sci., 89, 1879.

Crook, J. A., Gillett, N. P., and Keeley, S. P. E.: Sensitivity of Southern Hemisphere climate to zonal asymmetry in ozone, Geophys. Res. Lett., 35, L07806, doi:10.1029/2007GL032698, 2008.

Crutzen, P. J.: The influence of nitrogen oxides on the atmospheric ozone content, Quart. J. Roy. Meteor. Soc., 96, 320-325, doi:10.1002/qj.49709640815, 1970.

Crutzen, P. J.: Photochemical reactions initiated by and influencing ozone in unpolluted tropospheric air, Tellus, 26, 47-57, doi:10.1111/j.2153-3490.1974.tb01951.x, 1974.

Crutzen, P. J.: Chlorofluoromethanes: Threats to the ozone layer, Rev. Geophys., 17, 1824-1832, doi:10.1029/RG017i007p01824, 1979.

Crutzen, P. J., and Arnold, F.: Nitric acid cloud formation in the cold Antarctic stratosphere: a major cause for the springtime 'ozone hole', Nature, 324, 651-655, doi:10.1038/324651a0, 1986.

Crutzen, P. J., Groo, J. U., xdf, Br, xfc, hl, C., xfc, ller, R., and Russell, J. M.: A Reevaluation of the Ozone Budget with HALOE UARS Data: No Evidence for the Ozone Deficit, Science, 268, 705-708, doi:10.1126/science.268.5211.705, 1995.

Dahlmann, K., Grewe, V., Ponater, M., and Matthes, S.: Quantifying the contributions of individual NOx sources to the trend in ozone radiative forcing, Atmos. Environ., 45, 2860-2868, doi:10.1016/j.atmosenv.2011.02.071, 2011.

Dall'Amico, M., Gray, L. J., Rosenlof, K. H., Scaife, A. A., Shine, K. P., and Stott, P. A.: Stratospheric temperature trends: impact of ozone variability and the QBO, Clim. Dynam., 34, 381-398, doi:10.1007/s00382-009-0604-x, 2010.

Dameris, M., and Baldwin, M.P.: Impact of climate change on the stratospheric ozone layer. In: Müller, R. (ed.) Stratospheric Ozone Depletion and Climate Change, pp. 214–252. RSC Publishing, Cambridge, 2011.

Daniel, J. S., Solomon, S., Portmann, R. W., and Garcia, R. R.: Stratospheric ozone destruction: The importance of bromine relative to chlorine, J. Geophys. Res., 104, 23871-23880, doi:10.1029/1999JD900381, 1999.

Danielsen, E. F., and Mohnen, V.: Project Duststorm report: Ozone transport, in situ measurements and meteorological analysis of troposphere folding, J. Geophys. Res., 82, 5833–5866, doi:10.1029/JC082i037p05867, 1977.

Davis, S. M., Rosenlof, K. H., Hassler, B., Hurst, D. F., Read, W. G., Vömel, H., Selkirk, H., Fujiwara, M., and Damadeo, R.: The Stratospheric Water and Ozone Satellite Homogenized (SWOOSH) database: a long-term database for climate studies, Earth Syst. Sci. Data, 8, 461-490, doi:10.5194/essd-8-461-2016, 2016.

De Grandpré, J., Sandilands, J. W., McConnell, J. C., Beagley, S. R., Croteau, P. C., and Danilin, M. Y.: Canadian middle atmosphere model: Preliminary results from the chemical transport module, Atmos.-Ocean, 35, 385-431, doi:10.1080/07055900.1997.9649598, 1997.

De Zafra, R. L., Jaramillo, M., Parrish, A., Solomon, P., Connor, B., and Barrett, J.: High concentrations of chlorine monoxide at low altitudes in the Antarctic spring stratosphere: Diurnal variation, Nature, 328, 408-411, doi:10.1038/328408a0, 1987.

Diallo, M., Legras, B., and Chédin, A.: Age of stratospheric air in the ERA-Interim, Atmos. Chem. Phys., 12, 12133-12154, doi:10.5194/acp-12-12133-2012, 2012.

Dietmüller, S., Ponater, M., and Sausen, R.: Interactive ozone induces a negative feedback in CO2-driven climate change simulations, J. Geophys. Res., 119, 1796-1805, doi:10.1002/2013JD020575, 2014.

Dobson, G. M. B., and Harrison, D. N.: Measurements of the Amount of Ozone in the Earth's Atmosphere and Its Relation to Other Geophysical Conditions, Proc. R. Soc. London Ser. A, 110, 660-693, doi:10.1098/rspa.1926.0040, 1926.

Dobson, G. M. B.: Origin and Distribution of the Polyatomic Molecules in the Atmosphere, Proc. R. Soc. London Ser. A, Mathematical and Physical Sciences, 236, 187-193, doi:10.1098/rspa.1956.0127, 1956.

Dobson, G. M. B.: Forty years' research on atmospheric ozone at Oxford: a history, Appl. Opt., 7, 387-405, doi:10.1364/AO.7.000387, 1968.

Donner, L. J., Wyman, B. L., Hemler, R. S., Horowitz, L. W., Ming, Y., Zhao, M., Golaz, J. C., Ginoux, P., Lin, S. J., Schwarzkopf, M. D., Austin, J., Alaka, G., Cooke, W. F., Delworth, T. L., Freidenreich, S. M., Gordon, C. T., Griffies, S. M., Held, I. M., Hurlin, W. J., Klein, S. A., Knutson, T. R., Langenhorst, A. R., Lee, H. C., Lin, Y., Magi, B. I., Malyshev, S. L., Milly, P. C. D., Naik, V., Nath, M. J., Pincus, R., Ploshay, J. J., Ramaswamy, V., Seman, C. J., Shevliakova, E., Sirutis, J. J., Stern, W. F., Stouffer, R. J., Wilson, R. J., Winton, M., Wittenberg, A. T., and Zeng, F.: The Dynamical Core, Physical Parameterizations, and Basic Simulation Characteristics of the Atmospheric Component AM3 of the GFDL Global Coupled Model CM3, J. Clim., 24, 3484-3519, doi:10.1175/2011JCLI3955.1, 2011.

Dvortsov, V. L., and Solomon, S.: Response of the stratospheric temperatures and ozone to past and future increases in stratospheric humidity, J. Geophys. Res., 106, 7505-7514, doi:10.1029/2000JD900637, 2001.

Emmons, L. K., Walters, S., Hess, P. G., Lamarque, J. F., Pfister, G. G., Fillmore, D., Granier, C., Guenther, A., Kinnison, D., Laepple, T., Orlando, J., Tie, X., Tyndall, G., Wiedinmyer, C., Baughcum, S. L., and Kloster, S.: Description and evaluation of the Model for Ozone and Related chemical Tracers, version 4 (MOZART-4), Geosci. Model Dev., 3, 43-67, doi:10.5194/gmd-3-43-2010, 2010.

Engel, A., Mobius, T., Bonisch, H., Schmidt, U., Heinz, R., Levin, I., Atlas, E., Aoki, S., Nakazawa, T., Sugawara, S., Moore, F., Hurst, D., Elkins, J., Schauffler, S., Andrews, A., and Boering, K.: Age of stratospheric air unchanged within

uncertainties over the past 30 years, Nature Geosci., 2, 28-31, doi:10.1038/ngeo388, 2009.

Eyring, V., Harris, N. R. P., Rex, M., Shepherd, T. G., Fahey, D. W., Amanatidis, G. T., Austin, J., Chipperfield, M. P., Dameris, M., Forster, P. M. D. F., Gettelman, A., Graf, H. F., Nagashima, T., Newman, P. A., Pawson, S., Prather, M. J., Pyle, J. A., Salawitch, R. J., Santer, B. D., and Waugh, D. W.: A Strategy for Process-Oriented Validation of Coupled Chemistry–Climate Models, Bull. Am. Meteorol. Soc., 86, 1117-1133, doi:10.1175/BAMS-86-8-1117, 2005.

Eyring, V., Butchart, N., Waugh, D. W., Akiyoshi, H., Austin, J., Bekki, S., Bodeker, G. E., Boville, B. A., Brühl, C., Chipperfield, M. P., Cordero, E., Dameris, M., Deushi, M., Fioletov, V. E., Frith, S. M., Garcia, R. R., Gettelman, A., Giorgetta, M. A., Grewe, V., Jourdain, L., Kinnison, D. E., Mancini, E., Manzini, E., Marchand, M., Marsh, D. R., Nagashima, T., Newman, P. A., Nielsen, J. E., Pawson, S., Pitari, G., Plummer, D. A., Rozanov, E., Schraner, M., Shepherd, T. G., Shibata, K., Stolarski, R. S., Struthers, H., Tian, W., and Yoshiki, M.: Assessment of temperature, trace species, and ozone in chemistry-climate model simulations of the recent past, J. Geophys. Res., 111, D22308, doi:10.1029/2006JD007327, 2006.

Eyring, V., Waugh, D. W., Bodeker, G. E., Cordero, E., Akiyoshi, H., Austin, J., Beagley, S. R., Boville, B. A., Braesicke, P., Brühl, C., Butchart, N., Chipperfield, M. P., Dameris, M., Deckert, R., Deushi, M., Frith, S. M., Garcia, R. R., Gettelman, A., Giorgetta, M. A., Kinnison, D. E., Mancini, E., Manzini, E., Marsh, D. R., Matthes, S., Nagashima, T., Newman, P. A., Nielsen, J. E., Pawson, S., Pitari, G., Plummer, D. A., Rozanov, E., Schraner, M., Scinocca, J. F., Semeniuk, K., Shepherd, T. G., Shibata, K., Steil, B., Stolarski, R. S., Tian, W., and Yoshiki, M.: Multimodel projections of stratospheric ozone in the 21st century, J. Geophys. Res., 112, D16303, doi:10.1029/2006JD008332, 2007.

Eyring, V., Cionni, I., Bodeker, G. E., Charlton-Perez, A. J., Kinnison, D. E., Scinocca, J. F., Waugh, D. W., Akiyoshi, H., Bekki, S., Chipperfield, M. P., Dameris, M., Dhomse, S., Frith, S. M., Garny, H., Gettelman, A., Kubin, A., Langematz, U., Mancini, E., Marchand, M., Nakamura, T., Oman, L. D., Pawson, S., Pitari, G., Plummer, D. A., Rozanov, E., Shepherd, T. G., Shibata, K., Tian, W., Braesicke, P., Hardiman, S. C., Lamarque, J. F., Morgenstern, O., Pyle, J. A., Smale, D., and Yamashita, Y.: Multi-model assessment of stratospheric ozone return dates and ozone recovery in CCMVal-2 models, Atmos. Chem. Phys., 10, 9451-9472, doi:10.5194/acp-10-9451-2010, 2010a.

Eyring, V., Cionni, I., Lamarque, J. F., Akiyoshi, H., Bodeker, G. E., Charlton-Perez, A. J., Frith, S. M., Gettelman, A., Kinnison, D. E., Nakamura, T., Oman, L. D., Pawson, S., and Yamashita, Y.: Sensitivity of 21st century stratospheric ozone to greenhouse gas scenarios, Geophys. Res. Lett., 37, L16807, doi:10.1029/2010GL044443, 2010b.

Eyring, V., Arblaster, J. M., Cionni, I., Sedláček, J., Perlwitz, J., Young, P. J., Bekki, S., Bergmann, D., Cameron-Smith, P., Collins, W. J., Faluvegi, G., Gottschaldt, K. D., Horowitz, L. W., Kinnison, D. E., Lamarque, J. F., Marsh, D. R., Saint-Martin, D., Shindell, D. T., Sudo, K., Szopa, S., and Watanabe, S.: Long-term ozone changes and associated climate impacts in CMIP5 simulations, J. Geophys. Res., 118, 5029-5060, doi:10.1002/jgrd.50316, 2013a.

Eyring, V., Lamarque, J. F., Hess, P., Arfeuille, F., Bowman, K., Chipperfield, M. P., Duncan, B., Fiore, A., Gettelman, A., Giorgetta, M. a., Granier, C., Hegglin, M. I., Kinnison, D., Kunze, M., Langematz, U., Luo, B., Martin, R., Matthes, K., Newman, P. a., Peter, T., Robock, A., Ryerson, T., Saiz-Lopez, A., Salawitch, R., Schultz, M., Shepherd, T. G., Shindell, D., Stähelin, J., Tegtmeier, S., Thomason, L., Tilmes, S., Vernier, J. P., Waugh, D. W., and Young, P. J.: Overview of IGAC/SPARC Chemistry-Climate Model Initiative (CCMI) Community Simulations in Support of Upcoming Ozone and Climate Assessments, WMO-WRCP, Geneva, Switzerland, 48-66, 2013b.

Farman, J. C.: Ozone measurements at British Antarctic Survey stations, Philos. Trans. R. Soc. London Ser. B, 261-271, doi:10.1098/rstb.1977.0088, 1977.

Farman, J. C., Gardiner, B. G., and Shanklin, J. D.: Large losses of total ozone in Antarctica reveal seasonal ClOx/NOx interaction, Nature, 315, 207-210, doi:10.1038/315207a0, 1985.

Ferraro, A. J., Collins, M., and Lambert, F. H.: A hiatus in the stratosphere?, Nature Clim. Change, 5, 497-498, doi:10.1038/nclimate2624, 2015.

Finney, D. L., Doherty, R. M., Wild, O., Young, P. J., and Butler, A.: Response of lightning NOx emissions and ozone production to climate change: Insights from the Atmospheric Chemistry and Climate Model Intercomparison Project, Geophys. Res. Lett., 43, 2016GL068825, doi:10.1002/2016GL068825, 2016.

Fioletov, V. E., Bodeker, G. E., Miller, A. J., McPeters, R. D., and Stolarski, R.: Global and zonal total ozone variations estimated from ground‐based and satellite measurements: 1964–2000, J. Geophys. Res., 107, 4647, doi:10.1029/2001JD001350, 2002.

Fioletov, V. E., Labow, G., Evans, R., Hare, E. W., Köhler, U., McElroy, C. T., Miyagawa, K., Redondas, A., Savastiouk, V., and Shalamyansky, A. M.: Performance of the ground-based total ozone network assessed using satellite data, J. Geophys. Res., 113, D14313, doi:10.1029/2008JD009809, 2008.

Fiore, A. M., Dentener, F. J., Wild, O., Cuvelier, C., Schultz, M. G., Hess, P., Textor, C., Schulz, M., Doherty, R. M., Horowitz, L. W., MacKenzie, I. A., Sanderson, M. G., Shindell, D. T., Stevenson, D. S., Szopa, S., Van Dingenen, R., Zeng, G., Atherton, C., Bergmann, D., Bey, I., Carmichael, G., Collins, W. J., Duncan, B. N., Faluvegi, G., Folberth, G., Gauss, M., Gong, S., Hauglustaine, D., Holloway, T., Isaksen, I. S. A., Jacob, D. J., Jonson, J. E., Kaminski, J. W., Keating, T. J., Lupu, A., Marmer, E., Montanaro, V., Park, R. J., Pitari, G., Pringle, K. J., Pyle, J. A., Schroeder, S., Vivanco, M. G., Wind, P., Wojcik, G., Wu, S., and Zuber, A.: Multimodel estimates of

intercontinental source-receptor relationships for ozone pollution, J. Geophys. Res., 114, D04301, doi:10.1029/2008JD010816, 2009.

Fishman, J.: Tropospheric Ozone, in: Handbook of weather, climate, and water [Potter, T. D. and Colman, B. R. (eds)], JohnWiley & Sons, Inc., Hoboken, NJ, USA, 47-59, 2003.

Flato, G., Marotzke, J., Abiodun, B., Braconnot, P., Chou, S. C., Collins, W., Cox, P., Driouech, F., Emori, S., Eyring, V., Forest, C., Gleckler, P., Guilyardi, E., Jakob, C., Kattsov, V., Reason, C., and Rummukainen, M.: Evaluation of Climate Models, in: Climate Change 2013: The Physical Science Basis. Contribution of Working Group I to the Fifth Assessment Report of the Intergovernmental Panel on Climate Change [Stocker, T. F., Qin, D., Plattner, G. K., Tignor, M., Allen, S. K., Boschung, J., Nauels, A., Xia, Y., Bex, V., and Midgley, P. M. (eds)], Cambridge University Press, Cambridge, United Kingdom, 741-866, 2013.

Fleming, E. L., Jackman, C. H., Stolarski, R. S., and Douglass, A. R.: A model study of the impact of source gas changes on the stratosphere for 1850–2100, Atmos. Chem. Phys., 11, 8515-8541, doi:10.5194/acp-11-8515-2011, 2011.

Forster, P. M., and Shine, K. P.: Radiative forcing and temperature trends from stratospheric ozone changes, J. Geophys. Res., 102, 10841-10855, doi:10.1029/96JD03510, 1997.

Forster, P. M., Ramaswamy, V., Artaxo, P., Berntsen, T., Betts, R., Fahey, D. W., Haywood, J., Lean, J., Lowe, D. C., Myhre, G., Nganga, J., Prinn, R., Raga, G., Schulz, M., and Van Dorland, R.: Changes in Atmospheric Constituents and in Radiative Forcing. In: Climate Change 2007: The Physical Science Basis. Contribution of Working Group I to the Fourth Assessment Report of the Intergovernmental Panel on Climate Change [Solomon, S., D. Qin, M. Manning, Z. Chen, M. Marquis, K.B. Averyt, M.Tignor and H.L. Miller (eds.)]. Cambridge University Press, Cambridge, United Kingdom and New York, NY, USA, 2007.

Forster, P. M., Thompson, D. W. J., Baldwin, M. P., Chipperfield, M. P., Dameris, M., Haigh, J. D., Karoly, D. J., Kushner, P. J., Randel, W. J., Rosenlof, K. H., Seidel, D. J., Solomon, S.: Stratospheric changes and climate, in Scientific Assessment of Ozone Depletion: 2010, Global Ozone Research and Monitoring Project, Rep. No. 52, Chapter 4, 516 pp., World Meteorol. Organ., Geneva, Switzerland, 2011.

Fortuin, J. P. F., and Kelder, H.: An ozone climatology based on ozonesonde and satellite measurements, J. Geophys. Res., 103, 31709-31734, doi:10.1029/1998JD200008, 1998.

Frame, T. H. A., and Gray, L. J.: The 11-Yr Solar Cycle in ERA-40 Data: An Update to 2008, J. Clim., 23, 2213-2222, doi:10.1175/2009JCLI3150.1, 2010.

Free, M., and Seidel, D. J.: Causes of differing temperature trends in radiosonde upper air data sets, J. Geophys. Res., 110, D07101, doi:10.1029/2004JD005481, 2005.

Free, M.: The Seasonal Structure of Temperature Trends in the Tropical Lower Stratosphere, J. Clim., 24, 859-866, doi:10.1175/2010JCLI3841.1, 2010.

Fu, Q., Solomon, S., and Lin, P.: On the seasonal dependence of tropical lower-stratospheric temperature trends, Atmos. Chem. Phys., 10, 2643-2653, doi:10.5194/acp-10-2643-2010, 2010.

Fu, Q., Lin, P., Solomon, S., and Hartmann, D. L.: Observational evidence of strengthening of the Brewer-Dobson circulation since 1980, J. Geophys. Res., 120, 2015JD023657, doi:10.1002/2015JD023657, 2015.

Fuglestvedt, J. S., Berntsen, T. K., Isaksen, I. S. A., Mao, H., Liang, X. Z., and Wang, W. C.: Climatic forcing of nitrogen oxides through changes in tropospheric ozone and methane; global 3D model studies, Atmos. Environ., 33, 961-977, doi:10.1016/S1352-2310(98)00217-9, 1999.

Fujiwara, M., Wright, J. S., Manney, G. L., Gray, L. J., Anstey, J., Birner, T., Davis, S., Gerber, E. P., Harvey, V. L., Hegglin, M. I., Homeyer, C. R., Knox, J. A., Krüger, K., Lambert, A., Long, C. S., Martineau, P., Molod, A., Monge-Sanz, B. M., Santee, M. L., Tegtmeier, S., Chabrillat, S., Tan, D. G. H., Jackson, D. R., Polavarapu, S., Compo, G. P., Dragani, R., Ebisuzaki, W., Harada, Y., Kobayashi, C., McCarty, W., Onogi, K., Pawson, S., Simmons, A., Wargan, K., Whitaker, J. S., and Zou, C. Z.: Introduction to the SPARC Reanalysis Intercomparison Project (S-RIP) and overview of the reanalysis systems, Atmos. Chem. Phys., 17, 1417-1452, doi:10.5194/acp-17-1417-2017, 2017.

Fyfe, J. C., Boer, G. J., and Flato, G. M.: The Arctic and Antarctic oscillations and their projected changes under global warming, Geophys. Res. Lett., 26, 1601-1604, doi:10.1029/1999GL900317, 1999.

Fyfe, J. C., Gillett, N. P., and Marshall, G. J.: Human influence on extratropical Southern Hemisphere summer precipitation, Geophys. Res. Lett., 39, L23711, doi:10.1029/2012GL054199, 2012.

Garcia, R. R., and Solomon, S.: A new numerical model of the middle atmosphere: 2. Ozone and related species, J. Geophys. Res., 99, 12937-12951, doi:10.1029/94JD00725, 1994.

Garcia, R. R., and Randel, W. J.: Acceleration of the Brewer–Dobson Circulation due to Increases in Greenhouse Gases, J. Atmos. Sci., 65, 2731-2739, doi:10.1175/2008JAS2712.1, 2008.

Garcia, R. R., Smith, A. K., Kinnison, D. E., Cámara, Á. d. l., and Murphy, D. J.: Modification of the Gravity Wave Parameterization in the Whole Atmosphere Community Climate Model: Motivation and Results, J. Atmos. Sci., 74, 275-291, doi:10.1175/JAS-D-16-0104.1, 2017.

Garfinkel, C. I., and Hartmann, D. L.: Different ENSO teleconnections and their effects on the stratospheric polar vortex, J. Geophys. Res., 113, D18114, doi:10.1029/2008JD009920, 2008.

Gauss, M., Myhre, G., Pitari, G., Prather, M. J., Isaksen, I. S. A., Berntsen, T. K., Brasseur, G. P., Dentener, F. J., Derwent, R. G., Hauglustaine, D. A., Horowitz, L. W., Jacob, D. J., Johnson, M., Law, K. S., Mickley, L. J., Müller, J. F., Plantevin, P. H., Pyle, J. A., Rogers, H. L., Stevenson, D. S., Sundet, J. K., van Weele, M., and Wild, O.: Radiative forcing in the 21st century due to ozone changes in the troposphere and the lower stratosphere, J. Geophys. Res., 108, 4292, doi:10.1029/2002JD002624, 2003.

Gent, P., Yeager, S., Neale, R., Levis, S., and Bailey, D.: Improvements in a half degree atmosphere/land version of the CCSM, Clim. Dynam., 34, 819-833, doi:10.1007/s00382-009-0614-8, 2010.

Gettelman, A., Birner, T., Eyring, V., Akiyoshi, H., Bekki, S., Brühl, C., Dameris, M., Kinnison, D. E., Lefevre, F., Lott, F., Mancini, E., Pitari, G., Plummer, D. A., Rozanov, E., Shibata, K., Stenke, A., Struthers, H., and Tian, W.: The Tropical Tropopause Layer 1960–2100, Atmos. Chem. Phys., 9, 1621-1637, doi:10.5194/acp-9-1621-2009, 2009.

Gillett, N. P., and Thompson, D. W. J.: Simulation of Recent Southern Hemisphere Climate Change, Science, 302, 273-275, doi:10.1126/science.1087440, 2003.

Gillett, N. P., Scinocca, J. F., Plummer, D. A., and Reader, M. C.: Sensitivity of climate to dynamically-consistent zonal asymmetries in ozone, Geophys. Res. Lett., 36, L10809, doi:10.1029/2009GL037246, 2009.

Gillett, N. P., Akiyoshi, H., Bekki, S., Braesicke, P., Eyring, V., Garcia, R., Karpechko, A. Y., McLinden, C. A., Morgenstern, O., Plummer, D. A., Pyle, J. A., Rozanov, E., Scinocca, J., and Shibata, K.: Attribution of observed changes in stratospheric ozone and temperature, Atmos. Chem. Phys., 11, 599-609, doi:10.5194/acp-11-599-2011, 2011.

Gillett, N. P., Arora, V. K., Flato, G. M., Scinocca, J. F., and von Salzen, K.: Improved constraints on 21st-century warming derived using 160 years of temperature observations, Geophys. Res. Lett., 39, 1944-8007, doi:10.1029/2011GL050226, 2012.

Gillett, N. P., Arora, V. K., Matthews, D., and Allen, M. R.: Constraining the Ratio of Global Warming to Cumulative CO2 Emissions Using CMIP5 Simulations, J. Clim., 26, 6844-6858, doi:10.1175/jcli-d-12-00476.1, 2013.

Gillett, N. P., and Fyfe, J. C.: Annular mode changes in the CMIP5 simulations, Geophys. Res. Lett., 40, 1189-1193, doi:10.1002/grl.50249, 2013.

Gong, D., and Wang, S.: Definition of Antarctic Oscillation index, Geophys. Res. Lett., 26, 459-462, doi:10.1029/1999GL900003, 1999.

Granier, C., Bessagnet, B., Bond, T., D'Angiola, A., Denier van der Gon, H., Frost, G. J., Heil, A., Kaiser, J. W., Kinne, S., Klimont, Z., Kloster, S., Lamarque, J. F., Liousse, C., Masui, T., Meleux, F., Mieville, A., Ohara, T., Raut, J. C., Riahi, K., Schultz, M. G., Smith, S. J., Thompson, A., van Aardenne, J., van der Werf, G. R., and van Vuuren, D. P.: Evolution of anthropogenic and biomass burning emissions of air pollutants at global and regional scales during the 1980–2010 period, Clim. Change, 109, 163, doi:10.1007/s10584-011-0154-1, 2011.

Gray, W. M., Sheaffer, J. D., and Knaff, J. A.: Hypothesized mechanism for stratospheric QBO influence on ENSO variability, Geophys. Res. Lett., 19, 107-110, doi:10.1029/91GL02950, 1992a.

Gray, W. M., Sheaffer, J. D., and Knaff, J. A.: Influence of the stratospheric QBO on ENSO variability, J. Meteor. Soc. Japan Ser. II, 70, 975-995, doi:10.2151/jmsj1965.70.5_975, 1992b.

Gray, L. J., Beer, J., Geller, M., Haigh, J. D., Lockwood, M., Matthes, K., Cubasch, U., Fleitmann, D., Harrison, G., Hood, L. L., Luterbacher, J., Meehl, G. A., Shindell, D., van Geel, B., and White, W.: Solar influences on climate, Rev. Geophys., 48, RG4001, doi:10.1029/2009RG000282, 2010.

Gregg, J. W., Jones, C. G., and Dawson, T. E.: Urbanization effects on tree growth in the vicinity of New York City, Nature, 424, 183-187, doi:10.1038/nature01728, 2003.

Grenfell, J. L., Lehmann, R., Mieth, P., Langematz, U., and Steil, B.: Chemical reaction pathways affecting stratospheric and mesospheric ozone, J. Geophys. Res., 111, D17311, doi:10.1029/2004JD005713, 2006.

Griffies, S. M., Winton, M., Donner, L. J., Horowitz, L. W., Downes, S. M., Farneti, R., Gnanadesikan, A., Hurlin, W. J., Lee, H. C., Liang, Z., Palter, J. B., Samuels, B. L., Wittenberg, A. T., Wyman, B. L., Yin, J., and Zadeh, N.: The GFDL CM3 Coupled Climate Model: Characteristics of the Ocean and Sea Ice Simulations, J. Clim., 24, 3520-3544, doi:10.1175/2011JCLI3964.1, 2011.

Grise, K. M., Thompson, D. W. J., and Forster, P. M.: On the Role of Radiative Processes in Stratosphere–Troposphere Coupling, J. Clim., 22, 4154-4161, doi:10.1175/2009JCLI2756.1, 2009.

Grytsai, A. V., Evtushevsky, O. M., Agapitov, O. V., Klekociuk, A. R., and Milinevsky, G. P.: Structure and long-term change in the zonal asymmetry in Antarctic total ozone during spring, Ann. Geophys., 25, 361-374, doi:10.5194/angeo-25-361-2007, 2007.

Guenther, A. B., Jiang, X., Heald, C. L., Sakulyanontvittaya, T., Duhl, T., Emmons, L. K., and Wang, X.: The Model of Emissions of Gases and Aerosols from Nature version 2.1 (MEGAN2.1): an extended and updated framework for modeling biogenic emissions, Geosci. Model Dev., 5, 1471-1492, doi:10.5194/gmd-5-1471-2012, 2012.

Haagen-Smit, A. J.: Chemistry and Physiology of Los Angeles Smog, Ind. Eng. Che., 44, 1342-1346, doi:10.1021/ie50510a045, 1952.

Haigh, J. D., and Pyle, J. A.: Ozone perturbation experiments in a two-dimensional circulation model, Quart. J. Roy. Meteor. Soc., 108, 551-574, doi:10.1002/qj.49710845705, 1982.

Haimberger, L., Tavolato, C., and Sperka, S.: Toward Elimination of the Warm Bias in Historic Radiosonde Temperature Records—Some New Results from a Comprehensive Intercomparison of Upper-Air Data, J. Clim., 21, 4587-4606, doi:10.1175/2008JCLI1929.1, 2008.

Haimberger, L., Tavolato, C., and Sperka, S.: Homogenization of the Global Radiosonde Temperature Dataset through Combined Comparison with Reanalysis Background Series and Neighboring Stations, J. Clim., 25, 8108-8131, doi:10.1175/JCLI-D-11-00668.1, 2012.

Hansen, J., Sato, M., Ruedy, R., Nazarenko, L., Lacis, A., Schmidt, G. A., Russell, G., Aleinov, I., Bauer, M., Bauer, S., Bell, N., Cairns, B., Canuto, V., Chandler, M., Cheng, Y., Del Genio, A., Faluvegi, G., Fleming, E., Friend, A., Hall, T., Jackman, C., Kelley, M., Kiang, N., Koch, D., Lean, J., Lerner, J., Lo, K., Menon, S., Miller, R., Minnis, P., Novakov, T., Oinas, V., Perlwitz, J., Perlwitz, J., Rind, D., Romanou, A., Shindell, D., Stone, P., Sun, S., Tausnev, N., Thresher, D., Wielicki, B., Wong, T., Yao, M., and Zhang, S.: Efficacy of climate forcings, J. Geophys. Res., 110, 2156-2202, doi:10.1029/2005JD005776, 2005.

Hansen, J., Sato, M., Kharecha, P., Beerling, D., Berner, R., Masson-Delmotte, V., Pagani, M., Raymo, M., Royer, D. L., and Zachos, J. C.: Target atmospheric CO2: where should humanity aim?, Open Atmos. Sci. J., 2, 217–231, doi:10.2174/1874282300802010217, 2008.

Hansen, J., Ruedy, R., Sato, M., and Lo, K.: Global surface temperature change, Rev. Geophys., 48, 1944-9208, doi:10.1029/2010RG000345, 2010.

Hansen, J., Sato, M., Kharecha, P., and von Schuckmann, K.: Earth's energy imbalance and implications, Atmos. Chem. Phys., 11, 13421-13449, doi:10.5194/acp-11-13421-2011, 2011.

Hardacre, C., Wild, O., and Emberson, L.: An evaluation of ozone dry deposition in global scale chemistry climate models, Atmos. Chem. Phys., 15, 6419-6436, doi:10.5194/acp-15-6419-2015, 2015.

Hardiman, S. C., Butchart, N., and Calvo, N.: The morphology of the Brewer–Dobson circulation and its response to climate change in CMIP5 simulations, Quart. J. Roy. Meteor. Soc., 140, 1958-1965, doi:10.1002/qj.2258, 2014.

Hartley, W. N.: On the probable absorption of solar radiation by atmospheric ozone, Chem. News, 42, 268, 1880.

Hartmann, D. L., Klein Tank, A. M. G., Rusticucci, M., Alexander, L. V., Brönnimann, S., Charabi, Y., Dentener, F. J., Dlugokencky, E. J., Easterling, D. R., Kaplan, A., Soden, B. J., Thorne, P. W., Wild, M., and Zhai, P. M.: Observations: Atmosphere and Surface. In: Climate Change 2013: The Physical Science Basis. Contribution of Working Group I to the Fifth Assessment Report of the Intergovernmental Panel on Climate Change [Stocker, T. F., Qin, D., Plattner, G. K., Tignor, M., Allen, S. K., Boschung, J., Nauels, A., Xia, Y., Bex, V., and Midgley, P. M. (eds.)]. Cambridge University Press, Cambridge, United Kingdom and New York, NY, USA, 2013.

Hassler, B., Young, P. J., Portmann, R. W., Bodeker, G. E., Daniel, J. S., Rosenlof, K. H., and Solomon, S.: Comparison of three vertically resolved ozone data sets: climatology, trends and radiative forcings, Atmos. Chem. Phys., 13, 5533-5550, doi:10.5194/acp-13-5533-2013, 2013.

Hauglustaine, D. A., and Brasseur, G. P.: Evolution of tropospheric ozone under anthropogenic activities and associated radiative forcing of climate, J. Geophys. Res., 106, 32337-32360, doi:10.1029/2001JD900175, 2001.

Hegerl, G. C., Crowley, T. J., Allen, M., Hyde, W. T., Pollack, H. N., Smerdon, J., and Zorita, E.: Detection of Human Influence on a New, Validated 1500-Year Temperature Reconstruction, J. Clim., 20, 650-666, doi:10.1175/JCLI4011.1, 2007.

Hegglin, M. I., and Shepherd, T. G.: Large climate-induced changes in ultraviolet index and stratosphere-to-troposphere ozone flux, Nature Geosci., 2, 687-691, doi:10.1038/ngeo604, 2009.

Hegglin, M. I., Plummer, D. A., Shepherd, T. G., Scinocca, J. F., Anderson, J., Froidevaux, L., Funke, B., Hurst, D., Rozanov, A., Urban, J., von Clarmann, T., Walker, K. A., Wang, H. J., Tegtmeier, S., and Weigel, K.: Vertical structure of stratospheric water vapour trends derived from merged satellite data, Nature Geosci., 7, 768-776, doi:10.1038/ngeo2236, 2014.

Hendrick, F., Pommereau, J. P., Goutail, F., Evans, R. D., Ionov, D., Pazmino, A., Kyrö, E., Held, G., Eriksen, P., and Dorokhov, V.: NDACC/SAOZ UV-visible total ozone measurements: improved retrieval and comparison with correlative ground-based and satellite observations, Atmos. Chem. Phys., 11, 5975-5995, doi:10.5194/acp-11-5975-2011, 2011.

Henley, B., Gergis, J., Karoly, D., Power, S., Kennedy, J., and Folland, C.: A Tripole Index for the Interdecadal Pacific Oscillation, Clim. Dynam., 1-14, doi:10.1007/s00382-015-2525-1, 2015.

Holmes, C. D., Prather, M. J., Søvde, O. A., and Myhre, G.: Future methane, hydroxyl, and their uncertainties: key climate and emission parameters for future predictions, Atmos. Chem. Phys., 13, 285-302, doi:10.5194/acp-13-285-2013, 2013.

Holton, J. R., and Tan, H. C.: The Influence of the Equatorial Quasi-Biennial Oscillation on the Global Circulation at 50 mb, J. Atmos. Sci., 37, 2200-2208, doi:10.1175/1520-0469(1980)037<2200:TIOTEQ>2.0.CO;2, 1980.

Holton, J. R., Haynes, P. H., McIntyre, M. E., Douglass, A. R., Rood, R. B., and Pfister, L.: Stratosphere-troposphere exchange, Rev. Geophys., 33, 403-439, doi:10.1029/95RG02097, 1995.

Hood, L. L., and Zaff, D. A.: Lower stratospheric stationary waves and the longitude dependence of ozone trends in winter, J. Geophys. Res., 100, 25791-25800, doi:10.1029/95JD01943, 1995.

Hood, L. L., and Soukharev, B. E.: The Lower-Stratospheric Response to 11-Yr Solar Forcing: Coupling to the Troposphere–Ocean Response, J. Atmos. Sci., 69, 1841-1864, doi:10.1175/jas-d-11-086.1, 2012.

Hossaini, R., Chipperfield, M. P., Feng, W., Breider, T. J., Atlas, E., Montzka, S. A., Miller, B. R., Moore, F., and Elkins, J.: The contribution of natural and anthropogenic very short-lived species to stratospheric bromine, Atmos. Chem. Phys., 12, 371-380, doi:10.5194/acp-12-371-2012, 2012.

Hossaini, R., Mantle, H., Chipperfield, M. P., Montzka, S. A., Hamer, P., Ziska, F., Quack, B., Krüger, K., Tegtmeier, S., Atlas, E., Sala, S., Engel, A., Bönisch, H., Keber, T., Oram, D., Mills, G., Ordóñez, C., Saiz-Lopez, A., Warwick, N., Liang, Q., Feng, W., Moore, F., Miller, B. R., Marécal, V., Richards, N. A. D., Dorf, M., and Pfeilsticker, K.: Evaluating global emission inventories of biogenic bromocarbons, Atmos. Chem. Phys., 13, 11819-11838, doi:10.5194/acp-13-11819-2013, 2013.

Hsu, J., and Prather, M. J.: Stratospheric variability and tropospheric ozone, J. Geophys. Res., 114, D06102, doi:10.1029/2008JD010942, 2009.

Huang, B., Banzon, V. F., Freeman, E., Lawrimore, J., Liu, W., Peterson, T. C., Smith, T. M., Thorne, P. W., Woodruff, S. D., and Zhang, H. M.: Extended

Reconstructed Sea Surface Temperature Version 4 (ERSST.v4). Part I: Upgrades and Intercomparisons, J. Clim., 28, 911-930, doi:10.1175/JCLI-D-14-00006.1, 2015.

Hurwitz, M. M., Newman, P. A., and Garfinkel, C. I.: The Arctic vortex in March 2011: a dynamical perspective, Atmos. Chem. Phys., 11, 11447-11453, doi:10.5194/acp-11-11447-2011, 2011.

Iglesias-Suarez, F., Young, P. J., and Wild, O.: Stratospheric ozone change and related climate impacts over 1850–2100 as modelled by the ACCMIP ensemble, Atmos. Chem. Phys., 16, 343-363, doi:10.5194/acp-16-343-2016, 2016.

IPCC: Climate Change 2007: The Physical Science Basis. Contribution of Working Group I to the Fourth Assessment Report of the Intergovernmental Panel on Climate Change [Solomon, S., Qin, D., Manning, M., Chen, Z., Marquis, M., Averyt, K. B., Tignor M., and Miller H. L. (eds)]. Cambridge University Press, Cambridge, United Kingdom and New York, NY, USA, 996 pp, 2007.

IPCC: Climate Change 2013: The Physical Science Basis. Contribution of Working Group I to the Fifth Assessment Report of the Intergovernmental Panel on Climate Change [Stocker, T. F., Qin, D., Plattner, G. K., Tignor, M., Allen, S. K., Boschung, J., Nauels, A., Xia, Y., Bex, V., and Midgley, P. M. (eds)]. Cambridge University Press, Cambridge, United Kingdom and New York, NY, USA, 1535 pp, 2013.

Isaksen, I. S. A., Granier, C., Myhre, G., Berntsen, T. K., Dalsøren, S. B., Gauss, M., Klimont, Z., Benestad, R., Bousquet, P., Collins, W., Cox, T., Eyring, V., Fowler, D., Fuzzi, S., Jöckel, P., Laj, P., Lohmann, U., Maione, M., Monks, P., Prevot, A. S. H., Raes, F., Richter, A., Rognerud, B., Schulz, M., Shindell, D., Stevenson, D. S., Storelvmo, T., Wang, W. C., van Weele, M., Wild, M., and Wuebbles, D.: Atmospheric composition change: Climate–Chemistry interactions, Atmos. Environ., 43, 5138-5192, doi:10.1016/j.atmosenv.2009.08.003, 2009.

Jacob, D.: Introduction to atmospheric chemistry, Princeton University Press, Princeton, USA, 1999.

Jacob, D. J., and Winner, D. A.: Effect of climate change on air quality, Atmos. Environ., 43, 51-63, doi:10.1016/j.atmosenv.2008.09.051, 2009.

Jadin, E. A., Wei, K., Zyulyaeva, Y. A., Chen, W., and Wang, L.: Stratospheric wave activity and the Pacific Decadal Oscillation, J. Atmospheric Sol.-Terr. Phys., 72, 1163-1170, doi:10.1016/j.jastp.2010.07.009, 2010.

Jenkin, M. E., and Clemitshaw, K. C.: Ozone and other secondary photochemical pollutants: chemical processes governing their formation in the planetary boundary layer, Atmos. Environ., 34, 2499-2527, doi:10.1016/S1352-2310(99)00478-1, 2000.

Jenkin, M. E., Watson, L. A., Utembe, S. R., and Shallcross, D. E.: A Common Representative Intermediates (CRI) mechanism for VOC degradation. Part 1: Gas phase mechanism development, Atmos. Environ., 42, 7185-7195, doi:10.1016/j.atmosenv.2008.07.028, 2008.

Jerrett, M., Burnett, R. T., Pope, C. A., Ito, K., Thurston, G., Krewski, D., Shi, Y., Calle, E., and Thun, M.: Long-Term Ozone Exposure and Mortality, New Engl. J. Med., 360, 1085-1095, doi:10.1056/NEJMoa0803894, 2009.

Johnson, C. E., Stevenson, D. S., Collins, W. J., and Derwent, R. G.: Role of climate feedback on methane and ozone studied with a Coupled Ocean-Atmosphere-Chemistry Model, Geophys. Res. Lett., 28, 1723-1726, doi:10.1029/2000GL011996, 2001.

Johnson, D. G., Traub, W. A., Chance, K. V., Jucks, K. W., and Stachnik, R. A.: Estimating the abundance of ClO from simultaneous remote sensing measurements of HO2, OH, and HOCl, Geophys. Res. Lett., 22, 1869-1871, doi:10.1029/95GL01249, 1995.

Johnston, H.: Reduction of Stratospheric Ozone by Nitrogen Oxide Catalysts from Supersonic Transport Exhaust, Science, 173, 517, doi:10.1126/science.173.3996.517, 1971.

Jones, C. D., Hughes, J. K., Bellouin, N., Hardiman, S. C., Jones, G. S., Knight, J., Liddicoat, S., O'Connor, F. M., Andres, R. J., Bell, C., Boo, K. O., Bozzo, A., Butchart, N., Cadule, P., Corbin, K. D., Doutriaux-Boucher, M., Friedlingstein, P., Gornall, J., Gray, L., Halloran, P. R., Hurtt, G., Ingram, W. J., Lamarque, J. F., Law, R. M., Meinshausen, M., Osprey, S., Palin, E. J., Parsons Chini, L., Raddatz, T., Sanderson, M. G., Sellar, A. A., Schurer, A., Valdes, P., Wood, N., Woodward, S., Yoshioka, M., and Zerroukat, M.: The HadGEM2-ES implementation of CMIP5 centennial simulations, Geosci. Model Dev., 4, 543-570, doi:10.5194/gmd-4-543-2011, 2011.

Jones, G. S., Stott, P. A., and Christidis, N.: Attribution of observed historical near–surface temperature variations to anthropogenic and natural causes using CMIP5 simulations, J. Geophys. Res., 118, 4001-4024, doi:10.1002/jgrd.50239, 2013.

Kawase, H., Nagashima, T., Sudo, K., and Nozawa, T.: Future changes in tropospheric ozone under Representative Concentration Pathways (RCPs), Geophys. Res. Lett., 38, 1944-8007, doi:10.1029/2010gl046402, 2011.

Kawatani, Y., and Hamilton, K.: Weakened stratospheric quasibiennial oscillation driven by increased tropical mean upwelling, Nature, 497, 478-481, doi:10.1038/nature12140, 2013.

Keeble, J., Braesicke, P., Abraham, N. L., Roscoe, H. K., and Pyle, J. A.: The impact of polar stratospheric ozone loss on Southern Hemisphere stratospheric circulation and climate, Atmos. Chem. Phys., 14, 13705-13717, doi:10.5194/acp-14-13705-2014, 2014.

Kiesewetter, G., Sinnhuber, B. M., Weber, M., and Burrows, J. P.: Attribution of stratospheric ozone trends to chemistry and transport: a modelling study,

Atmos. Chem. Phys., 10, 12073-12089, doi:10.5194/acp-10-12073-2010, 2010.

Kinnison, D. E., Brasseur, G. P., Walters, S., Garcia, R. R., Marsh, D. R., Sassi, F., Harvey, V. L., Randall, C. E., Emmons, L., Lamarque, J. F., Hess, P., Orlando, J. J., Tie, X. X., Randel, W., Pan, L. L., Gettelman, A., Granier, C., Diehl, T., Niemeier, U., and Simmons, A. J.: Sensitivity of chemical tracers to meteorological parameters in the MOZART-3 chemical transport model, J. Geophys. Res., 112, D20302, doi:10.1029/2006JD007879, 2007.

Knutson, T. R., Zeng, F., and Wittenberg, A. T.: Multimodel Assessment of Regional Surface Temperature Trends: CMIP3 and CMIP5 Twentieth-Century Simulations, J. Clim., 26, 8709-8743, doi:10.1175/jcli-d-12-00567.1, 2013.

Koch, D., Schmidt, G. A., and Field, C. V.: Sulfur, sea salt, and radionuclide aerosols in GISS ModelE, J. Geophys. Res., 111, D06206, doi:10.1029/2004JD005550, 2006.

Kodera, K., Chiba, M., Koide, H., Kitoh, A., and Nikaidou, Y.: Interannual Variability of the Winter Stratosphere and Troposphere in the Northern Hemisphere, J. Meteor. Soc. Japan. Ser. II, 74, 365-382, doi:10.2151/jmsj1965.74.3_365, 1996.

Komhyr, W. D., Grass, R. D., and Leonard, R. K.: Total ozone decrease at South Pole, Antarctica, 1964-1985, Geophys. Res. Lett., 13, 1248-1251, doi:10.1029/GL013i012p01248, 1986.

Kopp, G., and Lean, J. L.: A new, lower value of total solar irradiance: Evidence and climate significance, Geophys. Res. Lett., 38, L01706, doi:10.1029/2010GL045777, 2011.

Kosaka, Y., and Xie, S. P.: Recent global-warming hiatus tied to equatorial Pacific surface cooling, Nature, 501, 403-407, doi:10.1038/nature12534, 2013.

Kovalenko, L. J., Jucks, K. W., Salawitch, R. J., Toon, G. C., Blavier, J. F., Johnson, D. G., Kleinböhl, A., Livesey, N. J., Margitan, J. J., Pickett, H. M., Santee, M. L., Sen, B., Stachnik, R. A., and Waters, J. W.: Observed and modeled HOCl profiles in the midlatitude stratosphere: Implication for ozone loss, Geophys. Res. Lett., 34, L19801, doi:10.1029/2007GL031100, 2007.

Kuttippurath, J., Lefèvre, F., Pommereau, J. P., Roscoe, H. K., Goutail, F., Pazmino, A., and Shanklin, J. D.: Antarctic ozone loss in 1979–2010: first sign of ozone recovery, Atmos. Chem. Phys., 13, 1625-1635, doi:10.5194/acp-13-1625-2013, 2013.

Lacis, A. A., Wuebbles, D. J., and Logan, J. A.: Radiative forcing of climate by changes in the vertical distribution of ozone, J. Geophys. Res., 95, 9971-9981, doi:10.1029/JD095iD07p09971, 1990.

Lamarque, J. F., and Hess, P. G.: Arctic Oscillation modulation of the Northern Hemisphere spring tropospheric ozone, Geophys. Res. Lett., 31, L06127, doi:10.1029/2003GL019116, 2004.

Lamarque, J. F., Hess, P., Emmons, L., Buja, L., Washington, W., and Granier, C.: Tropospheric ozone evolution between 1890 and 1990, J. Geophys. Res., 110, D08304, doi:10.1029/2004JD005537, 2005.

Lamarque, J. F., and Solomon, S.: Impact of Changes in Climate and Halocarbons on Recent Lower Stratosphere Ozone and Temperature Trends, J. Clim., 23, 2599-2611, doi:10.1175/2010JCLI3179.1, 2010.

Lamarque, J. F., Emmons, L. K., Hess, P. G., Kinnison, D. E., Tilmes, S., Vitt, F., Heald, C. L., Holland, E. A., Lauritzen, P. H., Neu, J., Orlando, J. J., Rasch, P. J., and Tyndall, G. K.: CAM-chem: description and evaluation of interactive atmospheric chemistry in the Community Earth System Model, Geosci. Model Dev., 5, 369-411, doi:10.5194/gmd-5-369-2012, 2012.

Lamarque, J. F., Dentener, F., McConnell, J., Ro, C. U., Shaw, M., Vet, R., Bergmann, D., Cameron-Smith, P., Dalsoren, S., Doherty, R., Faluvegi, G., Ghan, S. J., Josse, B., Lee, Y. H., MacKenzie, I. A., Plummer, D., Shindell, D. T., Skeie, R. B., Stevenson, D. S., Strode, S., Zeng, G., Curran, M., Dahl-Jensen, D., Das, S., Fritzsche, D., and Nolan, M.: Multi-model mean nitrogen and sulfur deposition from the Atmospheric Chemistry and Climate Model Intercomparison Project (ACCMIP): evaluation of historical and projected future changes, Atmos. Chem. Phys., 13, 7997-8018, doi:10.5194/acp-13-7997-2013, 2013a.

Lamarque, J. F., Shindell, D. T., Josse, B., Young, P. J., Cionni, I., Eyring, V., Bergmann, D., Cameron-Smith, P., Collins, W. J., Doherty, R., Dalsoren, S., Faluvegi, G., Folberth, G., Ghan, S. J., Horowitz, L. W., Lee, Y. H., MacKenzie, I. A., Nagashima, T., Naik, V., Plummer, D., Righi, M., Rumbold, S. T., Schulz, M., Skeie, R. B., Stevenson, D. S., Strode, S., Sudo, K., Szopa, S., Voulgarakis, A., and Zeng, G.: The Atmospheric Chemistry and Climate Model Intercomparison Project (ACCMIP): overview and description of models, simulations and climate diagnostics, Geosci. Model Dev., 6, 179-206, doi:10.5194/gmd-6-179-2013, 2013b.

Lary, D. J.: Gas phase atmospheric bromine photochemistry, J. Geophys. Res., 101, 1505-1516, doi:10.1029/95JD02463, 1996.

Lary, D. J., Chipperfield, M. P., Toumi, R., and Lenton, T.: Heterogeneous atmospheric bromine chemistry, J. Geophys. Res., 101, 1489-1504, doi:10.1029/95JD02839, 1996.

Lary, D. J.: Catalytic destruction of stratospheric ozone, J. Geophys. Res., 102, 21515-21526, doi:10.1029/97JD00912, 1997.

Lee, Y. H., Lamarque, J. F., Flanner, M. G., Jiao, C., Shindell, D. T., Berntsen, T., Bisiaux, M. M., Cao, J., Collins, W. J., Curran, M., Edwards, R., Faluvegi, G., Ghan, S., Horowitz, L. W., McConnell, J. R., Ming, J., Myhre, G., Nagashima, T., Naik, V., Rumbold, S. T., Skeie, R. B., Sudo, K., Takemura, T., Thevenon,

F., Xu, B., and Yoon, J. H.: Evaluation of preindustrial to present-day black carbon and its albedo forcing from Atmospheric Chemistry and Climate Model Intercomparison Project (ACCMIP), Atmos. Chem. Phys., 13, 2607-2634, doi:10.5194/acp-13-2607-2013, 2013.

Lelieveld, J., and Dentener, F. J.: What controls tropospheric ozone?, J. Geophys. Res., 105, 3531-3551, doi:10.1029/1999JD901011, 2000.

Li, F., Austin, J., and Wilson, J.: The Strength of the Brewer–Dobson Circulation in a Changing Climate: Coupled Chemistry–Climate Model Simulations, J. Clim., 21, 40-57, doi:10.1175/2007JCLI1663.1, 2008.

Li, F., Stolarski, R. S., and Newman, P. A.: Stratospheric ozone in the post-CFC era, Atmos. Chem. Phys., 9, 2207-2213, doi:10.5194/acp-9-2207-2009, 2009.

Liaskos, C. E., Allen, D. J., and Pickering, K. E.: Sensitivity of tropical tropospheric composition to lightning NOx production as determined by replay simulations with GEOS-5, J. Geophys. Res., 120, 2014JD022987, doi:10.1002/2014JD022987, 2015.

Lin, P., and Fu, Q.: Changes in various branches of the Brewer–Dobson circulation from an ensemble of chemistry climate models, J. Geophys. Res., 118, 73-84, doi:10.1029/2012JD018813, 2013.

Logan, J. A.: Tropospheric ozone: Seasonal behavior, trends, and anthropogenic influence, J. Geophys. Res., 90, 10463-10482, doi:10.1029/JD090iD06p10463, 1985.

Lott, F. C., Stott, P. A., Mitchell, D. M., Christidis, N., Gillett, N. P., Haimberger, L., Perlwitz, J., and Thorne, P. W.: Models versus radiosondes in the free atmosphere: A new detection and attribution analysis of temperature, J. Geophys. Res., 118, 2609-2619, doi:10.1002/jgrd.50255, 2013.

Mann, M. E.: On long range dependence in global surface temperature series, Clim. Change, 107, 267-276, doi:10.1007/s10584-010-9998-z, 2011.

Manney, G. L., Santee, M. L., Rex, M., Livesey, N. J., Pitts, M. C., Veefkind, P., Nash, E. R., Wohltmann, I., Lehmann, R., Froidevaux, L., Poole, L. R., Schoeberl, M. R., Haffner, D. P., Davies, J., Dorokhov, V., Gernandt, H., Johnson, B., Kivi, R., Kyro, E., Larsen, N., Levelt, P. F., Makshtas, A., McElroy, C. T., Nakajima, H., Parrondo, M. C., Tarasick, D. W., von der Gathen, P., Walker, K. A., and Zinoviev, N. S.: Unprecedented Arctic ozone loss in 2011, Nature, 478, 469-475, doi:10.1038/nature10556, 2011.

Mantua, N. J., Hare, S. R., Zhang, Y., Wallace, J. M., and Francis, R. C.: A Pacific Interdecadal Climate Oscillation with Impacts on Salmon Production, Bull. Am. Meteorol. Soc., 78, 1069-1079, doi:10.1175/1520-0477(1997)078<1069:APICOW>2.0.CO;2, 1997.

Marenco, A., Gouget, H., Nédélec, P., Pagés, J. P., and Karcher, F.: Evidence of a long-term increase in tropospheric ozone from Pic du Midi data series: Consequences: Positive radiative forcing, J. Geophys. Res., 99, 16617-16632, doi:10.1029/94JD00021, 1994.

Marsh, D. R., and Garcia, R. R.: Attribution of decadal variability in lower-stratospheric tropical ozone, Geophys. Res. Lett., 34, L21807, doi:10.1029/2007GL030935, 2007.

Marsh, D. R., Mills, M. J., Kinnison, D. E., Lamarque, J. F., Calvo, N., and Polvani, L. M.: Climate Change from 1850 to 2005 Simulated in CESM1(WACCM), J. Clim., 26, 7372-7391, doi:10.1175/JCLI-D-12-00558.1, 2013.

Marshall, G. J.: Trends in the Southern Annular Mode from Observations and Reanalyses, J. Clim., 16, 4134-4143, doi:10.1175/1520-0442(2003)016<4134:TITSAM>2.0.CO; 2, 2003.

Marshall, G. J., Stott, P. A., Turner, J., Connolley, W. M., King, J. C., and Lachlan-Cope, T. A.: Causes of exceptional atmospheric circulation changes in the Southern Hemisphere, Geophys. Res. Lett., 31, L14205, doi:10.1029/2004GL019952, 2004.

Marshall, G. J.: Half-century seasonal relationships between the Southern Annular mode and Antarctic temperatures, Int. J. Climatol., 27, 373-383, doi:10.1002/joc.1407, 2007.

Martin, G. M., Bellouin, N., Collins, W. J., Culverwell, I. D., Halloran, P. R., Hardiman, S. C., Hinton, T. J., Jones, C. D., McDonald, R. E., McLaren, A. J., O'Connor, F. M., Roberts, M. J., Rodriguez, J. M., Woodward, S., Best, M. J., Brooks, M. E., Brown, A. R., Butchart, N., Dearden, C., Derbyshire, S. H., Dharssi, I., Doutriaux-Boucher, M., Edwards, J. M., Falloon, P. D., Gedney, N., Gray, L. J., Hewitt, H. T., Hobson, M., Huddleston, M. R., Hughes, J., Ineson, S., Ingram, W. J., James, P. M., Johns, T. C., Johnson, C. E., Jones, A., Jones, C. P., Joshi, M. M., Keen, A. B., Liddicoat, S., Lock, A. P., Maidens, A. V., Manners, J. C., Milton, S. F., Rae, J. G. L., Ridley, J. K., Sellar, A., Senior, C. A., Totterdell, I. J., Verhoef, A., Vidale, P. L., and Wiltshire, A.: The HadGEM2 family of Met Office Unified Model climate configurations, Geosci. Model Dev., 4, 723-757, doi:10.5194/gmd-4-723-2011, 2011.

McElroy, M. B., Salawitch, R. J., Wofsy, S. C., and Logan, J. A.: Reductions of Antarctic ozone due to synergistic interactions of chlorine and bromine, Nature, 321, 759-762, doi:10.1038/321759a0, 1986.

McElroy, M. B., Salawitch, R. J., and Minschwaner, K.: The changing stratosphere, Planet. Space Sci., 40, 373-401, doi:10.1016/0032-0633(92)90070-5, 1992.

McLandress, C., Shepherd, T. G., Scinocca, J. F., Plummer, D. A., Sigmond, M., Jonsson, A. I., and Reader, M. C.: Separating the Dynamical Effects of Climate Change and Ozone Depletion. Part II: Southern Hemisphere Troposphere, J. Clim., 24, 1850-1868, doi:10.1175/2010JCLI3958.1, 2011.

McLinden, C. A., Olsen, S. C., Hannegan, B., Wild, O., Prather, M. J., and Sundet, J.: Stratospheric ozone in 3-D models: A simple chemistry and the cross-tropopause flux, J. Geophys. Res., 105, 14653-14665, doi:10.1029/2000JD900124, 2000.

McPeters, R. D., Bhartia, P. K., Haffner, D., Labow, G. J., and Flynn, L.: The version 8.6 SBUV ozone data record: An overview, J. Geophys. Res., 118, 8032-8039, doi:10.1002/jgrd.50597, 2013.

Mears, C. A., and Wentz, F. J.: Construction of the Remote Sensing Systems V3. 2 atmospheric temperature records from the MSU and AMSU microwave sounders, J. Atmospheric Ocean. Technol., 26, doi:10.1175/2008JTECHA1176.1, 2009.

Mears, C. A., Wentz, F. J., Thorne, P., and Bernie, D.: Assessing uncertainty in estimates of atmospheric temperature changes from MSU and AMSU using a Monte-Carlo estimation technique, J. Geophys. Res., 116, D08112, doi:10.1029/2010JD014954, 2011.

Meehl, G. A., Hu, A., Santer, B. D., and Xie, S. P.: Contribution of the Interdecadal Pacific Oscillation to twentieth-century global surface temperature trends, Nature Clim. Change, 6, 1005-1008, doi:10.1038/nclimate3107, 2016.

Meinshausen, M., Smith, S. J., Calvin, K., Daniel, J. S., Kainuma, M. L. T., Lamarque, J. F., Matsumoto, K., Montzka, S. A., Raper, S. C. B., Riahi, K., Thomson, A., Velders, G. J. M., and Vuuren, D. P. P.: The RCP greenhouse gas concentrations and their extensions from 1765 to 2300, Clim. Change, 109, 213-241, doi:10.1007/s10584-011-0156-z, 2011.

Meul, S., Langematz, U., Oberländer, S., Garny, H., and Jöckel, P.: Chemical contribution to future tropical ozone change in the lower stratosphere, Atmos. Chem. Phys., 14, 2959-2971, doi:10.5194/acp-14-2959-2014, 2014.

Molina, M. J., and Rowland, F. S.: Stratospheric sink for chlorofluoromethanes: chlorine atomc-atalysed destruction of ozone, Nature, 249, 810-812, doi:10.1038/249810a0, 1974.

Molina, L. T., and Molina, M. J.: Production of chlorine oxide (Cl2O2) from the self-reaction of the chlorine oxide (ClO) radical, The Journal of Physical Chemistry, 91, 433-436, doi:10.1021/j100286a035, 1987.

Monge-Sanz, B. M., Chipperfield, M. P., Dee, D. P., Simmons, A. J., and Uppala, S. M.: Improvements in the stratospheric transport achieved by a chemistry transport model with ECMWF (re)analyses: identifying effects and remaining challenges, Quart. J. Roy. Meteor. Soc., 139, 654-673, doi:10.1002/qj.1996, 2013.

Monks, P. S., Archibald, A. T., Colette, A., Cooper, O., Coyle, M., Derwent, R., Fowler, D., Granier, C., Law, K. S., Mills, G. E., Stevenson, D. S., Tarasova, O., Thouret, V., von Schneidemesser, E., Sommariva, R., Wild, O., and Williams, M. L.: Tropospheric ozone and its precursors from the urban to the global scale from air quality to short-lived climate forcer, Atmos. Chem. Phys., 15, 8889-8973, doi:10.5194/acp-15-8889-2015, 2015.

Morgenstern, O., Akiyoshi, H., Bekki, S., Braesicke, P., Butchart, N., Chipperfield, M. P., Cugnet, D., Deushi, M., Dhomse, S. S., Garcia, R. R., Gettelman, A., Gillett, N. P., Hardiman, S. C., Jumelet, J., Kinnison, D. E., Lamarque, J. F., Lott, F., Marchand, M., Michou, M., Nakamura, T., Olivié, D., Peter, T., Plummer, D., Pyle, J. A., Rozanov, E., Saint-Martin, D., Scinocca, J. F., Shibata, K., Sigmond, M., Smale, D., Teyssèdre, H., Tian, W., Voldoire, A., and Yamashita, Y.: Anthropogenic forcing of the Northern Annular Mode in CCMVal-2 models, J. Geophys. Res., 115, D00M03, doi:10.1029/2009JD013347, 2010a.

Morgenstern, O., Giorgetta, M. A., Shibata, K., Eyring, V., Waugh, D. W., Shepherd, T. G., Akiyoshi, H., Austin, J., Baumgaertner, A. J. G., Bekki, S., Braesicke, P., Brühl, C., Chipperfield, M. P., Cugnet, D., Dameris, M., Dhomse, S., Frith,

S. M., Garny, H., Gettelman, A., Hardiman, S. C., Hegglin, M. I., Jöckel, P., Kinnison, D. E., Lamarque, J. F., Mancini, E., Manzini, E., Marchand, M., Michou, M., Nakamura, T., Nielsen, J. E., Olivié, D., Pitari, G., Plummer, D. A., Rozanov, E., Scinocca, J. F., Smale, D., Teyssèdre, H., Toohey, M., Tian, W., and Yamashita, Y.: Review of the formulation of present-generation stratospheric chemistry-climate models and associated external forcings, J. Geophys. Res., 115, D00M02, doi:10.1029/2009JD013728, 2010b.

Morgenstern, O., Zeng, G., Luke Abraham, N., Telford, P. J., Braesicke, P., Pyle, J. A., Hardiman, S. C., O'Connor, F. M., and Johnson, C. E.: Impacts of climate change, ozone recovery, and increasing methane on surface ozone and the tropospheric oxidizing capacity, J. Geophys. Res., 118, 1028-1041, doi:10.1029/2012JD018382, 2013.

Morgenstern, O., Hegglin, M. I., Rozanov, E., O'Connor, F. M., Abraham, N. L., Akiyoshi, H., Archibald, A. T., Bekki, S., Butchart, N., Chipperfield, M. P., Deushi, M., Dhomse, S. S., Garcia, R. R., Hardiman, S. C., Horowitz, L. W., Jöckel, P., Josse, B., Kinnison, D., Lin, M., Mancini, E., Manyin, M. E., Marchand, M., Marécal, V., Michou, M., Oman, L. D., Pitari, G., Plummer, D. A., Revell, L. E., Saint-Martin, D., Schofield, R., Stenke, A., Stone, K., Sudo, K., Tanaka, T. Y., Tilmes, S., Yamashita, Y., Yoshida, K., and Zeng, G.: Review of the global models used within phase 1 of the Chemistry–Climate Model Initiative (CCMI), Geosci. Model Dev., 10, 639-671, doi:10.5194/gmd-10-639-2017, 2017.

Morice, C. P., Kennedy, J. J., Rayner, N. A., and Jones, P. D.: Quantifying uncertainties in global and regional temperature change using an ensemble of observational estimates: The HadCRUT4 data set, J. Geophys. Res., 117, D08101, doi:10.1029/2011JD017187, 2012.

Murphy, D. M., Solomon, S., Portmann, R. W., Rosenlof, K. H., Forster, P. M., and Wong, T.: An observationally based energy balance for the Earth since 1950, J. Geophys. Res., 114, D17107, doi:10.1029/2009JD012105, 2009.

Myhre, G., Shindell, D., Breìon, F. M., Collins, W., Fuglestvedt, J., Huang, J., Koch, D., Lamarque, J. F., Lee, D., Mendoza, B., Nakajima, T., Robock, A., Stephens, G., Takemura, T., and Zhang, H.: Anthropogenic and Natural Radiative Forcing, in: Climate Change: The Physical Science Basis. Contribution of Working Group I to the Fifth Assessment Report of the Intergovernmental Panel on Climate Change, [Stocker, T. F., Qin, D., Plattner, G. K., Tignor, M., Allen, S. K., Boschung, J., Nauels, A., Xia, Y., Bex, V., and Midgley, P. M. (eds)], Cambridge University Press, Cambridge, United Kingdom and New York, NY, USA, 659-740, 2013.

Nagai, T., Liley, B., Sakai, T., Shibata, T., and Uchino, O.: Post-Pinatubo Evolution and Subsequent Trend of the Stratospheric Aerosol Layer Observed by Mid-Latitude Lidars in Both Hemispheres, SOLA, 6, 69-72, doi:10.2151/sola.2010-018, 2010.

Naik, V., Horowitz, L. W., Fiore, A. M., Ginoux, P., Mao, J., Aghedo, A. M., and Levy, H.: Impact of preindustrial to present-day changes in short-lived pollutant emissions on atmospheric composition and climate forcing, J. Geophys. Res., 118, 8086-8110, doi:10.1002/jgrd.50608, 2013a.

Naik, V., Voulgarakis, A., Fiore, A. M., Horowitz, L. W., Lamarque, J. F., Lin, M., Prather, M. J., Young, P. J., Bergmann, D., Cameron-Smith, P. J., Cionni, I., Collins, W. J., Dalsören, S. B., Doherty, R., Eyring, V., Faluvegi, G., Folberth, G. A., Josse, B., Lee, Y. H., MacKenzie, I. A., Nagashima, T., van Noije, T. P. C., Plummer, D. A., Righi, M., Rumbold, S. T., Skeie, R., Shindell, D. T., Stevenson, D. S., Strode, S., Sudo, K., Szopa, S., and Zeng, G.: Preindustrial to present-day changes in tropospheric hydroxyl radical and methane lifetime from the Atmospheric Chemistry and Climate Model Intercomparison Project (ACCMIP), Atmos. Chem. Phys., 13, 5277-5298, doi:10.5194/acp-13-5277-2013, 2013b.

Naoe, H., and Shibata, K.: Equatorial quasi-biennial oscillation influence on northern winter extratropical circulation, J. Geophys. Res., 115, D19102, doi:10.1029/2009JD012952, 2010.

Nedoluha, G. E., Siskind, D. E., Lambert, A., and Boone, C.: The decrease in mid-stratospheric tropical ozone since 1991, Atmos. Chem. Phys., 15, 4215-4224, doi:10.5194/acp-15-4215-2015, 2015.

Neely, R. R., Toon, O. B., Solomon, S., Vernier, J. P., Alvarez, C., English, J. M., Rosenlof, K. H., Mills, M. J., Bardeen, C. G., Daniel, J. S., and Thayer, J. P.: Recent anthropogenic increases in SO2 from Asia have minimal impact on stratospheric aerosol, Geophys. Res. Lett., 40, 999-1004, doi:10.1002/grl.50263, 2013.

Newman, M., Alexander, M. A., Ault, T. R., Cobb, K. M., Deser, C., Lorenzo, E., Mantua, N. J., Miller, A. J., Minobe, S., Nakamura, H., Schneider, N., Vimont, D. J., Phillips, A. S., Scott, J. D., and Smith, C. A.: The Pacific Decadal Oscillation, Revisited, J. Clim., 29, 4399–4427, doi:10.1175/JCLI-D-15-0508.1, 2016.

Newman, P. A., Nash, E. R., and Rosenfield, J. E.: What controls the temperature of the Arctic stratosphere during the spring?, J. Geophys. Res., 106, 19999-20010, doi:10.1029/2000JD000061, 2001.

Newman, P. A., Nash, E. R., Kawa, S. R., Montzka, S. A., and Schauffler, S. M.: When will the Antarctic ozone hole recover?, Geophys. Res. Lett., 33, L12814, doi:10.1029/2005GL025232, 2006.

Newman, P. A., Daniel, J. S., Waugh, D. W., and Nash, E. R.: A new formulation of equivalent effective stratospheric chlorine (EESC), Atmos. Chem. Phys., 7, 4537-4552, doi:10.5194/acp-7-4537-2007, 2007.

Nowack, P. J., Luke Abraham, N., Maycock, A. C., Braesicke, P., Gregory, J. M., Joshi, M. M., Osprey, A., and Pyle, J. A.: A large ozone-circulation feedback and its implications for global warming assessments, Nature Clim. Change, 5, 41-45, doi:10.1038/nclimate2451, 2015.

O'Connor, F. M., Johnson, C. E., Morgenstern, O., Abraham, N. L., Braesicke, P., Dalvi, M., Folberth, G. A., Sanderson, M. G., Telford, P. J., Voulgarakis, A., Young, P. J., Zeng, G., Collins, W. J., and Pyle, J. A.: Evaluation of the new UKCA climate-composition model – Part 2: The Troposphere, Geosci. Model Dev., 7, 41-91, doi:10.5194/gmd-7-41-2014, 2014.

Oberländer, S., Langematz, U., and Meul, S.: Unraveling impact factors for future changes in the Brewer-Dobson circulation, J. Geophys. Res., 118, 10,296-210,312, doi:10.1002/jgrd.50775, 2013.

Olsen, S. C., McLinden, C. A., and Prather, M. J.: Stratospheric N2O–NOy system: Testing uncertainties in a three-dimensional framework, J. Geophys. Res., 106, 28771-28784, doi:10.1029/2001JD000559, 2001.

Oman, L., Waugh, D. W., Pawson, S., Stolarski, R. S., and Nielsen, J. E.: Understanding the Changes of Stratospheric Water Vapor in Coupled Chemistry–Climate Model Simulations, J. Atmos. Sci., 65, 3278-3291, doi:10.1175/2008JAS2696.1, 2008.

Oman, L., Waugh, D. W., Pawson, S., Stolarski, R. S., and Newman, P. A.: On the influence of anthropogenic forcings on changes in the stratospheric mean age, J. Geophys. Res., 114, D03105, doi:10.1029/2008JD010378, 2009.

Oman, L. D., Plummer, D. A., Waugh, D. W., Austin, J., Scinocca, J. F., Douglass, A. R., Salawitch, R. J., Canty, T., Akiyoshi, H., Bekki, S., Braesicke, P., Butchart, N., Chipperfield, M. P., Cugnet, D., Dhomse, S., Eyring, V., Frith, S., Hardiman, S. C., Kinnison, D. E., Lamarque, J. F., Mancini, E., Marchand, M., Michou, M., Morgenstern, O., Nakamura, T., Nielsen, J. E., Olivié, D., Pitari, G., Pyle, J., Rozanov, E., Shepherd, T. G., Shibata, K., Stolarski, R. S., Teyssèdre, H., Tian, W., Yamashita, Y., and Ziemke, J. R.: Multimodel assessment of the factors driving stratospheric ozone evolution over the 21st century, J. Geophys. Res., 115, D24306, doi:10.1029/2010JD014362, 2010.

Osterman, G. B., Kulawik, S. S., Worden, H. M., Richards, N. A. D., Fisher, B. M., Eldering, A., Shephard, M. W., Froidevaux, L., Labow, G., Luo, M., Herman, R. L., Bowman, K. W., and Thompson, A. M.: Validation of Tropospheric Emission Spectrometer (TES) measurements of the total, stratospheric, and tropospheric column abundance of ozone, J. Geophys. Res., 113, D15S16, doi:10.1029/2007JD008801, 2008.

Palmeiro, F. M., Calvo, N., and Garcia, R. R.: Future Changes in the Brewer–Dobson Circulation under Different Greenhouse Gas Concentrations in WACCM4, J. Atmos. Sci., 71, 2962-2975, doi:10.1175/JAS-D-13-0289.1, 2014.

Parrella, J. P., Jacob, D. J., Liang, Q., Zhang, Y., Mickley, L. J., Miller, B., Evans, M. J., Yang, X., Pyle, J. A., Theys, N., and Van Roozendael, M.: Tropospheric bromine chemistry: implications for present and pre-industrial ozone and mercury, Atmos. Chem. Phys., 12, 6723-6740, doi:10.5194/acp-12-6723-2012, 2012.

Parrish, D. D., Lamarque, J. F., Naik, V., Horowitz, L., Shindell, D. T., Staehelin, J., Derwent, R., Cooper, O. R., Tanimoto, H., Volz-Thomas, A., Gilge, S., Scheel, H. E., Steinbacher, M., and Fröhlich, M.: Long-term changes in lower tropospheric baseline ozone concentrations: Comparing chemistry-climate models and observations at northern midlatitudes, J. Geophys. Res., 119, 5719–5736, doi:10.1002/2013JD021435, 2014.

Pawson, S., Kodera, K., Hamilton, K., Shepherd, T. G., Beagley, S. R., Boville, B. A., Farrara, J. D., Fairlie, T. D. A., Kitoh, A., Lahoz, W. A., Langematz, U., Manzini, E., Rind, D. H., Scaife, A. A., Shibata, K., Simon, P., Swinbank, R., Takacs, L., Wilson, R. J., Al-Saadi, J. A., Amodei, M., Chiba, M., Coy, L., de Grandpré, J., Eckman, R. S., Fiorino, M., Grose, W. L., Koide, H., Koshyk, J. N., Li, D., Lerner, J., Mahlman, J. D., McFarlane, N. A., Mechoso, C. R., Molod, A., O'Neill, A., Pierce, R. B., Randel, W. J., Rood, R. B., and Wu, F.: The GCM–Reality Intercomparison Project for SPARC (GRIPS): Scientific Issues and Initial Results, Bull. Am. Meteorol. Soc., 81, 781-796, doi:10.1175/1520-0477(2000)081<0781:TGIPFS>2.3.CO;2, 2000.

Pawson, S., Steinbrecht, W., Charlton-Perez, A. J., Fujiwara, M., Karpechko, A.Yu., Petropavlovskikh, I., Urban, J., and Weber, M., Update on global ozone: Past, present, and future, Chapter 2 in Scientific Assessment of Ozone Depletion: 2014, Global Ozone Research and Monitoring Project – Report No. 55, World Meteorological Organization, Geneva, Switzerland, 2014.

Perlwitz, J., and Graf, H. F.: The Statistical Connection between Tropospheric and Stratospheric Circulation of the Northern Hemisphere in Winter, J. Clim., 8, 2281-2295, doi:10.1175/1520-0442(1995)008<2281:TSCBTA>2.0.CO;2, 1995.

Perlwitz, J., Pawson, S., Fogt, R. L., Nielsen, J. E., and Neff, W. D.: Impact of stratospheric ozone hole recovery on Antarctic climate, Geophys. Res. Lett., 35, L08714, doi:10.1029/2008GL033317, 2008.

Perlwitz, J.: Atmospheric science: Tug of war on the jet stream, Nature Clim. Change, 1, 29-31, doi:10.1038/nclimate1065, 2011.

Plumb, R. A.: Stratospheric Transport, Journal of the Meteorological Society of Japan. Ser. II, 80, 793-809, doi:10.2151/jmsj.80.793, 2002.

Plumb, R. A.: Tracer interrelationships in the stratosphere, Rev. Geophys., 45, RG4005, doi:10.1029/2005RG000179, 2007.

Plummer, D. A., Scinocca, J. F., Shepherd, T. G., Reader, M. C., and Jonsson, A. I.: Quantifying the contributions to stratospheric ozone changes from ozone depleting substances and greenhouse gases, Atmos. Chem. Phys., 10, 8803-8820, doi:10.5194/acp-10-8803-2010, 2010.

Polvani, L. M., Waugh, D. W., Correa, G. J. P., and Son, S. W.: Stratospheric Ozone Depletion: The Main Driver of Twentieth-Century Atmospheric Circulation Changes in the Southern Hemisphere, J. Clim., 24, 795-812, doi:10.1175/2010JCLI3772.1, 2010.

Polvani, L. M., Previdi, M., and Deser, C.: Large cancellation, due to ozone recovery, of future Southern Hemisphere atmospheric circulation trends, Geophys. Res. Lett., 38, L04707, doi:10.1029/2011GL046712, 2011.

Polvani, L. M., and Solomon, S.: The signature of ozone depletion on tropical temperature trends, as revealed by their seasonal cycle in model integrations with single forcings, J. Geophys. Res., 117, D17102, doi:10.1029/2012JD017719, 2012.

Portmann, R. W., and Solomon, S.: Indirect radiative forcing of the ozone layer during the 21st century, Geophys. Res. Lett., 34, L02813, doi:10.1029/2006GL028252, 2007.

Portmann, R. W., Daniel, J. S., and Ravishankara, A. R.: Stratospheric ozone depletion due to nitrous oxide: influences of other gases, Philos. T. Roy. Soc. B, 367, 1256-1264, doi:10.1098/rstb.2011.0377, 2012.

Poulet, G., Pirre, M., Maguin, F., Ramaroson, R., and Le Bras, G.: Role of the BRO + HO2 reaction in the stratospheric chemistry of bromine, Geophys. Res. Lett., 19, 2305-2308, doi:10.1029/92GL00781, 1992.

Prather M., Ehhalt, D., Dentener, F., Derwent, R., Dlugokencky, E., Holland, E., Isaksen, I., Katima, J., Kirchhoff, V., Matson, P., Midgley, P., Wang, M., Atmospheric chemistry and greenhouse gases. In: Climate change: The scientific basis. Contribution of Working Group I to the Third Assessment Report of the Intergovernmental Panel on Climate Change, [Houghton J. T., Ding, Y., Griggs, D. J., Noguer, M., van der Linden, P. J., Dai, X., Maskell, K., Johnson, C. A. (eds)], Cambridge University Press, Cambridge, UK, 2001.

Prather, M. J., Zhu, X., Tang, Q., Hsu, J., and Neu, J. L.: An atmospheric chemist in search of the tropopause, J. Geophys. Res., 116, D04306, doi:10.1029/2010JD014939, 2011.

Prather, M. J., Holmes, C. D., and Hsu, J.: Reactive greenhouse gas scenarios: Systematic exploration of uncertainties and the role of atmospheric chemistry, Geophys. Res. Lett., 39, L09803, doi:10.1029/2012GL051440, 2012.

Previdi, M., and Polvani, L. M.: Climate system response to stratospheric ozone depletion and recovery, Quart. J. Roy. Meteor. Soc., 140, 2401-2419, doi:10.1002/qj.2330, 2014.

Pyle, J. A.: A calculation of the possible depletion of ozone by chlorofluorocarbons using a two-dimensional model, pure and applied geophysics, 118, 355-377, doi:10.1007/BF01586458, 1980.

Pyle, J. A., Shepherd, T., Bodeker, G. E., Canziani, P., Dameris, M., Forster, P. M., Gruzdev, A., Müller, R., Muthama, N., Pitari, G., and Randel, W. J.: Ozone and climate: a review of interconnections, in: Special report on safeguarding the ozone layer and global climate system, IPCC/TEAP, Cambridge, 2005.

Ramaswamy, V., Schwarzkopf, M. D., Randel, W. J., Santer, B. D., Soden, B. J., and Stenchikov, G. L.: Anthropogenic and Natural Influences in the Evolution of Lower Stratospheric Cooling, Science, 311, 1138-1141, doi:10.1126/science.1122587, 2006.

Randel, W. J., and Wu, F.: Cooling of the Arctic and Antarctic Polar Stratospheres due to Ozone Depletion, J. Clim., 12, 1467-1479, doi:10.1175/1520-0442(1999)012<1467:COTAAA>2.0.CO;2, 1999.

Randel, W. J., Wu, F., Vömel, H., Nedoluha, G. E., and Forster, P.: Decreases in stratospheric water vapor after 2001: Links to changes in the tropical tropopause and the Brewer-Dobson circulation, J. Geophys. Res., 111, D12312, doi:10.1029/2005JD006744, 2006.

Randel, W. J., Park, M., Wu, F., and Livesey, N.: A Large Annual Cycle in Ozone above the Tropical Tropopause Linked to the Brewer–Dobson Circulation, J. Atmos. Sci., 64, 4479-4488, doi:10.1175/2007JAS2409.1, 2007.

Randel, W. J., and Wu, F.: A stratospheric ozone profile data set for 1979–2005: Variability, trends, and comparisons with column ozone data, J. Geophys. Res., 112, D06313, doi:10.1029/2006JD007339, 2007.

Randel, W. J., Garcia, R. R., Calvo, N., and Marsh, D.: ENSO influence on zonal mean temperature and ozone in the tropical lower stratosphere, Geophys. Res. Lett., 36, L15822, doi:10.1029/2009GL039343, 2009a.

Randel, W. J., Shine, K. P., Austin, J., Barnett, J., Claud, C., Gillett, N. P., Keckhut, P., Langematz, U., Lin, R., Long, C., Mears, C., Miller, A., Nash, J., Seidel, D. J., Thompson, D. W. J., Wu, F., and Yoden, S.: An update of observed stratospheric temperature trends, J. Geophys. Res., 114, D02107, doi:10.1029/2008JD010421, 2009b.

Randeniya, L. K., Vohralik, P. F., and Plumb, I. C.: Stratospheric ozone depletion at northern mid latitudes in the 21st century: The importance of future concentrations of greenhouse gases nitrous oxide and methane, Geophys. Res. Lett., 29, 10-11-10-14, doi:10.1029/2001GL014295, 2002.

Rap, A., Richards, N. A. D., Forster, P. M., Monks, S. A., Arnold, S. R., and Chipperfield, M. P.: Satellite constraint on the tropospheric ozone radiative effect, Geophys. Res. Lett., 42, 2015GL064037, doi:10.1002/2015GL064037, 2015.

Ravishankara, A. R., Daniel, J. S., and Portmann, R. W.: Nitrous Oxide (N2O): The Dominant Ozone-Depleting Substance Emitted in the 21st Century, Science, 326, 123-125, doi:10.1126/science.1176985, 2009.

Ray, E. A., Moore, F. L., Rosenlof, K. H., Davis, S. M., Sweeney, C., Tans, P., Wang, T., Elkins, J. W., Bönisch, H., Engel, A., Sugawara, S., Nakazawa, T., and Aoki, S.: Improving stratospheric transport trend analysis based on SF6 and CO2 measurements, J. Geophys. Res., 119, 2014JD021802, doi:10.1002/2014JD021802, 2014.

Reader, M. C., Plummer, D. A., Scinocca, J. F., and Shepherd, T. G.: Contributions to twentieth century total column ozone change from halocarbons, tropospheric ozone precursors, and climate change, Geophys. Res. Lett., 40, 6276-6281, doi:10.1002/2013GL057776, 2013.

Revell, L. E., Bodeker, G. E., Smale, D., Lehmann, R., Huck, P. E., Williamson, B. E., Rozanov, E., and Struthers, H.: The effectiveness of N2O in depleting stratospheric ozone, Geophys. Res. Lett., 39, L15806, doi:10.1029/2012GL052143, 2012.

Rienecker, M. M., Suarez, M. J., Gelaro, R., Todling, R., Bacmeister, J., Liu, E., Bosilovich, M. G., Schubert, S. D., Takacs, L., Kim, G. K., Bloom, S., Chen, J., Collins, D., Conaty, A., da Silva, A., Gu, W., Joiner, J., Koster, R. D., Lucchesi, R., Molod, A., Owens, T., Pawson, S., Pegion, P., Redder, C. R., Reichle, R., Robertson, F. R., Ruddick, A. G., Sienkiewicz, M., and Woollen, J.: MERRA: NASA's Modern-Era Retrospective Analysis for Research and Applications, J. Clim., 24, 3624-3648, doi:10.1175/JCLI-D-11-00015.1, 2011.

Riese, M., Ploeger, F., Rap, A., Vogel, B., Konopka, P., Dameris, M., and Forster, P.: Impact of uncertainties in atmospheric mixing on simulated UTLS composition and related radiative effects, J. Geophys. Res., 117, D16305, doi:10.1029/2012JD017751, 2012.

Roelofs, G. J., and Lelieveld, J.: Model study of the influence of cross-tropopause O3 transports on tropospheric O3 levels, Tellus Ser. B Chem. Phys. Meteorol., 49, 38-55, doi:10.3402/tellusb.v49i1.15949, 1997.

Rosenfield, J. E., Douglass, A. R., and Considine, D. B.: The impact of increasing carbon dioxide on ozone recovery, J. Geophys. Res., 107, ACH 7-1-ACH 7-9, doi:10.1029/2001JD000824, 2002.

Salby, M., Titova, E., and Deschamps, L.: Rebound of Antarctic ozone, Geophys. Res. Lett., 38, L09702, doi:10.1029/2011GL047266, 2011.

Salby, M. L., Titova, E. A., and Deschamps, L.: Changes of the Antarctic ozone hole: Controlling mechanisms, seasonal predictability, and evolution, J. Geophys. Res., 117, doi:10.1029/2011JD016285, 2012.

Sander, S. P., Finlayson-Pitts, B. J., Friedl, R. R., Golden, D. M., Huie, R. E., Keller-Rudek, H., Kolb, C. E., Kurylo, M. J., Molina, M. J., Moortgat, G. K., Orkin, V. L., Ravishankara, A. R., and Wine, P. H.: Chemical Kinetics and Photochemical Data for Use in Atmospheric Studies, JPL Publication 06-2, Jet Propulsion Laboratory, Pasadena, 2006.

Sander, S. P., Abbatt, J., Barker, J. R., Burkholder, J. B., Friedl, R. R., Golden, D. M., Huie, R. E., Kolb, C. E., Kurylo, M. J., Moortgat, G. K., Orkin, V. L., and Wine, P. H.: Chemical Kinetics and Photochemical Data for Use in Atmospheric Studies JPL Publication 09-31, Jet Propulsion Laboratory, Pasadena, 2009.

Sankey, D., and Shepherd, T. G.: Correlations of long-lived chemical species in a middle atmosphere general circulation model, J. Geophys. Res., 108, 4494, doi:10.1029/2002JD002799, 2003.

Santer, B. D., Wigley, T. M. L., Boyle, J. S., Gaffen, D. J., Hnilo, J. J., Nychka, D., Parker, D. E., and Taylor, K. E.: Statistical significance of trends and trend differences in layer-average atmospheric temperature time series, J. Geophys. Res., 105, 7337-7356, doi:10.1029/1999JD901105, 2000.

Santer, B. D., Sausen, R., Wigley, T. M. L., Boyle, J. S., AchutaRao, K., Doutriaux, C., Hansen, J. E., Meehl, G. A., Roeckner, E., Ruedy, R., Schmidt, G., and Taylor, K. E.: Behavior of tropopause height and atmospheric temperature in models, reanalyses, and observations: Decadal changes, J. Geophys. Res., 108, 4002, doi:10.1029/2002JD002258, 2003a.

Santer, B. D., Wehner, M. F., Wigley, T. M. L., Sausen, R., Meehl, G. A., Taylor, K. E., Ammann, C., Arblaster, J., Washington, W. M., Boyle, J. S., and

Brüggemann, W.: Contributions of Anthropogenic and Natural Forcing to Recent Tropopause Height Changes, Science, 301, 479-483, doi:10.1126/science.1084123, 2003b.

Santer, B. D., Painter, J. F., Bonfils, C., Mears, C. A., Solomon, S., Wigley, T. M. L., Gleckler, P. J., Schmidt, G. A., Doutriaux, C., Gillett, N. P., Taylor, K. E., Thorne, P. W., and Wentz, F. J.: Human and natural influences on the changing thermal structure of the atmosphere, Proc. Natl. Acad. Sci., doi:10.1073/pnas.1305332110, 2013.

Schmidt, G. A., Ruedy, R., Hansen, J. E., Aleinov, I., Bell, N., Bauer, M., Bauer, S., Cairns, B., Canuto, V., Cheng, Y., Del Genio, A., Faluvegi, G., Friend, A. D., Hall, T. M., Hu, Y., Kelley, M., Kiang, N. Y., Koch, D., Lacis, A. A., Lerner, J., Lo, K. K., Miller, R. L., Nazarenko, L., Oinas, V., Perlwitz, J., Perlwitz, J., Rind, D., Romanou, A., Russell, G. L., Sato, M., Shindell, D. T., Stone, P. H., Sun, S., Tausnev, N., Thresher, D., and Yao, M. S.: Present-Day Atmospheric Simulations Using GISS ModelE: Comparison to In Situ, Satellite, and Reanalysis Data, J. Clim., 19, 153-192, doi:10.1175/JCLI3612.1, 2006.

Schumann, U., and Huntrieser, H.: The global lightning-induced nitrogen oxides source, Atmos. Chem. Phys., 7, 3823-3907, doi:10.5194/acp-7-3823-2007, 2007.

Scinocca, J. F., McFarlane, N. A., Lazare, M., Li, J., and Plummer, D.: Technical Note: The CCCma third generation AGCM and its extension into the middle atmosphere, Atmos. Chem. Phys., 8, 7055-7074, doi:10.5194/acp-8-7055-2008, 2008.

Seviour, W. J. M., Butchart, N., and Hardiman, S. C.: The Brewer–Dobson circulation inferred from ERA-Interim, Quart. J. Roy. Meteor. Soc., 138, 878-888, doi:10.1002/qj.966, 2012.

Sexton, D. M. H.: The effect of stratospheric ozone depletion on the phase of the Antarctic Oscillation, Geophys. Res. Lett., 28, 3697-3700, doi:10.1029/2001GL013376, 2001.

Shepherd, T. G.: Dynamics, stratospheric ozone, and climate change, Atmos.-Ocean, 46, 117-138, doi:10.3137/ao.460106, 2008.

Shepherd, T. G., Plummer, D. A., Scinocca, J. F., Hegglin, M. I., Fioletov, V. E., Reader, M. C., Remsberg, E., von Clarmann, T., and Wang, H. J.: Reconciliation of halogen-induced ozone loss with the total-column ozone record, Nature Geosci., 7, 443-449, doi:10.1038/ngeo2155, 2014.

Sherwood, S. C., Meyer, C. L., Allen, R. J., and Titchner, H. A.: Robust Tropospheric Warming Revealed by Iteratively Homogenized Radiosonde Data, J. Clim., 21, 5336-5352, doi:10.1175/2008JCLI2320.1, 2008.

Shindell, D. T., and Schmidt, G. A.: Southern Hemisphere climate response to ozone changes and greenhouse gas increases, Geophys. Res. Lett., 31, L18209, doi:10.1029/2004GL020724, 2004.

Shindell, D. T., Faluvegi, G., Stevenson, D. S., Krol, M. C., Emmons, L. K., Lamarque, J. F., Pétron, G., Dentener, F. J., Ellingsen, K., Schultz, M. G., Wild, O., Amann, M., Atherton, C. S., Bergmann, D. J., Bey, I., Butler, T., Cofala, J., Collins, W. J., Derwent, R. G., Doherty, R. M., Drevet, J., Eskes, H. J., Fiore, A. M., Gauss, M., Hauglustaine, D. A., Horowitz, L. W., Isaksen, I. S. A., Lawrence, M. G., Montanaro, V., Müller, J. F., Pitari, G., Prather, M. J., Pyle, J. A., Rast, S., Rodriguez, J. M., Sanderson, M. G., Savage, N. H., Strahan, S. E., Sudo, K., Szopa, S., Unger, N., van Noije, T. P. C., and Zeng, G.: Multimodel simulations of carbon monoxide: Comparison with observations and projected near-future changes, J. Geophys. Res., 111, D19306, doi:10.1029/2006JD007100, 2006.

Shindell, D., Faluvegi, G., Nazarenko, L., Bowman, K., Lamarque, J. F., Voulgarakis, A., Schmidt, G. A., Pechony, O., and Ruedy, R.: Attribution of historical

ozone forcing to anthropogenic emissions, Nature Clim. Change, 3, 567-570, doi:10.1038/nclimate1835, 2013a.

Shindell, D. T., Lamarque, J. F., Schulz, M., Flanner, M., Jiao, C., Chin, M., Young, P. J., Lee, Y. H., Rotstayn, L., Mahowald, N., Milly, G., Faluvegi, G., Balkanski, Y., Collins, W. J., Conley, A. J., Dalsören, S., Easter, R., Ghan, S., Horowitz, L., Liu, X., Myhre, G., Nagashima, T., Naik, V., Rumbold, S. T., Skeie, R., Sudo, K., Szopa, S., Takemura, T., Voulgarakis, A., Yoon, J. H., and Lo, F.: Radiative forcing in the ACCMIP historical and future climate simulations, Atmos. Chem. Phys., 13, 2939-2974, doi:10.5194/acp-13-2939-2013, 2013b.

Shindell, D. T., Pechony, O., Voulgarakis, A., Faluvegi, G., Nazarenko, L., Lamarque, J. F., Bowman, K., Milly, G., Kovari, B., Ruedy, R., and Schmidt, G. A.: Interactive ozone and methane chemistry in GISS-E2 historical and future climate simulations, Atmos. Chem. Phys., 13, 2653-2689, doi:10.5194/acp-13-2653-2013, 2013c.

Sillman, S.: The relation between ozone, NOx and hydrocarbons in urban and polluted rural environments, Atmos. Environ., 33, 1821-1845, doi:10.1016/S1352-2310(98)00345-8, 1999.

Simmonds, I., and Keay, K.: Variability of Southern Hemisphere Extratropical Cyclone Behavior, 1958–97, J. Clim., 13, 550-561, doi:10.1175/1520-0442(2000)013<0550:VOSHEC>2.0.CO;2, 2000.

Skeie, R. B., Berntsen, T. K., Myhre, G., Tanaka, K., Kvalevåg, M. M., and Hoyle, C. R.: Anthropogenic radiative forcing time series from pre-industrial times until 2010, Atmos. Chem. Phys., 11, 11827-11857, doi:10.5194/acp-11-11827-2011, 2011.

Solomon, S., Garcia, R. R., and Stordal, F.: Transport processes and ozone perturbations, J. Geophys. Res., 90, 12981-12989, doi:10.1029/JD090iD07p12981, 1985.

Solomon, S., Garcia, R. R., Rowland, F. S., and Wuebbles, D. J.: On the depletion of Antarctic ozone, Nature, 321, 755-758, doi:10.1038/321755a0, 1986.

Solomon, S., Portmann, R. W., Garcia, R. R., Thomason, L. W., Poole, L. R., and McCormick, M. P.: The role of aerosol variations in anthropogenic ozone depletion at northern midlatitudes, J. Geophys. Res., 101, 6713-6727, doi:10.1029/95JD03353, 1996.

Solomon, S.: Stratospheric ozone depletion: A review of concepts and history, Rev. Geophys., 37, 275-316, doi:10.1029/1999rg900008, 1999.

Solomon, S., Young, P. J., and Hassler, B.: Uncertainties in the evolution of stratospheric ozone and implications for recent temperature changes in the tropical lower stratosphere, Geophys. Res. Lett., 39, L17706, doi:10.1029/2012gl052723, 2012.

Solomon, S., Haskins, J., Ivy, D. J., and Min, F.: Fundamental differences between Arctic and Antarctic ozone depletion, Proc. Natl. Acad. Sci., 111, 6220-6225, doi:10.1073/pnas.1319307111, 2014.

Solomon, S., Kinnison, D., Bandoro, J., and Garcia, R.: Simulation of polar ozone depletion: An update, J. Geophys. Res., 120, 2015JD023365, doi:10.1002/2015JD023365, 2015.

Solomon, S., Ivy, D. J., Kinnison, D., Mills, M. J., Neely, R. R., and Schmidt, A.: Emergence of healing in the Antarctic ozone layer, Science, doi:10.1126/science.aae0061, 2016.

Son, S. W., Polvani, L. M., Waugh, D. W., Akiyoshi, H., Garcia, R., Kinnison, D., Pawson, S., Rozanov, E., Shepherd, T. G., and Shibata, K.: The Impact of Stratospheric Ozone Recovery on the Southern Hemisphere Westerly Jet, Science, 320, 1486-1489, doi:10.1126/science.1155939, 2008.

Son, S. W., Tandon, N. F., Polvani, L. M., and Waugh, D. W.: Ozone hole and Southern Hemisphere climate change, Geophys. Res. Lett., 36, L15705, doi:10.1029/2009GL038671, 2009.

Son, S. W., Gerber, E. P., Perlwitz, J., Polvani, L. M., Gillett, N. P., Seo, K. H., Eyring, V., Shepherd, T. G., Waugh, D., Akiyoshi, H., Austin, J., Baumgaertner, A., Bekki, S., Braesicke, P., Brühl, C., Butchart, N., Chipperfield, M. P., Cugnet, D., Dameris, M., Dhomse, S., Frith, S., Garny, H., Garcia, R., Hardiman, S. C., Jöckel, P., Lamarque, J. F., Mancini, E., Marchand, M., Michou, M., Nakamura, T., Morgenstern, O., Pitari, G., Plummer, D. A., Pyle, J., Rozanov, E., Scinocca, J. F., Shibata, K., Smale, D., Teyssèdre, H., Tian, W., and Yamashita, Y.: Impact of stratospheric ozone on Southern Hemisphere circulation change: A multimodel assessment, J. Geophys. Res., 115, D00M07, doi:10.1029/2010JD014271, 2010.

Soukharev, B. E., and Hood, L. L.: Solar cycle variation of stratospheric ozone: Multiple regression analysis of long-term satellite data sets and comparisons with models, J. Geophys. Res., 111, D20314, doi:10.1029/2006JD007107, 2006.

Søvde, O. A., Hoyle, C. R., Myhre, G., and Isaksen, I. S. A.: The HNO3 forming branch of the HO2 + NO reaction: pre-industrial-to-present trends in atmospheric species and radiative forcings, Atmos. Chem. Phys., 11, 8929-8943, doi:10.5194/acp-11-8929-2011, 2011.

Ko, M., Newman, P., Reimann, S. and Strahan, S. (eds), SPARC Report on the Lifetimes of Stratospheric Ozone-Depleting Substances, TheirReplacements, and Related Species, SPARC Rep. 6, WCRP-15/2013 , World Climate Research Program, World Meteorological Organization,Geneva, Switzerland, 2013.

SPARC CCMVal, SPARC report on the evaluation of chemistry- climate models, in SPARC Report No. 5, WCRP-132, WMO/TD-No, [Eyring, V., Shepherd, T. G, and Waugh, D. W. (eds)], pp. 1526, 2010.

Squire, O. J., Archibald, A. T., Abraham, N. L., Beerling, D. J., Hewitt, C. N., Lathière, J., Pike, R. C., Telford, P. J., and Pyle, J. A.: Influence of future climate and cropland expansion on isoprene emissions and tropospheric ozone, Atmos. Chem. Phys., 14, 1011-1024, doi:10.5194/acp-14-1011-2014, 2014.

Stenke, A., and Grewe, V.: Simulation of stratospheric water vapor trends: impact on stratospheric ozone chemistry, Atmos. Chem. Phys., 5, 1257-1272, doi:10.5194/acp-5-1257-2005, 2005.

Stevenson, D. S., Dentener, F. J., Schultz, M. G., Ellingsen, K., van Noije, T. P. C., Wild, O., Zeng, G., Amann, M., Atherton, C. S., Bell, N., Bergmann, D. J., Bey, I., Butler, T., Cofala, J., Collins, W. J., Derwent, R. G., Doherty, R. M., Drevet, J., Eskes, H. J., Fiore, A. M., Gauss, M., Hauglustaine, D. A., Horowitz, L. W., Isaksen, I. S. A., Krol, M. C., Lamarque, J. F., Lawrence, M. G., Montanaro, V., Müller, J. F., Pitari, G., Prather, M. J., Pyle, J. A., Rast, S., Rodriguez, J. M., Sanderson, M. G., Savage, N. H., Shindell, D. T., Strahan, S. E., Sudo, K., and Szopa, S.: Multimodel ensemble simulations of present-day and near-future tropospheric ozone, J. Geophys. Res., 111, D08301, doi:10.1029/2005JD006338, 2006.

Stevenson, D. S., Young, P. J., Naik, V., Lamarque, J. F., Shindell, D. T., Voulgarakis, A., Skeie, R. B., Dalsoren, S. B., Myhre, G., Berntsen, T. K., Folberth, G. A., Rumbold, S. T., Collins, W. J., MacKenzie, I. A., Doherty, R. M., Zeng, G., van Noije, T. P. C., Strunk, A., Bergmann, D., Cameron-Smith, P., Plummer, D. A., Strode, S. A., Horowitz, L., Lee, Y. H., Szopa, S., Sudo, K., Nagashima, T., Josse, B., Cionni, I., Righi, M., Eyring, V., Conley, A., Bowman, K. W., Wild, O., and Archibald, A.: Tropospheric ozone changes, radiative forcing and attribution to emissions in the Atmospheric Chemistry and Climate Model Intercomparison Project (ACCMIP), Atmos. Chem. Phys., 13, 3063-3085, doi:10.5194/acp-13-3063-2013, 2013.

Stevenson, D. S.: Atmospheric chemistry: Climate's chemical sensitivity, Nature Clim. Change, 5, 21-22, doi:10.1038/nclimate2477, 2015.

Stiller, G. P., von Clarmann, T., Haenel, F., Funke, B., Glatthor, N., Grabowski, U., Kellmann, S., Kiefer, M., Linden, A., Lossow, S., and López-Puertas, M.: Observed temporal evolution of global mean age of stratospheric air for the 2002 to 2010 period, Atmos. Chem. Phys., 12, 3311-3331, doi:10.5194/acp-12-3311-2012, 2012.

Stolarski, R. S., and Cicerone, R. J.: Stratospheric Chlorine: a Possible Sink for Ozone, Can. J. Chem., 52, 1610-1615, doi:10.1139/v74-233, 1974.

Stolarski, R. S., Hays, P. B., and Roble, R. G.: atmospheric heating by solar EUV radiation, J. Geophys. Res., 80, 2266-2276, doi:10.1029/JA080i016p02266, 1975.

Stolarski, R. S., Krueger, A. J., Schoeberl, M. R., McPeters, R. D., Newman, P. A., and Alpert, J. C.: Nimbus 7 satellite measurements of the springtime Antarctic ozone decrease, Nature, 322, 808-811, doi:10.1038/322808a0, 1986.

Stolarski, R. S., and Frith, S. M.: Search for evidence of trend slow-down in the long-term TOMS/SBUV total ozone data record: the importance of instrument drift uncertainty, Atmos. Chem. Phys., 6, 4057-4065, doi:10.5194/acp-6-4057-2006, 2006.

Struthers, H., Bodeker, G. E., Austin, J., Bekki, S., Cionni, I., Dameris, M., Giorgetta, M. A., Grewe, V., Lefèvre, F., Lott, F., Manzini, E., Peter, T., Rozanov, E., and Schraner, M.: The simulation of the Antarctic ozone hole by chemistry-climate models, Atmos. Chem. Phys., 9, 6363-6376, doi:10.5194/acp-9-6363-2009, 2009.

Sudo, K., Takahashi, M., Kurokawa, J.-i., and Akimoto, H.: CHASER: A global chemical model of the troposphere 1. Model description, J. Geophys. Res., 107, 4339, doi:10.1029/2001JD001113, 2002.

Sudo, K., Takahashi, M., and Akimoto, H.: Future changes in stratosphere-troposphere exchange and their impacts on future tropospheric ozone simulations, Geophys. Res. Lett., 30, 2256, doi:10.1029/2003GL018526, 2003.

Taylor, K. E., Stouffer, R. J., and Meehl, G. A.: An Overview of CMIP5 and the Experiment Design, Bull. Am. Meteorol. Soc., 93, 485–498, doi:10.1175/BAMS-D-11-00094.1, 2012.

Thompson, D. W. J., and Wallace, J. M.: Annular Modes in the Extratropical Circulation. Part I: Month-to-Month Variability*, J. Clim., 13, 1000-1016, doi:10.1175/1520-0442(2000)013<1000:AMITEC>2.0.CO;2, 2000.

Thompson, D. W. J., and Solomon, S.: Interpretation of Recent Southern Hemisphere Climate Change, Science, 296, 895-899, doi:10.1126/science.1069270, 2002.

Thompson, D. W. J., Baldwin, M. P., and Solomon, S.: Stratosphere–Troposphere Coupling in the Southern Hemisphere, J. Atmos. Sci., 62, 708-715, doi:10.1175/JAS-3321.1, 2005.

Thompson, D. W. J., and Solomon, S.: Understanding Recent Stratospheric Climate Change, J. Clim., 22, 1934-1943, doi:10.1175/2008JCLI2482.1, 2009.

Thompson, D. W. J., Solomon, S., Kushner, P. J., England, M. H., Grise, K. M., and Karoly, D. J.: Signatures of the Antarctic ozone hole in Southern Hemisphere surface climate change, Nature Geosci., 4, 741-749, doi:10.1038/ngeo1296, 2011.

Thompson, D. W. J., Seidel, D. J., Randel, W. J., Zou, C. Z., Butler, A. H., Mears, C., Osso, A., Long, C., and Lin, R.: The mystery of recent stratospheric temperature trends, Nature, 491, 692-697, doi:10.1038/nature11579, 2012.

Thorne, P. W., Parker, D. E., Tett, S. F. B., Jones, P. D., McCarthy, M., Coleman, H., and Brohan, P.: Revisiting radiosonde upper air temperatures from 1958 to 2002, J. Geophys. Res., 110, D18105, doi:10.1029/2004JD005753, 2005.

Tilmes, S., Lamarque, J. F., Emmons, L. K., Conley, A., Schultz, M. G., Saunois, M., Thouret, V., Thompson, A. M., Oltmans, S. J., Johnson, B., and Tarasick, D.: Technical Note: Ozonesonde climatology between 1995 and 2011: description, evaluation and applications, Atmos. Chem. Phys., 12, 7475-7497, doi:10.5194/acp-12-7475-2012, 2012.

Tilmes, S., Lamarque, J. F., Emmons, L. K., Kinnison, D. E., Ma, P. L., Liu, X., Ghan, S., Bardeen, C., Arnold, S., Deeter, M., Vitt, F., Ryerson, T., Elkins, J. W., Moore, F., Spackman, J. R., and Val Martin, M.: Description and evaluation of tropospheric chemistry and aerosols in the Community Earth System Model (CESM1.2), Geosci. Model Dev., 8, 1395-1426, doi:10.5194/gmd-8-1395-2015, 2015.

Tilmes, S., Lamarque, J. F., Emmons, L. K., Kinnison, D. E., Marsh, D., Garcia, R. R., Smith, A. K., Neely, R. R., Conley, A., Vitt, F., Val Martin, M., Tanimoto, H., Simpson, I., Blake, D. R., and Blake, N.: Representation of the Community Earth System Model (CESM1) CAM4-chem within the Chemistry-Climate Model Initiative (CCMI), Geosci. Model Dev., 9, 1853-1890, doi:10.5194/gmd-9-1853-2016, 2016.

Toon, O. B., Hamill, P., Turco, R. P., and Pinto, J.: Condensation of HNO3 and HCl in the winter polar stratospheres, Geophys. Res. Lett., 13, 1284-1287, doi:10.1029/GL013i012p01284, 1986.

Toumi, R., Jones, R. L., and Pyle, J. A.: Stratospheric ozone depletion by CIONO2 photolysis, Nature, 365, 37-39, doi:10.1038/365037a0, 1993.

Trenberth, K. E., Caron, J. M., Stepaniak, D. P., and Worley, S.: Evolution of El Niño–Southern Oscillation and global atmospheric surface temperatures, J. Geophys. Res., 107, AAC 5-1-AAC 5-17, doi:10.1029/2000JD000298, 2002.

Trenberth, K. E., Fasullo, G. T., and Kiehl, J.: Earth's Global Energy Budget, Bull. Am. Meteorol. Soc., 90, 311-323, doi:10.1175/2008bams2634.1, 2009.

Trenberth, K. E., and Fasullo, J. T.: An apparent hiatus in global warming?, Earth's Future, 1, 19-32, doi:10.1002/2013EF000165, 2013.

Tung, K. K., Ko, M. K. W., Rodriguez, J. M., and Dak Sze, N.: Are Antarctic ozone variations a manifestation of dynamics or chemistry?, Nature, 322, 811-814, doi:10.1038/322811a0, 1986.

UNEP: Environmental effects of ozone depletion and its interaction with climate change: 2014 assessment, United Nations Environment Programme (UNEP), Nairobi, 2015.

Val Martin, M., Heald, C. L., and Arnold, S. R.: Coupling dry deposition to vegetation phenology in the Community Earth System Model: Implications for the simulation of surface O3, Geophys. Res. Lett., 41, 2988-2996, doi:10.1002/2014GL059651, 2014.

van Vuuren, Detlef, P., Edmonds, J., Kainuma, M., Riahi, K., Thomson, A., Hibbard, K., Hurtt, G., Kram, T., Krey, V., Lamarque, J. F., Masui, T., Meinshausen, M., Nakicenovic, N., Smith, S., and Rose, S.: The representative concentration pathways: an overview, Clim. Change, 109, 5-31, doi:10.1007/s10584-011-0148-z, 2011.

Vernier, J. P., Thomason, L. W., Pommereau, J. P., Bourassa, A., Pelon, J., Garnier, A., Hauchecorne, A., Blanot, L., Trepte, C., Degenstein, D., and Vargas, F.: Major influence of tropical volcanic eruptions on the stratospheric aerosol layer during the last decade, Geophys. Res. Lett., 38, L12807, doi:10.1029/2011GL047563, 2011.

von Kuhlmann, R., Lawrence, M. G., Crutzen, P. J., and Rasch, P. J.: A model for studies of tropospheric ozone and nonmethane hydrocarbons: Model evaluation of ozone-related species, J. Geophys. Res., 108, 4729, doi:10.1029/2002JD003348, 2003.

Vose, R. S., Arndt, D., Banzon, V. F., Easterling, D. R., Gleason, B., Huang, B., Kearns, E., Lawrimore, J. H., Menne, M. J., Peterson, T. C., Reynolds, R. W., Smith, T. M., Williams, C. N., and Wuertz, D. B.: NOAA's Merged Land–Ocean Surface Temperature Analysis, Bull. Am. Meteorol. Soc., 93, 1677-1685, doi:10.1175/bams-d-11-00241.1, 2012.

Voulgarakis, A., Naik, V., Lamarque, J. F., Shindell, D. T., Young, P. J., Prather, M. J., Wild, O., Field, R. D., Bergmann, D., Cameron-Smith, P., Cionni, I., Collins, W. J., Dalsören, S. B., Doherty, R. M., Eyring, V., Faluvegi, G., Folberth, G. A., Horowitz, L. W., Josse, B., MacKenzie, I. A., Nagashima, T., Plummer, D. A., Righi, M., Rumbold, S. T., Stevenson, D. S., Strode, S. A., Sudo, K., Szopa, S., and Zeng, G.: Analysis of present day and future OH and methane lifetime in the ACCMIP simulations, Atmos. Chem. Phys., 13, 2563-2587, doi:10.5194/acp-13-2563-2013, 2013.

Wang, X. L., Feng, Y., Compo, G. P., Swail, V. R., Zwiers, F. W., Allan, R. J., and Sardeshmukh, P. D.: Trends and low frequency variability of extra-tropical cyclone activity in the ensemble of twentieth century reanalysis, Clim. Dynam., 40, 2775-2800, doi:10.1007/s00382-012-1450-9, 2013.

Watanabe, S., Hajima, T., Sudo, K., Nagashima, T., Takemura, T., Okajima, H., Nozawa, T., Kawase, H., Abe, M., Yokohata, T., Ise, T., Sato, H., Kato, E., Takata, K., Emori, S., and Kawamiya, M.: MIROC-ESM 2010: model description and basic results of CMIP5-20c3m experiments, Geosci. Model Dev., 4, 845-872, doi:10.5194/gmd-4-845-2011, 2011.

Watson, P. A. G., and Gray, L. J.: How Does the Quasi-Biennial Oscillation Affect the Stratospheric Polar Vortex?, J. Atmos. Sci., 71, 391-409, doi:10.1175/JAS-D-13-096.1, 2013.

Waugh, D. W., Randel, W. J., Pawson, S., Newman, P. A., and Nash, E. R.: Persistence of the lower stratospheric polar vortices, J. Geophys. Res., 104, 27191-27201, doi:10.1029/1999JD900795, 1999.

Waugh, D. W., and Eyring, V.: Quantitative performance metrics for stratospheric-resolving chemistry-climate models, Atmos. Chem. Phys., 8, 5699-5713, doi:10.5194/acp-8-5699-2008, 2008.

Waugh, D. W., Oman, L., Kawa, S. R., Stolarski, R. S., Pawson, S., Douglass, A. R., Newman, P. A., and Nielsen, J. E.: Impacts of climate change on stratospheric ozone recovery, Geophys. Res. Lett., 36, L03805, doi:10.1029/2008GL036223, 2009a.

Waugh, D. W., Oman, L., Newman, P. A., Stolarski, R. S., Pawson, S., Nielsen, J. E., and Perlwitz, J.: Effect of zonal asymmetries in stratospheric ozone on simulated Southern Hemisphere climate trends, Geophys. Res. Lett., 36, L18701, doi:10.1029/2009GL040419, 2009b.

Wayne, R. P., Poulet, G., Biggs, P., Burrows, J. P., Cox, R. A., Crutzen, P. J., Hayman, G. D., Jenkin, M. E., Le Bras, G., Moortgat, G. K., Platt, U., and Schindler, R. N.: Halogen oxides: Radicals, sources and reservoirs in the laboratory and in the atmosphere, Atmos. Environ., 29, 2677-2881, doi:10.1016/1352-2310(95)98124-Q, 1995.

Weber, M., Dikty, S., Burrows, J. P., Garny, H., Dameris, M., Kubin, A., Abalichin, J., and Langematz, U.: The Brewer-Dobson circulation and total ozone from seasonal to decadal time scales, Atmos. Chem. Phys., 11, 11221-11235, doi:10.5194/acp-11-11221-2011, 2011.

Wegner, T., Kinnison, D. E., Garcia, R. R., and Solomon, S.: Simulation of polar stratospheric clouds in the specified dynamics version of the whole atmosphere community climate model, J. Geophys. Res., 118, 4991-5002, doi:10.1002/jgrd.50415, 2013.

Wesely, M. L., and Hicks, B. B.: A review of the current status of knowledge on dry deposition, Atmos. Environ., 34, 2261-2282, doi:10.1016/S1352-2310(99)00467-7, 2000.

Wilcox, L. J., Charlton-Perez, A. J., and Gray, L. J.: Trends in Austral jet position in ensembles of high- and low-top CMIP5 models, J. Geophys. Res., 117, D13115, doi:10.1029/2012JD017597, 2012.

Wild, O., and Prather, M. J.: Excitation of the primary tropospheric chemical mode in a global three-dimensional model, J. Geophys. Res., 105, 24647-24660, doi:10.1029/2000JD900399, 2000.

Wild, O.: Modelling the global tropospheric ozone budget: exploring the variability in current models, Atmos. Chem. Phys., 7, 2643-2660, doi:10.5194/acp-7-2643-2007, 2007.

Wild, O., and Palmer, P. I.: How sensitive is tropospheric oxidation to anthropogenic emissions?, Geophys. Res. Lett., 35, L22802, doi:10.1029/2008GL035718, 2008.

Williams, E. R.: Lightning and climate: A review, Atmospheric Res., 76, 272-287, doi:10.1016/j.atmosres.2004.11.014, 2005.

WMO, Scientific assessment of ozone depletion: 1998, Global Ozone Research and Monitoring Project-Report No. 44, Geneva, Switzerland, 1999.

WMO: Scientific Assessment of Ozone Depletion: 2006, World Meteorological Organization, Geneva, Switzerland, 572 pp., 2007.

WMO: Scientific Assessment of Ozone Depletion: 2010, World Meteorological Organization, Geneva, Switzerland, 516 pp., 2011.

WMO: Scientific Assessment of Ozone Depletion: 2014, World Meteorological Organization, Global Ozone Research and Monitoring Project, Geneva, Switzerland, 2014.

Wofsy, S. C., McElroy, M. B., and Yung, Y. L.: The chemistry of atmospheric bromine, Geophys. Res. Lett., 2, 215-218, doi:10.1029/GL002i006p00215, 1975.

Worden, H. M., Bowman, K. W., Kulawik, S. S., and Aghedo, A. M.: Sensitivity of outgoing longwave radiative flux to the global vertical distribution of ozone characterized by instantaneous radiative kernels from Aura-TES, J. Geophys. Res., 116, D14115, doi:10.1029/2010JD015101, 2011.

Wu, S., Liu, Z., Zhang, R., and Delworth, T.: On the observed relationship between the Pacific Decadal Oscillation and the Atlantic Multi-decadal Oscillation, J. Oceanogr., 67, 27-35, doi:10.1007/s10872-011-0003-x, 2011.

Young, P. J., Rosenlof, K. H., Solomon, S., Sherwood, S. C., Fu, Q., and Lamarque, J. F.: Changes in Stratospheric Temperatures and Their Implications for Changes in the Brewer-Dobson Circulation, 1979-2005, J. Clim., 25, 1759-1772, doi:10.1175/2011jcli4048.1, 2011.

Young, P. J., Archibald, A. T., Bowman, K. W., Lamarque, J. F., Naik, V., Stevenson, D. S., Tilmes, S., Voulgarakis, A., Wild, O., Bergmann, D., Cameron-Smith, P., Cionni, I., Collins, W. J., Dalsoren, S. B., Doherty, R. M., Eyring, V., Faluvegi, G., Horowitz, L. W., Josse, B., Lee, Y. H., MacKenzie, I. A., Nagashima, T., Plummer, D. A., Righi, M., Rumbold, S. T., Skeie, R. B., Shindell, D. T., Strode, S. A., Sudo, K., Szopa, S., and Zeng, G.: Pre-industrial to end 21st century projections of tropospheric ozone from the Atmospheric Chemistry and Climate Model Intercomparison Project (ACCMIP), Atmos. Chem. Phys., 13, 2063-2090, doi:10.5194/acp-13-2063-2013, 2013a.

Young, P. J., Butler, A. H., Calvo, N., Haimberger, L., Kushner, P. J., Marsh, D. R., Randel, W. J., and Rosenlof, K. H.: Agreement in late twentieth century Southern Hemisphere stratospheric temperature trends in observations and CCMVal-2, CMIP3, and CMIP5 models, J. Geophys. Res., 118, 605-613, doi:10.1002/jgrd.50126, 2013b.

Young, P. J., Davis, S. M., Hassler, B., Solomon, S., and Rosenlof, K. H.: Modeling the climate impact of Southern Hemisphere ozone depletion: The importance of the ozone data set, Geophys. Res. Lett., 41(24), 9033-9039, doi:10.1002/2014GL061738, 2014.

Young, P. J., Naik, V., Fiore, A. M., Gaudel, A., Guo, J., Lin, M. Y., Neu, J., Parrish, D. D., Rieder, H. E., Schnell, J. L., Tilmes, S., Wild, O., Zhang, L., Ziemke, J., Brandt, J., Delcloo, A., Doherty, R. M., Geels, C., Hegglin, M. I., Hu, L., Im, U., Kumar, R., Luhar, A., Murray, L., Plummer, D., Rodriguez, J., Saiz-Lopez, A., Schultz, M. G., Woodhouse, M., and Zeng, G., Tropospheric Ozone Assessment Report: Assessment of global-scale model performance for global and regional ozone distributions, variability, and trends, Elementa Science of the Anthropocene, 6, 10, doi:10.1525/elementa.265, 2018.

Yung, Y. L., Pinto, J. P., Watson, R. T., and Sander, S. P.: Atmospheric Bromine and Ozone Perturbations in the Lower Stratosphere, J. Atmos. Sci., 37, 339-353, doi:10.1175/1520-0469(1980)037<0339:ABAOPI>2.0.CO;2, 1980.

Zeng, G., and Pyle, J. A.: Changes in tropospheric ozone between 2000 and 2100 modeled in a chemistry-climate model, Geophys. Res. Lett., 30, 1392, doi:10.1029/2002GL016708, 2003.

Zeng, G., Pyle, J. A., and Young, P. J.: Impact of climate change on tropospheric ozone and its global budgets, Atmos. Chem. Phys., 8, 369-387, doi:10.5194/acp-8-369-2008, 2008.

Zeng, G., Morgenstern, O., Braesicke, P., and Pyle, J. A.: Impact of stratospheric ozone recovery on tropospheric ozone and its budget, Geophys. Res. Lett., 37, L09805, doi:10.1029/2010GL042812, 2010.

Zhang, H., Wu, S., Huang, Y., and Wang, Y.: Effects of stratospheric ozone recovery on photochemistry and ozone air quality in the troposphere, Atmos. Chem. Phys., 14, 4079-4086, doi:10.5194/acp-14-4079-2014, 2014.

Zou, C. Z., Goldberg, M. D., Cheng, Z., Grody, N. C., Sullivan, J. T., Cao, C., and Tarpley, D.: Recalibration of microwave sounding unit for climate studies using simultaneous nadir overpasses, J. Geophys. Res., 111, D19114, doi:10.1029/2005JD006798, 2006.

Zou, C. Z., Gao, M., and Goldberg, M. D.: Error Structure and Atmospheric Temperature Trends in Observations from the Microwave Sounding Unit, J. Clim., 22, 1661-1681, doi:10.1175/2008JCLI2233.1, 2009.

Zou, C. Z., and Wang, W.: Stability of the MSU-Derived Atmospheric Temperature Trend, J. Atmos. Ocean. Tech., 27, 1960-1971, doi:10.1175/2009jtecha1333.1, 2010.